Institute of Movement and Neurosciences

German Sport University Cologne

Head of Institute: Univ.-Prof. Dr. H. K. Strüder

Biomechanical and physiological aspects of handcycling propulsion under various exercise modalities in able-bodied participants

Doctoral thesis

accepted for the degree

Doktor der Sportwissenschaft

by

Oliver Jan Quittmann

from Dortmund, Germany

Cologne, 2020

First reviewer:

Univ.-Prof. Dr. Thomas Abel, Institute of Movement and Neurosciences,

German Sport University Cologne, Germany.

Second reviewer:

Jun.-Prof. Dr. Kirsten Albracht, Institute of Biomechanics and Orthopaedics,

German Sport University Cologne, Germany.

Chair of the doctorate committee:

Univ.-Prof. Dr. Mario Thevis, Institute of Biochemistry,

German Sport University Cologne, Germany.

Thesis defended on: 18 December 2019

Affidavits pursuant to §7 section 2 No. 4 and 5 of the doctoral regulations of the German Sport University Cologne, 20 February, 2013:

I hereby declare: the work presented in this thesis is the original work of the author except where acknowledged in the text. This material has not been submitted either in whole or in part for a degree at this or any other institution. Those parts or single sentences, which have been taken verbatim from other sources, are identified as citations. I further declare that I complied with the current "guidelines of qualified scientific work" of the German Sport University Cologne.

Oliver J. Quittmann

18 January 2020

"The highest reward for a person's toil is not what they get for it,

but what they become by it."

(John Ruskin, 1819–1900)

Table of contents

General comments

Six manuscripts as lead-author are integrated into the appraisal of the achievements befitting my doctoral candidate status. Two of those have already been accepted after a peer-review process in PubMed-listed and impact factor ranked international journals. These journals permitted the author to reuse the two articles within the thesis. The remaining four manuscripts are currently under review in PubMed-listed and impact factor ranked international journals. The articles presented within this cumulative thesis have been processed to ensure uniformity in abbreviations, citation style, figures and tables. Hence, the originally published articles may slightly differ from the chapters of this thesis.

Abbreviations

A	Amplitude parameter describing post-exercise lactate kinetics of the 15-s all-out test
ANOVA	analysis of variance
ATP	Adenosine triphosphate
BB	M. biceps brachii, Caput breve
BMI	Body mass index [$kg \cdot m^{-2}$]
b_{ST}	Increase in power output with each step of the incremental step test
C	Cycling
c_1	Linear coefficient of the quadratic polynomial for the incremental step test
c_2	Quadratic coefficient of the quadratic polynomial for the incremental step test
Cad	cadence
C_D	aerodynamic drag coefficient
CLT	continuous load trial
CSA	Cross-sectional area
d	Cohen's d (effect size)
DA	M. deltoideus, Pars clavicularis
DP	M. deltoideus, Pars spinalis
EC	M. extensor carpi ulnaris (forearm extensors)
EF	elbow-flexion
ESC	European Society of Cardiology
FC	M. flexor carpi radialis (forearm flexors)
GSUC	German Sport University Cologne
H^+	Proton (H^+-Ion)
HC	Handcycling
HIIT	High intensity interval training
HR	Heart rate [min^{-1}]
ICC	intraclass correlation coefficient
iEMG	integrated EMG (muscular effort)
IPC	International Paralympic Committee
k_1	Velocity constant describing the exchange of lactate from the previously active muscles
k_2	Velocity constant describing the removal of lactate during passive recovery
La	Lactate concentration [$mmol \cdot l^{-1}$]
La(0)	Lactate concentration at rest [$mmol \cdot l^{-1}$]
La(P)	Lactate concentration for a given power output [$mmol \cdot l^{-1}$]
$La_{Crit,CT}$	Maximal increase in lactate concentration within the last 20 minutes of the continuous load test [$mmol \cdot l^{-1}$]
$La_{max,AO15}$	Maximal lactate concentration after the 15-s all-out sprint trial [$mmol \cdot l^{-1}$]
$La_{max,CT}$	Maximal lactate concentration within the continuous load test [$mmol \cdot l^{-1}$]
$La_{max,ST}$	Maximal lactate concentration within the incremental step test [$mmol \cdot l^{-1}$]
LD	M. latissimus dorsi

LoA	limits of agreement
LSM	lean segment mass
LT	lactate threshold
M	torque
MAP	muscular activation pattern
MCT	monocarboxylate transporter
MICT	Moderate intensity continuous training
MLSS	Maximal lactate steady state
MVIC	maximal voluntary isometric contraction
P	power (output)
p	Probability of committing a type I error
P_4	calculated power output at a fixed lactate concentration of 4 $mmol \cdot l^{-1}$
PCr	creatine phosphate
PFK	Phosphofructokinase
P_{last}	Power output within the last (unfinished) step of the incremental step test
$P_{max,AO15}$	Maximal power output within the 15-s all-out test
$P_{max,ST}$	Maximal power output within the incremental step test
PM	M. pectoralis major, Pars sternalis
r	Correlation coefficient
R^2	Determination coefficient
RA	M. rectus abdominis
RD	radial-duction
RoA	range of activation [°]
RoM	range of motion [°]
SA	shoulder-abduction
SCI	spinal cord injury
RPE	Rate of perceived exertion
SD	standard deviation
sEMG	surface electromyography
SF	shoulder-flexion
SR	shoulder internal-rotation
t_{alac}	Period at the beginning of exercise for which no lactate formation is assumed [s]
TB	M. triceps brachii, Caput laterale
TD	M. trapezius, Pars descendens
TE	Technical error [%]
TF	trunk-flexion
t_{last}	Exercise duration within the last (unfinished) step of the incremental step test [s]
t_{ST}	Prescribed duration of each step during the incremental step test [s].
t_{pmax}	Time to peak power output [s]
$t_{pmax-3.5\%}$	time when power decreased by 3.5% from peak power output [s]
UCI	Union Cycliste Internationale
$\dot{V}La_{max}$	Maximal lactate accumulation rate (lactic power, maximal glycolytic rate) [$mmol \cdot l^{-1} \cdot s^{-1}$]
$\dot{V}O_2max$	Maximal oxygen consumption (aerobic power) [$ml \cdot min^{-1} \cdot kg^{-1}$]
$\bar{x}$	Mean value
θ	angle
η_p^2	partial eta squared
ω	angular velocity

List of figures

List of tables

Introduction

General introduction

Endurance performance is quantified as the time required to cover a given distance. Even though its quantification is rather simple, the exercise-related mechanisms underlying endurance performance are highly complex. Several biomechanical, physiological and cellular processes have to mesh precisely in order to realise a certain movement that can be observed from the outside. Accordingly, interdisciplinary approaches are required to gain a holistic and profound understanding of the various aspects underlying endurance exercise.

In cycling, the velocity of the athlete depends on both external and internal factors. External factors influencing velocity arise from the gradient of the terrain, frictional force between the tires and the surface and aerodynamic drag (Olds et al. 1995). Aerodynamic drag is highly dependent on total frontal area (A_f) and the shape of the athlete-bike interface, which is expressed in the drag coefficient (C_D). Besides these external factors, the athlete can affect velocity by means of mechanical power that is applied on the cranks. Mechanical power (P) is the product of the tangential torque (M) and crank angular velocity (ω) (or cadence, Cad). In other words, the more power generated by the athlete, the higher the velocity. To apply force on the cranks and accelerate them in a cyclic manner, the participating limbs have to change their configuration. These changes in limb configuration are influenced by the bike settings and expressed in terms of joint kinematics. Joint kinematics cover the angles, angular velocities and angular accelerations of the joints involved in the propulsion movement. Alterations in joint kinematics require a net joint moment that acts around the joint's axis. Besides gravitational and inertial aspects, the highest impact on net joint moment is inherent in the muscles surrounding the joint. Besides their anatomical insertion and moment arm properties, the muscles' force is the most important determinant of muscle torques. For higher muscle forces, additional motor-units have to be recruited which are accompanied by more pronounced electrical signals needed for muscle excitation (Merletti et al. 1990). Measuring these signals allows for estimating the muscles' effort, coordination and fatigue (Abbiss and Laursen 2005). Repetitive muscular activity increases the demand of energy that has to be supplied by the metabolic system.

Based on the physiological model of Michael Joyner, endurance performance can be predicted by three metabolic parameters (Joyner 1991, Joyner and Coyle 2008). Firstly, the highest rate of aerobic metabolism – in terms of maximal oxygen consumption ($\dot{V}O_2max$) – is a widely accepted and frequently examined factor of endurance performance. $\dot{V}O_2max$ is limited by several central and peripheral processes that influence oxygen uptake, transport and combustion (Basset and Howley 2000).

Secondly, the percentage of $\dot{V}O_2max$ that can be maintained during the race indicates the maximal rate of aerobic energy supply that can be provided in the absence of fatigue. This parameter is called 'performance $\dot{V}O_2max$' (%$\dot{V}O_2max$) and can be interpreted analogously to the maximal lactate steady-state (MLSS) (Beneke 2003a, 2003b). Even though there is an ongoing debate about parameters defining (maximal) metabolic homeostasis (Billat et al. 2003, Hauser et al. 2014b, Messias et al. 2017, Jones et al. 2019), explanations for the metabolic processes underlying %$\dot{V}O_2max$ are limited. Joyner and Coyle (2008) suggested: *"[…] that $\dot{V}O_2max$ and lactate threshold [LT] interact to determine how long a given rate of aerobic and anaerobic metabolism can be sustained […]."* Simulation approaches of cellular phosphorylation, on the contrary, assumed that (maximal) metabolic homeostasis arises from a system of differential equations which are based on two essential parameters: $\dot{V}O_2max$ as a measure of aerobic power and maximal lactate accumulation rate ($\dot{V}La_{max}$) as a measure of anaerobic power (Mader et al. 1983, Mader 2003, Heck et al. 2003). $\dot{V}La_{max}$ is determined by using post-exercise lactate kinetics following an all-out sprint test of 10 to 15 seconds (Heck et al. 2003, Hauser 2012). In cycling and swimming, $\dot{V}La_{max}$ was found to be altered depending on certain deliberate training loads (Sperlich et al. 2010, Manunzio et al. 2016, Hommel et al. 2019). Calculated MLSS demonstrated high reliability (Adam et al. 2015) and acceptable agreement to experimentally determined MLSS in cycling (Hauser et al. 2014a).

Lastly, the economy or efficiency of the movement (ME) determines the amount of speed or power that can be generated from a given metabolic rate (e. g. at $\%\dot{V}O_2max$). ME is most frequently expressed as the (normalised) amount of oxygen that is consumed for a given distance (e. g. $ml \cdot kg^{-1} \cdot km^{-1}$) or power (e. g. $ml \cdot kg^{-1} \cdot W^{-1}$). The better the efficiency, the less energy is required to maintain a given velocity (or power). Efficiency is influenced by a variety of physiological and biomechanical factors including cadence, bike settings, training intensity distribution, fatigue, compliance of the tendons, muscle fibre type and cellular aspects of muscle contraction (Allen et al. 2008, Goosey-Tolfrey et al. 2008, Ettema and Lorås 2009, Hopker et al. 2009, Fletcher et al. 2010, Lundby et al. 2017, Groot et al. 2018, Stone et al. 2019b).

Based on the aspects described so far, it seems obvious that endurance performance depends on various components. Furthermore, there are a lot of interdependencies between biomechanical and physiological perspectives that have not yet been fully examined. These interdisciplinary perspectives (from mechanical power to cellular metabolism) can be summarised as the 'mechanics and energetics of (hand-)cycling' (Fig. 1).

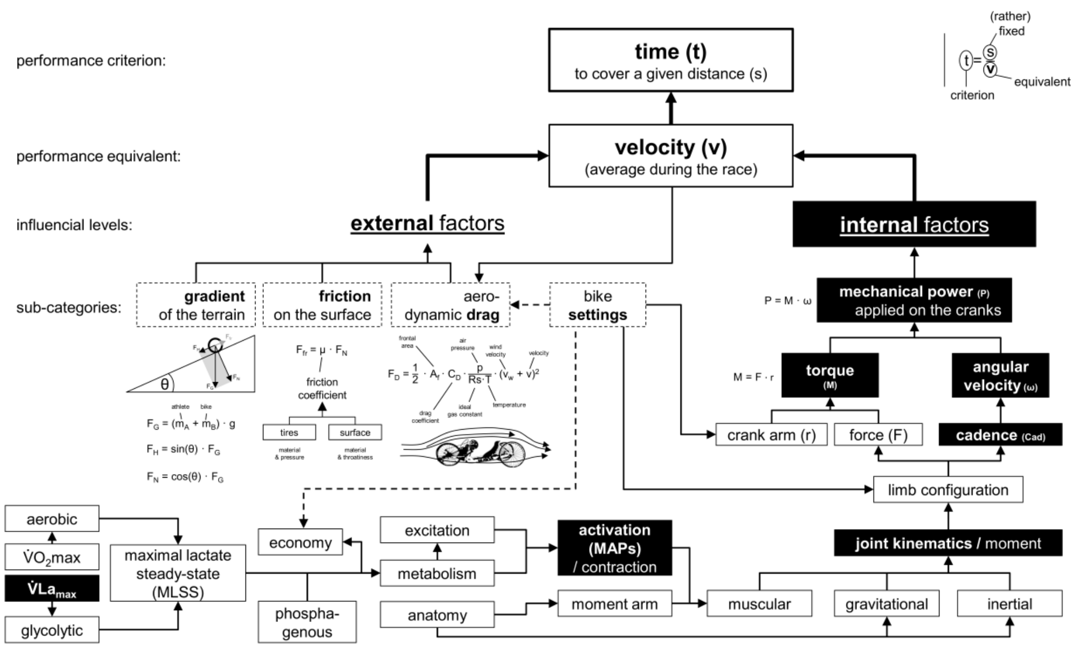

Fig. 1 Deterministic model of (hand-)cycling performance

This model aims to illustrate and categorise important aspects of cycling performance without any claim to completeness. The fields highlighted in black represent the main topics covered in this thesis. A_f = frontal area; Cad = cadence; C_D = drag coefficient; F = force; F_D = aerodynamic drag force; F_{fr} = frictional force; F_G = gravitational force; F_H = net force that accelerates an object in decline direction; F_N = normal force (projected orthogonal to the surface); g = gravitational acceleration (9.81 $m \cdot s^{-2}$); M = (crank) torque; m_A = mass of the athlete; MAPs = muscular activation patterns; MLSS = maximal lactate steady-state; m_B = mass of the bike; p = air pressure; r = crank arm; Rs = ideal gas constant (287.058 $J \cdot kg^{-1} \cdot K^{-1}$); s = (race) distance; t = time (to cover a given distance); T = temperature [°K]; v = velocity; $\dot{V}O_2max$ = maximal oxygen consumption (aerobic power); $\dot{V}La_{max}$ = maximal lactate accumulation rate (anaerobic power); v_w = wind velocity; θ = (incline) angle; μ = friction coefficient; ω = angular velocity.

Handcycling

Since 2007 paracycling has officially been administered by the Union Cycliste Internationale (UCI). Besides the bicycle, tricycle and tandem division, handcycling is a sub-category of paracycling. Handcycling is predominantly performed by athletes with an spinal-cord injury (SCI) and/or amputation of the lower limb/s. Handcycling celebrated its Paralympic debut in Athens 2004. At the Paralympics and the World Championships, the athletes compete in a road race (up to 80 km) and an individual time-trial (up to 30 km).

Handcycling is performed in a three wheeled vehicle called handcycle (or handbike) that is propelled with synchronous cranks driven by the athletes' upper extremities. Due to the synchronous crank mode, the propulsion movement in handcycling consists of a consecutive pull and push phase. *"The handcycle shall be propelled solely, through a chainset and conventional cycle drive train, of crank arms, chainwheels, chain and gears, with handgrips replacing foot pedals."* (Union Cycliste Internationale (UCI) 2019). It has an open frame of tubular construction, which conforms to the general principles and regulations of the UCI (Union Cycliste Internationale (UCI) 2019). Depending on the sport class, the athletes propel their handcycle in a lying (recumbent) or kneeling position.

In the recumbent position, the horizontal of the eye line must be above the crank housing/crank set, when the athlete is sitting with the hands on the handlebars at foremost position at full extent and the tip of the shoulder blades as well as the head in contact with the backrest and headrest, respectively. *"In the kneeling position, the athlete's legs and feet must be supported and protected from the ground surface."* (Union Cycliste Internationale (UCI) 2019). Due to the differences in body position, recumbent and kneeling handcycling can hardly be compared in terms of biomechanics (Lindschulten 2008). The size of a handcycle shall not exceed 250 centimetres in length and 75 centimetres in width. In road race events, the handcycle must be equipped with a safety bar to prevent the front wheel of a handcycle behind it from entering the space between the rear wheels at a height of 28 ± 1 centimetre. However, there are no regulations for crank length and width, which seem to be highly variable between handcycle athletes.

Athletes are assigned to a certain sport class to minimize the impact of impairment on sport performance and provide comparable and fair conditions in competition (Union Cycliste Internationale (UCI) 2019). The allocation to a certain sport class should not be affected by fitness level, technical proficiency and aging. Depending on the remaining function of the limbs and the trunk, the athletes are assigned to one of the five sport classes (from H1 with the most to H5 with the least impairment). In SCI athletes, the remaining function of the limbs highly depends on the height and degree (complete vs. incomplete) of the lesion. Previous research highlighted the necessity for evidence-based classification in handcycling (Kouwijzer et al. 2018). An overview of sport classes in handcycling is provided in Table 1.

In another race format, the team relay, three athletes of various sport classes can group together to compete against other teams. Depending on the sport class and sex, every athlete of the team contributes certain points to the team. The regulations state that the sum of all teammates must not exceed six and that at least one team member must have a point of one. For endurance sports with an emphasis on the upper extremity (e. g. swimming, rowing or triathlon) handcycling can be performed as a suitable cross-training option in able-bodied athletes as well.

Tab. 1 Overview of sport classes in handcycling

Sport class:	**H1**	**H2**	**H3**	**H4**	**H5**
Impaired muscle power	– tetraplegic (≤ C6) – no trunk stability / lower limb function – elbow-extension limited – loss of handgrip	– tetraplegic (≤ C7/C8) – no trunk stability / lower limb function – impaired triceps and biceps strength – impaired handgrip	– paraplegic (Th1 - Th10) – variable trunk stability (very limited to limited)	– paraplegic (≥ Th11) – impaired/no lower limb function – (almost) normal trunk stability	– paraplegic (≥ Th11) – normal trunk stability and function
Hypertonia	– bilateral involvement (quadriplegia) symmetrical or asymmetrical – grade ≥ 3 spasticity (in lower and upper limbs)	– bilateral involvement symmetrical or asymmetrical – grade ≥ 2 spasticity (in lower and upper limbs)	– bilateral involvement symmetrical or asymmetrical – grade ≥ 2 spasticity (in lower limb/s) – grade ≥ 1 spasticity (in upper limb/s)	– uni- or bilateral involvement (symmetrical or asymmetrical) – grade ≥ 2 spasticity (in lower limbs) – grade 0-1 spasticity (in upper limbs)	– lower limbs affected and upper limbs (near) normal – mild to normal trunk involvement – grade ≥ 2 spasticity (in lower limbs) / grade 0-1 spasticity (in upper limbs)
Ataxia / Athetosis / Dystonia	– Severe athetosis / dystonia & ataxia – Moderate to severe trunk involvement – limited elbow-extension (≥ grade 3 spasticity)	– Severe athetosis / dystonia & ataxia – Moderate to severe trunk involvement – no passive elbow extension limitation	– upper limbs less affected – grade ≥ 2 spasticity (in lower limb/s) – unilateral severely with ≥ grade 3 spasticity in lower limb	– mild to moderate athetosis / dystonia & ataxia – mild trunk involvement – poor balance and righting reactions in trunk	– mild to moderate athetosis / dystonia & ataxia – mild/normal trunk involvement
Distances	– Road Race: 45 to 60 km (men), 37 to 50 km (women). – Time-trial: 12 to 25 km (men), 10 to 20 km (women)	– Road Race: 45 to 60 km (men), 37 to 50 km (women). – Time-trial: 12 to 25 km (men), 10 to 20 km (women)	– Road Race: 60 to 80 km (men), 52 to 70 km (women). – Time-trial: 17 to 35 km (men), 10 to 20 km (women)	– Road Race: 60 to 80 km (men), 52 to 70 km (women). – Time-trial: 17 to 35 km (men), 15 to 30 km (women)	– Road Race: 60 to 80 km (men), 52 to 70 km (women). – Time-trial: 17 to 35 km (men), 15 to 30 km (women)
Points for team relay	men: 1, women: 1	men: 1, women: 1	men: 2, women: 1	men: 3, women: 2	men: 3, women: 2

According to the regulations of the UCI (Union Cycliste Internationale (UCI) 2019). Impaired passive range of motion (H4) and limb deficiency (H4 and H5) are not mentioned in Table 1.

Literature review

In general, studies in handcycling can be classified on three levels: Based on the study design (single case vs. several participants), the type of vehicle (recreational attach-unit vs. racing handcycle) and the recruitment of participants (handcycle athletes vs. able-bodied participants) (Fig. 2). Since the findings and generalisation of a study might be affected by the design, vehicle type and recruitment, these variables should be taken into account when results are interpreted and generalised. In this section, the findings of previous research are summarised according to the model described in the general introduction. At first, the physiological aspects of handcycling exercise are illustrated and biomechanical aspects of handcycling propulsion are described thereafter.

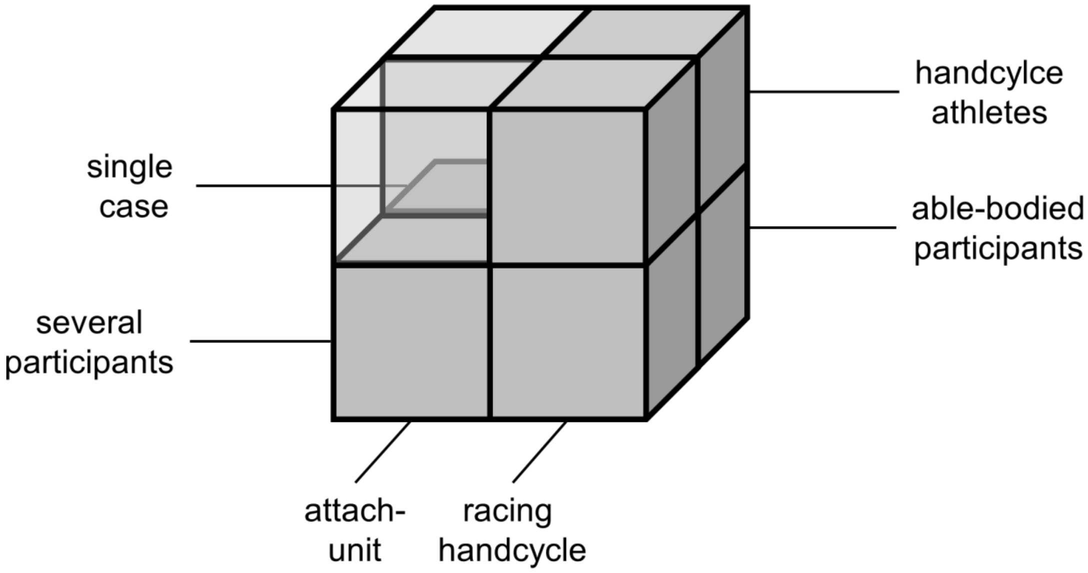

Fig. 2 Design, vehicle type and recruitment of studies in handcycling

This cube illustrates methodological differences of studies performed in the field of handcycling.

Handcycling was found to be a suitable endurance exercise for improving aerobic metabolism in paraplegic individuals during clinical rehabilitation (Valent et al. 2008, Valent 2009). Compared to manual wheelchair propulsion, arm-cranking and handcycling demonstrated less metabolic demands (Sawka et al. 1980, Hintzy et al. 2002, Abel et al. 2003, Dallmeijer et al. 2004b) and less mechanical strain (Arnet et al. 2012a, Arnet et al. 2013), especially on the shoulder and rotator cuff muscles. These findings were based on former inverse dynamic musculoskeletal modelling approaches of the upper extremity (van der Helm 1994, Veeger et al. 1991, Veeger et al. 1997, Nikooyan et al. 2010). Updated models of the shoulder are available in more recent research (Nikooyan et al. 2011, Nikooyan et al. 2012, Wu et al. 2016). However, elite athletes who compete at the Paralympics were found to be prone to overuse injuries, especially in the shoulder (17.7%), wrist (11.4%) and elbow (8.8%) region (Athanasopoulos et al. 2009, Willick et al. 2013). Even though handcycling was considered to be more efficient compared to wheelchair propulsion and thus more suitable for covering long distances, several contextual reasons (e. g. lack of interest, inability, unfamiliarity and financial constraints) were found for SCI individuals refraining from handcycling (Arnet et al. 2016).

Studies of handcycling propulsion have compared the synchronous and asynchronous crank mode, with the latter being applied in conventional (leg) cycling and arm-cranking exercise. Whereas earlier studies tended to favour asynchronous crank mode in terms of efficiency (Hopman et al. 1995) and subjective reports of the participants (Mossberg et al. 1999), most of the literature indicates that synchronous crank mode is more adventurous in terms of efficiency (van der Woude et al. 2000, Dallmeijer et al. 2004a, Bafghi et al. 2008) as well as force application and locally perceived discomfort (Bafghi et al. 2008). This is probably due to the need for stabilising the trunk in medio-lateral direction during asynchronous crank, which is limited in SCI individuals (van der Woude et al. 2000). Whereas asynchronous crank mode resulted in higher trunk lateral flexion and rotation, crank kinetics were not affected by crank mode in several (n = 7) able-bodied individuals (Faupin et al. 2011).

Competitions in handcycling come along with a considerable demand of power output, energy expenditure and lactate metabolism and lead to a substantial increase in body temperature (Abel et al. 2006, Lindschulten 2008, Groen et al. 2010, de Groot et al. 2014, Fischer et al. 2015). Very high body temperatures (> 40° C) at the end of a race may additionally result from the reduced ability of SCI athletes to sweat below their lesion level (Abel et al. 2006). Previous research consistently agrees that peak power output, $\dot{V}O_2max$ and efficiency are major predictors of race performance in handcycling (Janssen et al. 2001, Lindschulten 2008, Lovell et al. 2012, de Groot et al. 2014, Fischer et al. 2015). In a simulated marathon race, several (n = 10) SCI handcyclists demonstrated a mean $\dot{V}O_2$ and lactate concentration of 27.3 ± 5.8 $ml \cdot min^{-1} \cdot kg^{-1}$ and 4.8 ± 1.8 $mmol \cdot l^{-1}$, respectively (Lindschulten 2008). In a 'power balance model for handcycling', a high empirically derived relationship (R^2 = 95%) between power output and velocity was calculated which was based on four members of the Dutch Paralympic team (Groen et al. 2010). These authors highlighted the efficiency of handcycling propulsion in upper body exercise. Even anthropometric variables, such as waist circumference, seem to be relevant for handcycling performance (de Groot et al. 2014). However, there are contrary findings concerning the influence of lesion level on race performance (Janssen et al. 2001, de Groot et al. 2014, Arnet et al. 2016). Maximal fat oxidation of trained handcyclists was found to be 0.28 ± 0.05 $g \cdot min^{-1}$ which occurred at a heart rate of 135 ± 6 min^{-1} and corresponded to an oxygen consumption of around 55% of their $\dot{V}O_2max$ (Knechtle et al. 2004). Since the incremental tests in this study were cancelled when a respiratory exchange ratio (RER) of 1.1 was reached, the $\dot{V}O_2max$ of the participants might be underestimated. However, trained handcyclists demonstrated considerably lower $\dot{V}O_2$, energy expenditure, carbohydrate and fat oxidation, but a significantly higher maximal lactate concentration compared to trained cyclists (Knechtle et al. 2004). This might be influenced by a different ratio of lactate accumulation and removal (oxidation).

The effects of endurance training on metabolic parameters in handcycling have been examined in various studies. In several (N = 24) able-bodied participants, a 7-week intervention of moderate intensity continuous training (MICT) led to a significant increase in peak power output (32.2 ± 8.1%) and $\dot{V}O_2max$ (10.7 ± 12.3%) attained in a ramp protocol (Schoenmakers et al. 2016). Following high intensity interval training (HIIT), improvements in peak power output (47.1 ± 20.7%) and $\dot{V}O_2max$ (22.2 ± 8.1%) were significantly higher compared to MICT. However, due to the recruitment and relatively short training period, these results cannot be generalised to the training of elite handcyclists. Two single case studies examined the effect of different training intensity distributions on metabolic parameters in elite handcyclists during a half-year training period (Abel et al. 2010, Zeller et al. 2017). Whereas high volume training (72%, 15% and 13% in training zones 1, 2 and 3, respectively) increased the lactate threshold (P_4) by 20.7% (Zeller et al. 2017), polarised training (57%, 10% and 33%) led to an increase in P_4 by 63.8% (Abel et al. 2010). However, due to the different sport classes and performance levels, the generalisation of these results is also limited. Perception-based intensity regulation resulted in similar power output, $\dot{V}O_2$, heart rate and lactate concentration when compared to imposed conditions indicating that ratings of perceived exertion (RPE) are effective in controlling endurance training intensities in SCI participants (Goosey-Tolfrey et al. 2010). Accordingly, the training load of SCI handcyclists in terms of training impulse (TRIMP) demonstrated a close agreement between internal (based on RPE) and external (based on heart rate) quantification (de Groot et al.

2018). This indicates that both approaches are appropriate for monitoring handcycling training load. Since the agreement of internal and external training load differed between individuals, it is recommended to use both measures for monitoring endurance training (de Groot et al. 2018).

Besides endurance training, other interventions and procedures were examined in their ability to improve handcycling performance. Whereas an 8-week concurrent strength and endurance training programme indicated a promising increase in time-trial performance (Nevin et al. 2018), short-term respiratory muscle endurance training does not seem to improve exercise performance in SCI athletes (Fischer et al. 2014). Whereas a caffeine supplementation of 4 to 6 $mg \cdot kg^{-1}$ improved simulated 20-km time trial performance in a paratriathlete (Graham-Paulson et al. 2018), the ingestion of equimolar doses of beetroot juice did not affect time-trial performance (Flueck et al. 2019). In a recent study, the effect of arm-crank position on aerodynamic drag was examined using simulations of computational fluid dynamics (CFD) which were validated using wind tunnel experiments at various yaw angles (0°, 5°, 10° and 15°) (Mannion et al. 2019). The findings indicated that holding the cranks in foremost position (cranks pointing in direction of movement) resulted in the lowest drag coefficient at all yaw angles, which is particularly relevant for high-velocity descents. Drafting behind a competitor (at 28 $km \cdot h^{-1}$) reduced the mechanical demand in terms of power output by 25% in (n = 12) able-bodied participants (Lindschulten 2008).

Exercise testing in handcycling is predominantly based on measures of oxygen consumption and lactate concentration. Previous studies on arm-cranking exercise in (non-specifically trained) able-bodied men extensively examined the effect of cadence on $\dot{V}O_2$ kinetics and efficiency (Smith et al. 2001, Smith et al. 2006a, Smith et al. 2006b, Smith et al. 2007, Price et al. 2007).

Whereas higher cadences (around 80 to 90 min^{-1}) demonstrated a higher $\dot{V}O_2$ and heart rate, lower cadences (around 50 min^{-1}) demonstrated a higher efficiency, $\dot{V}O_2$ slow component and locally perceived exertion. Similar findings were demonstrated in handcycling stating that higher cadences result in a lower mechanical efficiency (Verellen et al. 2004). Additionally, spontaneously chosen cadence was found to increase with increasing power output (Verellen et al. 2004). At submaximal workloads, the joints' range of motion (RoM) tended to be lower at higher cadences (Price et al. 2007). The determination of ventilatory thresholds in SCI individuals demonstrated a high random error within and between examiners (Kouwijzer et al. 2019). Moreover, a clear determination of ventilatory thresholds was not possible in all (especially tetraplegic) individuals. The authors concluded that exercise testing in handcycling should be augmented by other intensity prescription methods (e. g. measures of lactate threshold) (Kouwijzer et al. 2019).

Lactate threshold in terms of power output equivalent to a concentration of 4 $mmol \cdot l^{-1}$ (P_4) demonstrated a significant correlation to simulated marathon race time ($r = -0.69$, $p \leq 0.05$) in ($n = 10$) SCI handcyclists (Lindschulten 2008). Two different lactate threshold concepts have been compared in ($n = 11$) SCI handcyclists and validated using a 30-min continuous load trial in a recent study (Stangier et al. 2019). Despite the large inter-individual differences, the lactate minimum and 4 $mmol \cdot l^{-1}$ concept demonstrated no significant difference in terms of power output, $\dot{V}O_2$ and heart rate. However, during the continuous load trials at lactate minimum, lactate concentration, heart rate and respiratory exchange ratio were lower compared to P_4. Since the percentage of continuous load trials that met the steady-state criterion (increase within the last 20 min of ≤ 1 $mmol \cdot l^{-1}$) was 83% in the lactate minimum and 67% in the 4 $mmol \cdot l^{-1}$ concept, the authors highlighted the necessity of verifying MLSS by means of several continuous load trials in elite handcyclists (Stangier et al. 2019). Post-exercise lactate kinetics following exhaustive arm-cranking exercise have been compared between able-bodied and paraplegic participants (Leicht and Perret 2008). Whereas paraplegic participants demonstrated a significantly lower power output, $\dot{V}O_2max$ and maximal lactate concentration, the lactate accumulation constant was higher compared to able-bodied participants. Since the lactate elimination constant showed no significant difference between groups, the authors concluded that the time of recovery after strenuous exercise does not have to be prolonged in trained paralysed individuals (Leicht and Perret 2008). Unfortunately, the anaerobic (lactic) power in terms of $\dot{V}La_{max}$ has not yet been quantified and examined for handcycling exercise; neither in a cross-sectional nor a longitudinal intervention study. Previous research highlighted the need for complex (aerobic and anaerobic) exercise testing procedures to improve performance in handcycling (Lindschulten 2008).

The settings of the handcycle have an impact on performance as well as physiological and biomechanical aspects of handcycling exercise. In several (n = 10) able-bodied participants, handcycling in a kneeling handcycle demonstrated a significantly higher sprint peak power output when compared to the recumbent position (Kouwijzer et al. 2018). Moreover, this study showed that the ability to make a closed chain in a recumbent handcycle – by placing both feet in the footrests – allows for a 25% higher peak power output during all-out sprinting. This has direct implications for evidence-based classification in handcycling, since some athletes who are classified as H4, would fit the H5 class but are unable to kneel. These athletes are adventurous to SCI H4 athletes due to their ability to make a closed chain (Kouwijzer et al. 2018).

Preferences and perceptions of expert handcyclists concerning their handbike configuration have been examined in a qualitative analysis (Stone et al.

2019a). The study indicated that power production, comfort and stability were primarily affected by crank position, width and length. Indeed, crank position was found to have an influence on mechanical efficiency (ME) in able-bodied (van Drongelen et al. 2009) and paraplegic participants (Stone et al. 2019b). Whereas van Drongelen at al. (2009) favoured a higher elbow-flexion angle (due to the flexors' higher moment arms), Stone et al. (2019b) concluded that a crank distance of 97% to 100% of the athletes' individual arm length (from acromion to the distal end of the fifth metacarpal) was most suitable for efficient propulsion. However, other studies demonstrated no differences in ME between crank positions in SCI individuals (Arnet et al. 2014) and able-bodied participants (Vegter et al. 2019). Similar results were found for $\dot{V}O_2$, heart rate and lactate concentration in an incremental step test at three different crank heights (Lindschulten 2008). Whereas crank width did not influence handle speed, power output and cadence, crank length was shown to significantly affect all of these parameters (Krämer et al. 2009a). For long cranks (190 ± 10 mm), power output and handle speed were highest, whereas cadence was lowest (107 ± 16 min^{-1}). However, another study measured $\dot{V}O_2$, heart rate and lactate concentration during handcycling for different crank lengths (180 and 220 mm) and cadences (70 and 85 min^{-1}) and found that the most efficient and least straining propulsion condition was the combination of short cranks and high cadence in (n = 8) wheelchair dependent athletes (Goosey-Tolfrey et al. 2008). By contrast, a recent study demonstrated a higher efficiency (at a very low power output of 35 W) in terms of both oxygen consumption and force application at a low cadence (52 min^{-1}) in several (n = 12) able-bodied participants (Kraaijenbrink et al. 2017). Different handgrip angles (horizontal, vertical and diagonal) and chainring configurations (circular and noncircular) had no effect on physiological parameters in terms of power output, $\dot{V}O_2$, ME, heart rate and lactate concentration except for a higher lactate concentration at submaximal load if a vertical handgrip was used (Abel et al. 2015, Zeller et al. 2015). Unfortunately, no biomechanical measurements were conducted in the latter two studies, which could have led to further insights into ergonomic considerations.

Biomechanical aspects of handcycling propulsion in terms of kinetics, kinematics and muscular activity were found to be affected by handbike settings in terms of backrest positioning, crank position and length, handgrip angle and chainring configuration. In several (n = 10) able-bodied participants, removing the backrest resulted in a higher maximal velocity and trunk-flexion/extension angle during the course of an 8 s sprint when compared to a high backrest tilt (65 to 70°); especially at higher gear ratios (Faupin et al. 2008). Both parameters demonstrated no difference between a high and medium (40 to 50°) backrest tilt. These findings were confirmed in a subsequent study which included measures of 2D crank kinetics demonstrating a similar efficiency in terms of fraction effective force between propulsion types (Faupin et al. 2011). Besides the common measure of fraction effective force, another parameter called 'postural force production index' (which takes the joint configuration into account) was calculated in an SCI athlete to describe force application handcycling (Jacquier-Bret et al. 2013). However, another study demonstrated that more upright (60°) backrest positions resulted in a lower shoulder load compared to more tilted backrests (0 to 30°) in several (n = 13) SCI participants (Arnet et al. 2014). In recreational handcyclists, as the authors stated, physical capacity should be improved in a shoulder-friendly way by using more upright positions. Accordingly, moving the seat downward was found to decrease shoulder-flexor and extensor and elbow internal-rotator moment, whereas shoulder-adductor, internal- and external-rotator and elbow-abductor moment increased (Li et al. 2015). However, findings from an elite handcyclist indicated that lower backrest angles are related to lower muscular effort (Litzenberger et al. 2015). Hence, the effect of backrest position on biomechanical aspects should always be interpreted in relation to the crank position.

The effect of crank position on joint kinematics was simulated and validated with 3D motion capturing of one paraplegic and one able-bodied participant (Faupin and Gorce 2008). The findings indicated that the joints' range of motion was lowest in a backward and downward position of the crank and that elbow-flexion/extension highly depends on the anterior-posterior position. The authors highlighted the need for a better knowledge of energetic and mechanical aspects of handcycling propulsion to promote this model (Faupin and Gorce 2008). The effect of anterior-posterior crank position on work distribution, joint kinematics and joint moments was examined in several (n = 12) able-bodied (Vegter et al. 2019) and (n = 16) wheelchair-dependent participants (Li et al. 2015) as well as (n = 15) handcycle athletes (Stone et al. 2019b). A higher distance to the cranks led to an increase in elbow-extension, shoulder-flexion, shoulder-abduction, shoulder internal-rotation, scapula internal-rotation and clavicle-protraction (Stone et al. 2019b), an increase in shoulder external rotator moment and a decrease in elbow-flexor, wrist-flexor and radial-deviation moment as well as an increase in trunk-flexion range of motion (Li et al. 2015). Moreover, higher distances demonstrated an increase in the work (62 ± 7 to 69 ± 8%) and peak torque attained in the pull phase, whereas the opposite was found in the push phase (Vegter et al. 2019). Contrary to the findings of Stone et al. (2019b), the authors favoured the crank position closest to the trunk (94% arm length) since it evens the load over crank cycle (Vegter et al. 2019). However, previous research indicated that subscapularis force is reduced in a more distant position, whereas shoulder load was not affected by crank position (Arnet et al. 2014). Hence, more distant crank positions seem to be advantageous in terms of economy and strain.

The effects of crank position and length on musclar activity were analysed in several (n = 13) able-bodied participants (Lindschulten 2008) and an elite handcyclist (Litzenberger et al. 2015, 2016). Muscular effort was not affected by different crank heights during the course of an incremental step test (Lindschulten 2008). Whereas little changes occurred for kinematics parameters, changes in crank position led to a shift in muscular timing (Litzenberger et al. 2016). The results indicated that a higher and longer crank tends to reduce muscular effort in an elite handcyclist (Litzenberger et al. 2015, 2016). Depending on other handbike settings, similar results were found for similar shoulder-crank distances (Litzenberger et al. 2015). The kinematic data of this study were used to perform a musculoskeletal modelling of muscular timing in a subsequent study (Felsner et al. 2016). Due to the electrode positioning on M. deltoideus (Pars acromialis) and the insufficient knowledge about the actual crank torque, high differences were observed between observed and simulated on- and offsets. Hence, the authors concluded that future studies need to combine measures of crank kinetics, joint kinematics and muscular activity to provide adequate input parameters for musculoskeletal modelling (Felsner et al. 2016).

Handgrip angle was found to affect work distribution during handcycling in several (n = 21) able-bodied participants (Krämer et al. 2009b). Whereas a pronated handgrip (+30°) improved crank torque during the pull-down sector (crank angle 30 to 90°), a slightly supinated handgrip (-15°) was found to be beneficial during the lift-up (crank angle 150 to 210°). To combine these advantages and to avoid premature fatigue due to a fixed position, the authors argue that a handgrip allowing a pronation-supination motion might be promising during prolonged handcycling exercise. However, since the pull-down sector accounted for the most work performed over crank cycle (25% higher than the mean) and a variable handgrip demonstrates only marginal benefits, a fixed pronated handgrip angle of 30° was claimed to be optimal for power generation (Krämer et al. 2009b). Findings in arm-cranking exercise showed that a neutral handgrip (0°) angle results in a higher amplitude (63%) of M. brachioradialis when compared to supinated (-90°) and pronated (+90°) handgrip (Bressel et al. 2001). At a supinated handgrip, M. infraspinatus demonstrated significantly lower amplitude (36%) when compared to neural and pronated handgrip angles, which might be clinically relevant for shoulder rehabilitation (Bressel et al. 2001).

Chainring configuration was optimised in a musculoskeletal modelling approach using AnyBody Modeling System (Damsgaard et al. 2006) and validated in experimental trials of several (n = 10) able-bodied participants (Juhl 2013). The optimised (noncircular) chainring resulted in a short duration of the transition from pull to push phase (cranks closest to the shoulders) and long duration during the pull phase. However, oxygen consumption in the experimental trials was higher with the non-circular chainring indicating a lower efficiency compared to a circular chainring (Juhl 2013).

Alterations of crank kinetics, joint kinematics and muscular activity have been investigated with respect to intensity and fatigue. At higher power outputs, tangential crank torque increased predominantly in the pull phase of propulsion (Lindschulten 2008). The variation coefficients of tangential crank torque demonstrated similar values for subsequent cycles, between participants, between different power outputs and with respect to fatigue (Verellen et al. 2008). Depending on the crank torque, the authors divided the crank cycle into four phases: an acceleration phase (from 335 to 90°), a turnover phase (from 90 to 140°), a deceleration phase (from 140 to 230°) and a second turnover phase (from 230 to 335°). In a subsequent study, an instrumented attach-unit handcycle was equipped with six degrees of freedom force sensor and validated in static and dynamic trials to examine 3D crank kinetics applied to the handgrips (van Drongelen et al. 2011). As suggested by the authors, these force data, combined with kinematic analyses and EMG measurements, can be used as input parameters for various biomechanical models. At a similar power output (35W), more work was achieved during the pull phase and press-down when higher velocities (cadences) were applied (Arnet et al. 2012c). According to a higher cadence, total and tangential force was significantly lower, whereas no changes were observed in lateral force. However, force characteristics were not affected by the method through which power (or resistance) was imposed (by incline vs. pulley system) and thus seem to be comparable (Arnet et al. 2012c). Applied procedures to estimate the inertial parameters of the upper limb in handcycling have been described in previous research (Azizpour et al. 2017a, Azizpour et al. 2017b). A combination approach of crank kinetics and musculoskeletal modelling has been described in previous research, even though these findings have not yet been applied in subsequent studies (Jakobsen and Ahlers 2016).

The effect of gear ratio on joint kinematics has been examined in several (n = 8) able-bodied participants performing 8 s sprints on a recumbent handcycle mounted on a home-trainer (Faupin et al. 2006). At higher gear ratios, a higher maximal velocity, higher trunk-flexion/extension and shoulder-abduction/adduction angle and lower shoulder and elbow-flexion/extension angular acceleration was observed. Compared to ergonomic recommendations (Veeger et al. 1998), wrist dorsal-flexion (25°) and ulnar deviation (15°) exceeded allowable limits of 15 and 10°, respectively. The authors concluded that all-out handcycling exercise might increase the risk of overuse injuries in terms of carpal tunnel syndrome (Faupin et al. 2006). In a very recent study, shoulder and thorax kinematics have been compared between (n = 7) competitive and (n = 6) recreational handcyclists at training, competition and sprint intensity using statistical parametric mapping (SPM) (Stone et al. 2019c). Competitive handcyclists demonstrated a higher trunk-flexion (~5°), shoulder extension (~10°), posterior scapula tilt and arm length (~3.5 cm) when compared to recreational athletes. The participants demonstrated no significant differences in kinematics during sprinting and in their handbike configuration, even though competitive handcyclists tended to configure their handbikes with a higher anterior-posterior distance to the crank and a lower arm length relative to crank length (Stone et al. 2019c). In several (n = 12) able-bodied participants, increasing power output resulted in a reinforced pull phase, lower shoulder-retroversion, higher shoulder-abduction, internal-rotation, elbow-flexion and trunk-flexion angle (Quittmann et al. 2018b). Since most of these changes were negatively associated with peak power output, maintaining the kinematic profile seems to be advantageous for higher performance in handcycling. In particular, the transition from pull to push phase during the lift-up sector (crank angle 180°) was claimed to be a limiting factor at high workloads (Quittmann et al. 2018b). However, muscular activity in terms of surface electromyography (sEMG) was not measured or described in these studies. A complex biomechanical investigation of handcycling propulsion combining crank kinetics, joint kinematics and muscular activity was performed in a single case study of an able-bodied participant (Faupin et al. 2010). The authors provided interesting findings on force application, limb configuration and muscular coordination characteristics of six muscles during low-intensity handcycling at a cadence of 70 min^{-1}. However, these findings cannot be generalised due to the design, intensity spectrum and number of muscles involved in this study (Faupin et al. 2010).

Purpose and outline

As demonstrated in the literature review, knowledge on handcycling exercise and propulsion lacks studies on measures of anaerobic metabolism and complex biomechanical investigations combining crank kinetics, joint kinematics and muscular activity at various exercise modalities in several participants, respectively. This thesis has a primary and a secondary aim which are covered in the following six chapters. The primary aim is to gain a more profound understanding of handcycling propulsion in terms of biomechanical and physiological aspects. The secondary aim is to improve exercise testing and biomechanical measurements of handcycling exercise by examining the suitability of the applied procedures.

Physiological aspects of handcycling propulsion are investigated in terms of lactate kinetics, since aerobic measures of handcycling exercise have frequently been examined. This thesis mainly focusses on maximal lactate accumulation rate ($\dot{V}La_{max}$) as a measure of anaerobic power. To assess whether $\dot{V}La_{max}$ is a promising parameter for exercise testing in handcycling, this parameter is examined in terms of reliability and its correlation to sport-specific performance measures. If $\dot{V}La_{max}$ was found to be a promising parameter, establishing this parameter in handcycling exercise testing could be beneficial for individualising endurance training needs.

The biomechanical aspects of handcycling propulsion can be divided into crank kinetics, joint kinematics and muscular activity. Crank kinetics are relevant for detecting in which crank position the most rotational work (W_{rot}) is accomplished and whether this is similar for various exercise modalities. Especially in comparison between the pull and push phase, these findings have a direct implication for the strength training of handcyclists. Joint kinematics are necessary to assess movement alterations due to different exercise modalities and indicate risks for overuse of the tendons and ligaments surrounding the joint in terms of ergonomic considerations. This might have an application for the manufacturers of individualised handbikes. As a main focus of this thesis, muscular activity is measured to reveal how handcycling propulsion is performed from the inside. Quantifying muscular effort and activation characteristics during various exercise modalities helps to assign a certain function to the several muscles of the upper extremity and trunk. In fact, some muscles (e. g. M. latissimus dorsi) have not yet been investigated in terms of their activation during handcycling propulsion which hinders estimating their relevance. This knowledge is highly important for improving sport-specific strength training and examining neuromuscular fatigue in handcycling. However, adequate procedures for normalisation of muscular activity in handcycling (Lindschulten 2008) have to be validated in order to improve the interpretation and generalisation of these results.

The manuscripts covered in the first five chapters of this thesis belong to a single study. Hence, the (n = 12) participants of these chapters are the same individuals. The sixth chapter represents a part of a subsequent study. Even though the population (competitive triathletes) is similar, the (n = 18) participants described in this study are – for the most part – different individuals. **Chapter 1** covers the lactate kinetics of handcycling during three exercise modalities (incremental step test, all-out sprint test and continuous load test) and their correlation with sport-specific performance measures. **Chapter 2** illustrates the muscular activation patterns (MAPs) during incremental handcycling in terms of reliability and their alterations due to increased intensity. **Chapters 3 and 4** illustrate the biomechanics of handcycling propulsion in a 15-s all-out test and a continuous load trial, respectively. **Chapter 3** highlights the biomechanical alterations during the course of a sprint test due to short-term fatigue. **Chapter 4** points out which muscles are predominantly suffering from neuromuscular fatigue during prolonged handcycling exercise. **Chapter 5** aims to compare sport and muscle-specific normalisation techniques in handcycling and derive an adequate setup for maximal voluntary isometric contractions (MVICs). **Chapter 6** investigates the lactate kinetics of handcycling and conventional (leg) cycling in terms of reliability, differences between and correlations among extremities. After these chapters, the main findings of this thesis are discussed between studies to point out the main findings and practical applications.

1 Lactate kinetics in handcycling

Lactate kinetics in handcycling under various exercise modalities and their relationship to performance measures in able-bodied participants

Oliver J. Quittmann[1], Thomas Abel[1,2], Sebastian Zeller[1,2], Tina Foitschik[1] & Heiko K. Strüder[1]

1 Institute of Movement and Neurosciences, German Sport University Cologne

2 European Research Group in Disability Sport (ERGiDS)

Published in:

European Journal of Applied Physiology, 2018, 118(7): 1493–1505. (Impact factor 2018: 3.055)

doi: 10.1007/s00421-018-3879-y

Submitted: 24 December, 2017 Accepted: 26 April, 2018

Abstract

Purpose: The aim of this study was to expand exercise testing in handcycling by (1) examining different approaches to determine lactate kinetics in handcycling under various exercise modalities and (2) identifying relationships between parameters of lactate kinetics and selected performance measures.

Methods: Twelve able-bodied nationally competitive triathletes performed a familiarisation, a sprint test, an incremental step test, and a continuous load trial at a power output corresponding to a lactate concentration (La) of 4 mmol·l^{-1} (P_4) in a racing handcycle that was mounted on an ergometer. During the tests, La and heart rate (HR) were determined.

Results: As performance measures, maximal power output during the 15-s all-out sprint test ($P_{max,AO15}$) and maximal power output during the incremental test ($P_{max,ST}$) were determined. As physiological parameters, coefficients of lactate kinetics, lactic power ($\dot{V}La_{max}$), maximal La following the sprint test and incremental test ($La_{max,AO15}$, $La_{max,ST}$) and the increase in La within the last 20 minutes of the continuous trial ($La_{Crit,CT}$) were determined. Mean values of $P_{max,AO15}$ (545.6 ± 69.9 W), $P_{max,ST}$ (131.3 ± 14.9 W), P_4 (86.73 ± 12.32 W), $\dot{V}La_{max}$ (0.45 ± 0.11 mmol·l^{-1}·s^{-1}), $La_{max,AO15}$ (6.64 ± 1.32 mmol·l^{-1}), $La_{max,ST}$ (9.64 ± 2.24 mmol·l^{-1}) and $La_{Crit,CT}$ (0.74 ± 0.74 mmol·l^{-1}) were in accordance to literature. $\dot{V}La_{max}$ was positively correlated with $La_{max,AO15}$ and $P_{max,AO15}$ and negatively correlated with $P_{max,ST}$. $P_{max,ST}$ was negatively correlated with $La_{max,AO15}$. P_4 was negatively correlated with $La_{max,ST}$.

Conclusions: $\dot{V}La_{max}$ was identified as a promising parameter for exercise testing in handcycling that can be supplemented by other parameters describing lactate kinetics following a sprint test.

1.1 Introduction

In most endurance events, performance and ranking in competition is determined by the time that is required to cover a given distance. To cover a certain distance in a short period of time, a high mean velocity is needed. In order to sustain a high race velocity, the athlete has to supply the active muscles with a considerable amount of energy in the form of adenosine triphosphate (ATP). Whereas a certain amount of energy can be defined as a capacity to perform work, the turnover of energy over time can be defined as power. The intensity-dependent ATP turnover is provided by aerobic and anaerobic metabolism.

When the ATP demand of muscle contraction exceeds mitochondrial respiration, a net proton (H^+) accumulation occurs that leads to metabolic acidosis (Robergs et al. 2004). Metabolic acidosis is reflected in a lowering of cellular pH that increasingly inhibits enzymes of glycolysis (e. g. phosphofructokinase, PFK). Thereby, exercise intensity on this level is limited. Because lactate accumulation coincides with cellular acidosis, it is regarded as a good indirect marker of cellular anaerobic metabolism (Robergs et al. 2004). Hence, the detection of blood lactate concentration (La) provides an indication of the usage of different energy-supplying systems. The changes in La due to certain exercise intensities and modalities are formally known as lactate kinetics (Freund and Gendry 1978, Moxnes and Sandbakk 2012).

Lactate kinetics depend on whole body lactate production and removal in which certain organs (e. g., muscles, brain, and heart) are involved to a different extent (van Hall 2010). The greatest influence on lactate turnover is applied by the active and passive skeletal muscles including their transporters (van Hall 2010). This is why measurements of lactate kinetics are commonly used in exercise testing. The predominant exercise modalities in lactate testing are (1) all-out sprint tests, (2) incremental step tests, and (3) continuous load trials.

All-out sprint tests are implemented to assess the athletes' sprint performance (e. g. in terms of maximal power output), to describe the athlete's ability to exchange and remove lactate, and to determine the athlete's anaerobic capability (Beneke et al. 2005, Heck et al. 2003). The athlete's ability to exchange and remove lactate is operationalised by parameters of biexponential interpolation approaches describing post-exercise lactate kinetics (Beneke et al. 2005, Messonnier et al. 2006, Leicht and Perret 2008). These approaches identify a parameter of amplitude (A), as well as exponential constants for lactate exchange (k_1) and removal (k_2) following strenuous exercise. However, studies using this approach vary in exercise modality (sprint tests, ramp protocols, or incremental step tests), as well as in recovery modality (active vs. passive) which is why the comparability between studies and their ability to determine lactic power is limited. So far, approaches to determine parameters of post-exercise lactate kinetics have not been compared to approaches to determine lactic power.

The athlete's lactic power can be described as the maximal lactate accumulation rate ($\dot{V}La_{max}$) (Mader 2003, Heck et al. 2003, Hauser et al. 2014a, Manunzio et al. 2016). In conventional cycling, $\dot{V}La_{max}$ is discussed as another important parameter (in addition to maximal oxygen uptake, $\dot{V}O_2max$) that affects endurance performance (Heck et al. 2003, Mader 2003, Manunzio et al. 2016). Furthermore, it allows for a wider interpretation of the physiological profile of the athlete (Mader 2003). For handcycling, an analysis of post-exercise lactate kinetics following a sprint test as well as $\dot{V}La_{max}$ has not yet been conducted.

Incremental step tests are implemented to determine lactate-based training zones and approximations of the maximal lactate steady-state (MLSS) as calculations of lactate threshold (LT) (Seiler 2010, Beneke 2003a). Whereas the MLSS is defined as the highest exercise intensity, where lactate production and removal are still at equilibrium, there are various approaches for determining LT, which are more mathematically than physiologically founded. Nevertheless, the shift in LT (e. g. at a defined La of 4 $mmol \cdot l^{-1}$) can be used as an indicator of physiological adaptations. However, simulation approaches indicate that the alterations of the physiological profile (resulting in a shift in LT) are affected by aerobic power ($\dot{V}O_2max$) and lactic power ($\dot{V}La_{max}$) (Mader 2003, Manunzio et al. 2016).

Continuous load trials are implemented to validate approximations of MLSS. The athletes have to perform several tests at a fixed load for about 30 minutes. MLSS is determined by the highest intensity, in which La increases not more than 1 $mmol \cdot l^{-1}$ within the last 20 minutes of the continuous trial (Beneke 2003b).

In contrast to conventional cyclists, handcycle athletes have a spinal cord injury (SCI) or amputation of the lower extremities. Consequently, the athletes have to propel the handcycle (a flat three-wheeled vehicle) through a chain set using their upper extremities. There are some indicators that there might be a difference between lower and upper extremities when it comes to cross-sectional area (CSA), strength, and fibre type (Schantz et al. 1983) as well as between able-bodied and paraplegic participants (Leicht and Perret 2008).

Performance testing in handcycling includes the determination of $\dot{V}O_2max$ (Smith et al. 2001, Smith et al. 2007, Abel et al. 2015, Zeller et al. 2015) LT, (Abel et al. 2010, Zeller et al. 2015) and movement economy (Smith et al.

2006a, Powers et al. 1984). Thus far, lactate kinetics in handcycling have been assessed only during competition (Abel et al. 2006), during an incremental test (Abel et al. 2010) and during active recovery following a ramp test until volitional exhaustion (Leicht and Perret 2008). In conventional cycling, performance improvements were shown to be related to alterations of lactate kinetics (Messonnier et al. 2006). For their implementation in handcycling exercise testing, the parameters in lactate kinetics have to prove their suitability by being associated with sport-specific performance measures. Furthermore, the parameters of different approaches for determining lactate kinetics under various exercise modalities have not yet been examined for interdependencies.

Thus, the aim of this study was to improve exercise testing in handcycling by (1) examining different approaches for determining lactate kinetics in handcycling under various exercise modalities and (2) identifying relationships between parameters of lactate kinetics and selected performance measures.

1.2 Methods

1.2.1 Participants

To improve transferability to SCI athletes, we wanted participants to be homogenously endurance-trained, especially with regard to the upper extremities as in previous studies (Leicht and Perret 2008, Zeller et al. 2015). Twelve able-bodied male competitive (national level) triathletes (26.0 ± 4.4 years, 1.83 ± 0.06 m, 74.3 ± 3.3 kg) without handcycling experience participated voluntarily in this study (see Tab. 2). The mean BMI of the participants was 22.2 ± 1.0 $kg \cdot m^{-2}$. The participants were used to a weekly training routine of 13.0 ± 4.9 $h \cdot wk^{-1}$ and had participated in triathlon competitions for 6.0 ± 3.6 yrs. Prior to any testing, the participants were given a medical check-up based on the guidelines of the European Society of Cardiology (ESC). This includes notation of the individuals' account of their own medical, family and personal history, a physical examination and a resting electrocardiogram (Corrado et al. 2005). Only participants without positive findings were included. All procedures received institutional ethics approval according to the Helsinki Declaration modified in 1983. Before the investigation, participants were personally informed of the aims, procedures and potential risks of this study, and gave their written consent.

Tab. 2 Individual values and descriptive statistics of the participants

ID	Triathlon experience [yrs.]	Training routine [$h \cdot wk^{-1}$]	$P_{max,AO15}$ [W]	$P_{max,ST}$ [W]	P_4 [W]	$\dot{V}La_{max}$ [$mmol \cdot l^{-1} \cdot s^{-1}$]
P01	6	10	560	120	72	0.44
P02	5	19	491	160	98	0.28
P03	8	20	627	148	115	0.40
P04	3	16.5	498	118	77	0.5
P05	2	9	668	106	89	0.63
P06	1.5	10	557	140	89	0.49
P07	10	12.5	572	123	78	0.42
P08	10	20	403	130	100	0.27
P09	4	15	581	122	78	0.57
P10	3	8	495	128	80	0.47
P11	13	10	518	140	87	0.51
P12	7	6	577	140	80	0.38
$\bar{x}$	6.0	13.0	546	131	87	0.45
SD	3.6	4.9	70	15	12	0.11
Max	13	20.0	668	160	115	0.63
Min	1.5	6.0	403	106	72	0.27

$\bar{x}$ = mean value; Max = maximal value; Min = minimal value; $P_{max,AO15}$ = Maximal power output within the 15-s all-out sprint test; $P_{max,ST}$ = Maximal power output within the incremental step test; P_4 = Power output equivalent to a lactate concentration of 4 $mmol \cdot l^{-1}$; SD = standard deviation; $\dot{V}La_{max}$ = Maximal lactate accumulation rate (glycolytic rate).

1.2.2 Instrumentation

The tests were performed in a racing handcycle (Shark S, Sopur, Sunrise Medical, Malsch, Germany) in synchronous crank mode that was mounted on a fully calibrated and validated ergometer (TE 2%, Cyclus 2, 8 Hz, RBM electronic automation GmbH, Leipzig, Germany) (Reiser et al. 2000). To ensure comparable conditions between participants, and between this and other studies, the backrest of the handcycle was tilted so that (1) the elbows were slightly flexed (5–10° while bringing shoulder blades together) in the foremost position and (2) that the axis of the shoulder joints were approximately at the same height as the crank axis (Faupin et al. 2010, Zeller et al. 2015). The crank length and width were kept fixed at 17.2 and 38.5 cm, respectively. The gear ratio was set to 52/12.

1.2.3 Design

The study contained (1) an initial familiarisation protocol, (2) a 15-s all-out sprint test, (3) an incremental step test and (4) a continuous load test (Fig. 3). Whereas the familiarisation and the 15-s all-out sprint test were performed on the same occasion, the other tests were conducted after a rest period of at least three days. The day before each test, participants had to refrain from consuming alcohol or caffeine and from performing heavy training loads (Zeller et al. 2015). At every visit to the laboratory, participants were instructed to arrive in a rested, carbohydrate-loaded and fully hydrated state (Jeacocke and Burke 2010).

To familiarise the participants with handcycling propulsion and sport-specific load, an incremental familiarisation protocol with decreasing stage durations was performed at their first visit to the laboratory (Fig. 3a). At the end of every stage, heart rate (HR) (Polar H7, Polar Electro Inc, Lake Success, NY, USA) and ratings of perceived exertion (RPE) on a global (cardio-pulmonary) and local (upper extremity) level were collected (Borg 1982, Smith et al. 2001). At the end of the highest workload (100 W), La of the right arterialised ear lobe was determined using a stationary analyser (Biosen C-Line, EKF-diagnostics GmbH, Barleben, Germany). Afterwards, participants performed an active recovery of 5 min at 20 W. To examine whether La was reduced during active recovery, another blood sample was collected at the end. The active recovery was followed by 5 min of passive recovery before performing the 15-s all-out sprint test.

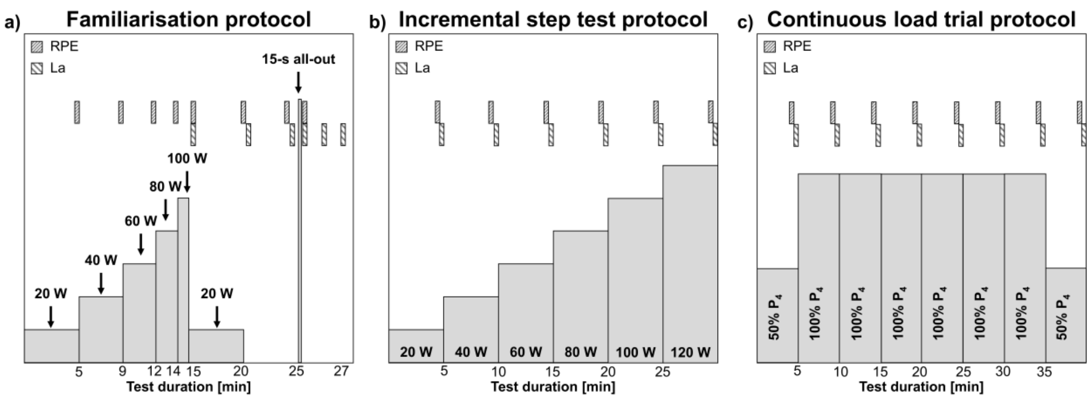

Fig. 3 Protocols and illustration of data collection times of the three different exercise modalities

a) Protocol of the familiarisation and the 15-s all-out sprint test; b) Protocol of the incremental step test; c) Protocol of the continuous load test; La = lactate concentration; P_4 = Power output equivalent to a lactate concentration of 4 mmol·l^{-1}; RPE = rate of perceived exertion.

The 15-s all-out sprint test was performed to assess the participants' anaerobic performance and lactic power. The initial torque and cadence defining the test start were set at 20 N m and 20 min^{-1}, respectively (Zeller et al. 2015). With regard to the results of Faupin et al. (2006), cadence was limited to 140 min^{-1} (Faupin et al. 2006). La was determined immediately before and after the 15-s all-out sprint test as well as every minute after exercise for 10 minutes. Throughout the 15-s all-out sprint test, participants were verbally encouraged to achieve and maintain maximal power output. To avoid active lactate elimination during the post-exercise phase, participants were instructed to keep as still as possible. Lactate kinetics of the 15-s all-out test were interpolated using a modified biexponential time function based on Michaelis–Menten kinetics as described in previous research (Eq. 1) (Beneke et al. 2005, Messonnier et al. 2006):

$$La(t) = La(0) + A \cdot \left(1 - e^{-k_1 \cdot t}\right) - A \cdot \left(1 - e^{-k_2 \cdot t}\right) \quad (1)$$

where La(t) = interpolated lactate concentration at a certain time [mmol·l^{-1}]; t = time [min]; La(0) = resting lactate concentration immediately before the test [mmol·l^{-1}]; A = amplitude parameter describing post-exercise lactate kinetics of the 15-s all-out test [mmol·l^{-1}]; k_1 = velocity constant describing the exchange of lactate from the previously active muscles [min^{-1}] and k_2 = velocity constant describing the removal of lactate during passive recovery [min^{-1}]. The parameters were determined using a nonlinear regression technique with a criterion of residual convergence lower than 10^{-8} (SPSS, 23, SPSS Inc., Chicago, Ill., USA). The starting values for A, k_1 and k_2 were 3, 0.5 and 0.05 respectively.

As applied in conventional cycling, $\dot{V}La_{max}$ was calculated as the difference between maximal post-exercise La and resting La that was divided by the difference between test time (15 s) and the period at the beginning of exercise for which no lactate formation is assumed (t_{alac}) according to Eq. (2) (Heck et al. 2003, Hauser et al. 2014a, Manunzio et al. 2016):

$$\dot{V}La_{max} = \frac{La_{max} - La(0)}{t_{test} - t_{alac}} \quad (2)$$

where La_{max} = maximal lactate concentration after the test (here $La_{maxAO15}$) [mmol·l^{-1}]; La(0) = resting lactate concentration immediately before the test [mmol·l^{-1}]; t_{test} = duration of the test [s] (15 seconds); and t_{alac} = period at the beginning of exercise for which no lactate formation is assumed. The t_{alac} was individually set as the time when P decreased by 3.5% from peak P ($P_{max,AO15}$) (Hauser et al. 2014a).

An example of the determination of lactate kinetics following the sprint test is illustrated in Figure 4.

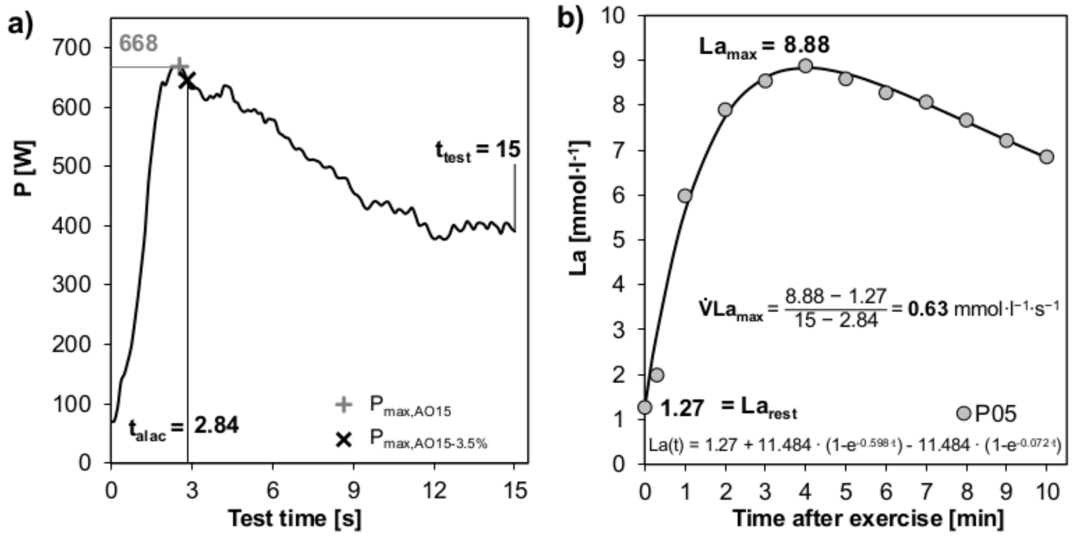

Fig. 4 Exemplary power output and post-exercise lactate kinetics of the 15-s all-out sprint test (P05)

a) Measured power output during the 15-s all-out sprint test; b) Post exercise lactate kinetics of the 15-s all-out sprint test; La(t) = Interpolated lactate concentration; La_{max} = Maximal lactate concentration following the sprint test; P = Power output; $P_{max,AO15}$ = Maximal power output within the 15-s all-out sprint test; $P_{max,AO15-3.5\%}$ = Interpolated power output that is decreased by 3.5% of maximal power output; t_{alac} = Time at the onset of exercise for which no formation of lactate is assumed.

To examine the participants' lactate kinetics due to increasing workloads, an incremental step test was performed. The step test started with an initial load of 20 W and increased every 5 min by 20 W until volitional exhaustion (Abel et al. 2010, Abel et al. 2015, Zeller et al. 2015) (Fig. 3b). Due to the ergometer's minimum of braking force (approximately 30–35 N), the participants were instructed to limit cadence for the 20 and 40 W steps to 30 and 50 min^{-1}, respectively (Zeller et al. 2015). From the 60 W step onwards, cadence was freely chosen. To quantify the participants' subjective and metabolic demands, La and HR were collected within the last 30 s of every power level (Fig. 3b). Throughout the incremental step test, participants were verbally encouraged to maintain the prescribed P. Because of their limited ability to sweat, SCI athletes are usually cooled during laboratory performance tests (Abel et al. 2006). To ensure comparable conditions between able-bodied and SCI athletes, a fan was used to cool participants from the 100 W step on. To quantify the participants' maximal effort in metabolic measurements, the maximal La during the incremental test ($La_{max,ST}$) was determined. As an approximation of MLSS, P corresponding to a fixed lactate concentration of 4 mmol·l⁻¹ (P_4, lactate threshold) was identified (Heck et al. 1985, Abel et al. 2010, Zeller et al. 2015). Lactate concentration at a certain P was interpolated using a quadratic polynomial interpolation approach according to Eq. (3):

$$La(P) = La(0) + c_1 \cdot P + c_2 \cdot P^2 \tag{3}$$

where La(P) = interpolated lactate concentration at a certain power output [mmol·l⁻¹]; La(0) = resting lactate concentration immediately before the test [mmol·l⁻¹]; c_1 and c_2 = coefficients describing the curvature of the polynomial; and P = power output [W].

For the polynomial interpolation, only lactate concentrations of fully completed steps were considered. P_4 was calculated by solving Eq. (3) for P (Eq. 4):

$$P_4 = \sqrt{\left(\frac{c_1}{2c_2}\right)^2 - \frac{La(0) - 4}{c_2}} - \frac{c_1}{2c_2} \tag{4}$$

where P_4 = interpolated power output at a lactate concentration of 4 mmol·l⁻¹ [W]; La(0) = resting lactate concentration immediately before the test [mmol·l⁻¹]; c_1 = the linear coefficient describing the curvature of the polynomial; and c_2 = the quadratic coefficient describing the curvature of the polynomial.

As an individual performance criterion, the maximal power output during the incremental step test ($P_{max,ST}$) was estimated for every participant according to Eq. (5) (Janssen et al. 2001):

$$P_{max,ST} = (P_{last} - b_{ST}) + \frac{t_{last}}{t_{ST}} \cdot b_{ST} \tag{5}$$

where P_{last} = power output of the last (unfinished) step; b_{ST} = increase in power output with each step; t_{last} = exercise duration within the last (unfinished) step; and t_{ST} = prescribed duration of each step (5 minutes).

To verify the suitability of P_4 to approximate MLSS, a continuous load test was performed. Prescribed workloads were based on the results of the incremental step test and the quadratic polynomial interpolation of P_4. The participants performed a 5-min warm-up at 50% P_4, a 30-min continuous trial at P_4 and a 5-min cool-down at 50% P_4 (Fig. 3c). Cadence was freely chosen throughout the test. During the continuous trial, a fan was used to cool the participants. La, and HR were collected every 5 min (Fig. 3c). The increase in La within the last 20 min of the continuous trial ($La_{Crit,CT}$) was checked to meet common criteria of ≤ 1 $mmol \cdot l^{-1}$ for MLSS detection (Heck et al. 1985, Beneke 2003b).

1.2.4 Statistics

Statistical analyses were done using Statistical Package for the Social Sciences software (23, SPSS Inc., Chicago, IL, USA). Parameters were initially checked for normal distribution using the Kolmogorov–Smirnov test with Lilliefors' correction. To verify the accuracy of interpolation methods, the coefficient of determination (R^2) was calculated. Correlations were calculated using Pearson's correlation coefficient. For parameters that violated the normal distribution assumption, the non-parametric correlation coefficient of Spearman was applied. As performance measures, $P_{max,AO15}$, $P_{max,ST}$ and P_4 were included. As parameters of lactate kinetics, coefficients of Eq. (1) (A, k_1 and k_2), $\dot{V}La_{max}$, t_{alac}, $La_{max,AO15}$, coefficients of Eq. (3) (c_1 and c_2), $La_{max,ST}$, $La_{max,CT}$ and $La_{Crit,CT}$ were included. The level of significance for inferential analyses was set at $\alpha = 0.05$. Values are presented as the mean value ($\bar{x}$) with standard deviation (SD).

1.3 Results

1.3.1 Familiarisation

All participants were able to complete the familiarisation protocol without volitional exhaustion. The mean La and HR values after the 100 W step were 2.12 ± 0.56 $mmol \cdot l^{-1}$ and 97.9 ± 13.9 min^{-1}, respectively.

1.3.2 15-s all-out sprint test

Immediately before the 15-s all-out sprint test, La decreased on resting levels of 1.13 ± 0.30 mmol·l^{-1}. The maximal power output during the 15-s all-out test ($P_{max,AO15}$) was 545.6 ± 69.9 W or relativized to body weight 7.36 ± 1.05 W kg^{-1}. The mean R^2 of the biexponential nonlinear interpolation approach of post-exercise lactate kinetics was 99.32 ± 0.53%. The mean interpolation parameters for the biexponential regression A, k_1 and k_2 values were 6.94 ± 2.07 mmol·l^{-1}, 0.995 ± 0.407 min^{-1} and 0.048 ± 0.020 min^{-1}, respectively. The participants' mean $La_{max,AO15}$ and $\dot{V}La_{max}$ were 6.64 ± 1.32 mmol·l^{-1} and 0.45 ± 0.11 mmol·l^{-1}·s^{-1}, respectively (Fig. 5a).

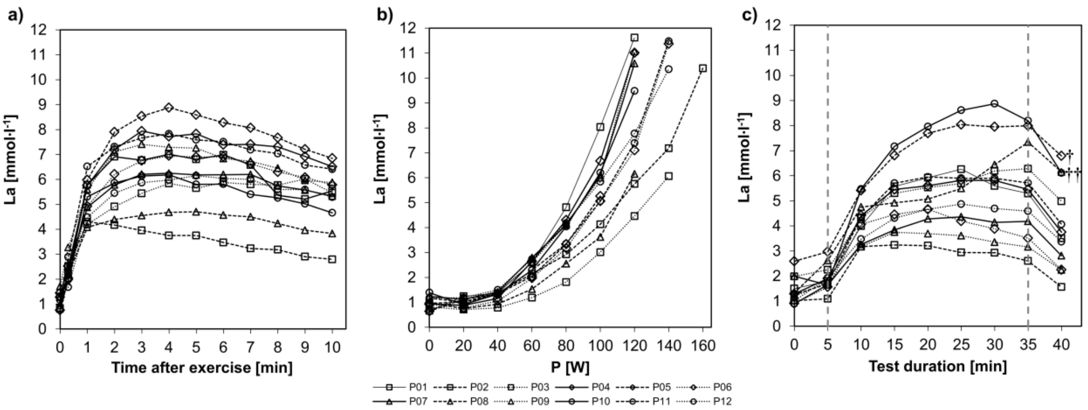

Fig. 5 Individual lactate kinetics of the three exercise modalities

a) 15-s all-out test; b) Incremental step test; c) continuous load test; La = lactate concentration; P = power output. The incremental step test (b) started with an initial load of 20 W, which increased every 5 minutes by 20 W until volitional exhaustion.† Participants with an increase in blood lactate concentration of > 1 mmol·l^{-1} within the last 20 minutes of the continuous load trial (c). The grey discontinuous lines represent the borders to the warm-up and cool-down sections (at 50% of P_4). In between, the participants had to maintain a power output equivalent to a lactate concentration of 4 mmol·l^{-1} (P_4) (c).

1.3.3 Incremental step test

The participants reached a $P_{max,ST}$ of 131.3 ± 14.9 W, which corresponded to 1.77 ± 0.24 W·kg^{-1} relativized to body weight. The mean La and HR at volitional exhaustion were 9.64 ± 2.24 mmol·l^{-1} and 167 ± 14 min^{-1}, respectively. Individual lactate kinetics of the incremental step test are illustrated in Fig. 5b. The mean interpolation parameters for the quadratic polynomial regression c_1 and c_2 were -0.026 ± 0.013 mmol·l^{-1}·W^{-1} and 0.00071 ± 0.00022 mmol·l^{-1}·W^{-2}, respectively (Eq. 3). The mean R^2 of the quadratic polynomial interpolation approach was 99.65 ± 0.28%.

1.3.4 Continuous load test

All participants were able to complete the continuous load test without volitional exhaustion. The mean La and HR at the end of the continuous load trial (at P_4) were 5.36 ± 1.85 mmol·l^{-1} and 126.8 ± 20.4 min^{-1}, respectively. Individual lactate kinetics of the continuous load trial are illustrated in Figure 5c. Three participants (P05, P08 and P10) exceeded the common criterion for MLSS (increase in La of > 1.0 mmol·l^{-1}). Hence, the mean $La_{Crit,CT}$ of all participants was 0.74 ± 0.74 mmol·l^{-1}.

1.3.5 Correlation analyses

Variables that violated the normal distribution assumption were k_1 ($p = 0.002$), t_{alac} ($p < 0.001$), and $La_{max,ST}$ ($P = 0.006$). Considering the parameters of the 15-s all-out sprint test, the amplitude parameter A was significantly correlated with the velocity constant k_1 ($r = -0.671$, $p = 0.017$) (Tab. 3). Furthermore, A showed high correlations with $\dot{V}La_{max}$ ($r = 0.904$, $p < 0.001$) and $La_{max,AO15}$ (0.941, $p < 0.001$). According to Eq. (2), $La_{max,AO15}$ and $\dot{V}La_{max}$ were positively correlated ($r = 0.942$, $p < 0.001$). The velocity constant k_2 was not significantly correlated with $La_{max,AO15}$ ($r = 0.168$, $p = 0.603$) and body weight ($r = 0.526$, $p = 0.079$). As parameters of the incremental step test, c_1 and c_2 were negatively correlated ($r = -0.814$, $p = 0.001$). The coefficient c_2 was also positively correlated with $La_{max,ST}$ ($r = 0.629$, $p = 0.028$). $La_{max,ST}$ was negatively correlated with $La_{Crit,CT}$ ($r = -0.636$, $p = 0.026$). $La_{Crit,CT}$ showed a significant correlation with $La_{max,CT}$ ($r = 0.814$, $p = 0.001$).

Tab. 3 Correlations between parameters of lactate kinetics

	$La_{Crit,CT}$	$La_{max,CT}$	$La_{max,ST}$	c_2	c_1	$La_{max,AO15}$	t_{alac}	$\dot{V}La_{max}$	k_2	k_1	A
A	-0.151	0.305	0.343$_s$	0.346	-0.038	**0.941*** **	0.042$_s$	**0.902*** **	0.409	**-0.671*$_s$**	-
k_1	-0.049$_s$	-0.056$_s$	0.028$_s$	-0.210$_s$	-0.217$_s$	-0.524$_s$	-0.070$_s$	-0.413$_s$	-0.203$_s$	-	
k_2	-0.101	0.014	0.070$_s$	0.205	0.176	0.168	0.546$_s$	0.207	-		
$\dot{V}La_{max}$	-0.256	0.210	-0.273$_s$	0.418	-0.229	**0.942*** **	0.266$_s$	-			
t_{alac}	-0.126$_s$	-0.126$_s$	-0.112$_s$	0.168$_s$	-0.112$_s$	0.049$_s$	-				
$La_{max,AO15}$	-0.246	0.232	0.350$_s$	0.408	-0.175	-					
c_1	0.041	-0.028	-0.385$_s$	**-0.814*** **	-						
c_2	-0.204	-0.022	**0.629*$_s$**	-							
$La_{max,ST}$	**-0.636*$_s$**	-0.483$_s$	-								
$La_{max,CT}$	**0.814***	-									
$La_{Crit,CT}$	-										

A = Amplitude parameter describing post-exercise lactate kinetics of the 15-s all-out test; c_1 and c_2 = Coefficients of the quadratic polynomial interpolation; k_1 = Velocity constant describing the exchange of lactate from the previously active muscles; k_2 = Velocity constant describing the removal of lactate during passive recovery; $La_{max,AO15}$ = Maximal lactate concentration after the 15-s all-out sprint trial; $La_{max,ST}$ = Maximal lactate concentration within the incremental step test; $La_{max,CT}$ = Maximal lactate concentration within the continuous load test; $La_{Crit,CT}$ = Maximal increase in lactate concentration within the last 20 minutes of the continuous load test; t_{alac} = Period at the beginning of exercise for which no lactate formation is assumed; $\dot{V}La_{max}$ = Maximal lactate accumulation rate (glycolytic rate); $_s$ Spearman's correlation coefficient; * significant correlation ($p \leq 0.05$); *** significant correlation ($p \leq 0.001$).

With regard to $P_{max,AO15}$, significant correlations could be found for k_1 ($r = -0.615$, $p = 0.033$) and $\dot{V}La_{max}$ ($r = 0.604$, $p = 0.037$) (Tab. 4). The amplitude parameter A was almost significantly correlated with $P_{max,AO15}$ ($r = 0.557$, $p = 0.060$). $P_{max,ST}$ was negatively correlated with A ($r = -0.733$, $p = 0.007$), $La_{max,AO15}$ ($r = -0.678$, $p = 0.015$), and $\dot{V}La_{max}$ ($r = -0.646$, $p = 0.023$). P_4 was negatively correlated with c_2 ($r = -0.795$, $p = 0.002$), and $La_{max,ST}$ ($r = -0.605$, $p = 0.037$). There were tendencies for A ($r = -0.490$, $p = 0.106$) and k_2 ($r = -0.515$, $p = 0.087$) that were not statistically significant. $\dot{V}La_{max}$ was the only parameter that was related to both anaerobic and aerobic performance (Fig. 6a-b).

Tab. 4 Correlations between performance measures and parameters of lactate kinetics

	$P_{max,AO15}$	$P_{max,ST}$	P_4
A	0.557	**-0.733***	-0.490
k_1	**-0.615***$_s$	0.535$_s$	0.344$_s$
k_2	-0.079	-0.353	-0.515
$\dot{V}La_{max}$	**0.604***	**-0.646***	-0.415
t_{alac}	-0.014$_s$	-0.282$_s$	-0.084$_s$
$La_{max,AO15}$	0.558	**-0.678***	-0.439
c_1	0.345	0.273	0.351
c_2	-0.131	-0.566	**-0.795****
$La_{max,ST}$	-0.168$_s$	-0.070$_s$	**-0.605***$_s$
$La_{max,CT}$	-0.056	-0.447	0.073
$La_{Crit,CT}$	-0.320	-0.260	0.281

A = Amplitude parameter describing post-exercise lactate kinetics of the 15-s all-out test; c_1 and c_2 = Coefficients of the quadratic polynomial interpolation; k_1 = Velocity constant describing the exchange of lactate from the previously active muscles; k_2 = Velocity constant describing the removal of lactate during passive recovery; $La_{max,AO15}$ = Maximal lactate concentration after the 15-s all-out sprint trial; $La_{max,ST}$ = Maximal lactate concentration within the incremental step test; $La_{max,CT}$ = Maximal lactate concentration within the continuous load test; $La_{Crit,CT}$ = Maximal increase in lactate concentration within the last 20 minutes of the continuous load test; $P_{max,AO15}$ = Maximal power output within the 15-s all-out sprint test; $P_{max,ST}$ = Maximal power output within the incremental step test; P4 = Power output equivalent to a lactate concentration of 4 $mmol \cdot l^{-1}$; t_{alac} = Period at the beginning of exercise for which no lactate formation is assumed; $\dot{V}La_{max}$ = Maximal lactate accumulation rate (glycolytic rate); s Spearman's correlation coefficient; * significant correlation ($P \leq 0.05$); ** significant correlation ($P \leq 0.01$).

Besides these correlations, two individual participants (P02 and P05) were opposed with respect to lactate kinetics and their rankings in performance measures (Fig. 6c). Interestingly, P05 was the participant with the highest $\dot{V}La_{max}$, the highest $P_{max,AO15}$ and the lowest $P_{max,ST}$. By contrast, P02 was the participant with the next-to-lowest $\dot{V}La_{max}$, the next-to-lowest $P_{max,AO15}$ and the highest $P_{max,ST}$.

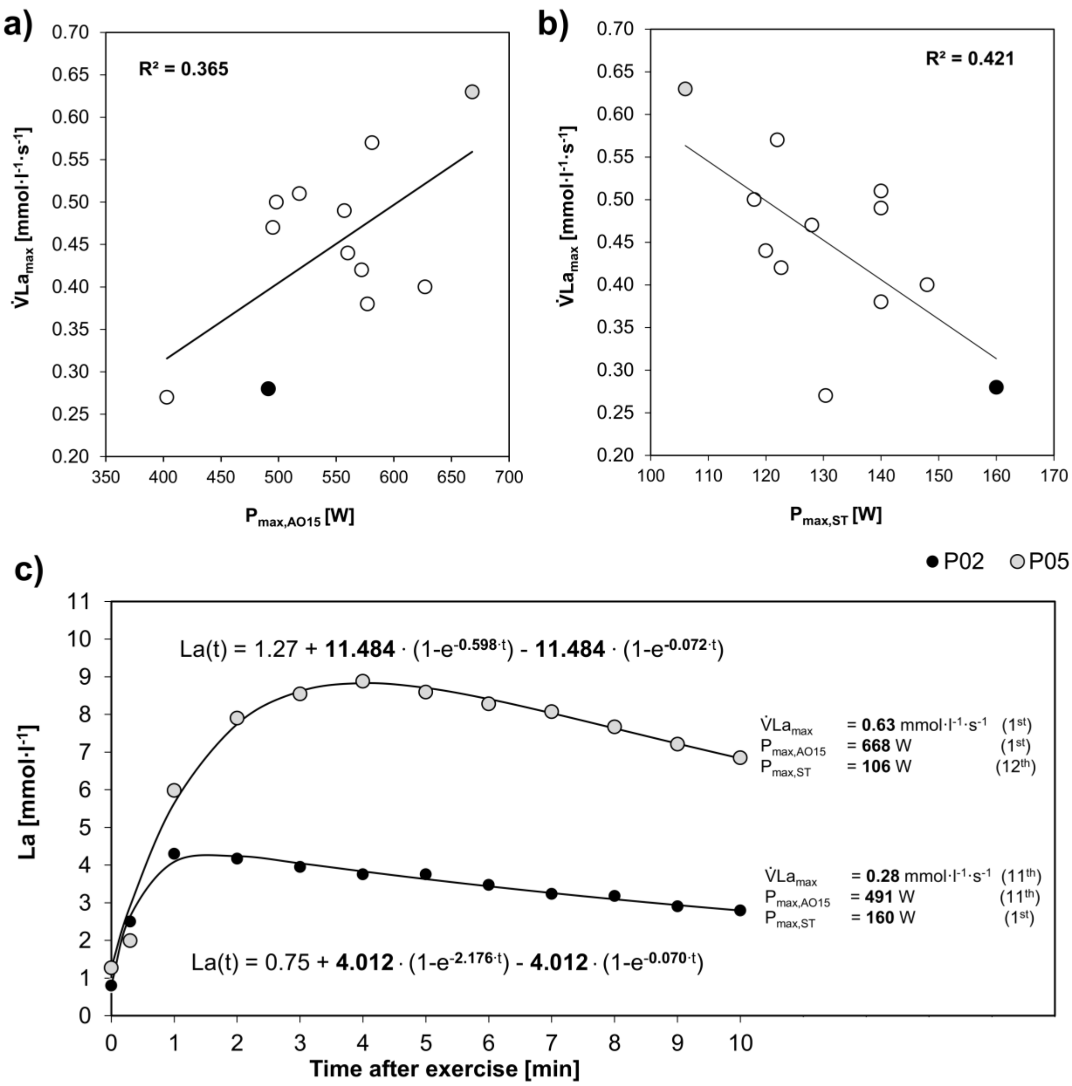

Fig. 6 Correlation plots and comparison between two individual participants (P02 and P05) in performance measures and lactate kinetics of the 15-s all-out sprint test

a) Correlation between anaerobic performance and $\dot{V}La_{max}$; b) Correlation between aerobic performance and $\dot{V}La_{max}$; c) Comparison between two individual participants (P02 and P05) in performance measures and post exercise lactate kinetics of the 15-s all-out test; La = lactate concentration; La(t) = Interpolated lactate concentration; P = power output; $P_{max,AO15}$ = Maximal power output within the 15-s all-out sprint test; $P_{max,ST}$ = Maximal power output within the incremental step test; $\dot{V}La_{max}$ = Maximal lactate accumulation rate (lactic power).

1.4 Discussion

The aim of this study was to improve exercise testing in handcycling by (1) examining different approaches to determine lactate kinetics in handcycling under various exercise modalities and (2) identifying relationships between parameters of lactate kinetics and selected performance measures.

1.4.1 Lactate kinetics following a 15-s all-out sprint test

The curvature of post-exercise lactate kinetics was characterised as an increase, with a decreasing slope up to the maximum of La followed by an almost linear decrease during the observed 10-min period (Fig. 4b, Fig. 6c). However, due to the biexponential interpolation approach, studies that assessed post-exercise La for a longer period of time (of 1 h or even longer) demonstrated a nonlinear decrease (Freund and Gendry 1978, Messonnier et al. 2006). This type of curvature is explainable by the fact that lactate transport (predominantly performed by monocarboxylate transporters, MCTs), is dependent on the lactate gradient between muscle and blood (Juel and Halestrap 1999, Wahl et al. 2011). The more lactate diffuses from active muscles to the blood, the lower the gradient and hence the slope of La increase.

During passive recovery, the decrease could be predominantly depend on lactate distribution volume (Medbø and Toska 2001). As a rough approximation of body volume, body weight accounted for approximately 28% of total variance in k_2, which tends to support this hypothesis. The values for the velocity constants of lactate exchange (k_1) and removal (k_2) are in accordance with the literature (Freund and Gendry 1978, Messonnier et al. 2006). There was no relationship between k_2 and performance measures, although other studies using a passive recovery demonstrated that changes in k_2 were related to improvements in performance measures (Messonnier et al. 2006). During active recovery at low intensity, lactate clearance is reinforced by oxidative capabilities which increases k_2 (Taoutaou et al. 1996, Leicht and Perret 2008). Therefore, the modality of recovery has to be taken into account when the curvature constant of the decrease in La is interpreted. Biexponential interpolation parameters were able to fit the curvature almost perfectly ($R^2 > 99\%$). In the context of this approach, high amplitudes of post-exercise La (A) were associated with lower increase constants (k_1). In other words, the athletes with high lactate accumulation capabilities and thus higher intramuscular La exhibited a net lactate release for a longer period of time. However, La gradients might initially be higher for participants with high maximal La. Hence, this negative relationship does not seem to be generalizable per se and should have been interpreted with caution.

Lactic power in terms of $\dot{V}La_{max}$ was related to the amplitude of lactate increase (A), which can be explained by the use of maximal La. In this domain, both approaches provide similar information about the lactic metabolism. Whereas the biexponential approach provides additional information about lactate increase and clearance behaviour, $\dot{V}La_{max}$ was the only parameter that was related to both anaerobic and aerobic performance measures. It seems that $\dot{V}La_{max}$ promotes anaerobic and somehow limits aerobic performance measures. This finding corresponds to simulation approaches of cellular metabolism (Mader 2003, Hauser et al. 2014a). Since the rate of lactic metabolism determines the ATP turnover of non-oxidative glycolysis, it seems to be reasonable that participants with a higher $\dot{V}La_{max}$ achieved higher power outputs during the sprint test. Due to the concomitant release of hydrogen ions (H^+) and the corresponding lowering of cellular pH during lactate metabolism, exercises of high intensity are increasingly inhibited over time. Hence, participants with high $\dot{V}La_{max}$ are more prone to suffer from an earlier metabolic acidosis during incremental exercises. On the other hand, participants with a low $\dot{V}La_{max}$ might not be able to achieve a high lactic ATP turnover and power output during the sprint test. Furthermore, a low $\dot{V}La_{max}$ might delay the metabolic acidosis towards higher workloads and thus support aerobic performance. However, the ability to metabolise lactate in the mitochondria is predominantly determined by aerobic power ($\dot{V}O_2max$). Since improvements in $\dot{V}O_2max$

come along with lower post-exercise lactate concentrations and a higher lactate removal ability, it is likely that lactic power ($\dot{V}La_{max}$) is reduced through aerobic exercise (Manunzio et al. 2016).

However, for training interventions of high-intensity interval training (HIIT) using the non-oxidative glycolytic pathway to a high extent, $\dot{V}La_{max}$ could exhibit more of an increase. Thus far, interventions in handcycling are primarily compared in their effect on $\dot{V}O_2max$ and lactate threshold (Abel et al. 2010, Schoenmakers et al. 2016). Hence, for exercise testing in handcycling, the determination of $\dot{V}La_{max}$ allows for new insights into applied exercise physiology. The alactic time interval (t_{alac}) was not related to performance measures. Simulation approaches indicate that t_{alac} is directly dependent on the capacity and power of (alactic) phosphate metabolism (e.g. creatine phosphate, PCr) (Hultman et al. 1991, Mader 2003). Because of the considerably higher ATP turnover of phosphate metabolism (compared to non-oxidative glycolysis) a noticeable reduction of peak power (−3.5%) was operationalised as t_{alac}, which was subtracted from exercise time. This approach to select t_{alac} could be the reason why t_{alac} was not related to anaerobic or aerobic performance measures. Hence, there seems to be a need to define anaerobic–alactic parameters of individual exercise physiology.

1.4.2 Lactate kinetics during an incremental step test

Quadratic exponential interpolation parameters (c_1 and c_2) were able to fit the curvature almost perfectly (R^2 > 99%). The higher correlations of c_2 to P_4 and $La_{max,ST}$ can be explained by the relative (mathematical) weight of c_2 (Eq. 3, Eq. 4). As a quadratic coefficient, the impact on c_2 to the curvature of La is higher relative to c_1. A higher c_2 results in a relative shift to the left (decrease) of P_4. However, c_2 was related only to the indirect performance measure P_4; not to $P_{max,AO15}$ or $P_{max,ST}$. Thus, interpolation coefficients (c_1 and c_2) are powerful to predict incremental La, but not suitable to predict performance measures.

1.4.3 Lactate kinetics during a continuous load test

Although continuous load trials were performed at a P corresponding to a fixed lactate concentration of 4 mmol·l^{-1} (P_4), during the continuous trials La showed great variation between participants (approximately 3–6 mmol·l^{-1}; Fig. 5c), which was consistent with findings in conventional cycling (Smekal et al. 2012). In contrast to another study, $La_{max,CT}$ tended to be related to $P_{max,ST}$ ($r = -0.447$), however, correlation was not significant (Smekal et al. 2012). Three out of twelve participants (25%) exceeded the MLSS criterion. Interestingly, participants with a low $La_{max,ST}$ exhibited a higher increase in La during the continuous load trial ($La_{Crit,CT}$). This indicates that P_4 seems to overestimate MLSS in handcycling for participants with relatively low maximal La during the incremental test. Even if nine participants reached a lactate steady state, we cannot say whether this was their MLSS. Hence, for a valid approximation of MLSS, several continuous load trials are needed (Beneke 2003a).

1.4.4 Limitations

The findings of this study are predominantly limited by the fact that the participants were able-bodied. Compared to athletes with an SCI, they have full function of their legs and trunk and are able to sweat all over. On the other hand, they were not specifically trained in handcycling, which is likely to influence their performance capabilities. The performance capabilities of the participants in terms of $P_{max,ST}$ and P_4 were comparable to other studies that examined able-bodied participants (Abel et al. 2015, Zeller et al. 2015, Schoenmakers et al. 2016). Compared with handcycle athletes, the participants achieved a P_4 (86.73 ± 12.32 W) that was similar to pre-season values (90.1 W) (Abel et al. 2010). However, after a 1-year training period, the handcyclist described in previous research increased his P_4 to 147.6 W, which is considerably higher than the P_4 of our participants.

Because lactate kinetics are strongly influenced by the activity and volume of skeletal muscles, differences arising from SCI and concomitant atrophy are likely (van Hall 2010). Although the amplitude and increase of La were shown to be different between able-bodied and paraplegic participants, the mechanisms underlying the behaviour of lactate appearance and disappearance seem to be the same (Leicht and Perret 2008). For inexperienced participants, technical aspects such as propulsion kinematics, kinetics and muscular activation patterns might have a greater influence on performance measures than in highly experienced athletes. We, therefore, believe that the correlations we found between physiological parameters and performance measures will be more pronounced when replicated with handcycle athletes.

1.4.5 Practical applications

From the present findings, it seems promising to augment exercise testing in handcycling. Previous studies focused primarily on aerobic performance ($P_{max,ST}$) and power ($\dot{V}O_2max$) (Abel et al. 2010, Schoenmakers et al. 2016). In the present study, measures of anaerobic performance and lactic power showed promising results and seem to contribute additional information on aspects of exercise physiology. Especially when different training regimes (e.g., HIIT and moderate intensity continuous training, MICT) are compared, a narrow focus on aerobic performance and power only displays a part of the physiological profile (Schoenmakers et al. 2016). To reveal the profound mechanisms underlying different training regimes, exercise testing in handcycling should be augmented by measures of anaerobic performance

($P_{max,AO15}$) and lactic power ($\dot{V}La_{max}$). This would be a helpful tool for athletes and coaches who seek to define individual training needs.

1.5 Conclusions

This study adds new findings for exercise testing in handcycling:

1. $\dot{V}La_{max}$ is identified as a promising parameter for exercise testing in handcycling, because it correlates positively with anaerobic and negatively with aerobic performance measures.

2. The parameters of post-exercise lactate kinetics and $\dot{V}La_{max}$ correlate with each other and allow for additional information of the athlete's physiology which is why both approaches should be applied.

3. Lactate kinetics following a sprint test, as well as during an incremental step test, can be precisely interpolated using biexponential or quadratic polynomial approaches ($R^2 > 99\%$).

4. The suitability of P_4 as an estimation of MLSS in handcycling tests seems to be influenced by individual lactate kinetics (e.g., expressed as $La_{max,ST}$) and needs further investigation.

5. To adequately represent (alterations in) the physiological profile of handcycle athletes, the determination of aerobic performance ($P_{max,ST}$) and power ($\dot{V}O_2max$) should be augmented by the measurement of anaerobic performance ($P_{max,AO15}$) and power ($\dot{V}La_{max}$).

2 Muscular activity in incremental handcycling

Reliability of muscular activation patterns and their alterations during incremental handcycling in able-bodied participants

Oliver J. Quittmann[1], Thomas Abel[1,2], Kirsten Albracht[3,4] & Heiko K. Strüder[1]

1 Institute of Movement and Neurosciences, German Sport University Cologne

2 European Research Group in Disability Sport (ERGiDS)

3 Institute of Biomechanics and Orthopaedics, German Sport University Cologne

4 Faculty of Medical Engineering and Technomathematics, University of Applied Sciences Aachen

Published in:

Sports Biomechanics, 2019, epub ahead of print. (Impact factor 2018: 1.714)

doi: 10.1080/14763141.2019.1593496

Submitted: 4 August, 2018 Accepted: 4 March, 2019

Abstract

Purpose: The aim of this study was to assess muscular activation patterns (MAPs) in handcycling in terms of reliability and their alterations due to increasing workload.

Methods: Twelve able-bodied triathletes performed an incremental step test until subjective exhaustion in a racing handcycle that was mounted on an ergometer. During the test, muscular activity of ten muscles of the upper extremity and trunk was measured using surface electromyography (sEMG). MAPs were examined by calculating integrated EMG (iEMG), the onset, offset and range of activation (RoA). Parameters of MAPs were analysed using intraclass correlation coefficient (ICC) and two-way ANOVA with repeated measures.

Results: ICCs ranged from 0.775 to 0.999 indicating ‘good’ to ‘excellent’ reliability. All muscles increased their iEMG from low to high intensity with differing effect sizes. Several muscles showed an earlier onset and increased RoA.

Conclusions: MAPs in handcycling are highly reliable and altered due to increasing workload in able-bodied participants. Whereas muscular effort can be examined in a single cycle, muscular activation characteristics require at least six to ten consecutive revolutions to achieve ‘good’ or ‘excellent’ reliability. At high intensity, many muscles demonstrated an earlier onset and larger RoA. Future studies should validate these findings in several elite handcyclists and investigate all-out sprint exercises.

2.1 Introduction

Handcycling is a Paralympic endurance sport for athletes with disabilities such as spinal cord injury or amputation of the lower extremities. As an aerobic exercise of the upper body, handcycling is a suitable cross-training option for able-bodied athletes, who train and/or compete in endurance sports with an emphasis on the arms such as swimming, rowing or triathlon. Due to the synchronous crank mode, handcycling propulsion consists of a consecutive pull and push phase. Insights into the complex interplay of muscles of the upper extremity and the trunk during handcycling propulsion demonstrate sport-specific demands and help to optimise movement coordination, training, equipment and performance. For such analyses, muscular coordination should attain an adequate level of reliability.

Musular activation patterns (MAPs) can be described in terms of muscular effort and muscle activation characteristics using surface electromyography (sEMG). Muscular effort [e.g. in terms of integrated EMG (iEMG)] of the upper extremities was shown to increase with workload (Bafghi et al. 2008, Smith et al. 2008). However, it has not yet been quantified to what extent muscular effort increases in certain muscles of the upper extremity. In order to improve the training of handcyclists, a comparison of these increases helps to understand which muscles are primarily involved in high intensity handcycling and thus probably more prone to fatigue. Muscle activation characteristics of an elite handcyclist have been quantified by the onset, offset and range of activation (RoA) above a certain threshold (Litzenberger et al. 2015, 2016). Muscle activation characteristics demonstrated differences between an able-bodied participant (Faupin et al. 2010) and an elite handcyclist (Litzenberger et al. 2015, 2016). This is important because handcycling is performed by both of these groups. Since most of the previous research was based on a single-case design, the reliability of MAPs in handcycling has not yet been examined.

Although different intensities were applied in previous research, the effect of workload on MAPs could not yet be certified (Litzenberger et al. 2015, 2016). Furthermore, it was recommended to expand the investigated muscles to include M. trapezius (Pars descendens), M. latissimus dorsi and M. rectus abdominis (Smith et al. 2008) to gain a more profound understanding of the muscular coordination characteristics underlying handcycling exercise. Due to the lacking generalisability, rather inconsistent findings and muscles that have not yet been included in investigations, MAPs during handcycling have remained uncertain. A more profound examination of inter- and intra-muscular coordination characteristics in handcycling could provide helpful information for athletes and coaches to develop sport-specific strength and conditioning training regimes.

The investigation of elite handcyclists is challenging for three reasons. Firstly, complex biomechanical procedures are rather time-consuming which is why it is hard to find several (n > 10) elite handcyclists who are willing to do such a study. Secondly, due to the different classifications, the prerequisites of the athletes are rather heterogeneous which would probably result in huge differences between athletes that influence statistical analyses. Lastly, handcycle athletes make use of a customised handcycle with an individualised crank position, length and width. These individual settings affect the standardisation and outcomes of the biomechanical measurements. Even though choosing to use able-bodied participants impedes generalisability to elite handcyclists, there are practical, methodical and standardisation-based advantages to using this kind of sample. Additionally, information on the MAPs during handcycling could be useful for exercise professionals in other sports who are considering prescribing handcycling to their able-bodied athletes and clients with respect to their performance goals and their injury history.

In order to evaluate a method to determine MAPs in handcycling and gain a deeper understanding of the muscular activation processes underlying handcycling propulsion, the aim of this study was to assess MAPs in terms of reliability and their alterations due to increasing workload in able-bodied participants. It is hypothesised that MAPs are different between handcycling at low and high intensity.

2.2 Methods

2.2.1 Participants

Twelve able-bodied male competitive triathletes (26.0 ± 4.4 yrs., 1.83 ± 0.06 m, 74.3 ± 3.6 kg) participated in the study. Participants gave their written informed consent before participating in the study. The study was approved by the German Sport University Cologne Ethics Committee (No. 52/2016) and complied with the ethical standards of the 1975 Helsinki Declaration modified in 1983.

2.2.2 Experimental protocol

The participants performed an initial familiarisation trial and incremental step test in a racing handcycle that was mounted on an ergometer until voluntary exhaustion (Quittmann et al. 2018b). The incremental test started with an initial load of 20 W and increased by 20 W every five minutes. Every participant was able to reach at least the 120 W step of the test. During the incremental test this study is based on, further biomechanical measures (including the kinematics and kinetics of handcycling propulsion) were examined. To ensure comparable conditions between participants and other studies, the backrest of the handcycle was tilted so that (1) the elbow was slightly flexed (5 to 10° while bringing shoulder blades together) in the foremost position (almost extended arm) and (2) the axis of the shoulder joint was approximately at the same height as the crank axis (Quittmann et al. 2018b). A detailed description of the experimental protocol and instrumentation of the handcycle is available in previous research (Quittmann et al. 2018b).

2.2.3 Data recording

Muscular activity of 10 muscles [M. trapezius, Pars descendens (TD); M. pectoralis major, Pars sternalis (PM); M. deltoideus, Pars clavicularis (DA); M. deltoideus, Pars spinalis (DP); M. biceps brachii, Caput breve (BB); M. triceps brachii, Caput laterale (TB); M. flexor carpi radialis (FC); M. extensor carpi ulnaris (EC); M. latissimus dorsi (LD) and M. rectus abdominis (RA)] was measured unilaterally on the dominant (right) side of the participants. Since the muscles of the forearm are tightly gathered and thus increase the risk of EMG crosstalk, FC and EC were identified to represent forearm flexors and extensors, respectively. Muscular activity was measured using a wireless sEMG system (DTSEMG Sensor®, 1,000 Hz, Noraxon Scottsdale, Arizona, USA). The sensor delay of 312 ms was corrected for synchronisation with kinetic and kinematic measures (Quittmann et al. 2018b). The skin of the participants was prepared according to the standards for reporting EMG Data of the International Society of Electromyography and Kinesiology. Two single-use wet gel Ag/AgCl-electrodes (Ambu BlueSensor N, Ambu A/S, Ballerup, Denmark) were applied on each muscle according to the guidelines of the SENIAM project (Fig. 7).

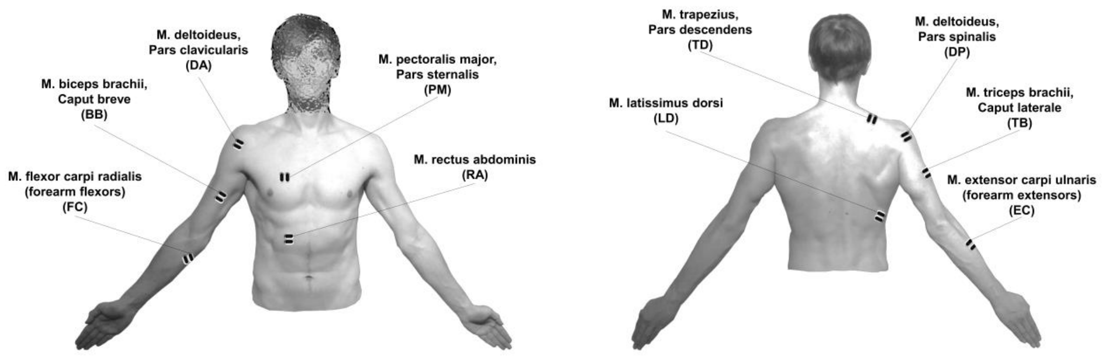

Fig. 7 Electrode positions of the investigated muscles from anterior (left) and posterior (right)

Muscular activity was measured unilaterally on the dominant (right) side of the participants.

Electrodes and senders were additionally fixed using kinesiology tape (Elyth®, WINpharma Herstellungs- und Vertriebs-GmbH, Wilhelmsburg, Germany). As a sport-specific normalisation of voltage signals, the participants performed maximal voluntary isometric contractions (MVICs) at the foremost (0°), lowest (90°), nearest (180°) and highest (270°) crank position (Fig. 8).

One week before the incremental tests, participants were familiarised with handcycling propulsion and MVIC trials using an incremental familiarisation protocol with decreasing stage durations (Quittmann et al. 2018b). The duty-cycle of MVIC contractions was 1.0 with two to three seconds time under tension for three consecutive contractions in each position. sEMG data were collected simultaneously to kinematic and kinetic measurements at the beginning and at the end of every step for 20 s (Quittmann et al. 2018b).

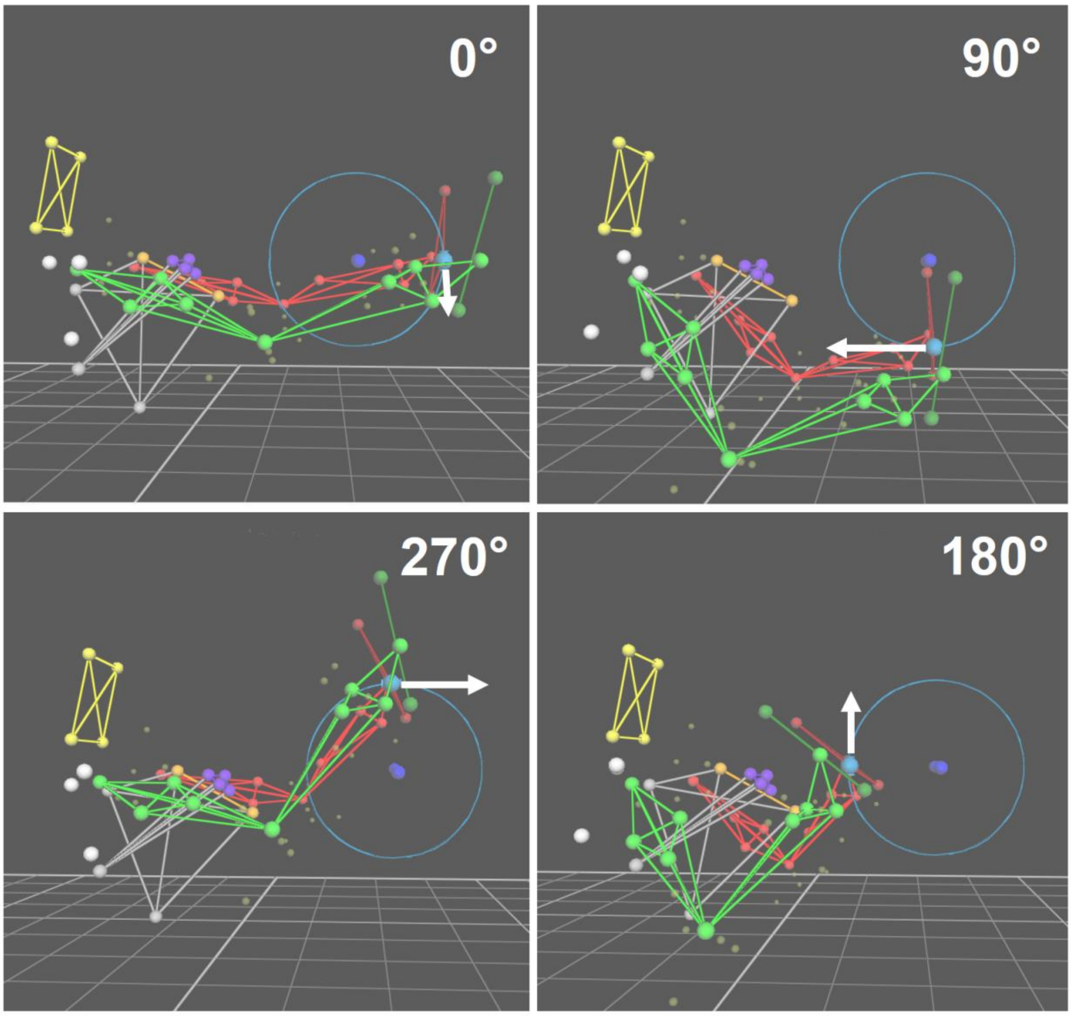

Fig. 8 Crank angles of sport-specific MVICs (0°, 90°, 180° and 270°)

The polygon represented in the figure was applied in a previous study focusing on the kinematics and kinetics of incremental handcycling which were obtained during the same test this study is based on (Quittmann et al. 2018b). The arrows indicate the cranks' direction of movement.

2.2.4 Data processing

sEMG data were rectified and smoothed using a zero-lag moving average filter with a window size of 200 ms using MATLAB (R2017b, MathWorks®, Natick, Massachusetts, USA) (Litzenberger et al., 2015). Based on synchronised crank kinematics, sEMG data were divided into single crank cycles, interpolated to a length of 360 frames and averaged over crank cycle (Litzenberger et al., 2016). In order to compare muscular activity between muscles, sEMG data were normalised to the MVICs that were performed immediately before the incremental test. For every muscle, the reference MVIC value (representing 100%) was set as the highest value attained in all MVIC positions and contractions. Muscular effort was assessed using the integral of normalised sEMG values (iEMG) which was expressed as a percentage of MVIC over crank cycle.

Muscle activation characteristics were assessed by using the crank angles where sEMG values exceeded a threshold of 30% of a muscle's local amplitude (Litzenberger et al. 2015, 2016). The threshold of 30% was normalised to the maximum and minimum within crank cycle to determine the onsets and offsets of muscular activation. However, cyclic movement are characterised by alternating phases of higher and lower activation. The wording onset and offset does not imply that the muscles are inactive as under resting conditions. Hence, muscles were considered to be less activated when muscular activity was falling below the given threshold and not inactive. For onsets and offsets that occurred around the foremost position where crank angles experience a large switch (from 359° to 0°), values were adjusted according to an either low or high definition of crank position. The crank cycle was divided into six consecutive sectors identified as press-down (330° to 30°), pull-down (30° to 90°), pull-up (90° to 150°), lift-up (150° to 210°), push-up (210° to 270°) and push-down (270 to 330°) (Krämer et al. 2009b).

2.2.5 Statistics

Statistical analyses were performed using the Statistical Package for the Social Sciences software (25, SPSS Inc., Chicago, Illinois, USA). To assess the reliability of iEMG, onset, offset and RoA, intraclass correlation coefficient (ICC, Model: Two-way mixed, Definition: Absolute agreement, Type: Mean of measurements) was applied (Koo and Li 2016). ICCs were separately determined for every muscle and workload resulting in a total of 80 ICCs. ICCs were calculated by analysing an n-times-k matrix, where n is the sample size and k is the least number of consecutive crank cycles within a workload (k = 14). ICCs were classified as ‘excellent’ (ICC ≥ 0.90), ‘good’ (0.90 > ICC ≥ 0.75), ‘moderate’ (0.75 > ICC ≥ 0.50) or ‘poor’ (0.5 > ICC) (Koo & Li, 2016). In order to assess how many crank cycles (revolutions) are required to achieve a ‘good’ or even ‘excellent’ level of reliability, ICCs were determined for k = 2 to k = 14 revolutions. Differences in MAP parameters between a moderate (60 W) and high intensity workload (120 W) as well as between muscles were analysed using a two-way (10 × 2) analysis of variance (ANOVA) with repeated measures. For obtaining MAP parameters, muscular activity was averaged over consecutive crank cycles within one particular trial for every participant and muscle. Mauchly’s test was used to examine sphericity. If the parameters showed significant differences in sphericity, the degrees of freedom were adjusted using the Greenhouse-Geisser method. Post hoc comparisons between workloads and muscles were adjusted using Bonferroni’s correction. The calculated effect sizes for factors and mean differences were partial eta squared (η_p^2) and Cohen’s d, respectively (Cohen 1988). The level of significance was set at $\alpha = 0.05$.

2.3 Results

2.3.1 Muscular activity with respect to crank angle

Since all participants reached the 120Wstep of the incremental test, muscular activity could be averaged across all participants from 20 to 120 W with respect to crank angle (Fig. 9). Averaged values of muscular activity indicated that alterations in MAPs due to increasing workloads vary between the investigated muscles. At low intensities, LD and RA demonstrated the lowest activation with respect to MVIC.

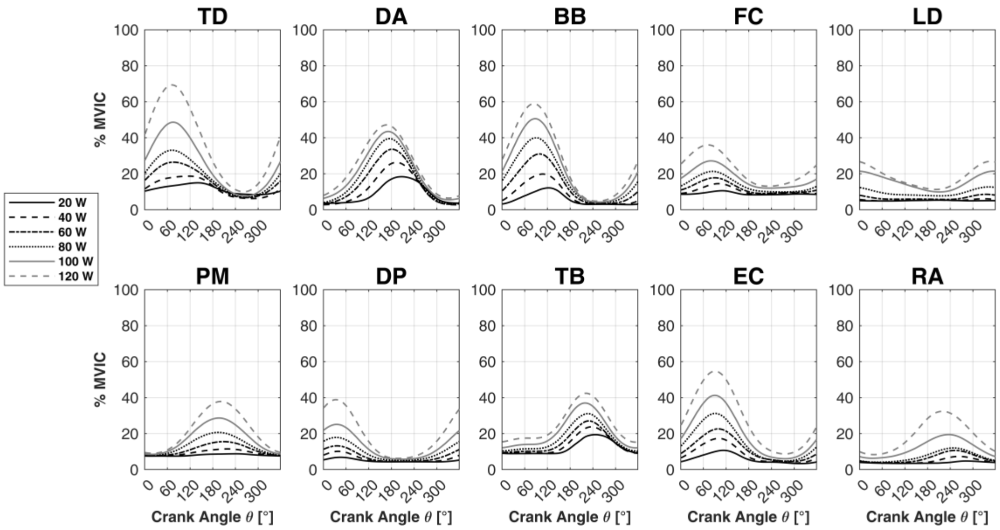

Fig. 9 Muscular activity at increasing workloads with respect to crank angle

The lines represent the mean values across all participants. BB = M. biceps brachii, Caput breve; DA = M. deltoideus, Pars clavicularis; DP = M. deltoideus, Pars spinalis; EC = M. extensor carpi ulnaris; FC = M. flexor carpi radialis; LD = M. latissimus dorsi; MVIC = maximal voluntary isometric contraction; PM = M. pectoralis major, Pars sternalis; RA = M. rectus abdominis; TB = M. triceps brachii, Caput laterale; TD = M. trapezius, Pars descendens.

2.3.2 Reliability analysis

For all (k = 14) revolutions, the range in ICCs of iEMG (0.979 to 0.996), onset (0.839 to 0.999), offset (0.775 to 0.993) and RoA (0.851 to 0.991) indicated 'good' to 'excellent' reliability (Tab. 5). Ten ICC values were below 0.90 and represented the offset and RoA of LD at 60 W (0.878, 0.872) and 120 W (0.794, 0.851), the offset of PM (0.775), DP (0.821) and FC (0.886) at 60 W, the onset (0.839) and RoA (0.880) of RA at 60 W and the RoA of DP at 60 W (0.884).

Tab. 5 Reliability analyses of MAP parameters at increasing workloads

		iEMG	Onset	Offset	RoA
TD	60 W	0.990 (0.979 - 0.997)	0.999 (0.999 - 0.999)	0.956 (0.909 - 0.985)	0.975 (0.947 - 0.991)
	120 W	0.995 (0.990 - 0.998)	0.999 (0.999 - 0.999)	0.975 (0.947 - 0.991)	0.957 (0.910 - 0.985)
PM	60 W	0.993 (0.985 - 0.998)	0.892 (0.774 - 0.963)	0.775 (0.528 - 0.923)	0.941 (0.877 - 0.980)
	120 W	0.989 (0.976 - 0.996)	0.965 (0.927 - 0.988)	0.974 (0.946 - 0.991)	0.951 (0.898 - 0.983)
DA	60 W	0.993 (0.985 - 0.997)	0.993 (0.985 - 0.998)	0.980 (0.959 - 0.993)	0.991 (0.981 - 0.997)
	120 W	0.981 (0.961 - 0.994)	0.997 (0.995 - 0.999)	0.917 (0.828 - 0.972)	0.925 (0.844 - 0.974)
DP	60 W	0.993 (0.985 - 0.997)	0.945 (0.886 - 0.981)	0.821 (0.625 - 0.939)	0.884 (0.758 - 0.960)
	120 W	0.979 (0.956 - 0.993)	0.984 (0.967 - 0.995)	0.965 (0.927 - 0.988)	0.957 (0.912 - 0.986)
FC	60 W	0.987 (0.973 - 0.996)	0.986 (0.971 - 0.995)	0.886 (0.763 - 0.961)	0.944 (0.883 - 0.981)
	120 W	0.997 (0.994 - 0.999)	0.973 (0.943 - 0.991)	0.976 (0.951 - 0.992)	0.947 (0.890 - 0.982)
EC	60 W	0.984 (0.967 - 0.995)	0.999 (0.999 - 0.999)	0.974 (0.945 - 0.991)	0.964 (0.924 - 0.988)
	120 W	0.990 (0.980 - 0.997)	0.99 (0.979 - 0.997)	0.99 (0.979 - 0.997)	0.975 (0.948 - 0.991)
LD	60 W	0.996 (0.992 - 0.999)	0.937 0.869 - 0.978)	0.878 (0.747 - 0.958)	0.872 (0.735 - 0.956)
	120 W	0.990 (0.980 - 0.997)	0.940 (0.875 - 0.979)	0.794 (0.573 - 0.930)	0.851 (0.690 - 0.949)
RA	60 W	0.995 (0.989 - 0.998)	0.839 (0.665 - 0.945)	0.932 (0.858 - 0.977)	0.880 (0.749 - 0.959)
	120 W	0.987 (0.974 - 0.996)	0.912 (0.818 - 0.970)	0.993 (0.986 - 0.998)	0.903 (0.797 - 0.967)

The values represent ICCs (Model: Two-way mixed, Type: Mean of measurements, Definition: Absolute agreement) in bold and their 95% confidence intervals in parenthesis. BB = M. biceps brachii, Caput breve; DA = M. deltoideus, Pars clavicularis; DP = M. deltoideus, Pars spinalis; EC = M. extensor carpi ulnaris; FC = M. flexor carpi radialis; ICC = intraclass correlation coefficient; LD = M. latissimus dorsi; PM = M. pectoralis major, Pars sternalis; RA = M. rectus abdominis; TB = M. triceps brachii, Caput laterale; TD = M. trapezius, Pars descendens.

The number of revolutions required to achieve a 'good' or even 'excellent' level of reliability varied between parameters (Tab. 6). Whereas an 'excellent' reliability in iEMG was achieved after three revolutions, the onsets, offsets and RoA require considerably more revolutions. Even after 14 revolutions, an 'excellent' level of reliability was not achieved for the onset and offset PM, the RoA of DP, the offset of FC, the offset and RoA of LD and the RoA of RA at 60 W as well as the offset and RoA of LD at 120 W. Mean ICCs for every revolution and parameter indicated that a 'good' level of reliability in iEMG, onset, offset and RoA is achieved after two, two, four and six revolutions, respectively (Fig. 10). For an 'excellent' level of reliability for iEMG, onset, offset and RoA, two, seven, nine and ten revolutions are required, respectively.

Tab. 6 Number of revolutions to achieve good (excellent) reliability

		iEMG	Onset	Offset	RoA
TD	60 W	2 (3)	2 (2)	4 (8)	3 (4)
	120 W	2 (2)	2 (2)	2 (3)	2 (2)
PM	60 W	2 (2)	5 (> 14)	3 (> 14)	7 (11)
	120 W	2 (2)	2 (4)	2 (4)	3 (5)
DA	60 W	2 (2)	2 (2)	2 (3)	2 (3)
	120 W	2 (3)	2 (2)	5 (13)	7 (11)
DP	60 W	2 (2)	2 (3)	2 (2)	10 (> 14)
	120 W	2 (2)	2 (2)	3 (4)	4 (8)
FC	60 W	2 (2)	2 (2)	7 (> 14)	2 (8)
	120 W	2 (2)	2 (2)	2 (3)	2 (3)
EC	60 W	2 (2)	2 (2)	3 (4)	3 (4)
	120 W	2 (2)	2 (2)	2 (2)	2 (4)
LD	60 W	2 (2)	2 (8)	7 (> 14)	10 (> 14)
	120 W	2 (2)	8 (11)	13 (> 14)	12 (> 14)
RA	60 W	2 (2)	2 (11)	2 (2)	11 (> 14)
	120 W	2 (2)	2 (14)	2 (2)	4 (14)

The values represent the number of revolutions that are required to achieve a good (ICC ≥ 0.80) reliability (Model: Two-way mixed, Type: Mean of measurements, Definition: Absolute agreement). Values in parenthesis represent the number of revolutions to achieve an excellent (ICC ≥ 0.90) reliability. BB = M. biceps brachii, Caput breve; DA = M. deltoideus, Pars clavicularis; DP = M. deltoideus, Pars spinalis; EC = M. extensor carpi ulnaris; FC = M. flexor carpi radialis; ICC = intraclass correlation coefficient; LD = M. latissimus dorsi; PM = M. pectoralis major, Pars sternalis; RA = M. rectus abdominis; TB = M. triceps brachii, Caput laterale; TD = M. trapezius, Pars descendens.

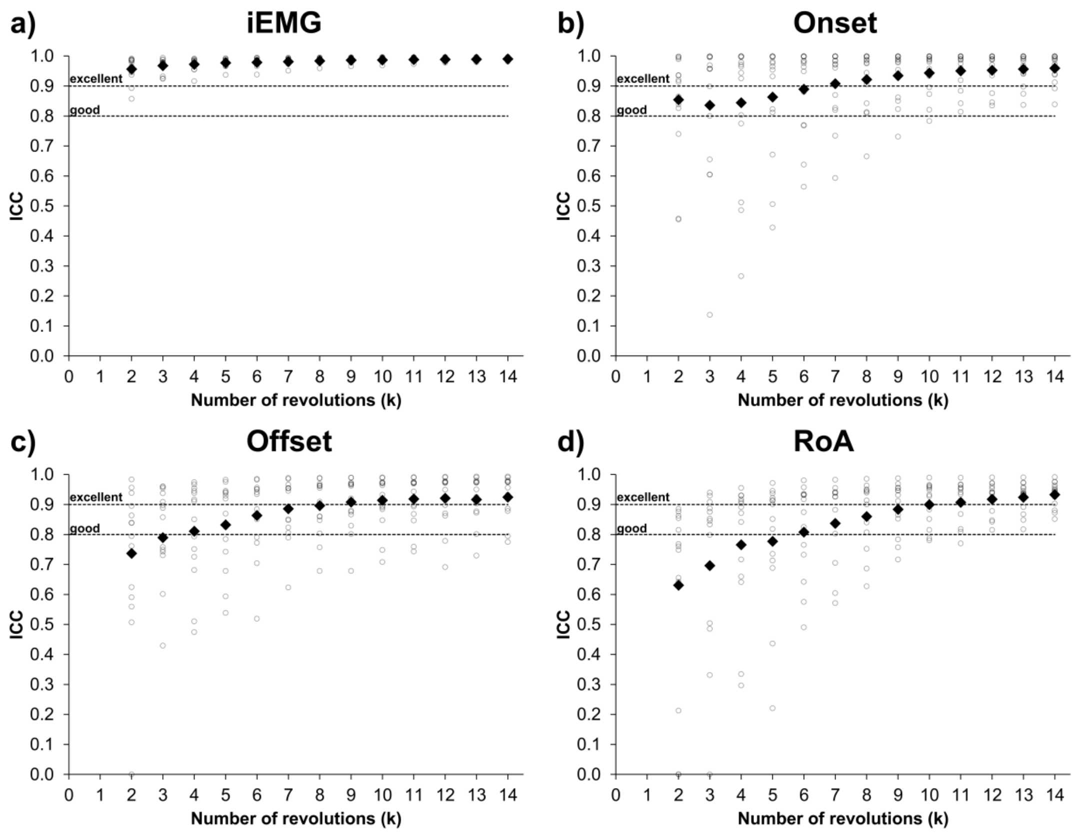

Fig. 10 Reliability with respect to the number of revolutions for muscular activation pattern parameters

a) Muscular effort (iEMG); b) Onset; c) Offset; d) Range of activation (RoA). The grey circles represent the single intraclass correlations coefficients (ICCs) for all muscles and workloads. The diamonds represent the mean ICC of the particular number of revolutions (k). The dotted lines represent the borders for 'good' (ICC = 0.80) and 'excellent' (ICC = 0.90) reliability (Koo and Li 2016).

2.3.3 Analysis of variance (ANOVA)

Two-way ANOVAs demonstrated a significant effect of the factor 'muscle' for iEMG ($\eta_P^2 = 0.274$, $p < 0.001$), onset ($\eta_P^2 = 0.967$, $p < 0.001$), offset ($\eta_P^2 = 0.924$, $p < 0.001$) and RoA ($\eta_P^2 = 0.490$, $p < 0.001$) (Tab. 7). A significant effect of 'workload' was observed for iEMG ($\eta_P^2 = 0.933$, $p < 0.001$), onset ($\eta_P^2 = 0.395$, $p = 0.021$) and RoA ($\eta_P^2 = 0.485$, $p = 0.004$). For all muscles combined, the offset was not significantly affected by workload ($\eta_P^2 = 0.223$, $p = 0.103$). There was no significant interaction between 'muscle' and 'workload' for iEMG, onset, offset and RoA.

Tab. 7 ANOVA results of sEMG parameters

		Muscle	Workload	Muscle×Workload
iEMG	p	< 0.001	< 0.001	0.076
	η_p^2	**0.274*** **	**0.933*** **	0.141
Onset	p	< 0.001^g	0.021	0.053^g
	η_p^2	**0.967*** **	**0.395***	0.249
Offset	p	< 0.001^g	0.103	0.067^g
	η_p^2	**0.924*** **	0.223	0.245
RoA	p	< 0.001	0.008	0.063^g
	η_p^2	**0.490*** **	**0.485** **	0.200

ANOVA = analysis of variance; ^{g} = Greenhouse-Geisser correction of the degrees of freedom; iEMG = amplitude of sEMG (area under the curve); p = probability of committing a type 1 error; RoA = range of activation; η_p^2 = effect size (partial eta squared); * = p ≤ 0.050; ** = p ≤ 0.010; *** = p ≤ 0.001.

2.3.4 Post-hoc comparisons between workloads

iEMG significantly increased from 60 W to 120 W in all investigated muscles (Tab. 8). Cohen's d of iEMG increase ranged from 1.12 (FC) to 2.21 (DP) demonstrating high effect sizes. The onset of muscular activation occurred significantly earlier in crank cycle for DA (d = −0.85, p = 0.024), DP (d = −0.81, p = 0.003), BB (d = −0.98, p = 0.002), TB (d = −0.94, p = 0.001), EC (d = −0.66, p = 0.002) and RA (d = −1.43, p = 0.001) (Tab. 9). The offset of muscular activation occurred significantly earlier for TD (d = −0.83, p = 0.016) and later for DP (d = 0.86, p = 0.001). RoA was significantly increased for DA (d = 0.77, p = 0.037), DP (d = 1.40, p < 0.001), BB (d = 1.08, p = 0.006), TB (d = 1.14, p = 0.003), EC (d = 0.97, p = 0.010) and RA (d = 1.69, p = 0.002). Muscle activation characteristics in terms of onset, offset and RoA were not significantly altered for PM, FC and LD.

Tab. 8 Post-hoc comparisons of iEMG between workloads

	60 W	120 W	d	p
TD	16 ± 6	36 ± 16	**1.30*** **	< 0.001
PM	11 ± 5	22 ± 8	**1.32*** **	< 0.001
DA	15 ± 7	24 ± 8	**1.11** **	0.002
DP	7 ± 3	19 ± 7	**1.76*** **	< 0.001
BB	14 ± 8	27 ± 17	**0.80*** **	0.001
TB	15 ± 4	25 ± 7	**1.46*** **	< 0.001
FC	12 ± 4	23 ± 13	**0.83** **	0.003
EC	12 ± 5	28 ± 13	**1.27*** **	< 0.001
LD	7 ± 3	18 ± 11	**1.08** **	0.002
RA	6 ± 3	19 ± 14	**0.92** **	0.004

Descriptive values are expressed as mean value ($\bar{x}$) and standard deviation (SD) [% MVIC]. Post-hoc comparisons were adjusted using Bonferroni's correction. BB = M. biceps brachii, Caput breve; d = effect size (Cohen's d); DA = M. deltoideus, Pars clavicularis; DP = M. deltoideus, Pars spinalis; EC = M. extensor carpi ulnaris; FC = M. flexor carpi radialis; LD = M. latissimus dorsi; p = probability of committing a type 1 error; PM = M. pectoralis major, Pars sternalis; RA = M. rectus abdominis; RoA = range of activation; TB = M. triceps brachii, Caput laterale; TD = M. trapezius, Pars descendens; Significant increase from 60 to 120 W ** = $p \leq 0.010$; *** = $p \leq 0.001$.

Tab. 9 Post-hoc comparisons of muscle activation characteristics between workloads

		60 W	120 W	d	p
TD	Onset [°]	347 ± 22	338 ± 19	-0.43	0.160
	Offset [°]	191 ± 18	175 ± 19	**-0.83***	0.016
	RoA [°]	204 ± 28	197 ± 17	-0.30	0.280
PM	Onset [°]	116 ± 27	108 ± 24	-0.31	0.260
	Offset [°]	303 ± 21	301 ± 21	-0.10	0.532
	RoA [°]	187 ± 26	195 ± 23	0.32	0.260
DA	Onset [°]	84 ± 28	63 ± 22	**-0.85***	0.024
	Offset [°]	264 ± 12	260 ± 14	-0.25	0.317
	RoA [°]	180 ± 29	198 ± 16	**0.77***	0.037
DP	Onset [°]	321 ± 25	301 ± 22	**-0.81****	0.003
	Offset [°]	106 ± 14	117 ± 13	**0.86*****	0.001
	RoA [°]	145 ± 22	176 ± 22	**1.40*****	< 0.001
BB	Onset [°]	16 ± 25	352 ± 23	**-0.98****	0.002
	Offset [°]	172 ± 18	174 ± 10	0.11	0.745
	RoA [°]	157 ± 27	182 ± 19	**1.08****	0.006
TB	Onset [°]	159 ± 13	143 ± 21	**-0.94*****	0.001
	Offset [°]	298 ± 11	298 ± 8	0.03	0.919
	RoA [°]	139 ± 10	155 ± 18	**1.14****	0.003
FC	Onset [°]	345 ± 50	350 ± 26	0.12	0.777
	Offset [°]	158 ± 10	158 ± 20	-0.01	0.974
	RoA [°]	173 ± 46	168 ± 24	-0.14	0.780
EC	Onset [°]	10 ± 26	353 ± 25	**-0.66****	0.002
	Offset [°]	180 ± 25	182 ± 26	0.07	0.723
	RoA [°]	170 ± 20	189 ± 18	**0.97****	0.010
LD	Onset [°]	188 ± 91	249 ± 69	0.75	0.124
	Offset [°]	151 ± 108	86 ± 42	-0.79	0.078
	RoA [°]	173 ± 58	167 ± 29	-0.13	0.780
RA	Onset [°]	176 ± 22	136 ± 33	**-1.43*****	0.001
	Offset [°]	326 ± 17	329 ± 27	0.11	0.759
	RoA [°]	150 ± 24	193 ± 27	**1.69****	0.002

Descriptive values are expressed as mean value ($\bar{x}$) and standard deviation (SD). Post-hoc comparisons were adjusted using Bonferroni's correction. BB = M. biceps brachii, Caput breve; d = effect size (Cohen's d); DA = M. deltoideus, Pars clavicularis; DP = M. deltoideus, Pars spinalis; EC = M. extensor carpi ulnaris; FC = M. flexor carpi radialis; LD = M. latissimus dorsi; p = probability of committing a type 1 error; PM = M. pectoralis major, Pars sternalis; RA = M. rectus abdominis; RoA = range of activation; TB = M. triceps brachii, Caput laterale; TD = M. trapezius, Pars descendens; Significant increase from 60 to 120 W * = p ≤ 0.050; ** = p ≤ 0.010; *** = p ≤ 0.001.

2.3.5 Muscular coordination during handcycling propulsion

At low intensity (60 W), the press-down (330 to 30°) is initiated by DP activation (Fig. 11). Around the foremost position (0°) TD, FC, EC and BB start supporting the press-down and pull-down (30° to 90°). The pull-up (90° to 150°) is initiated by DA that is activated shortly before the crank starts lifting (at 90°) and DP reduces activation. The period of co-contraction between DP and DA lasts approximately 20 degrees. The second half of the pull-up (120° to 150°) is supported by PM activation. The first half of the lift-up (150° to 180°) is supported by TD, EC and BB, while FC already reduced activation. Shortly before TD, EC and BB set off (around 180°), TB performs the lift-up (150° to 210°). The period of co-contraction between BB and TB lasts approximately 15 degrees. The push-up (210° to 270°) is performed by DA, PM, and TB activation. The offset of DA occurs shortly before the crank's highest position (270°). While PM and TB support the first half of the push-down (270° to 300°), DP sets in again at the beginning of the press-down (330°).

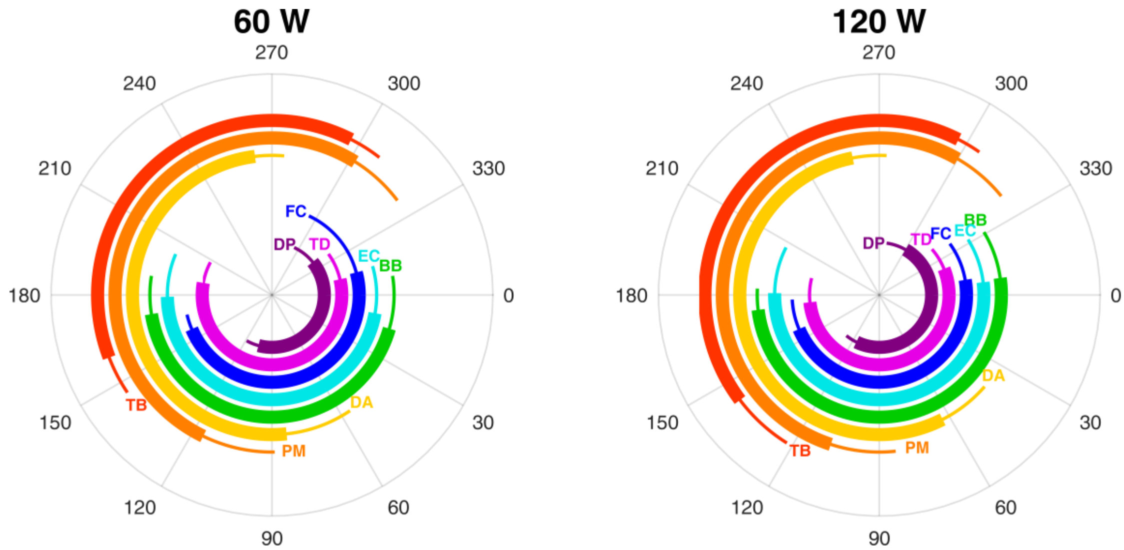

Fig. 11 Muscular activity above threshold with respect to crank angle at 60 W (left) and 120 W (right)

The thick lines represent muscular activity above 30%. The thin lines represent the standard deviation addition of the onsets and offsets. BB = M. biceps brachii, Caput breve; DA = M. deltoideus, Pars clavicularis; DP = M. deltoideus, Pars spinalis; EC = M. extensor carpi ulnaris; FC = M. flexor carpi radialis; PM = M. pectoralis major, Pars sternalis; TB = M. triceps brachii, Caput laterale; TD = M. trapezius, Pars descendens.

At high intensity (120 W), DP even supports the second half of the push-down followed by an almost similar onset of TD, FC, EC and BB around the foremost position. DA supports the second half of the pull-down that is performed by DP, TD, FC, EC and BB. DP demonstrates a later offset and even supports the first half of the pull-up. The period of co-contraction between DP and DA is enlarged at high intensity and lasts approximately 50 degrees. As at low intensity, the second half of the pull-up is supported by PM activation. The lift-up is initiated by TB and RA activation. Shortly after the beginning of the lift-up, FC reduces activation. TD, EC and BB support the first half of the lift-up, although TD demonstrated an earlier offset. The period of co-contraction between BB and TB is almost doubled at high intensity to approximately 30 degrees. The second half of the lift-up and the push-up is performed by DA, PM, and TB. PM and TB remain active until activation of DP sets in again at the beginning of the second half of the push-down.

2.4 Discussion

The aim of this study was to assess the reliability of MAPs in handcycling and their alterations due to increasing workload.

2.4.1 Reliability of MAPs in handcycling

The ‘good’ to ‘excellent’ ICCs based on the ‘mean of measurements’ indicate that it is appropriate to assess all MAP parameters obtained from several (k = 14) consecutive cycles recorded in each trial which are averaged over crank cycle. However, the number of revolutions required to achieve an appropriate reliability varies between parameters. Whereas muscular effort in terms of iEMG demonstrated a high (initial) reliability, muscle activation characteristics require more revolutions to achieve ‘good’ or even ‘excellent’ reliability. Since RoA demonstrated the highest number of revolutions required to achieve a ‘good’ (k = 6) or even ‘excellent’ (k = 10) reliability, it can be deduced that six to ten revolutions allow for an adequate assessment of muscle activation characteristics in terms of onset, offset and RoA in inexperienced participants. Future studies need to investigate movement variability in elite handcyclists to assess whether fewer or more revolutions are required to quantify MAPs in experienced athletes (Bartlett et al. 2007).

2.4.2 Alterations of MAPs due to increasing workload

Muscular effort in terms of iEMG increased due to increasing workload which agrees with findings from previous studies focussing on arm-cranking exercise (Bressel et al. 2001) and recreational handcycling with an attach-unit (Bafghi et al. 2008). Due to the incremental test design, it is hard to distinguish whether the increase in muscular effort was exclusively due to increasing workload or additionally affected by neuromuscular fatigue. Since three of the twelve participants were exhausted within the 120 W step and locally perceived exertion was rather high (Quittmann et al. 2018b) an additional effect of fatigue (especially in DP) seems to be likely. In order to quantify the effect of fatigue without the aspect of an increased workload, future studies should examine muscular effort during prolonged continuous load handcycling. The increase in muscular effort might be explained by additional recruitment of (non-fatigued) motor-units (Merletti et al. 1990, Martinez-Valdes et al. 2016). The rather high increase in iEMG of DP might additionally be explained by alterations of shoulder kinematics presented in the previous study. At higher workloads, an increased shoulder-abduction could have caused a higher EMG amplitude (Phillips and Karduna 2017, Quittmann et al. 2018b).

Muscle activation characteristics of TD and FC could be presented, although difficulties in their measurement are described in previous research

(Litzenberger et al. 2016). Due to the participants' position in the handcycle, the electrodes of TD would have had contact to the backrest which is why undisturbed measurement was prevented (Litzenberger et al. 2016). For FC, a distinct onset or offset could not be detected due to insufficient amplitude fluctuations (Litzenberger et al. 2016).

Whereas muscle activation characteristics remained constant for PM and FC, several muscles (DA, DP, BB, TB, EC and RA) demonstrated a larger RoA due to an earlier onset that results in reduced recovery during crank cycle. The earlier onset could be a strategy to enlarge the period of force transmission which is necessary to remain a high cadence. However, there was no overall effect of workload for the offset indicating that the alterations were quite different between muscles. Indeed, there were tendencies for an earlier (TD and LD), later (DP and RA) and rather similar offset (PM, DA, BB, TB, FC and EC). DP was the only muscle that demonstrated a significantly later offset of activation at high intensity compared to handcycling propulsion at low intensity. Even though DP was mainly activated during the press-down and pull-down, DP showed an additional function by assisting the pull-up at a high intensity. This could be due to the fact that the minimum of tangential crank torque occurs during the following lift-up (Quittmann et al. 2018b). A prolonged DP activation might help to remain crank angular velocity during the pull-up and thus improve force transmission during the lift-up.

2.4.3 Limitations

Since this study investigated able-bodied participants, direct transferability to MAPs in elite handcyclists with a spinal cord injury is impeded. The choice to use able-bodied participants involves advantages in the standardisation of the handcycle and prerequisites of the participants and allows for new insights on the muscular coordination of able-bodied handcyclists that might be helpful for coaches in other upper-body dominant sports. In order to minimise the lack in transferability, the participants with high aerobic fitness (especially with respect to the upper extremities) and homogeneous performance were recruited. Previous research of an elite handcyclist demonstrated rather similar muscle activation characteristics with higher RoA in able-bodied participants that could be due to lack of experience (Litzenberger et al. 2016). The similarity in muscle activation characteristics could be due to the fact that the propulsion movement in handcycling has rather few degrees of freedom.

Since the back has contact with the back rest, and the hands are holding the crank grips, the movement possibilities are relatively constrained, suggesting that the movement and MAPs may exhibit lower degrees of functional variability than in less constrained upper-body dominant activities such as kayaking and swimming. In able-bodied participants RA was shown to support the push phase according to findings in kinematics (Quittmann et al. 2018b). However, in athletes with a spinal cord injury who are at most able to activate the upper parts of the trunk muscles and use even more recumbent backrest positions, it is likely that RA support is rather small.

The backrest position provided in this study is rather common for able-bodied participants in both biomechanical investigations and recreational exercise (Faupin et al. 2010). However, compared to very low backrest positions that are frequently used in elite handcyclists, the backrest position of this study was higher (less tilted). Indeed, muscle activation characteristics were shown to be influenced by handcycle settings (Litzenberger et al. 2015, 2016, Smith et al. 2008). Providing a similar distance between the shoulders and the crank axis, the use of a lower backrest caused a counter-clockwise shift in the onsets and offsets of approximately 20 to 30 degrees (Litzenberger et al. 2015). This might be explained by the fact that a lower backrest results in an increase of the relative height of the crank axis with respect to the shoulder axis that shifts the most extended position of the elbow from around 0° to around 325°. If the results of this study should be transferred to a lower backrest position, this shift needs to be taken into account.

Muscle activation characteristics of LD and RA demonstrated a high variability that is due to the low activation and oscillation with respect to MVIC. However, an appropriate assessment of muscle activation characteristics in terms of onset, offset and RoA requires a certain oscillation. In order to avoid false positives, values should be considered with respect to sport-specific MVICs. Since participants had contact to the backrest of the handcycle, LD measurements in handcycling are prone to artefacts caused by movement and sweat that might affect the detections of onsets and offsets.

Because of the unilateral assessment of muscular activity, this study fails to quantify synchrony between extremities. Findings of an elite handcyclist indicate that differences in muscle activation characteristics between extremities are rather small (approximately 10°) (Litzenberger et al. 2015, 2016). However, with regard to the missing experience in handcycling propulsion, larger differences between extremities are assumed for able-bodied participants.

2.4.4 Practical applications

Since DP faced the highest increase in muscular effort during the incremental test and demonstrated a shift in muscle function, DP could be prone to neuromuscular fatigue. To validate this assumption, muscular effort during a prolonged continuous load test should be examined. Additionally, DP is not supported by large muscle groups at the onset which could indicate high muscular load. Hence, coaches and athletes are encouraged to pay particular attention to this muscle and develop propulsion-specific strength exercises to improve the athletes' performance.

Due to the high variability and low amplitudes compared to MVICs, the function of LD in handcycling propulsion remains unclear. Our findings indicate that LD seems to support handcycling propulsion throughout the crank cycle with two (slightly) reinforced phases which is why it is assumed that LD has a rather stabilising function. Since LD activation was increased during the later steps of the incremental test, future studies should examine LD activation during all-out sprint exercises. In order to examine the function of other back muscles (e.g. M. teres major and M. trapezius, Pars transversus) that cannot be measured directly (because of the contact to the backrest), inverse dynamic modelling approaches might help to gain deeper insight into handcycling propulsion mechanics.

2.5 Conclusions

MAP parameters in handcycling are highly reliable and different between low and high intensities in able-bodied participants. Whereas muscular effort can even be examined in a single crank cycle, muscle activation characteristics require at least six to ten averaged revolutions. Muscular effort (iEMG) increased due to workload in every muscle demonstrating high effect sizes from $d = 1.02$ (BB) to $d = 2.21$ (DP). Muscle activation characteristics demonstrated a higher RoA in several muscles (DA, DP, BB, TB, EC and RA) that was due to an earlier onset. DP demonstrated a later offset and even assisted the pull-up at a high intensity. Muscle activation characteristics of PM and FC were not affected by workload.

For an appropriate interpretation of muscle activation characteristics, values should be expressed with respect to sport-specific MVICs. Since DP faced the larges alterations of muscular effort and muscle activation characteristics due to increasing workload and is not supported by large muscle groups at the onset, athletes and coaches might pay particular attention to this muscle in sport-specific strength and endurance training.

3 Biomechanics of all-out handcycling exercise

Biomechanics of all-out handcycling exercise: Kinetics, kinematics and muscular activity of a 15-s sprint test in able-bodied participants

Oliver J. Quittmann[1], Thomas Abel[1,2], Kirsten Albracht[3,4] & Heiko K. Strüder[1]

1 Institute of Movement and Neurosciences, German Sport University Cologne

2 European Research Group in Disability Sport (ERGiDS)

3 Institute of Biomechanics and Orthopaedics, German Sport University Cologne

4 Faculty of Medical Engineering and Technomathematics, University of Applied Sciences Aachen

Under Review in:

Sports Biomechanics (Impact factor 2018: 1.714)

Submitted: 24 March, 2019 Revised: 12 August, 2019

Abstract

Purpose: The aim of this study was to quantify the kinematics, kinetics and muscular activity of all-out handcycling exercise and examine their alterations during the course of a 15-s sprint test.

Methods: Twelve able-bodied competitive triathletes performed a 15-s all-out sprint test in a recumbent racing handcycle that was attached to an ergometer. During the sprint test, tangential crank kinetics, 3D joint kinematics and muscular activity of ten muscles of the upper extremity and trunk were examined using motion capturing and surface electromyography (sEMG). Parameters were compared between revolution one (R1), revolution two (R2), the average of revolution three to thirteen (R3) and the average of the remaining revolutions (R4).

Results: Shoulder-abduction and internal-rotation increased, whereas maximal retroversion decreased during the course of the sprint. Except for the wrist angles, angular velocity increased for every joint of the upper extremity. Several muscles demonstrated an increase in muscular effort, an earlier onset of muscular activation in crank cycle and an increased range of activation.

Conclusions: Since the most notable alterations during the course of a 15-s sprint test occurred in shoulder kinematics and the activation of the muscles associated with the push phase, there is need to pay particular attention to strength and conditioning.

3.1 Introduction

Handcycling is a Paralympic endurance sport that is performed by people with a spinal cord injury (SCI) or amputation of the lower extremities. The athletes make use of a three wheeled vehicle called handcycle that is propelled with synchronous cranks driven by the athletes' upper extremities. Due to the type of propulsion, handcycling can be used to improve the endurance capacity of able-bodied athletes who make use of their upper extremities (e. g. in swimming, rowing or triathlon) as well. To provide comparable and fair conditions in competition and to minimize the impact of impairment on sport performance, athletes are assigned to a certain sport class (Internaional Paralympic Commitee 2015). Classification into one of the five sport classes (from H1 with the most to H5 with the least impairment) highly depends on the remaining function of the limbs and the trunk. To improve evidence-based classification in handcycling, profound knowledge of the mechanisms underlying exercise and performance is necessary (Kouwijzer et al. 2018). Since the performance and ranking in competition is determined by the time to cover a certain distance, the athletes have to attain a high mean race velocity. Due to the dynamics of a handcycle race, the athletes need to temporarily increase their effort and race velocity at certain events of the race e. g. at the start, for passing manoeuvres or the final sprint (Abel et al. 2006). Among rather technical aspects (e. g. aerodynamics and rolling resistance), the race velocity is primarily caused by the mechanical power transmitted to the cranks that is caused by the biomechanical aspects of handcycling propulsion (Lindschulten 2008).

The mechanical power of handcycling propulsion is equal to the product of the tangential crank torque and crank angular velocity (or cadence). Since the hands remain fixed on the cranks during propulsion, the athletes have to change the displacement, velocity and acceleration of their limbs in order to apply a high torque (or force) on the cranks and maintain a high cadence. In other words, crank kinetics and kinematics are directly dependent on the athletes' joint kinematics. Joint kinematics, in turn, are directly dependent on the surrounding muscles generating force on the limbs that is based on the intensity and characteristics of their activation. However, high and repetitive muscle forces increase the load of muscle fibres, tendons and ligaments that might suffer from overuse injuries (Willick et al. 2013). Hence, the combined quantification of kinetics, kinematics and muscular activity allow for a more profound understanding of the biomechanical mechanisms underlying handcycling propulsion and estimating risks of overuse.

Previous studies that examined biomechanical aspects of handcycling vary in the use of investigation methods [kinematics, kinetics, surface electromyography (sEMG) and/or inverse dynamics], type of vehicle (racing handcycle vs. attach-unit), recruitment of participants (inexperienced able-bodied participants vs. handcycle athletes) and exercise intensity. Most of the previous studies examined biomechanical aspects of handcycling at a rather moderate intensity (Arnet et al. 2012a, Arnet et al. 2012b, Arnet et al. 2012c, 2013, Arnet et al. 2014, Faupin et al. 2010, Faupin et al. 2011, Kraaijenbrink et al. 2017, van Drongelen et al. 2011). At a similar power output (around 15 W), it was shown that glenohumeral contact forces were remarkably lower in attach-unit handcycling compared to manual wheelchair propulsion indicating that the former is mechanically less straining (Arnet et al. 2012a). Due to the very low intensity and the fact that the highest relative muscles forces were found in M. deltoideus and the muscles of the rotator cuff, it is suggested that high-intensity (or even all-out) handcycling causes high stress to the shoulder region and thus increases the risk of overuse injuries. In retrospective studies, the most frequently injured regions in Paralympic wheelchair athletes were found to be the shoulder, followed by the wrist and elbow (Athanasopoulos et al. 2009, Willick et al. 2013). To develop preventive exercises for sport-specific conditioning, a profound understanding of the sport-specific movement is needed.

A combined quantification of kinematics, kinetics and muscular activity during handcycling propulsion in a racing handcycle at moderate intensity was performed for one able-bodied participant (Faupin et al. 2010). Even though exercise intensity was rather low; power output could not be quantified in this study. Litzenberger et al. investigated the kinematics and muscular activity of one elite handcycle athlete at three concrete power outputs (130, 160 and 190 W) and demonstrated little alterations in joint kinematics due to higher workloads (Litzenberger et al. 2015, 2016). In a recent study, however, alterations of crank kinetics (e. g. higher torque during the pull phase) and joint kinematics (e. g. increased shoulder internal-rotation and abduction and reduced retroversion and elbow-flexion) could be observed with respect to crank position during the course of an incremental step test in able-bodied participants (Quittmann et al. 2018b). Additionally, muscular activation in handcycling was shown to be affected by exercise intensity in terms of higher muscular effort and altered muscular activation characteristics (Quittmann et al. 2019). Even though kinetics, kinematics and muscular activity during an incremental test were quantified at an almost exhausted state, maximal power output (120 to 160 W) was not even close to all-out sprint conditions (546 ± 70 W) (Quittmann et al. 2018a, Quittmann et al. 2018b).

The kinematics of all-out handcycling exercise have been investigated by two studies. The first investigation in this field examined the influence of gear ratio on the joint angles' range of motion (RoM) and angular acceleration during an 8-s all-out sprint in a racing handcycle which was mounted on a computer-linked ergo-cycle (Elite, Axiom, Italy) in able-bodied participants (n = 8) (Faupin et al. 2006). For increasing gear ratios, a significant increase in the RoM of the trunk and shoulder-abduction was found. It was stated that the RoM of the wrist during the sprint are slightly above the tolerable limits to prevent overuse injuries (e. g. carpal tunnel syndrome). The second study very recently quantified joint kinematics of competitive (n = 7) and recreational (n = 6) handcyclists at training, competition and sprint intensity (Stone et al. 2019c). Whereas competitive handcyclists demonstrated higher shoulder retroversion and trunk-flexion at training and competition intensities, no differences were observed during sprinting. However, the authors argued that the combination of subtle differences in handbike configuration influenced the observed differences in joint kinematics and that “[f]uture studies could employ electromyography and cycle kinetics to explore handcycling biomechanics further” (Stone et al. 2019c).

To the best of our knowledge, the combined quantification of kinetics, kinematics and muscle activation patterns (MAPs) of all-out handcycling have not yet been investigated. Additionally, alterations within an all-out sprint condition (e. g. 15 seconds) could be interesting in terms of short-duration fatigue and highlight regions with a risk of overuse (injuries) and a need for sport-specific conditioning. As previously stated, the measurement of elite handcyclists is challenging due to time-consuming tests and highly individual handcycle settings and perquisites (Quittmann et al. 2019). Additionally, there is no practical option to measure crank kinetics in the athlete’s individual handcycle. Hence, the aim of this study was to quantify the biomechanics of all-out handcycling exercise in terms of kinematics, kinetics and muscular activity and examine alterations during the course of a 15-s sprint test in able-bodied participants. It is hypothesised that biomechanical parameters are remarkably high and altered during the course of a 15-s sprint test due to short-term fatigue.

3.2 Methods

3.2.1 Participants

A total of 12 able-bodied male competitive triathletes (26.0 ± 4.4 yrs., 1.83 ± 0.06 m, 74.3 ± 3.6 kg) participated in the study. In order to improve the transferability of results from able-bodied participants to handcycle athletes, participants should have high aerobic fitness (especially with respect to the upper extremities). All participants stated their right arm was dominant. Medical peculiarities and acute complaints of the upper extremity were exclusion criteria. The study was approved by the ethics committee of the German Sport University Cologne (No. 52/2016) and complied with the ethical standards of the 1975 Helsinki Declaration modified in 1983. Participants gave their written informed consent before participating in the study.

3.2.2 Experimental protocol

Participants were instructed to arrive in a rested, carbohydrate-loaded and fully hydrated state, refrain from consuming alcohol or caffeine and performing heavy training loads the day before each test (Jeacocke and Burke 2010, Zeller et al. 2015). One week prior to the investigation, participants performed an initial familiarisation trial. The familiarisation trial consisted of five incremental workload steps with decreasing stage durations and a 15-s all-out sprint test (Quittmann et al. 2018a, Quittmann et al. 2018b). The 15-s all-out sprint test was performed with maximal effort in isokinetic-mode against a crank-rate-dependent braking force. Post-exercise lactate kinetics were used to determine maximal lactate accumulation rate ($\dot{V}La_{max}$). In the week of biomechanical measurements, another 15-s all-out sprint test was performed approximately five minutes after the participants had performed an incremental step test until voluntary exhaustion (Quittmann et al. 2018b, Zeller et al. 2015). This second sprint test was the original investigation trial this study is based on.

The tests were performed in a racing handcycle (Shark S, Sopur, Sunrise Medical, Malsch, Germany) that was mounted on a calibrated and validated ergometer (Cyclus 2, TE 2%, 8 Hz, RBM electronic-automation GmbH, Leipzig, Germany) (Reiser et al. 2000). According to previous literature, the type of propulsion can be characterised as a closed-chain arm-power recumbent handcycle (Kouwijzer et al. 2018). To ensure comparable conditions between participants and other studies, the backrest of the handcycle was tilted so that (1) the elbow was slightly flexed (5 to 10° while bringing the shoulder blades together) in the foremost position (almost extended arm) and (2) the axis of the shoulder joint was approximately at the same height as the crank axis (Faupin et al. 2010, Quittmann et al. 2018b). These settings resulted in a backrest tilt between 46.4° and 53.4° which is comparable to previous research on sprint exercise in handcycling (Faupin et al. 2006). The crank length and width were kept fixed at 17.2 and 38.5 cm, respectively. The gear ratio was set to 52/12. For the 15-s all-out sprint test, the initial torque and cadence defining the test start were set at 20 Nm and 20 min^{-1}, respectively (Quittmann et al. 2018a, Zeller et al. 2015). Cadence was limited to 140 min^{-1}, which was due to the isokinetic mode of the ergometer (Faupin et al. 2006, Quittmann et al. 2018a). The start position of the cranks was determined at foremost position. Biomechanical measurements of crank kinetics, kinematics and muscular activity were performed throughout the 15-s all-out sprint test.

3.2.3 Data recording

Crank kinetics were estimated using a power meter [1000 Hz, Schoberer Rad Messtechnik (SRM) GmbH, Jülich, Germany] installed in the crank. The device was equipped with eight strain gauges, which transferred the tangential deformation of the crank (due to the crank torque) into a voltage signal. To transfer the voltage signals into torque signals, the system was calibrated using free weights from 5 to 40 kg with the crank fixed at foremost position (R^2 = 99.8%). Following convention, the crank angle was defined as 0° or 360° (foremost position), 90° (crank arm pointing downward), 180° (crank arm pointing to the participant) and 270° (crank arm pointing upward) (Faupin et al. 2010, Litzenberger et al. 2016, Quittmann et al. 2018b, Quittmann et al. 2019). Crank kinetics were filtered using a fourth-order low-pass Butterworth filter with a cut-off frequency of 10 Hz.

Seven high-speed infrared cameras (100 Hz, MX-F40 and MX-3+, Vicon Nexus 2.3, Vicon Motion Systems Ltd., Oxford, UK) were placed around the handcycle. Spherical retro-reflective markers (in all 44) were placed on the crank, ergometer and anatomical landmarks according to the Upper Limb Model (Vicon Motion Systems) (Quittmann et al. 2018b). Using the Upper Limb Model, angles and angular velocities of shoulder-flexion (SF), shoulder-abduction (SA), shoulder internal-rotation (SR), elbow-flexion (EF), palmar-flexion (PF) and radial-duction (RD) of the dominant (right) arm were considered (Quittmann et al. 2018b, Vicon Motion Systems 2007). Trunk-flexion angle (TF) was determined in accordance with ISB recommendations as the angle between the horizontal plane and the line connecting the midpoints between the 7th cervical vertebra (C7) and jugular notch (CLAV) and the 10th thoracic vertebra (T10) and xiphoid process (STRN) (Wu et al. 2005, Quittmann et al. 2018b). Kinematic measures were resampled to 1000 Hz using pchip interpolation method and filtered using a fourth-order low-pass Butterworth filter with a cut-off frequency of 10 Hz. Crank angle and angular velocity [expressed as cadence (Cad)] was estimated using the crank markers on the axis and the crank arm (Quittmann et al. 2018b). Power with respect to crank angle was calculated as the product of angular velocity and the torque of the SRM crank (1000 Hz). Additionally, the Cyclus 2 ergometer (8 Hz) estimated power output based on the braking force and cadence.

Muscular activity of ten muscles [M. trapezius, Pars descendens (TD); M. pectoralis major, Pars sternalis (PM); M. deltoideus, Pars clavicularis (DA); M. deltoideus, Pars spinalis (DP); M. biceps brachii, Caput breve (BB); M. triceps brachii, Caput laterale (TB); M. flexor carpi radialis (FC); M. extensor carpi ulnaris (EC); M. latissimus dorsi (LD) and M. rectus abdominis (RA)] was measured unilaterally on the dominant (right) side of the participants. Since the muscles of the forearm are tightly gathered and thus increase the risk of EMG crosstalk, FC and EC were identified to represent forearm flexors and extensors, respectively. Muscular activity was measured using a wireless sEMG system (DTSEMG Sensor®, 1000 Hz, Noraxon Scottsdale, Arizona, USA) and processed as recently published (Quittmann et al. 2019).

3.2.4 Data processing

All biomechanical measures were resampled to 360 values per cycle for every revolution during the 15-s all-out sprint test. Previous research has frequently analysed upper limb kinematics over ten consecutive cycles (Stone et al. 2019c, Verellen et al. 2012). For muscular activity, recent research demonstrated that 10 consecutive cycles are required to attain an 'excellent' reliability (ICC ≥ 0.90) in muscular activation patterns (MAPs) (Quittmann et al. 2019). Hence, ten consecutive cycles seem to be a suitable window for analysing handcycling biomechanics. Since the first two revolutions are required to overcome the initial resistance and set the cranks in motion, revolutions were compared between revolution one (R1), revolution two (R2), the average of revolutions three to thirteen (R3) and the average of the remaining revolutions (R4). Depending on the crank angular velocity of the participants, the number of remaining revolutions ranged from 10 to 14. The investigated parameters for kinematics and kinetics included the maximum value (Max), minimum value (Min) and range over crank cycle as well as the (absolute and relative) work components within the sectors and phases. The range of joint angles was expressed as range of motion (RoM). For muscular activity, iEMG, onset, offset and RoA were analysed.

3.2.5 Statistics

Alterations in kinetics, kinematics and muscular activity during the sprint test were examined using a one-way analysis of variance (ANOVA) with repeated measures. The assumption of sphericity was tested using Mauchly's test. For parameters with a significant violation of sphericity, the degrees of freedom were adjusted according to Greenhouse-Geisser. As an effect size, partial eta squared (η_P^2) was calculated. Post-hoc comparisons between R1, R2, R3 and R4 were adjusted according to Bonferroni's correction. The level of significance was set at $\alpha = 0.05$. In order to gain a deeper understanding of the complex interplay of and alterations in muscular activation and joint kinematics, muscular activity was observed with respect to the corresponding joint angle as described in previous research (Leedham and Dowling 1995).

3.3 Results

Figure 12 illustrates the torque, cadence and power profile of one individual participant during the course of the 15-s all-out sprint test. Initially, the torque applied onto the cranks increased and reached its maximum after 0.88 s. Afterwards, crank torque declined fast (until maximal cadence was reached) and declined steadily towards the end of the sprint. Initially, cadence increased rapidly up to around three seconds. Afterwards, a slight but steady increase in cadence up to the end of the sprint was observed.

Power, as a product of torque and cadence, reached the maximum at around three seconds and remained rather constant towards the end of the sprint. However, a high oscillation in power was found within the crank cycle.

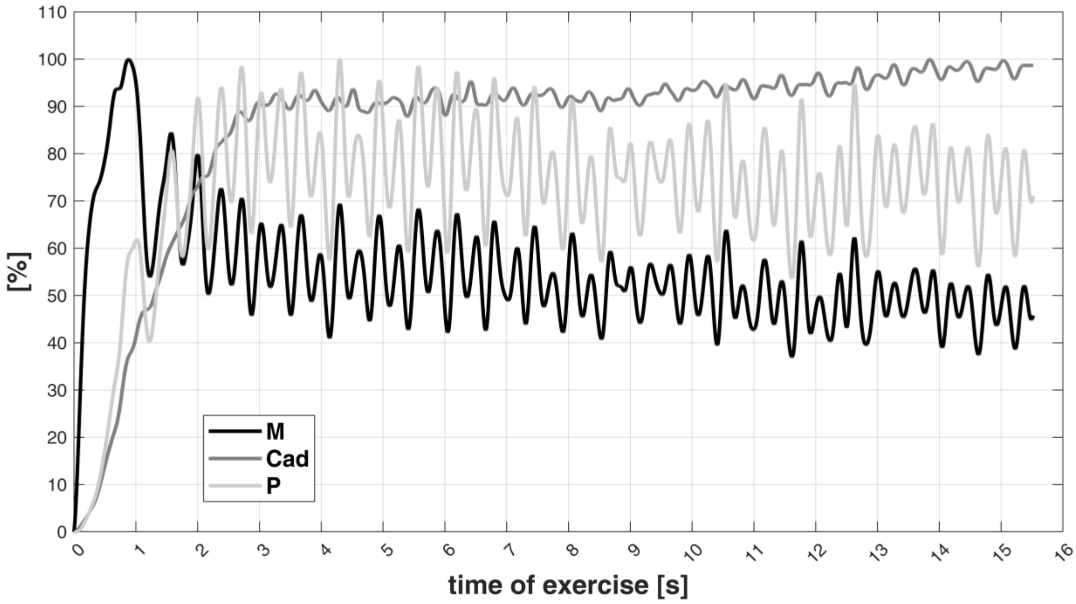

Fig. 12 Torque, cadence and power variation of one exemplary participant (P01) during the course of the 15-s all-out sprint test

Values are expressed as a percentage of the maximum value during the whole trial. Cad = cadence; M = torque; P = power.

3.3.1 Torque, cadence and power

Figure 13 illustrates the mean torque, cadence and power profiles with respect to crank angle during the course of the 15-s all-out sprint test. The torque profile demonstrated two distinct maxima in the pull (at around 90°) and push phase (at around 280°) with mean peak values at R1 of around 113 and 90 Nm, respectively. According to the crank length of 17.2 cm, the corresponding force values are 657 and 523 N, respectively. At R4, mean peak torque (69 and 67 N) and force (400 and 390 N) were considerably lower during the pull and push phase. Whereas the difference between these maxima was relatively high at R1 (around 23 Nm), the difference diminished during the course of the sprint and became negligible (around 2 Nm) at R4. Maximal ($\eta_P^2 = 0.881$, $p < 0.001$), minimal ($\eta_P^2 = 0.745$, $p < 0.001$) and the range of torque ($\eta_P^2 = 0.837$, $p < 0.001$) significantly decreased during the course of the sprint test (Tab. 10). Except for the difference between R1 and R2 in minimal torque, post-hoc comparisons demonstrated significant differences between all revolutions in all parameters of torque.

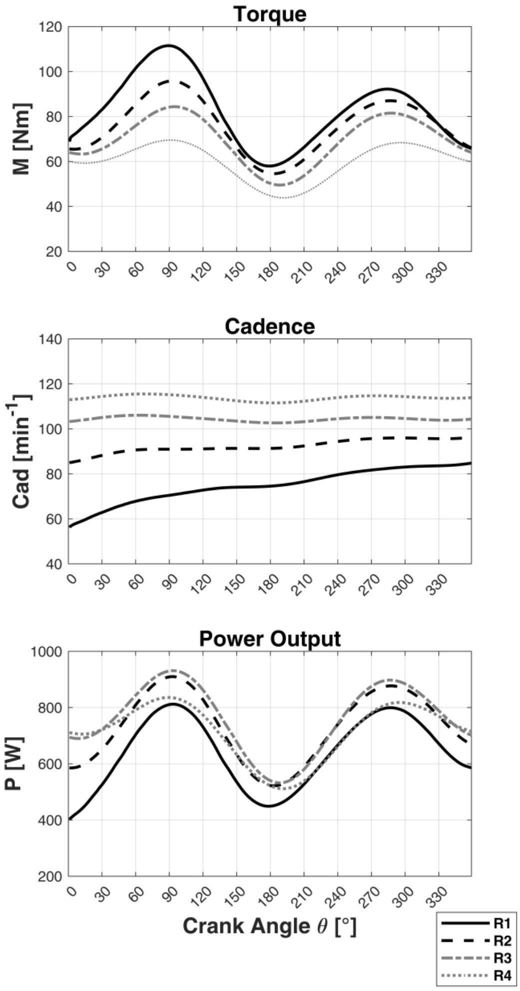

Fig. 13 Torque, cadence and power with respect to crank angle during the course of the 15-s all-out sprint test

Values are expressed as the mean curves across all participants. Cad = cadence; M = torque; P = power; R1 = first revolution of the sprint; R2 = second revolution of the sprint; R3 = mean over the third to thirteenth revolution; R4 = mean over the fourteenth to last revolution.

Tab. 10 Alterations of torque, cadence and power with respect to crank angle during the course of the 15-s all-out sprint test

		R1	R2	R3	R4	η_P^2	p
M	Max [Nm]	113 ± 13^{b,c,d}	97 ± 7^{a,c,d}	87 ± 5^{a,b,d}	72 ± 5^{a,b,c}	**0.881*** **	< 0.001^{g}
	Min [Nm]	56 ± 7^{c,d}	54 ± 5^{c,d}	49 ± 4^{a,b,d}	43 ± 3^{a,b,c}	**0.745*** **	< 0.001
	Range [Nm]	58 ± 9^{b,c,d}	44 ± 5^{a,c,d}	38 ± 4^{a,b,d}	29 ± 6^{a,b,c}	**0.837*** **	< 0.001^{g}
Cad	Max [min^{-1}]	85 ± 8^{b,c,d}	97 ± 6^{a,c,d}	106 ± 6^{a,b,d}	116 ± 8^{a,b,c}	**0.887*** **	< 0.001^{g}
	Min [min^{-1}]	56 ± 25^{b,c,d}	85 ± 8^{a,c,d}	102 ± 6^{a,b,d}	111 ± 8^{a,b,c}	**0.789*** **	< 0.001^{g}
	Range [min^{-1}]	29 ± 18^{b,c,d}	12 ± 5^{a,c,d}	4 ± 1^{a,b}	4 ± 2^{a,b}	**0.674*** **	< 0.001^{g}
P	Max [W]	845 ± 125^{b,c}	938 ± 86^{a,d}	968 ± 85^{a,d}	871 ± 66^{b,c}	**0.452** **	0.004^{g}
	Min [W]	366 ± 181	505 ± 57	529 ± 60	508 ± 55	**0.393* **	0.017^{g}
	Range [W]	478 ± 92^{d}	433 ± 58	439 ± 47^{d}	364 ± 60^{a,c}	**0.417** **	0.004^{g}

Values are expressed as mean value ($\bar{x}$) and standard deviation (SD). ^{a} = significant difference in post-hoc comparison to R1 ($p \leq 0.05$); b = significant difference in post-hoc comparison to R2 ($p \leq 0.05$); c = significant difference in post-hoc comparison to R3 ($p \leq 0.05$); d = significant difference in post-hoc comparison to R4 ($p \leq 0.05$); ^{g} = degrees of freedom were adjusted based on Greenhouse-Geisser due to missing sphericity assumption. Post-hoc comparisons were adjusted using Bonferroni's correction. Significant time effects * $p \leq 0.05$; ** $p \leq 0.01$; *** $p \leq 0.001$. Cad = cadence; M = torque; Max = maximal value; Min = minimal value; p = probability of committing a type 1 error; P = power; R1 = first revolution of the sprint; R2 = second revolution of the sprint; R3 = mean over the third to thirteenth revolution; R4 = mean over the fourteenth to last revolution; η_P^2 = partial eta squared.

Cadence increased during the course of the 15-s all-out sprint test (Fig. 12). Within R1, cadence increased on average from almost 60 to more than 80 min^{-1}. At R4, the mean cadence was slightly higher than 110 min^{-1}. Maximal ($\eta_P^2 = 0.887$, $p < 0.001$) and minimal ($\eta_P^2 = 0.789$, $p < 0.001$) values of cadence significantly increased, whereas the range ($\eta_P^2 = 0.674$, $p < 0.001$) decreased during the course of the sprint test (Tab. 10). Except for the difference in the range of cadence between R3 and R4, post-hoc comparisons demonstrated significant differences between all revolutions in all parameters of cadence.

According to the profiles of torque and cadence, the power profile demonstrated two distinct maxima as well (Fig. 13). Maximal power ($\eta_P^2 = 0.452$, $p = 0.004$), minimal power ($\eta_P^2 = 0.393$, $p = 0.017$) and the range ($\eta_P^2 = 0.417$, $p = 0.004$) were significantly affected by revolution (Tab 10). Maximal power increased from R1 to R2 and decreased from R3 to R4. For minimal power, no post-hoc comparison demonstrated significant differences. The range of power was lower at R4 compared to R1 and R3. Since power was measured using the calibrated SRM crank (combined with crank kinematics) and the Cyclus 2 ergometer, there were different values for maximal power output ($P_{max,AO15}$). $P_{max,AO15}$ of the SRM crank was almost twice as high (1039 ± 82 W) compared to the Cyclus 2 (578 ± 78 W).

3.3.2 Joint angles

Figure 14 illustrates the joint angles with respect to crank angle during the course of the sprint test. Maximal retroversion, SF, SA and EF occurred at crank angles of around 140, 290, 220, and 180°, respectively. SR demonstrated two distinct maxima between 70° to 100° and at around 260°. Minimal EF angle was about 50°. Maximal dorsal-flexion and ulnar-duction were attained at around 220°. TF angle peaked at around 140°.

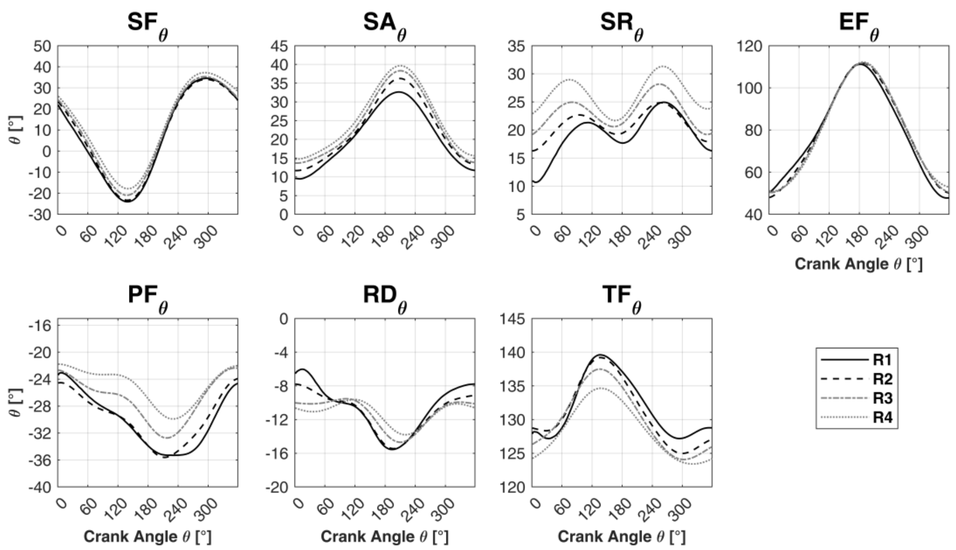

Fig. 14 Joint angles with respect to crank angle during the course of the 15-s all-out sprint test

Values are expressed as the mean curves across all participants. EF_θ = elbow-flexion angle; PF_θ = palmar-flexion angle; R1 = first revolution of the sprint; R2 = second revolution of the sprint; R3 = mean over the third to thirteenth revolution; R4 = mean over the fourteenth to last revolution; RD_θ = radial-duction angle; SA_θ = shoulder-abduction angle; SF_θ = shoulder-flexion angle; SR_θ = shoulder internal-rotation angle; TF_θ = trunk-flexion angle

The only RoM that was significantly altered during the course of the sprint test was found for SR (η_P^2 = 0.219, p = 0.040) (Tab. 11). For SF, the maximum (η_P^2 = 0.333, p = 0.004) and minimum (η_P^2 = 0.721, p < 0.001) increased, indicating a higher shoulder-flexion and reduced retroversion, respectively. For SA and SR, the maximum (η_P^2 = 0.638, p < 0.001; η_P^2 = 0.474, p < 0.001) and minimum (η_P^2 = 0.669, p < 0.001; η_P^2 = 0.563, p < 0.001) demonstrated a significant increase. Both, the maximum and minimum of EF (η_P^2 = 0.086, p = 365; η_P^2 = 0.230, p = 0.079) and RD (η_P^2 = 0.110, p = 0.273; η_P^2 = 0.021, p = 0.663) were not significantly affected by revolution. The minimum of PF demonstrated a significant increase (η_P^2 = 0.440, p = 0.005) indicating reduced dorsal-flexion. Whereas the minimal angle of TF remained rather constant (η_P^2 = 0.061, p = 0.449), an increase in the maximum was found (η_P^2 = 0.580, p < 0.001).

Tab. 11 Alterations of joint angles during the course of the 15-s all-out sprint test

		R1	R2	R3	R4	η_P^2	p
SF_θ	Max [°]	35 ± 5	34 ± 4^{d}	35 ± 3	37 ± 3^{b}	**0.333****	0.004
	Min [°]	-24 ± 6^{c,d}	-24 ± 6^{c,d}	-21 ± 5^{a,b,d}	-18 ± 5^{a,b,c}	**0.721*****	< 0.001^{g}
	RoM [°]	59 ± 9	58 ± 7	57 ± 7	56 ± 6	0.252	0.051^{g}
SA_θ	Max [°]	33 ± 8^{c,d}	37 ± 9^{c,d}	39 ± 9^{a,b}	40 ± 10^{a,b}	**0.638*****	< 0.001^{g}
	Min [°]	9 ± 4^{b,c,d}	11 ± 4^{a,d}	13 ± 4^{a}	14 ± 4^{a,b}	**0.669*****	< 0.001^{g}
	RoM [°]	25 ± 6	25 ± 7	26 ± 7	26 ± 7	0.059	0.487^{g}
SR_θ	Max [°]	30 ± 8	29 ± 8^{c,d}	32 ± 10^{b}	35 ± 10^{b}	**0.474*****	< 0.001
	Min [°]	8 ± 7^{c,d}	13 ± 9^{c,d}	15 ± 8^{a,b}	17 ± 8^{a,b}	**0.563*****	< 0.001^{g}
	RoM [°]	21 ± 8	16 ± 6	18 ± 7	18 ± 7	**0.219***	0.040
EF_θ	Max [°]	112 ± 5	112 ± 5	112 ± 6	113 ± 7	0.086	0.365^{g}
	Min [°]	46 ± 10	47 ± 9	49 ± 10	49 ± 10	0.230	0.079^{g}
	RoM [°]	66 ± 7	65 ± 6	64 ± 7	63 ± 8	0.102	0.300^{g}
PF_θ	Max [°]	-21 ± 5	-22 ± 5	-20 ± 6	-19 ± 7	0.147	0.193^{g}
	Min [°]	-39 ± 10^{c,d}	-38 ± 9	-34 ± 7^{a}	-32 ± 7^{a}	**0.440****	0.005^{g}
	RoM [°]	18 ± 6	16 ± 8	14 ± 7	13 ± 7	0.196	0.114^{g}
RD_θ	Max [°]	-5 ± 7	-6 ± 6	-6 ± 5	-7 ± 6	0.110	0.273^{g}
	Min [°]	-17 ± 7	-17 ± 7	-16 ± 6	-16 ± 6	0.021	0.663^{g}
	RoM [°]	12 ± 6	11 ± 5	10 ± 4	9 ± 4	0.171	0.155^{g}
TF_θ	Max [°]	141 ± 7^{d}	140 ± 8^{d}	139 ± 8^{d}	136 ± 8^{a,b,c}	**0.580*****	< 0.001
	Min [°]	123 ± 6	123 ± 7	122 ± 7	121 ± 7	0.061	0.449^{g}
	RoM [°]	18 ± 5	18 ± 6	17 ± 7	15 ± 8	0.130	0.224^{g}

Values are expressed as mean value ($\bar{x}$) and standard deviation (SD). [a] = significant difference in post-hoc comparison to R1 ($p \leq 0.05$); [b] = significant difference in post-hoc comparison to R2 ($p \leq 0.05$); [c] = significant difference in post-hoc comparison to R3 ($p \leq 0.05$); [d] = significant difference in post-hoc comparison to R4 ($p \leq 0.05$); [g] = degrees of freedom were adjusted based on Greenhouse-Geisser due to missing sphericity assumption. Post-hoc comparisons were adjusted using Bonferroni's correction. Significant time effects * $p \leq 0.05$; ** $p \leq 0.01$; *** $p \leq 0.001$. EF_θ = elbow-flexion angle; Max = maximal value; Min = minimal value; p = probability of committing a type 1 error; PF_θ = palmar-flexion angle; R1 = first revolution of the sprint; R2 = second revolution of the sprint; R3 = mean over the third to thirteenth revolution; R4 = mean over the fourteenth to last revolution; RD_θ = radial-duction angle; RoM = range of motion; SA_θ = shoulder-abduction angle; SF_θ = shoulder-flexion angle; SR_θ = shoulder internal-rotation angle; TF_θ = trunk-flexion angle; η_p^2 = partial eta squared.

3.3.3 Joint angular velocity

For SF, joint angular velocity ranged between around 400 (shoulder-flexion velocity) and -300° s^{-1} (retroversion velocity) at crank angles of around 210 and 70°, respectively (Fig. 15). The transition from retroversion to shoulder-flexion occurred at a crank angle of about 130°. SA demonstrated a maximum of around 150 and a minimum of approximately 180° s^{-1}. The transition from shoulder-abduction to -adduction occurred at about 210°. SR demonstrated two distinct maxima and minima with a total range between around ± 90° s^{-1}. The transitions from shoulder internal-rotation to external-rotation occurred at a crank angle of around 0, 90, 170 and 260°. Elbow-flexion velocity ranged between almost ± 400° s^{-1} with a maximum and minimum at a crank angle of around 110 and 260°, respectively. The transition from elbow-flexion to extension occurred at 180°. The angular velocity of the wrist ranged between -60 to almost 80° s^{-1} for PF and ± 40° s^{-1} for RD, respectively. A distinct transition from ulnar to radial-duction occurred at around 200°, whereas the transition from dorsal to palmar flexion occurred at around 220°. During the pull phase, the trunk demonstrated a flexion, whereas an extension movement was performed during the push phase. The range of angular velocity was between around ± 80° s^{-1}. The transition from trunk-flexion to extension occurred at around 140°. An illustration of the joint angular velocity profiles with respect to crank cycle is provided as supplementary material.

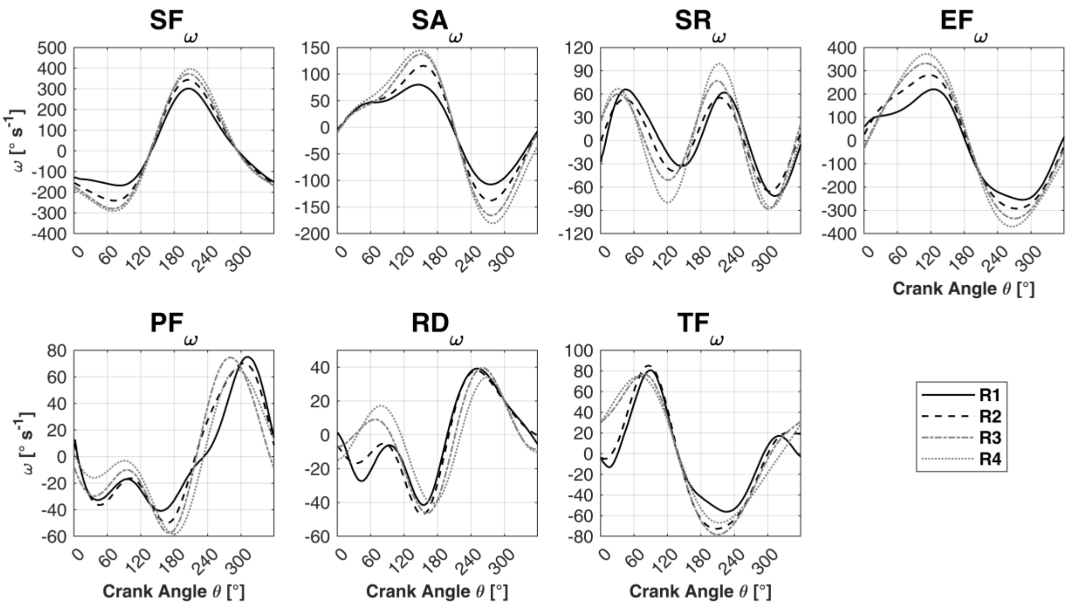

Fig. 15 Joint angular velocities with respect to crank angle during the course of the 15-s all-out sprint test

Values are expressed as the mean curves across all participants. EF_{ω} = elbow-flexion angular velocity; PF_{ω} = palmar-flexion angular velocity; R1 = first revolution of the sprint; R2 = second revolution of the sprint; R3 = mean over the third to thirteenth revolution; R4 = mean over the fourteenth to last revolution; RD_{ω} = radial-duction angular velocity; SA_{ω} = shoulder-abduction angular velocity; SF_{ω} = shoulder-flexion angular velocity; SR_{ω} = shoulder internal-rotation angular velocity; TF_{ω} = trunk-flexion angular velocity.

For SF, maximal ($\eta_P^2 = 0.700$, $p < 0.001$), minimal ($\eta_P^2 = 0.776$, $p < 0.001$) and the range of angular velocity ($\eta_P^2 = 0.766$, $p < 0.001$) were reinforced during the course of the sprint indicating a faster flexion and retroversion velocity (Tab. 12). The same accounts for the maximum ($\eta_P^2 = 0.662$, $p < 0.001$; $\eta_P^2 = 0.392$, $p = 0.001$), minimum ($\eta_P^2 = 0.677$, $p < 0.001$; $\eta_P^2 = 0.246$, $p = 0.024$) and range ($\eta_P^2 = 0.703$, $p < 0.001$; $\eta_P^2 = 0.373$, $p = 0.001$) of SA and SR, respectively. For SF, SA and SR there was no significant difference between R3 and R4 in the maximum, minimum or range. However, maximum ($\eta_P^2 = 0.824$, $p < 0.001$), minimum ($\eta_P^2 = 0.679$, $p < 0.001$) and range ($\eta_P^2 = 0.799$, $p < 0.001$) of EF were significantly affected by revolution and demonstrated significant post-hoc differences between R3 and R4. The angular velocities of the wrist (PF and RD) were not significantly altered during the course of the sprint test.

For TF, a significant increase in maximal extension velocity (η_P^2 = 0.334, p = 0.021) was observed, whereas maximal flexion velocity (η_P^2 = 0.045, p = 0.524) and the range (η_P^2 = 0.132, p = 0.222) were not significantly different. Between R3 and R4 there was no difference in TF extension velocity.

Tab. 12 Alterations of joint angular velocity during the course of the 15-s all-out sprint test

		R1	R2	R3	R4	η_P^2	p
SF_ω	Max [° s^{-1}]	305 ± 61^{b,c,d}	350 ± 56^{a,c,d}	380 ± 65^{a,b}	405 ± 64^{a,b}	**0.700*** **	< 0.001^g
	Min [° s^{-1}]	-183 ± 46^{b,c,d}	-245 ± 48^{a,c,d}	-284 ± 50^{a,b}	-296 ± 55^{a,b}	**0.776*** **	< 0.001^g
	Range [° s^{-1}]	489 ± 102^{b,c,d}	595 ± 100^{a,c,d}	664 ± 108^{a,b}	701 ± 111^{a,b}	**0.766*** **	< 0.001^g
SA_ω	Max [° s^{-1}]	104 ± 34^{b,c,d}	126 ± 46^{a,c,d}	146 ± 44^{a,b}	154 ± 49^{a,b}	**0.662*** **	< 0.001^g
	Min [° s^{-1}]	-117 ± 34^{b,c,d}	-148 ± 41^{a,c,d}	-173 ± 45^{a,b}	-189 ± 53^{a,b}	**0.677*** **	< 0.001^g
	Range [° s^{-1}]	221 ± 65^{b,c,d}	274 ± 82^{a,c,d}	319 ± 84^{a,b}	343 ± 97^{a,b}	**0.703*** **	< 0.001^g
SR_ω	Max [° s^{-1}]	111 ± 33^{d}	111 ± 41^{d}	137 ± 53	150 ± 50^{a,b}	**0.392*** **	0.001
	Min [° s^{-1}]	-116 ± 39	-103 ± 32^{d}	-123 ± 41	-138 ± 38^{b}	**0.246***	0.024
	Range [° s^{-1}]	227 ± 69	213 ± 68^{c,d}	260 ± 83^{b}	288 ± 77^{b}	**0.373*** **	0.001
EF_ω	Max [° s^{-1}]	233 ± 50^{b,c,d}	298 ± 43^{a,c,d}	347 ± 45^{a,b,d}	387 ± 55^{a,b,c}	**0.824*** **	< 0.001^g
	Min [° s^{-1}]	-267 ± 39^{b,c,d}	-308 ± 40^{a,d}	-342 ± 63^{a,d}	-378 ± 76^{a,b,c}	**0.679*** **	< 0.001^g
	Range [° s^{-1}]	500 ± 70^{b,c,d}	606 ± 64^{a,c,d}	689 ± 92^{a,b,d}	766 ± 113^{a,b,c}	**0.799*** **	< 0.001^g
PF_ω	Max [° s^{-1}]	101 ± 52	104 ± 61	97 ± 58	96 ± 55	0.014	0.781^g
	Min [° s^{-1}]	-82 ± 27	-77 ± 30	-82 ± 26	-89 ± 46	0.030	0.644^g
	Range [° s^{-1}]	183 ± 75	182 ± 86	179 ± 79	185 ± 95	0.002	0.931^g
RD_ω	Max [° s^{-1}]	58 ± 36	60 ± 32	66 ± 27	71 ± 27	0.173	0.135^g
	Min [° s^{-1}]	-58 ± 17	-64 ± 28	-63 ± 14	-63 ± 20	0.032	0.666^g
	Range [° s^{-1}]	116 ± 46	124 ± 52	129 ± 37	134 ± 44	0.085	0.398
TF_ω	Max [° s^{-1}]	90 ± 27	100 ± 27	97 ± 37	101 ± 46	0.045	0.524^g
	Min [° s^{-1}]	-83 ± 31^{b,c}	-97 ± 32^{a}	-105 ± 42^{a,d}	-92 ± 47^{d}	**0.334***	0.021^g
	Range [° s^{-1}]	173 ± 52^{b}	197 ± 53^{a}	202 ± 76	193 ± 91	0.132	0.222^g

Values are expressed as mean value (x̄) and standard deviation (SD). ^{a} = significant difference in post-hoc comparison to R1 ($p \leq 0.05$); ^{b} = significant difference in post-hoc comparison to R2 ($p \leq 0.05$); ^{c} = significant difference in post-hoc comparison to R3 ($p \leq 0.05$); ^{d} = significant difference in post-hoc comparison to R4 ($p \leq 0.05$); ^{g} = degrees of freedom were adjusted based on Greenhouse-Geisser due to missing sphericity assumption. Post-hoc comparisons were adjusted using Bonferroni's correction. Significant time effects * $p \leq 0.05$; ** $p \leq 0.01$; *** $p \leq 0.001$. EF_ω = elbow-flexion angular velocity; Max = maximal value; Min = minimal value; p = probability of committing a type 1 error; PF_ω = palmar-flexion angular velocity; R1 = first revolution of the sprint; R2 = second revolution of the sprint; R3 = mean over the third to thirteenth revolution; R4 = mean over the fourteenth to last revolution; RD_ω = radial-duction angular velocity; SA_ω = shoulder-abduction angular velocity; SF_ω = shoulder-flexion angular velocity; SR_ω = shoulder internal-rotation angular velocity; TF_ω = trunk-flexion angular velocity; η_P2 = partial eta squared.

3.3.4 Muscular activity

Figure 16 illustrates the mean muscular activity with respect to crank angle during the course of the sprint test. TD demonstrated the highest mean activation with maximal values of more than 100% at a crank angle of about 70 degrees and a minimum between around 20% and 40% at 260°. The onset and offset of TD occurred at around 330° and 195°, respectively (Tab. 13). PM had a minimum of less than 20% at a crank angle of 40° and a maximum of 80% at 210°. The onset and offset of PM occurred at around 120° and 330°, respectively. The antagonistic shoulder muscles DA and DP attained opposed profiles. Whereas DA had a maximum of around 80% at 180° and a minimum between 5 to 20% around the foremost position, DP demonstrated a maximum of around 70% at 30° and 10% at 210°, respectively. The onset and offset of DA occurred at around 70° and 280°, while they occurred at around 290° and 130° for DP, respectively. The co-activation period of DA and DP was around 60°. The same was found for BB and TB. BB had a maximum of more than 80% at 70° and a minimum of around 15% at 240°. The onset and offset of BB occurred at around 330° and 180°, respectively. TB showed a maximum of slightly below 80% at 230° and a minimum of around 30% at 30°. The onset and offset of TB occurred at around 130° and 320°, respectively. The co-activation period of BB and TB was around 50°. FC and EC attained similar muscular activity profiles with a maximum of 80% and 85% at a crank angle of 60° and 80° and a minimum of 30% and 40% at 210° and 250°, respectively. The onset and offset of FC occurred at around 290° and 150°, while they occurred at around 330° and 180° for EC, respectively. Except for R1, LD demonstrated a single maximum of 70% at around 330° and a minimum between 20% and 25% at around 150°. At R1, one participant (P12) used a totally different activation profile of LD compared to the other participants, which is why an additional maximum appeared at 150°. The onset and offset of TD occurred at around 240° and 80°, respectively. RA attained maximal values of muscular activity of (even more than) 100% MVIC at 220° and a minimum between 15% and 30% at around 50°. The onset and offset of RA occurred at around 120° and between 260° and 330°, respectively.

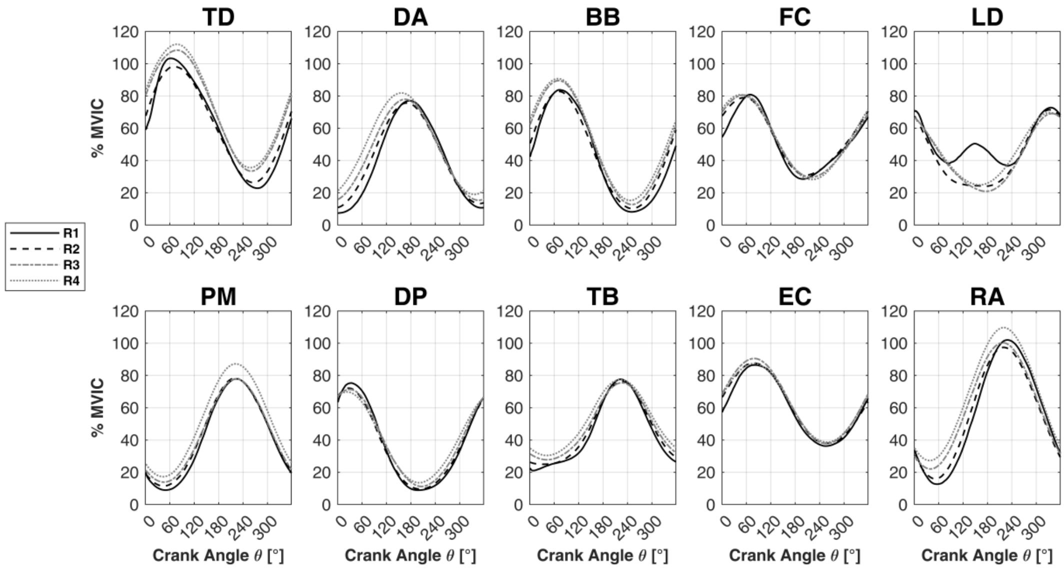

Fig. 16 Muscular activity with respect to crank angle during the course of the 15-s all-out sprint test

Values are expressed as a percentage of maximal voluntary isometric contraction (MVIC) and mean curves across all participants. BB = M. biceps brachii, Caput breve; DA = M. deltoideus, Pars clavicularis; DP = M. deltoideus, Pars spinalis; EC = M. extensor carpi ulnaris; FC = M. flexor carpi radialis; LD = M. latissimus dorsi; PM = M. pectoralis major, Pars sternalis; R1 = first revolution of the sprint; R2 = second revolution of the sprint; R3 = mean over the third to thirteenth revolution; R4 = mean over the fourteenth to last revolution; RA = M. rectus abdominis; RoA = range of activation; TB = M. triceps brachii, Caput laterale; TD = M. trapezius, Pars descendens.

Muscular effort in terms of iEMG significantly increased for TD ($\eta_P^2 = 0.486$, $p = 0.003$), PM ($\eta_P^2 = 0.460$, $p = 0.004$), DA ($\eta_P^2 = 0.547$, $p < 0.001$), BB ($\eta_P2 = 0.387$, $p = 0.001$) and RA ($\eta_P^2 = 0.407$, $p = 0.007$) (Tab. 13). For TD, post-hoc comparisons in iEMG between revolutions were only significant from R1 to R3 and R1 to R4. Muscular activation characteristics in terms of onset, offset and RoA were not significantly affected by evolutions. For PM, iEMG was significantly higher for R4 compared to R1 and R3.

Tab. 13 Alterations of muscular activity during the course of the 15-s all-out sprint test

		R1	R2	R3	R4	η_p^2	p
TD	iEMG [% MVIC]	62 ± 24^{c,d}	62 ± 22	71 ± 29^{a}	74 ± 29^{a}	**0.486****	0.003^{g}
	Onset [°]	337 ± 12^{c}	335 ± 18	328 ± 15^{a}	328 ± 16	0.218	0.071^{g}
	Offset [°]	197 ± 32	199 ± 27	194 ± 21	191 ± 19	0.103	0.299^{g}
	RoA [°]	221 ± 26	225 ± 23	227 ± 13	224 ± 9	0.037	0.666^{g}
PM	iEMG [% MVIC]	41 ± 9^{d}	43 ± 10	44 ± 9^{d}	51 ± 12^{a,c}	**0.460****	0.004^{g}
	Onset [°]	125 ± 15^{b,d}	118 ± 11^{a}	119 ± 13	116 ± 15^{a}	**0.326****	0.004
	Offset [°]	330 ± 17	333 ± 15	330 ± 15	332 ± 17	0.050	0.635
	RoA [°]	206 ± 16	216 ± 15	212 ± 9	216 ± 6	**0.263***	0.034^{g}
DA	iEMG [% MVIC]	40 ± 12^{c,d}	42 ± 11^{d}	46 ± 13^{a,d}	50 ± 15^{a,b,c}	**0.547*****	< 0.001^{g}
	Onset [°]	83 ± 18^{b,c,d}	69 ± 19^{a,c,d}	60 ± 17^{a,b,d}	49 ± 18^{a,b,c}	**0.855*****	< 0.001^{g}
	Offset [°]	287 ± 23^{d}	280 ± 17^{d}	277 ± 14^{d}	267 ± 17^{a,b,c}	**0.376****	0.008^{g}
	RoA [°]	206 ± 20	213 ± 17	217 ± 12	220 ± 10	0.243	0.066^{g}
DP	iEMG [% MVIC]	38 ± 13	37 ± 12	39 ± 13	40 ± 13	0.117	0.257^{g}
	Onset [°]	292 ± 17^{c,d}	295 ± 37	282 ± 17^{a,d}	274 ± 19^{a,c}	0.273	0.061^{g}
	Offset [°]	123 ± 14c	135 ± 31	133 ± 14^{a,d}	129 ± 15^{c}	0.097	0.307^{g}
	RoA [°]	192 ± 15^{c,d}	200 ± 18^{d}	212 ± 10^{a}	216 ± 7^{a,b}	**0.622*****	< 0.001^{g}
BB	iEMG [% MVIC]	43 ± 23	45 ± 28^{c,d}	50 ± 29^{b}	52 ± 31^{b}	**0.387*****	0.001
	Onset [°]	335 ± 15^{b,c,d}	320 ± 13^{a}	321 ± 8^{a}	320 ± 10^{a}	**0.508*****	< 0.001
	Offset [°]	175 ± 15	176 ± 14	178 ± 8	179 ± 8	0.085	0.372^{g}
	RoA [°]	200 ± 26^{b}	217 ± 17^{a}	218 ± 9	221 ± 6	**0.415****	0.006^{g}
TB	iEMG [% MVIC]	45 ± 7	46 ± 10	49 ± 11	52 ± 15	0.245	0.068^{g}
	Onset [°]	141 ± 15	133 ± 15	129 ± 16^{d}	124 ± 15^{c}	**0.300***	0.032^{g}
	Offset [°]	317 ± 15	323 ± 15	325 ± 15	328 ± 17	**0.272***	0.014
	RoA [°]	178 ± 18^{d}	190 ± 11^{d}	196 ± 12^{d}	205 ± 12^{a,b,c}	**0.519****	0.002^{g}
FC	iEMG [% MVIC]	52 ± 20	54 ± 19	53 ± 17	53 ± 21	0.016	0.780^{g}
	Onset [°]	277 ± 46	279 ± 51	287 ± 35	288 ± 31	0.084	0.380^{g}
	Offset [°]	132 ± 36	165 ± 65	147 ± 22	149 ± 25	0.094	0.310^{g}
	RoA [°]	216 ± 41	217 ± 25	221 ± 18	222 ± 11	0.016	0.801^{g}
EC	iEMG [% MVIC]	60 ± 19	62 ± 24	63 ± 30	63 ± 35	0.034	0.582^{g}
	Onset [°]	328 ± 38	334 ± 26	326 ± 20	324 ± 19	0.078	0.400^{g}
	Offset [°]	182 ± 30	181 ± 24	183 ± 19	184 ± 21	0.006	0.840^{g}
	RoA [°]	215 ± 33	209 ± 17	218 ± 10	221 ± 8	0.086	0.359^{g}
LD	iEMG [% MVIC]	51 ± 58	42 ± 32	42 ± 31	46 ± 38	0.069	0.400^{g}
	Onset [°]	244 ± 52^{b}	234 ± 48^{a}	242 ± 24^{d}	231 ± 27^{c}	0.025	0.613^{g}
	Offset [°]	81 ± 50	88 ± 69	84 ± 33	83 ± 35	0.022	0.667^{g}
	RoA [°]	168 ± 11^{c,d}	185 ± 21^{c,d}	203 ± 14^{a,b,d}	213 ± 13^{a,b,c}	**0.753*****	< 0.001^{g}
RA	iEMG [% MVIC]	56 ± 25	56 ± 22^{d}	61 ± 24^{d}	68 ± 26^{b,c}	**0.407****	0.007^{g}
	Onset [°]	135 ± 27^{b,c,d}	119 ± 20^{a}	112 ± 25^{a}	110 ± 29^{a}	**0.519*****	< 0.001
	Offset [°]	318 ± 93	312 ± 90	306 ± 85	331 ± 24	0.051	0.467^{g}
	RoA [°]	214 ± 19	223 ± 15	224 ± 9	222 ± 8	0.173	0.095

Values are expressed as mean value ($\bar{x}$) and standard deviation (SD). ^{a} = significant difference in post-hoc comparison to R1 ($p \leq 0.05$); ^{b} = significant difference in post-hoc comparison to R2 ($p \leq 0.05$); ^{c} = significant difference in post-hoc comparison to R3 ($p \leq 0.05$); ^{d} = significant difference in post-hoc comparison to R4 ($p \leq 0.05$); ^{g} = degrees of freedom were adjusted based on Greenhouse-Geisser due to missing sphericity assumption. Post-hoc comparisons were adjusted using Bonferroni's correction.

Significant time effects * $p \leq 0.05$; ** $p \leq 0.01$; *** $p \leq 0.001$. BB = M. biceps brachii, Caput breve; DA = M. deltoideus, Pars clavicularis; DP = M. deltoideus, Pars spinalis; EC = M. extensor carpi ulnaris; FC = M. flexor carpi radialis; iEMG = integrated EMG (muscular effort); LD = M. latissimus dorsi; Max = maximal value; Min = minimal value; p = probability of committing a type 1 error; PM = M. pectoralis major, Pars sternalis; R1 = first revolution of the sprint; R2 = second revolution of the sprint; R3 = mean over the third to thirteenth revolution; R4 = mean over the fourteenth to last revolution; RA = M. rectus abdominis; RoA = range of activation; TB = M. triceps brachii, Caput laterale; TD = M. trapezius, Pars descendens.

The onset of PM occurred earlier in crank cycle (at lower crank angles) during later stages of the sprint ($\eta_P^2 = 0.326$, $p = 0.004$), which resulted in a significantly higher RoA ($\eta_P^2 = 0.263$, $p = 0.034$) (Fig. 17). The onset occurred significantly later at R1, compared to R2 and R4. Post-hoc comparisons of RoA were not statistically significant. The iEMG of DA was higher at R4 compared to R1, R2 and R3. During the course of the 15-s all-out test, an earlier onset ($\eta_P^2 = 0.855$, $p < 0.001$) and offset ($\eta_P^2 = 0.376$, $p = 0.008$) was found. At R4, the onset and offset occurred significantly earlier compared to R1, R2 and R3. However, the RoA was not significantly affected by revolutions ($\eta_P^2 = 0.243$, $p = 0.066$). For DP, RoA was significantly higher at later revolutions ($\eta_P^2 = 0.622$, $p < 0.001$). At R4 and R3, a higher RoA was observed compared to R1. The onset ($\eta_P^2 = 0.273$, $p = 0.061$) and offset ($\eta_P2 = 0.097$, $p = 0.307$) were not significantly altered during the sprint. iEMG of BB at R3 and R4 was higher compared to R2. During the sprint test, an earlier onset ($\eta_P^2 = 0.508$, $p < 0.001$) and increase in RoA ($\eta_P^2 = 0.415$, $p = 0.006$) was observed. At R1, the onset occurred at significantly higher crank angles compared to R2, R3 and R4. The only significant difference in RoA was found between R1 and R2. The offset of BB was not significantly altered during the course of the sprint ($\eta_P^2 = 0.085$, $p = 0.372$). For TB, an earlier onset ($\eta_P^2 = 0.300$, $p = 0.032$) and increase in RoA ($\eta_P^2 = 0.519$, $p = 0.002$) was observed. The onset occurred significantly earlier at R4 compared to R3 and the RoA was significantly higher at R4 compared to R1, R2 and R3. For the wrist muscles FC and EC, muscular effort and activation characteristics were not significantly altered during the course of the all-out sprint test. For LD, only the RoA was significantly affected by revolutions ($\eta_p^2 = 0.753$, $p < 0.001$). RoA was significantly higher at R3 and R4 compared to R1 and R2. Even between R3 and R4, a significant increase in RoA was found. For RA, iEMG was higher at R4 compared to R2 and R3. The onset occurred significantly earlier at later revolutions ($\eta_p^2 = 0.519$, $p < 0.001$). At R1, the onset occurred significantly earlier compared to R2, R3 and R4. The offset ($\eta_p^2 = 0.051$, $p < 0.001$) and RoA ($\eta_p^2 = 0.173$, $p = 0.095$) was not significantly altered during the course of the sprint test.

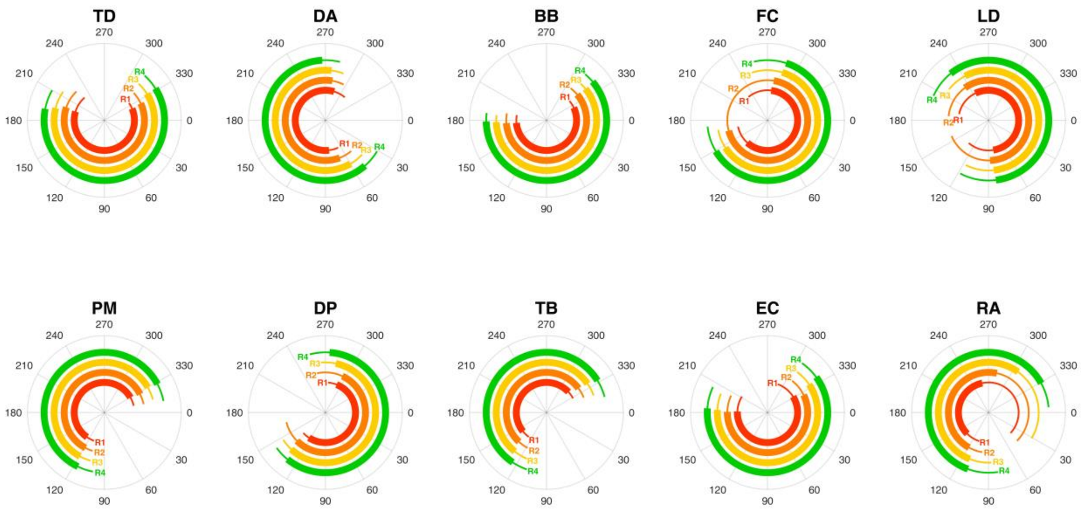

Fig. 17 Muscular activity above threshold with respect to crank angle during the course of the 15-s all-out sprint test

The thick lines represent muscular activity above 30%. The thin lines represent the standard deviation addition of the on- and offsets. BB = M. biceps brachii, Caput breve; DA = M. deltoideus, Pars clavicularis; DP = M. deltoideus, Pars spinalis; EC = M. extensor carpi ulnaris; FC = M. flexor carpi radialis; LD = M. latissimus dorsi; PM = M. pectoralis major, Pars sternalis; ; R1 = first revolution of the sprint; R2 = second revolution of the sprint; R3 = mean over the third to thirteenth revolution; R4 = mean over the fourteenth to last revolution; RA = M. rectus abdominis; RoA = range of activation; TB = M. triceps brachii, Caput laterale; TD = M. trapezius, Pars descendens.

Figure 18 illustrates muscular activity of the ten investigated muscles with respect to a corresponding joint angle during the course of the 15-s all-out sprint test. At R1, the maximal activation of TD occurred at an SA angle of 12°, whereas it increased to 18° at R4. Maximal PM activation occurred at a lower SR angle at R1 (22°) compared to R4 (27°). For DA, a narrowing of the angle-activation profile was observed during the course of the sprint test. The highest DA activation was always observed at the lowest SF angle (maximal retroversion). The angle-activation profile of DP remained rather constant during the sprint. A high DP activation was observed for an almost maximal SF angle. Whereas a high BB activation was found at low EF angles, TB activation was highest at maximal EF. The angle-activation profile of the wrist muscles (FC and EC) demonstrated a shift towards less dorsal-flexion and less ulnar-duction, respectively. They also showed a narrower profile during the later revolutions of the sprint. LD activation was relatively high for a low SA angle and lowest for high SA. For RA, maximal activation was found in the middle (between maximal and minimal) of TF angle. The profile tended to be narrower for later revolutions.

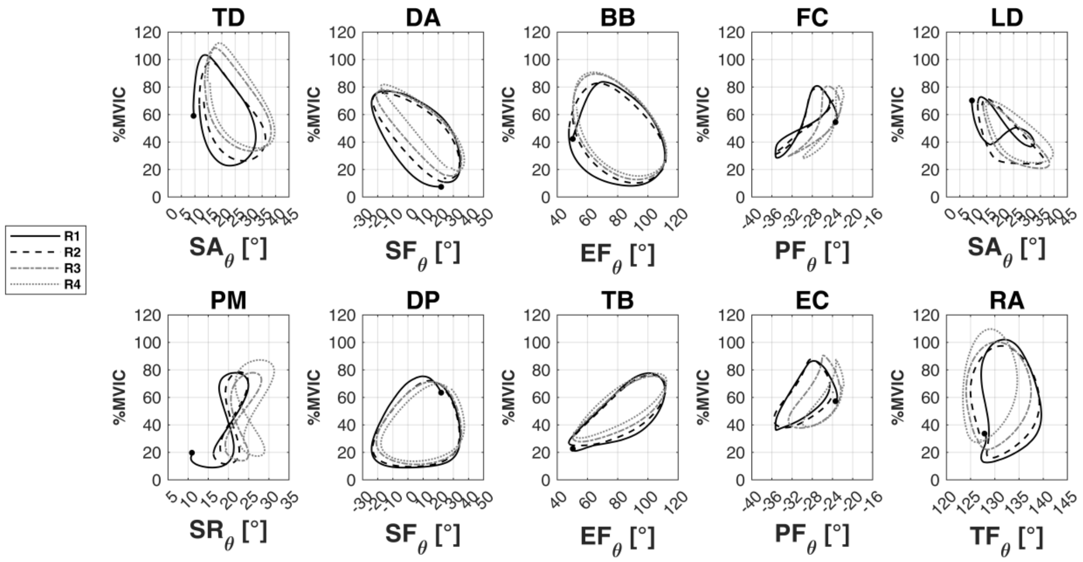

Fig. 18 Muscular activity with respect to a corresponding joint angle during the course of the 15-s all-out sprint test

BB = M. biceps brachii, Caput breve; DA = M. deltoideus, Pars clavicularis; DP = M. deltoideus, Pars spinalis; EC = M. extensor carpi ulnaris; EF_θ = elbow-flexion angle; FC = M. flexor carpi radialis; LD = M. latissimus dorsi; MVIC = maximal voluntary isometric contraction; PF_θ = palmar-flexion angle; PM = M. pectoralis major, Pars sternalis; ; R1 = first revolution of the sprint; R2 = second revolution of the sprint; R3 = mean over the third to thirteenth revolution; R4 = mean over the fourteenth to last revolution; RA = M. rectus abdominis; RD_θ = radial-duction angle; RoA = range of activation; SA_θ = shoulder-abduction angle; SF_θ = shoulder-flexion angle; SR_θ = shoulder internal-rotation angle; TB = M. triceps brachii, Caput laterale; TD = M. trapezius, Pars descendens; TF_θ = trunk-flexion angle.

3.4 Discussion

The aim of this study was to quantify the biomechanics of all-out handcycling exercise and examine alterations in kinematics, kinetics and muscular activity during the course of a 15-s all-out sprint test in able-bodied participants. To our knowledge, this was the first study to combine torque measurements, 3D movement analysis and surface electromyography during all-out handcycling exercise in several participants.

3.4.1 Torque and cadence

The high values of crank kinetics indicate that all-out handcycling exercise is associated with a considerable load on the upper extremities. The highest torque was observed during the initial pull of R1 that caused an increase of cadence as in the start of a handcycle race. According to previous research, crank torque peaked at a crank angle of 90° and demonstrated a local minimum during the lift-up (Quittmann et al. 2018b). During the push-up, crank torque increased again and peaked at the end of this sector. This torque profile can be explained by the muscles primarily generating the crank forces that are either assigned to the pull (e. g. BB, DP and TD) or push phase (e. g. PM, DA and TB). The local minima at 180° and 0° might be due to an unfavourable configuration of the upper extremity joints in terms of ergonomics (Stone et al. 2019c).

Compared to recent findings in incremental handcycling, peak torque was found to be more than five times higher during the initial pull at R1 (Quittmann et al. 2018b). This is due to the fact that the intensity of this study was all-out and the cranks had to be set in motion. These findings indicate that sprints in handcycling come along with remarkably higher forces compared to handcycling propulsion at a high aerobic intensity. Thus, the usage of maximal sprints in the training of elite handcyclists should be taken with caution. In this context, joint moments and muscle forces of the upper extremity would have been interesting to quantify and compare the load on and contribution of certain regions.

3.4.2 Trunk

The participants supported the pull and push phase by an active usage of their trunk. This corresponds to previous research indicating reinforced trunk activation for higher workloads (Quittmann et al. 2018b, Quittmann et al. 2019). This movement might have been facilitated by closed chain propulsion (2-feet support) in which the footrests are used as an abutment of the legs. Previous research demonstrated that the ability to make a closed chain significantly improves sprint performance (Kouwijzer et al. 2018). However, the initial press-down of R1 was performed with a slight and rather constant flexion angle of the trunk. In doing so the trunk was used as an abutment of the shoulder muscles in order to overcome the initial resistance and set the cranks in motion. During the pull-down and pull-up, a reinforced RA activation caused an increasing flexion of the trunk. The higher trunk-flexion in this sector reduced the lever arm for the shoulder and elbow and probably improved the force transmission of TD, DP and BB. At the transition from pull-up to lift-up, an extension movement of the trunk was initiated and led to a maximal extension velocity and RA activity at the end of the lift-up. It might seem paradoxical that TF increased even though RA activity decreased. A reason for this could be that the participants rather pulled themselves forward by their shoulder and arm muscles than initiating the movement using their trunk muscles. Since maximal extension velocity occurred at a crank angle of around 210°, it is likely that a reinforced extension movement of the trunk was applied in order to quickly overcome the lift up and support the push phase.

TF angle demonstrated a higher flexion and RoM compared to previous research (Faupin et al. 2006, Quittmann et al. 2018b). This might be due to the fact that the method to impose power was slightly different between studies. Whereas the frame of the handcycle (front wheel removed) was directly attached to the ergometer, (Faupin et al. 2006) provided a constant friction onto the front wheel (roller) to calculate power and velocity by cadence. The rather stiff connection to the ergometer in this study might facilitate a powerful usage of the trunk and hence a higher RoM. Compared to handcycling at a high aerobic intensity, TF angular velocity was around four times higher in an all-out exercise condition (Quittmann et al. 2018b). This supports the hypothesis that trunk action in handcycling is only added at high intensities. It was recently shown that TF demonstrates a higher variance and different profile over crank cycle at sprint compared to training and competition intensity (Stone et al. 2019c). It can be concluded, that the usage of the trunk in SCI handcyclists highly depends on individual perquisites and handcycle settings.

3.4.3 Shoulder

As the most proximal joint of the upper extremity, the shoulder provides the most degrees of freedom at the expense of reduced stability (Murray et al. 2013). In wheelchair athletes, the functionality of the upper extremity is essential for both exercise and daily living which increases the load on the upper extremity. Accordingly, the shoulder (17.7%) was found to be the most frequently injured region in Paralympic athletes followed by the wrist (11.4%) and elbow (8.8%) joints (Willick et al. 2013). Due to the high angular velocities and activation of corresponding muscles, this study demonstrates that the shoulder is facing a high load during all-out handcycling exercise.

During the course of the sprint, shoulder kinematics and muscular activity of surrounding muscles demonstrated various alterations. Angular velocities of the shoulder joint demonstrated an increase although no differences were found between R3 and R4. As observed in incremental handcycling, shoulder retroversion angle decreased whereas abduction and internal-rotation increased (Quittmann et al. 2018b). Accordingly, DA and PM demonstrated a high increase in muscular effort and an earlier onset of muscular activation. Since muscular effort of DP was not significantly altered during the test, there is reason to believe that primarily the muscles associated with the push phase suffered from short-duration fatigue. It seems that the lift-up sector is a limiting factor of high-intensity propulsion due to the challenging positions of the upper-body segments in terms of force generation transmission (Stone et al. 2019c). DA's high increase in muscular effort and shift of muscular activation onset might be due to the fact that DA initiates the lift-up and is a rather small muscle. Reinforced activation of DA and PM might be used to quickly overcome the lift-up and reduce its limiting effect. The increase in TD activation could be interpreted as an increasing elevation of the scapula during the sprint. This might be another strategy to assist force generation of DA and PM during the lift-up and push-up. On the other hand, the increase in TD activation was found over the whole crank cycle that might be an indicator of fatigue. It is hypothesised that repetitive sprints and thus high activation of TD might increase the risk of neck tension symptoms in handcyclists. Even though LD muscular effort was not significantly altered during the sprint, LD demonstrated an increase in RoA from R3 to R4 indicating a wider activation profile. This is probably due to an increasing need to stabilise the humerus and thus improve the force transmission of the shoulder muscles.

Shoulder kinematics observed in this agreed with previous research (Faupin et al. 2010, Quittmann et al. 2018b, Stone et al. 2019c). Due to the higher intensity and cadence, higher values of angular velocity (especially in SF) were found compared to incremental handcycling. Whereas RoM of SF and SA was similar compared to handcycling at a high aerobic intensity, minimal and maximal SR angle was remarkably higher and RoM lower in the all-out exercise condition (Quittmann et al. 2018b).

3.4.4 Elbow

Based on EF's high joint angular velocity and the high activation of BB and TB, the elbow seems to be a major contributor to mechanical power in handcycling propulsion. Due to the fixed positions of the hands on the cranks and the trunk leaning against the backrest of the handcycle, EF angle is dependent on crank position (Stone et al. 2019c). The period of BB and TB co-activation (located from the late pull-up to the early lift-up) was rather high (around 50°) compared to previous research (Faupin et al. 2010, Litzenberger et al. 2016, Quittmann et al. 2019). This was probably due to the fact that force transmission during the lift-up is rather challenging in terms of ergonomics and thus co-activation might improve force transmission (Stone et al. 2019c, van Ingen Schenau 1989). Another argument for the high period of co-activation is the fact that it was an all-out sprint exercise condition and participants were rather inexperienced in handcycling (O'Bryan et al. 2014). It was observed that BB activation peaked at an only slightly flexed position of the elbow when the moment arm of BB is rather small and the muscle length is rather high (Leedham and Dowling 1995, Pigeon et al. 1996). Simultaneously, EF angular velocity demonstrated a rapid increase up to almost 400° s^{-1} at R4 that was around 100° s^{-1} higher compared to findings in incremental handcycling (Quittmann et al. 2018b). Since elite handcycle athletes perform a high training volume of considerable intensity, these aspects might cause overuse symptoms of the elbow flexors' insertion region (Abel et al. 2010, Zeller et al. 2017).

During the course of the 15-s all-out test, EF demonstrated an increase in maximal flexion and extension velocity, whereas EF angle was not altered. The increase in flexion velocity was even higher compared to extension velocity. Accordingly, BB demonstrated an increase in muscular effort and earlier onset of muscular activation whereas muscular effort was not significantly altered in TB. However, TB demonstrated a later offset of activation at the beginning of the press-down. Whereas minimal EF angle was about 10° higher, maximal EF was about 10° lower compared to findings in incremental handcycling (Quittmann et al. 2018b). This was probably due to the active usage of the trunk and higher SF angles that decreased maximal elbow-extension and flexion.

3.4.5 Wrist

Whereas the force is primarily generated by the shoulder and elbow (muscles), the wrists' main function is to ensure force transmission by increasing the wrists' joint stiffness to the cranks. An argument for this hypothesis is that the MAPs of FC and EC were found to be quite similar even though they are considered as antagonists. Possibly, this type of activation causes high joint moments (Gonzalez et al. 1997). Due to the position of the wrist, the activity values of the forearm extensors were higher compared to the forearm flexors. Between the first (R3) and second half (R4) of the sprint no alterations of kinematics and muscular activity could be found in the wrist region. This indicates that fatigue-based alterations do not appear in the wrist region within a 15-s all-out sprint test.

Whereas the values of maximal ulnar-duction corresponded to previous research, this study demonstrated even higher values of maximal dorsal-flexion (Faupin et al. 2006, Quittmann et al. 2018b) and PF RoM (Litzenberger et al. 2016). Based on ergonomic recommendations stating allowable ranges of the wrist (15° dorsalflexion and 5° radial-duction), the kinematics of this study were above these limits (Veeger et al. 1998). The highest activation of FC and EC was observed at around 25° dorsal-flexion and 10° radial-duction. At maximal dorsal-flexion and radial-duction, muscular activity of the wrist muscles was lowest, but still between 30 to 40% of MVIC. Based on these findings, the wrist region might be prone to overuse injuries if a considerable volume of high-intensity handcycling is performed which agrees with retrospective findings in Paralympic sports (Athanasopoulos et al. 2009, Fagher and Lexell 2014).

3.4.6 Limitations

As in other studies that investigated inexperienced and able-bodied participants, the transferability of the results to elite handcycle athletes is impeded. Athletes with an SCI have a limited function of their trunk depending on the height and extent of their lesion. The participants of this study demonstrated high usage of the trunk (muscles) that SCI athletes could not afford. Furthermore, the elite handcyclists primarily use an even more recumbent (rather lying) position that increases the inertia moment of the trunk. Due to these aspects, it is likely that joint kinematics und muscular activity of the shoulder, elbow and wrist are even more pronounced in elite handcycle athletes. However, recent research demonstrated that competitive handcyclists demonstrate a higher TF compared to recreational handcyclists. Power output of the SRM crank and the Cyclus 2 ergometer demonstrated rather high discrepancies. These discrepancies are influenced by the fact that the measurement frequency was 125 times higher in the SRM crank. However, this factor does not account for the whole discrepancy between methods. For the purposes of this study the difference between investigation methods does not limit the essence of the findings. All participants started the sprint in the foremost crank position leading to an initial pull. This might have affected the alterations during the course of the sprint test. Future studies should examine the effect of starting position (e. g. at 180°) and its effects on performance and biomechanics. As previously mentioned, the kinematic model of this study did not quantify the movement of the scapula. Based on the high activation of TD and previous findings (Stone et al. 2019c) there is reason to believe that a vigorous movement of the scapula was performed. Future studies are encouraged to further analyse the scapula movement of all-out handcycling. Even though maximal cadence was set at 140 min^{-1}, the participants attained only 116 min^{-1} on average. This was probably due to a flaw in the Cyclus 2 regulation technology.

3.4.7 Practical applications

As a recent study demonstrated, eight weeks of concurrent training (strength and endurance programs) lead to a higher improvement in elite handcyclists' performance as endurance training only (Nevin et al. 2018). Accordingly, handcycle athletes might be encouraged to augment their training by additional strength-oriented exercises. Based on the findings of this study, there are a few aspects that should be considered to improve handcycling performance and prevent overuse injuries in (elite) handcyclists. It was assumed that PM and BB are the major contributors of the push and pull phase, respectively. DA and DP act as important initiators of the push and pull phase and assist larger muscles such as PM and BB, respectively. To improve the strength of PM and DA, flat and incline bench press exercises could be applied. The strength abilities of BB and DP could be improved by pulling exercises (e. g. on a cable tower) with similar conditions as in handcycling (shoulders abducted, TD activated). However, such exercises need to be treated with caution since the insertion region of the elbow flexors examines a high load in sprint handcycling exercise. Since the lift-up was considered as a limiting factor of propulsion, sport-specific strength training exercises imitating this movement should be performed. A sport-specific exercise for the lift-up could be a fast and repetitive clean and jerk motion of a (medicine) ball that has to be passed in a high trajectory towards a partner (or against a wall). Since shoulder stability improves the force transmission of larger (more distal) muscles and reduces the prevalence of overuse injuries, particular attention should be paid to the conditioning of the rotator cuff muscles (Murray et al. 2013). The functionality and strength of the rotator cuff muscles can be improved by shoulder-rotation exercises with the use of elastic bands (Batalha et al. 2015).

However, due to the wheelchair athletes' vigorous use of the upper extremity in daily living and exercise, additional strength training exercises should be applied with caution. Especially when sport-specific endurance training is performed at high-intensity, resistance training should be minimized and restricted to rather low weights during competition periods. During preparation periods, a higher volume and intensity of strength training might be applied. In order to prevent tension and overuse symptoms, relaxation techniques as applied in physiotherapy seem to be essential in handcycle athletes.

3.5 Conclusions

Kinematics, kinetics and muscular activity are remarkably high and altered during the course of a 15-s all-out sprint test in handcycling. It seems that the shoulder region is exposed to high stress, reacts rather sensitively to fatigue-based alterations and is probably prone to overuse injuries. DA and DP act as important initiators of the push and pull phase and assist larger muscles such as PM and BB, respectively. This knowledge can be used to improve performance and prevent overuse injuries in handcycling.

4 Biomechanics of continuous load handcycling

Biomechanics of handcycling propulsion in a 30-min continuous load test at lactate threshold: Kinetics, kinematics and muscular activity in able-bodied participants

Oliver J. Quittmann[1], Thomas Abel[1,2], Kirsten Albracht[3,4], Joshua Meskemper[3], Tina Foitschik[1] & Heiko K. Strüder[1]

1 Institute of Movement and Neurosciences, German Sport University Cologne

2 European Research Group in Disability Sport (ERGiDS)

3 Institute of Biomechanics and Orthopaedics, German Sport University Cologne

4 Faculty of Medical Engineering and Technomathematics, University of Applied Sciences Aachen

Submitted in:

European Journal of Applied Physiology (Impact factor 2018: 3.055)

Submitted: 16 December, 2019

Abstract

Purpose: This study aims to assess fatigue-related alterations of handcycling biomechanics during the course of a continuous load trial (CLT).

Methods: Twelve able-bodied triathletes performed a 30-min CLT at lactate threshold in a racing recumbent handcycle mounted on a stationary ergometer. During the CLT, tangential crank kinetics, 3D joint kinematics and muscular activity of ten muscles of the upper extremity and trunk were examined using motion capturing and surface electromyography (sEMG).

Results: During the course of the CLT, spontaneously chosen cadence increased whereas crank torque decreased. Ratings of perceived exertion (RPE) were higher on a local level compared to global RPE. Joint range of motion decreased for elbow-flexion and radial-duction. Muscular effort demonstrated an increase in the forearm flexors, forearm extensors and M. deltoideus (Pars spinalis). An earlier onset of activation was found for M. deltoideus (Pars clavicularis), M. pectoralis major, M. rectus abdominis, M. biceps brachii and the forearm flexors.

Conclusions: These findings indicate that handcycling is predominantly limited by peripheral mechanisms in inexperienced individuals. An increase in cadence might delay locally-based fatigue by a reduced muscle force and concomitant reduced vascular occlusion. It is assumed that the gap between peripheral and central fatigue is reduced due to sport-specific endurance training.

4.1 Introduction

Endurance performance can be defined as the ability to sustain a high mechanical power or load during prolonged exercise in the absence of fatigue. Since fatigue is a complex phenomenon, the meaning of this term differs between disciplines (Abbiss and Laursen 2005). In psychology, fatigue may be viewed as a sensation of tiredness since maintaining exercise is a volitional decision (Kayser 2003). In physiology, fatigue is considered as a failure of a specific (metabolic) system that leads to insufficient energy supply to the involved muscles (Green 1997). In biomechanics, fatigue is described as a decline in muscular force production and/or altered muscular activation which is called 'neuromuscular fatigue' (Kent-Braun et al. 2012, Millet and Lepers 2004). Interdisciplinary knowledge of the mechanisms underlying fatigue during prolonged exercise helps to improve performance in endurance sports.

In cycling, neuromuscular fatigue has already been examined in several studies (Lepers et al. 2000, Lepers et al. 2001, Lepers et al. 2002, Hettinga et al. 2006, Amann 2011, de Morree and Marcora 2012, Decorte et al. 2012, Martinez-Valdes et al. 2016). It was shown that muscular activity during prolonged exercise does not only change in terms of intensity, but also in terms of muscular activation patterns (MAPs) (Blake and Wakeling 2012, Hug and Dorel 2009). This may lead to a shift in the pedalling movement which can be assessed by crank kinetics and joint kinematics (Bini et al. 2010, Momeni et al. 2014, Sayers et al. 2012, Suzuki et al. 1982). Based on these findings, certain functions were assigned to the particular joints of the lower extremity. Whereas the knee and hip joint are considered the major power producers (Bini et al. 2008), it is supposed that the function of the ankle joint and its surrounding muscles is to transfer force from the legs to the cranks (Mornieux et al. 2007, Ryan and Gregor 1992, Zajac 2002). As the most distal joint, the ankle demonstrated the highest fatigue (Elmer et al. 2012) and a reduced contribution to total joint moments (Bini et al. 2010).

As part of paracycling, handcycling is a Paralympic endurance sport that is predominantly performed by athletes with a spinal cord injury (SCI) or amputation of the lower extremities. In contrast to conventional (leg) cycling, the athletes propel their three wheeled vehicle (called handcycle or handbike) by the power of their upper extremity. Physiological responses during prolonged handcycling exercise in terms of power output, lactate concentration, oxygen uptake, energy expenditure and body temperature have already been reported in previous research (Abel et al. 2006, Fischer et al. 2014, Fischer et al. 2015, Stangier et al. 2019). During the course of an incremental step test until voluntary exhaustion, handcycling biomechanics demonstrated alterations in terms of crank kinetics, joint kinematics and muscular activity and indicated locally based fatigue (Quittmann et al. 2018b, Quittmann et al. 2019). However, the findings of these studies are influenced by both exercise intensity and duration. To isolate the effect of exercise duration on propulsion characteristics and to gain further insights into sport-specific fatigue in handcycling, this study aims to examine biomechanics during the course of a 30-min continuous load trial (CLT) at lactate threshold. It is hypothesised that fatigue-related alterations apply analogously in handcycling and cycling.

4.2 Methods

4.2.1 Participants

Twelve able-bodied male competitive triathletes (26.0 ± 4.4 yrs., 1.83 ± 0.06 m, 74.3 ± 3.6 kg) participated in this study. All participants stated their right arm was dominant. Medical peculiarities and acute complaints of the upper extremity were exclusion criteria. Participants gave their written informed consent before participating in the study. The study was approved by the German Sport University Cologne Ethics Committee (No. 52 / 2016) and complied with the ethical standards of the 1975 Helsinki Declaration modified in 1983.

4.2.2 Instrumentation

The tests were performed in a racing handcycle (Shark S, Sopur, Sunrise Medical, Malsch, Germany) in synchronous crank mode that was mounted on a fully calibrated and validated ergometer (TE 2%, Cyclus 2, 8 Hz, RBM electronic automation GmbH, Leipzig, Germany) (Reiser et al. 2000). Handcycle settings were standardised between participants and resulted in backrest tilt between 46° and 53° as described elsewhere (Quittmann et al. 2018b, Quittmann et al. 2019).

4.2.3 Design

Participants performed various exercise tests on three distinct occasions within a two-week period to become familiarised with handcycling propulsion. On the first occasion, the participants performed an incremental familiarisation protocol up to 100 W with decreasing stage durations and a 15-s all-out sprint test in isokinetic mode (Quittmann et al. 2018a). Post-exercise lactate kinetics following the 15-s sprint test were used to determine maximal lactate accumulation rate ($\dot{V}La_{max}$). On the second occasion, the participants performed an incremental step test until voluntary exhaustion and a second 15-s sprint test thereafter (Quittmann et al. 2018b, Quittmann et al. 2019). At the end of every stage of the incremental test, blood lactate concentration was measured to determine the lactate threshold as the power output corresponding to a lactate concentration of 4 mmol·l^{-1} (P_4) (Heck et al. 1985). On the third occasion, participants performed a CLT for 30 minutes at their individual lactate threshold. As a warm-up and cool-down, the participants performed five minutes at 50% of lactate threshold power before and after the CLT, respectively (Quittmann et al. 2018a). Lactate concentration was determined every five minutes using an enzymatic-amperometric sensor chip system (Biosen C-Line, EKF-diagnostics GmbH, Barleben, Germany). The increase in lactate concentration within the last 20 minutes of the CLT was checked to meet common criteria of ≤ 1 $mmol \cdot l^{-1}$ for detecting steady-state conditions (Stangier et al. 2019). Lactate kinetics of the exercise tests performed (including the CLT of this study) are described in previous research (Quittmann et al. 2018a). Cadence was freely chosen throughout the test. During the CLT, a fan was facing the participants to minimise sweat contamination of sEMG signals. During all exercise tests, medical background was provided to ensure professional first aid in case of emergency. To analyse alterations in handcycling propulsion over time, the CLT was divided into six five minute stages. Biomechanical measures were recorded at the end of the first and beginning of the last minute of each stage for 20 s. The values attained in the two files of each stage were resampled to 360° and averaged over crank cycle.

4.2.4 Measures

Tangential crank torque (M) was measured using a power meter (1000 Hz, Schoberer Rad Messtechnik (SRM) GmbH, Jülich, Germany) installed in the crank and integrated in motion capturing software (Vicon Nexus 2.3, Vicon Motion Systems Ltd., Oxford, UK). Voltage signals were calibrated using free weights from 5 to 40 kg at a crank fixed at the foremost position. Crank angle was defined as foremost (0°), lowest (90°), nearest (180°) and highest (270°) crank position according to conventions. Crank kinetics were filtered using a fourth-order low-pass Butterworth filter with a cut-off frequency of 10 Hz. Rotational work (W_{rot}) was calculated for the pull (330° to 150°) and push phase (150° to 330°) as described elsewhere (Quittmann et al. 2018b).

Additionally, ratings of perceived exertion (RPE) were collected every five minutes of the CLT on a global (cardio pulmonary) and local (upper extremities) level.

Joint kinematics were calculated according to the Upper Limb Model of Vicon Nexus. A total of 44 spherical retro-reflective markers were placed on the crank, ergometer and anatomical landmarks (Quittmann et al. 2018b). Marker positions were captured by seven high-speed infrared cameras that were placed around the handcycle (100 Hz, MX-F40 and MX-3+, Vicon Nexus 2.3, Vicon Motion Systems Ltd., Oxford, UK). Angles and angular velocities of shoulder-flexion (SF), shoulder-abduction (SA), shoulder internal-rotation (SR), elbow-flexion (EF), palmar-flexion (PF) and radial-duction (RD) of the dominant (right) arm were considered by the Upper Limb Model. According to ISB recommendations and previous research, trunk-flexion angle (TF) was determined as the angle between the horizontal plane and the line connecting the midpoints between the 7th cervical vertebra (C7) and jugular notch (CLAV) and the 10th thoracic vertebra (T10) and xiphoid process (STRN) (Quittmann et al. 2018b). Kinematic measures were resampled to 1000 Hz using pchip interpolation method and filtered using a fourth-order low-pass Butterworth filter with a cut-off frequency of 10 Hz. Crank angular velocity or cadence (Cad) was estimated using markers on the axis and the crank arm.

Surface electromyography (sEMG) was performed for ten muscles of the upper extremity and trunk using a wireless sEMG system (DTSEMG Sensor®, 1000 Hz, Noraxon Scottsdale, Arizona, USA). Muscular activity was assessed for M. trapezius, Pars descendens (TD); M. pectoralis major, Pars sternalis (PM); M. deltoideus, Pars clavicularis (DA); M. deltoideus, Pars spinalis (DP); M. biceps brachii, Caput breve (BB); M. triceps brachii, Caput laterale (TB); M. flexor carpi radialis (FC); M. extensor carpi ulnaris (EC); M.

latissimus dorsi (LD) and M. rectus abdominis (RA). Due to the risk of sEMG crosstalk contamination between tightly gathered agonists, FC and EC were identified to represent forearm flexors and extensors, respectively. Electrode positions and skin preparation procedures were in accordance with the SENIAM guidelines (Hermens et al. 2000) and are precisely described in a preliminary study (Quittmann et al. 2019). Muscular effort in terms of integrated EMG (iEMG) and MAPs in terms of the onset, offset and range of activation (RoA) was determined according to previous research (Quittmann et al. 2019). Biomechanical measures were processed and prepared for statistical analyses using MATLAB (R2017b, MathWorks®, Natick, Massachusetts, USA).

4.2.5 Statistics

Statistical analyses were done using the Statistical Package for the Social Sciences software (26, SPSS Inc., Chicago, Ill., USA). Alterations of biomechanics during the course of the CLT were examined using a one-way analysis of variance (ANOVA) with repeated measures. Mauchly's test was performed to check for sphericity. In case sphericity was violated, Greenhouse-Geisser correction of the degrees of freedom was applied. For M, Cad and joint kinematics, the minimum, maximum and range over crank cycle was analysed. Muscular activity was examined in terms of iEMG, onset, offset and RoA. For W_{rot} and RPE, a two-way ANOVA was performed to examine differences in the relative contribution of W_{rot} between phases and stages (2 × 6) and between levels of perceived exertion and time (2 × 6), respectively. Post-hoc comparisons were adjusted according to Bonferroni. Partial eta squared (η_p^2) and Cohen's d (d) were calculated as effect sizes. The level of significance was set at $\alpha = 0.05$.

4.3 Results

4.3.1 Kinetics and RPE

Crank torque demonstrated a decrease during the course of the CLT for maximal (η_p^2 = 0.328, p = 0.006) and minimal (η_p^2 = 0.415, p = 0.003) values, whereas minimal cadence increased (η_p^2 = 0.328, p = 0.014) (Tab. 14). W_{rot} during the pull phase was higher compared to the push phase (η_p^2 = 0.820, p < 0.001) (Fig. 19). During the CLT, the difference between pull and push phase increased in favour of pulling. RPE demonstrated a significant effect for time (η_p^2 = 0.500, p = 0.001) and the level (η_p^2 = 0.688, p < 0.001). Post-hoc comparisons demonstrated that locally perceived exertion was significantly higher compared to globally perceived exertion throughout the CLT (Fig. 19b). RPE increased during the first half of the test and remained stable thereafter.

Tab. 14 Crank torque and cadence during the continuous load trial

		5 min	10 min	15 min	20 min	25 min	30 min	η_p^2	p
M	Max [Nm]	13.8 ± 2.0^{c}	13.6 ± 2.3	13.2 ± 1.9^{a}	13.1 ± 2.0	13.0 ± 2.1	13.1 ± 1.9	**0.328****	0.006^{g}
	Min [Nm]	9.2 ± 1.2^{b,c,e}	8.8 ± 1.3^{a}	8.5 ± 1.0^{a}	8.4 ± 1.2	8.3 ± 0.9^{a}	8.0 ± 1.1	**0.415****	0.003^{g}
	Range [Nm]	4.6 ± 0.9	4.8 ± 1.2	4.7 ± 1.2	4.7 ± 1.2	4.7 ± 1.5	5.1 ± 1.7	0.067	0.473^{g}
Cad	Max [min^{-1}]	77 ± 10^{b,c,d,f}	81 ± 12^{a}	83 ± 13^{a}	85 ± 15^{a}	95 ± 32	88 ± 17^{a}	0.254	0.067^{g}
	Min [min^{-1}]	73 ± 10^{c,d,f}	77 ± 12	79 ± 12^{a}	82 ± 15^{a}	80 ± 16	84 ± 15^{a}	**0.328***	0.014^{g}
	Range [min^{-1}]	3 ± 1	4 ± 2	4 ± 3	4 ± 2	15 ± 36	4 ± 3	0.313	0.093^{g}

Values are expressed as mean value (x̄) and standard deviation (SD). ^{a} = significant difference in post-hoc comparison to 5 min (p ≤ 0.05); ^{b} = significant difference in post-hoc comparison to 10 min (p ≤ 0.05); ^{c} = significant difference in post-hoc comparison to 15 min (p ≤ 0.05); ^{d} = significant difference in post-hoc comparison to 20 min (p ≤ 0.05); ^{e} = significant difference in post-hoc comparison to 25 min (p ≤ 0.05); ^{f} = significant difference in post-hoc comparison to 30 min (p ≤ 0.05); g = degrees of freedom adjusted based on Greenhouse-Geisser due to missing sphericity assumption. Post-hoc comparisons were adjusted using Bonferroni's correction. Significant time effects * p ≤ 0.05; ** p ≤ 0.01. Cad = cadence; M = torque; Max = maximal value; Min = minimal value; p = probability of committing a type 1 error; η_p^2 = partial eta squared.

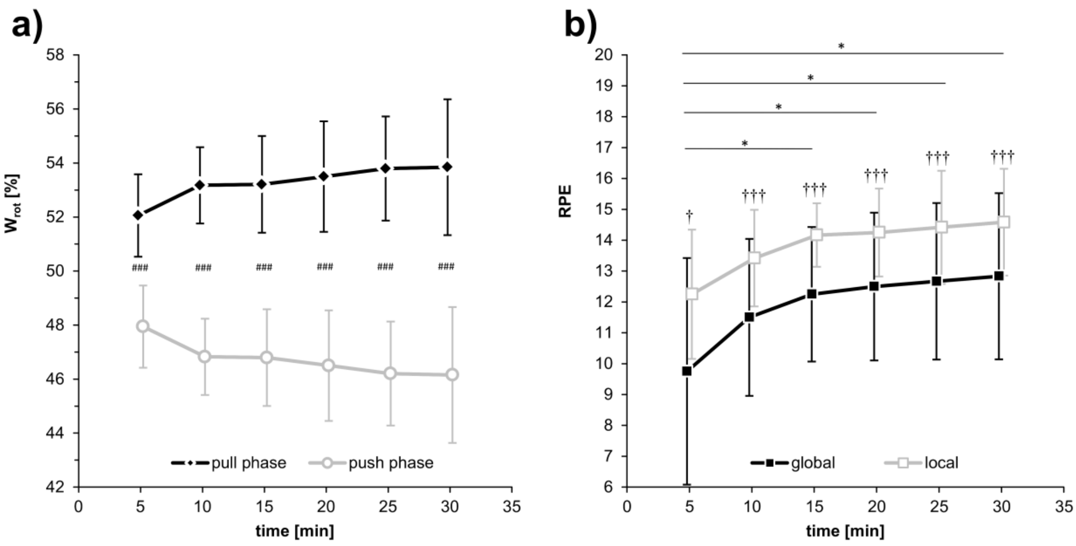

Fig. 19 Rotational work (W_{rot}) (left) and ratings of perceived exertion (RPE) (right) during the course of the 30-min continuous load trial

Values are expressed as mean value ($\bar{x}$) and standard deviation (SD). ### significant difference between pull and push phase ($p \leq 0.001$); * significant difference over time ($p \leq 0.05$); † significant difference between globally and locally perceived exertion ($p \leq 0.05$); ††† significant difference between globally and locally perceived exertion ($p \leq 0.001$).

4.3.2 Kinematics

Joint angles demonstrated hardly any changes during the CLT (Tab. 15, Fig. 20). EF demonstrated a decrease in RoM ($\eta_p^2 = 0.273$, $p = 0.026$) due to a reduced flexion ($\eta_p^2 = 0.267$, $p = 0.040$). RoM was also reduced in RD ($\eta_p^2 = 0.243$, $p = 0.008$). Maximum, minimum and range of joint angular velocities increased for SF and EF (Tab. 16, Fig. 21). For SA, SR and PF, only minimal values demonstrated an increase.

Tab. 15 Joint angles during the continuous load trial

		5 min	10 min	15 min	20 min	25 min	30 min	η_P^2	p
SF_θ	Max [°]	38 ± 4	37 ± 4	38 ± 4	37 ± 4	37 ± 4	37 ± 4	0.027	0.762[g]
	Min [°]	-17 ± 6	-16 ± 6	-17 ± 5	-16 ± 5	-17 ± 5	-18 ± 4	0.057	0.651
	RoM [°]	55 ± 5	54 ± 4	54 ± 4	54 ± 5	55 ± 5	55 ± 5	0.096	0.334
SA_θ	Max [°]	31 ± 6	32 ± 6	32 ± 5	32 ± 6	31 ± 5	31 ± 5	0.035	0.702[g]
	Min [°]	7 ± 3	7 ± 3	8 ± 3	8 ± 4	8 ± 3	8 ± 4	0.181	0.092[g]
	RoM [°]	24 ± 5	24 ± 5	24 ± 4	24 ± 4	23 ± 3	23 ± 3	0.072	0.452[g]
SR_θ	Max [°]	28 ± 6	28 ± 7	28 ± 6	28 ± 7	27 ± 6	27 ± 6	0.031	0.875
	Min [°]	14 ± 6	13 ± 6	13 ± 6	13 ± 7	12 ± 7	11 ± 8	0.106	0.290[g]
	RoM [°]	14 ± 3	15 ± 3	15 ± 3	15 ± 4	15 ± 5	15 ± 5	0.077	0.429[g]
EF_θ	Max [°]	116 ± 3	116 ± 4	116 ± 4	116 ± 4	116 ± 4	116 ± 4	0.073	0.508
	Min [°]	38 ± 7	39 ± 8	39 ± 8	41 ± 8	41 ± 8	41 ± 9	**0.267***	0.040[g]
	RoM [°]	78 ± 6	77 ± 6	76 ± 6	75 ± 6	75 ± 5	75 ± 6	**0.273***	0.026[g]
PF_θ	Max [°]	-17 ± 5	-16 ± 5	-14 ± 6	-16 ± 4	-15 ± 4	-15 ± 5	0.129	0.211[g]
	Min [°]	-31 ± 6	-31 ± 7	-29 ± 9	-30 ± 7	-29 ± 6	28 ± 7	0.122	0.233[g]
	RoM [°]	14 ± 5	15 ± 6	15 ± 6	14 ± 6	14 ± 5	13 ± 5	0.102	0.306[g]
RD_θ	Max [°]	-8 ± 6	-8 ± 6	-9 ± 7	-9 ± 6	-10 ± 6	-10 ± 6	0.167	0.066
	Min [°]	-17 ± 8	-16 ± 9	-16 ± 8	-16 ± 8	-16 ± 7	-17 ± 7	0.087	0.370[g]
	RoM [°]	8 ± 4	8 ± 4	7 ± 4	7 ± 4	7 ± 4	7 ± 4	**0.243****	0.008
TF_θ	Max [°]	135 ± 5	134 ± 5	135 ± 5	134 ± 5	134 ± 5	135 ± 5	0.057	0.564[g]
	Min [°]	130 ± 6	130 ± 6	131 ± 6	130 ± 5	130 ± 5	130 ± 6	0.062	0.497[g]
	RoM [°]	5 ± 2	5 ± 2	4 ± 2	4 ± 2	4 ± 2	5 ± 4	0.088	0.362[g]

Values are expressed as mean value ($\bar{x}$) and standard deviation (SD). [a] = significant difference in post-hoc comparison to 5 min ($p \leq 0.05$); [b] = significant difference in post-hoc comparison to 10 min ($p \leq 0.05$); [c] = significant difference in post-hoc comparison to 15 min ($p \leq 0.05$); [d] = significant difference in post-hoc comparison to 20 min ($p \leq 0.05$); [e] = significant difference in post-hoc comparison to 25 min ($p \leq 0.05$); [f] = significant difference in post-hoc comparison to 30 min ($p \leq 0.05$); [g] = degrees of freedom adjusted based on Greenhouse-Geisser due to missing sphericity assumption. Significant time effects * $p \leq 0.05$; ** $p \leq 0.01$; *** $p \leq 0.001$. EF_θ = elbow-flexion angle; Max = maximal value; Min = minimal value; p = probability of committing a type 1 error; PF_θ = palmar-flexion angle; RD_θ = radial-duction angle; RoM = range of motion; SA_θ = shoulder-abduction angle; SF_θ = shoulder-flexion angle; SR_θ = shoulder internal-rotation angle; TF_θ = trunk-flexion angle; η_P^2 = partial eta squared.

Tab. 16 Joint angular velocity during the continuous load trial

		5 min	10 min	15 min	20 min	25 min	30 min	η_p^2	p
SF_ω	Max [$°\cdot s^{-1}$]	$265 \pm 42^{c,d,e,f}$	272 ± 44^{f}	281 ± 42^{a}	287 ± 50^{a}	293 ± 49^{a}	$300 \pm 55^{a,b}$	**0.576*** **	$< 0.001^{g}$
	Min [$°\cdot s^{-1}$]	$-197 \pm 30^{e,f}$	-204 ± 36^{f}	-211 ± 38	-212 ± 41^{f}	-220 ± 39^{a}	$-224 \pm 43^{a,b,d}$	**0.467*** **	< 0.001
	Range [$°\cdot s^{-1}$]	$462 \pm 70^{c,d,e,f}$	476 ± 78^{f}	492 ± 79^{a}	500 ± 89^{a}	513 ± 87^{a}	$524 \pm 96^{a,b}$	**0.569*** **	< 0.001
SA_ω	Max [$°\cdot s^{-1}$]	88 ± 21	94 ± 25	96 ± 21	101 ± 28	95 ± 27	98 ± 27	0.104	0.298^{g}
	Min [$°\cdot s^{-1}$]	-106 ± 29^{f}	-115 ± 32	-118 ± 29	-122 ± 36	-120 ± 32	-122 ± 31^{a}	**0.265***	0.015^{g}
	Range [$°\cdot s^{-1}$]	195 ± 48	208 ± 55	214 ± 48	223 ± 63	215 ± 54	220 ± 54	0.201	0.069^{g}
SR_ω	Max [$°\cdot s^{-1}$]	96 ± 33	105 ± 26	104 ± 26	109 ± 41	110 ± 42	113 ± 40	0.134	0.150
	Min [$°\cdot s^{-1}$]	-85 ± 20	-94 ± 28	-99 ± 28	-95 ± 31	-102 ± 34	-106 ± 35	**0.269***	0.026^{g}
	Range [$°\cdot s^{-1}$]	181 ± 51	199 ± 50	202 ± 47	204 ± 66	212 ± 71	220 ± 71	0.221	0.058^{g}
EF_ω	Max [$°\cdot s^{-1}$]	$290 \pm 37^{c,d,e,f}$	298 ± 41	308 ± 42^{a}	314 ± 50^{a}	318 ± 48^{a}	323 ± 54^{a}	**0.504*** **	$< 0.001^{g}$
	Min [$°\cdot s^{-1}$]	$-305 \pm 40^{c,e,f}$	-314 ± 46	-325 ± 46^{a}	-328 ± 52	-335 ± 50^{a}	-334 ± 48^{a}	**0.435*** **	0.001^{g}
	Range [$°\cdot s^{-1}$]	$595 \pm 74^{c,d,e,f}$	611 ± 85	632 ± 85^{a}	643 ± 101^{a}	653 ± 96^{a}	658 ± 99^{a}	**0.499*** **	$< 0.001^{g}$
PF_ω	Max [$°\cdot s^{-1}$]	67 ± 22	73 ± 24	80 ± 26	76 ± 30	78 ± 29	74 ± 30	0.116	0.254^{g}
	Min [$°\cdot s^{-1}$]	-68 ± 20	-68 ± 24	-76 ± 24	-75 ± 25	-78 ± 24	-77 ± 21	**0.246** **	0.007
	Range [$°\cdot s^{-1}$]	135 ± 38	141 ± 46	156 ± 45	152 ± 51	156 ± 50	150 ± 48	0.192	0.088^{g}
RD_ω	Max [$°\cdot s^{-1}$]	42 ± 17	40 ± 21	37 ± 26	39 ± 25	38 ± 31	41 ± 27	0.040	0.619^{g}
	Min [$°\cdot s^{-1}$]	-41 ± 24	-37 ± 23	-35 ± 21	-38 ± 25	-40 ± 29	-42 ± 23	0.115	0.254^{g}
	Range [$°\cdot s^{-1}$]	83 ± 38	77 ± 43	72 ± 46	77 ± 49	77 ± 59	83 ± 49	0.089	0.363^{g}
TF_ω	Max [$°\cdot s^{-1}$]	23 ± 14	22 ± 11	23 ± 13	23 ± 14	21 ± 14	27 ± 22	0.079	0.396^{g}
	Min [$°\cdot s^{-1}$]	-23 ± 13	-23 ± 13	-24 ± 14	-23 ± 13	-23 ± 15	-29 ± 22	0.093	0.326^{g}
	Range [$°\cdot s^{-1}$]	46 ± 27	45 ± 23	47 ± 26	46 ± 26	45 ± 28	56 ± 44	0.089	0.345^{g}

Values are expressed as mean value ($\bar{x}$) and standard deviation (SD). [a] = significant difference in post-hoc comparison to 5 min ($p \leq 0.05$); [b] = significant difference in post-hoc comparison to 10 min ($p \leq 0.05$); [c] = significant difference in post-hoc comparison to 15 min ($p \leq 0.05$); [d] = significant difference in post-hoc comparison to 20 min ($p \leq 0.05$); [e] = significant difference in post-hoc comparison to 25 min ($p \leq 0.05$); [f] = significant difference in post-hoc comparison to 30 min ($p \leq 0.05$); [g] = degrees of freedom adjusted based on Greenhouse-Geisser due to missing sphericity assumption. Significant time effects * $p \leq 0.05$; ** $p \leq 0.01$; *** $p \leq 0.001$. EF_ω = elbow-flexion angular velocity; Max = maximal value; Min = minimal value; p = probability of committing a type 1 error; PF_ω = palmar-flexion angular velocity; RD_ω = radial-duction angular velocity; SA_ω = shoulder-abduction angular velocity; SF_ω = shoulder-flexion angular velocity; SR_ω = shoulder internal-rotation angular velocity; TF_ω = trunk-flexion angular velocity; η_p2 = partial eta squared.

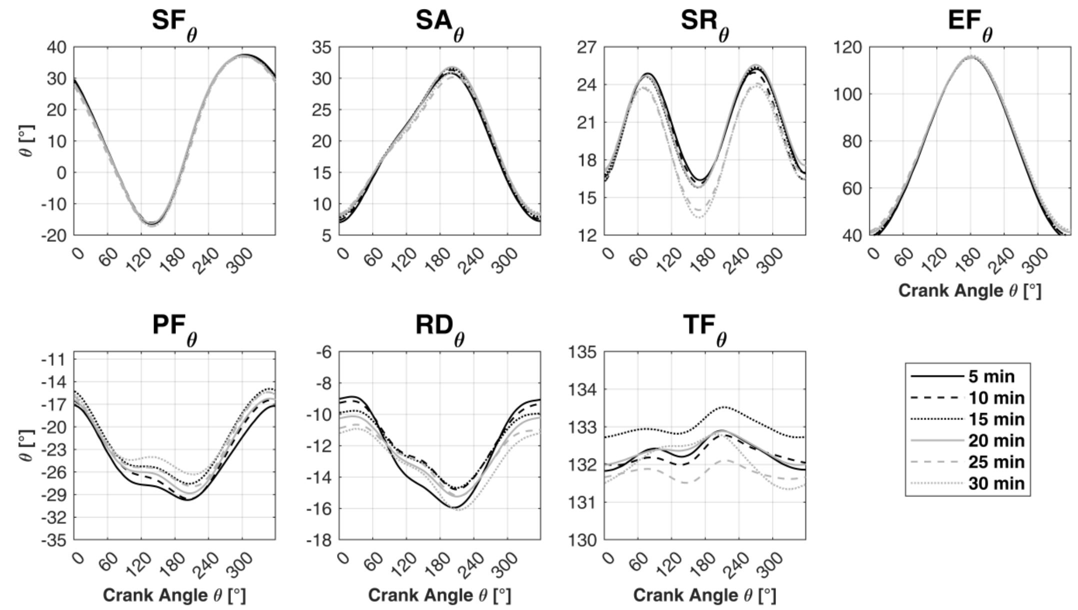

Fig. 20 Joint angles with respect to crank angle during the course of the continuous load trial

Values are expressed as the mean curves across all participants. EF_θ = elbow-flexion angle; PF_θ = palmar-flexion angle; RD_θ = radial-duction angle; SA_θ = shoulder-abduction angle; SF_θ = shoulder-flexion angle; SR_θ = shoulder internal-rotation angle; TF_θ = trunk-flexion angle.

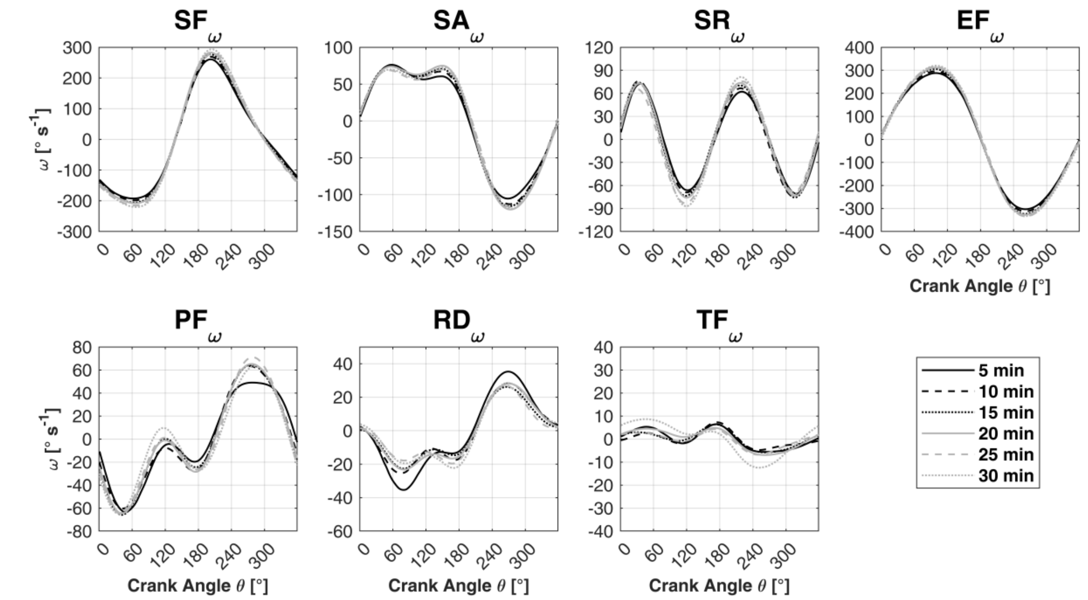

Fig. 21 Joint angular velocity with respect to crank angle during the course of the continuous load trial

Values are expressed as the mean curves across all participants. EF_ω = elbow-flexion angular velocity; PF_ω = palmar-flexion angular velocity; RD_ω = radial-duction angular velocity; SA_ω = shoulder-abduction angular velocity; SF_ω = shoulder-flexion angular velocity; SR_ω = shoulder internal-rotation angular velocity; TF_ω = trunk-flexion angular velocity.

4.3.3 Muscular activity

Muscular effort in terms of iEMG increased in EC ($\eta_P^2 = 0.336$, $p = 0.005$), FC ($\eta_P^2 = 0.336$, $p = 0.006$) and DP $\eta_P^2 = 0.310$, $p = 0.025$) (Tab. 17, Fig. 22). Since LD demonstrated very low activation throughout the CLT, MAPs were not considered for this muscle. Due to sweat contamination, LD signal was lost in one participant (P08) from minute 25 onwards. Onset of activation appeared earlier in crank cycle for DA ($\eta_P^2 = 0.469$, $p = 0.001$), PM ($\eta_P^2 = 0.454$, $p = 0.001$), RA ($\eta_P^2 = 0.335$, $p = 0.023$), BB ($\eta_P^2 = 0.276$, $p = 0.014$) and FC ($\eta_P^2 = 0.252$, $p = 0.025$). The RoA increased for RA ($\eta_P^2 = 0.462$, $p < 0.001$), DA ($\eta_P^2 = 0.357$, $p = 0.008$), FC ($\eta_P^2 = 0.282$, $p = 0.019$) and TD ($\eta_P^2 = 0.223$, $p = 0.014$). PM demonstrated an earlier offset during the course of the CLT ($\eta_P^2 = 0.289$, $p = 0.015$). The period of co-contraction between DP and DA increased from 44° at 5 min to 50° at 30 min (Fig. 23). For BB and TB, the period of co-contraction decreased from 51° to 43°.

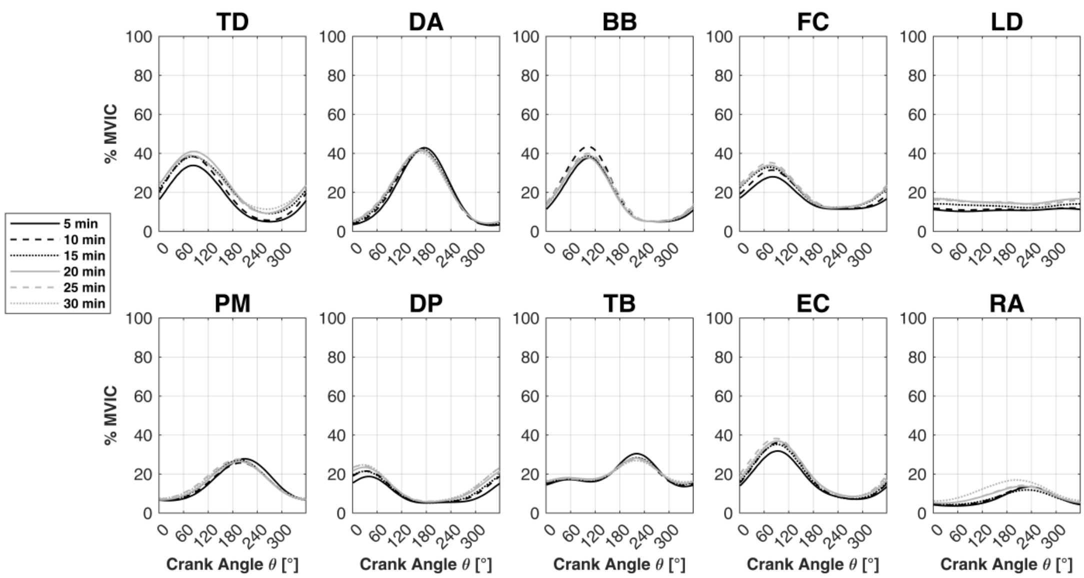

Fig. 22 Muscular activity with respect to crank angle during the course of the continuous load trial
Values are expressed as a percentage of maximal voluntary isometric contraction (MVIC) and mean curves across all participants. BB = M. biceps brachii, Caput breve; DA = M. deltoideus, Pars clavicularis; DP = M. deltoideus, Pars spinalis; EC = M. extensor carpi ulnaris (forearm extensors); FC = M. flexor carpi radialis (forearm flexors); LD = M. latissimus dorsi; PM = M. pectoralis major, Pars sternalis; RA = M. rectus abdominis; TB = M. triceps brachii, Caput laterale; TD = M. trapezius, Pars descendens.

Tab. 17 Muscular activity during the continuous load trial

		5 min	10 min	15 min	20 min	25 min	30 min	η_p^2	p
TD	iEMG [%]	17 ± 12	20 ± 16	22 ± 15	24 ± 18	23 ± 17	23 ± 17	0.222	0.081[g]
	Onset [°]	353 ± 18	353 ± 21	355 ± 33	353 ± 33	352 ± 37	355 ± 37	0.007	0.824[g]
	Offset [°]	182 ± 22	185 ± 23	195 ± 44	191 ± 32	195 ± 40	195 ± 49	0.078	0.375[g]
	RoA [°]	189 ± 18	192 ± 17	199 ± 19	198 ± 17	203 ± 18	201 ± 18	**0.223***	0.014
PM	iEMG [%]	15 ± 8	15 ± 8	15 ± 7	15 ± 7	16 ± 8	16 ± 8	0.122	0.239[g]
	Onset [°]	116 ± 20[c,e,f]	108 ± 22	105 ± 23[a]	104 ± 27	97 ± 30[a]	99 ± 28[a]	**0.454*****	0.001[g]
	Offset [°]	299 ± 13	293 ± 16	291 ± 15	290 ± 14	288 ± 16	289 ± 17	**0.289***	0.015[g]
	RoA [°]	183 ± 20	185 ± 20	185 ± 19	186 ± 21	191 ± 23	190 ± 21	0.223	0.055[g]
DA	iEMG [%]	19 ± 5	19 ± 5	20 ± 5	20 ± 5	20 ± 6	19 ± 5	0.073	0.431[g]
	Onset [°]	85 ± 22[b,d,e,f]	77 ± 24[a]	74 ± 28[e]	71 ± 30[a]	67 ± 28[a,c]	71 ± 26[a]	**0.469*****	0.001[g]
	Offset [°]	261 ± 10	257 ± 11	256 ± 13	255 ± 12	255 ± 11	256 ± 11	0.211	0.046[g]
	RoA [°]	176 ± 17[f]	180 ± 19	182 ± 19	184 ± 21	188 ± 22	185 ± 18[a]	**0.357****	0.008[g]
DP	iEMG [%]	10 ± 4	11 ± 5	11 ± 5	13 ± 7	13 ± 7	14 ± 7	**0.310***	0.025[g]
	Onset [°]	324 ± 24	316 ± 32	314 ± 33	313 ± 41	307 ± 43	310 ± 44	0.194	0.108[g]
	Offset [°]	129 ± 53	123 ± 41	126 ± 52	122 ± 33	130 ± 60	121 ± 23	0.082	0.363[g]
	RoA [°]	165 ± 41	167 ± 26	172 ± 40	168 ± 25	182 ± 34	172 ± 23	0.103	0.295[g]
BB	iEMG [%]	17 ± 7	20 ± 9	18 ± 9	18 ± 9	19 ± 11	18 ± 10	0.148	0.165[g]
	Onset [°]	17 ± 20	11 ± 25	10 ± 26	6 ± 29	5 ± 27	7 ± 27	**0.276***	0.014
	Offset [°]	180 ± 15	177 ± 12	178 ± 12	178 ± 13	182 ± 16	181 ± 13	0.105	0.296[g]
	RoA [°]	163 ± 17	167 ± 19	168 ± 20	171 ± 22	177 ± 26	174 ± 23	**0.250***	0.037[g]
TB	iEMG [%]	20 ± 6	19 ± 6	20 ± 6	20 ± 6	20 ± 6	20 ± 6	0.027	0.910
	Onset [°]	129 ± 34	138 ± 18	138 ± 25	136 ± 24	130 ± 33	138 ± 21	0.056	0.518[g]
	Offset [°]	300 ± 49	315 ± 52	312 ± 43	311 ± 42	310 ± 48	316 ± 43	0.127	0.231[g]
	RoA [°]	170 ± 43	177 ± 46	175 ± 33	176 ± 33	180 ± 38	178 ± 39	0.037	0.670[g]
FC	iEMG [%]	17 ± 10[f]	19 ± 12	20 ± 13	21 ± 14	22 ± 14	21 ± 12[a]	**0.336****	0.006[g]
	Onset [°]	360 ± 24	357 ± 24	351 ± 28	349 ± 30	346 ± 31	346 ± 30	**0.252***	0.025[g]
	Offset [°]	159 ± 13	164 ± 14	160 ± 14	162 ± 12	164 ± 15	160 ± 12	0.049	0.626[g]
	RoA [°]	159 ± 21	167 ± 19	169 ± 18	173 ± 23	178 ± 33	175 ± 24	**0.282***	0.019[g]
EC	iEMG [%]	17 ± 7	19 ± 7	19 ± 7	20 ± 10	21 ± 9	20 ± 9	**0.336****	0.005[g]
	Onset [°]	366 ± 19	363 ± 19	360 ± 17	360 ± 18	355 ± 23	358 ± 23	0.164	0.132[g]
	Offset [°]	189 ± 23	190 ± 21	187 ± 17	191 ± 19	191 ± 23	190 ± 23	0.032	0.712[g]
	RoA [°]	184 ± 17	187 ± 14	187 ± 16	190 ± 17	196 ± 22	192 ± 17	0.159	0.149[g]
RA	iEMG [%]	7 ± 4	8 ± 5	8 ± 5	9 ± 6	9 ± 6	11 ± 10	0.200	0.113[g]
	Onset [°]	156 ± 27	150 ± 31	144 ± 31	132 ± 44	135 ± 41	133 ± 46	**0.335***	0.023[g]
	Offset [°]	319 ± 23	321 ± 28	320 ± 22	312 ± 18	313 ± 14	314 ± 20	0.100	0.306[g]
	RoA [°]	163 ± 28[d,e,f]	171 ± 35	176 ± 36	180 ± 38[a]	178 ± 38[a]	181 ± 40[a]	**0.462*****	< 0.001[g]
LD	iEMG [%]	11 ± 5	11 ± 5	13 ± 7	15 ± 9	15 ± 9	15 ± 8	0.135	0.205[g]

Values are expressed as mean value (x̄) and standard deviation (SD). [a] = significant difference in post-hoc comparison to 5 min ($p \leq 0.05$); [b] = significant difference in post-hoc comparison to 10 min ($p \leq 0.05$); c = significant difference in post-hoc comparison to 15 min ($p \leq 0.05$); [d] = significant difference in post-hoc comparison to 20 min ($p \leq 0.05$); [e] = significant difference in post-hoc comparison to 25 min ($p \leq 0.05$); [f] = significant difference in post-hoc comparison to 30 min ($p \leq 0.05$); [g] = degrees of freedom adjusted based on Greenhouse-Geisser due to missing sphericity assumption. Significant time effects: * $p \leq 0.05$; ** $p \leq 0.01$; *** $p \leq 0.001$. BB = M. biceps brachii, Caput breve; DA = M. deltoideus, Pars clavicularis; DP = M. deltoideus, Pars spinalis; EC = M. extensor carpi ulnaris; FC = M. flexor carpi radialis; iEMG = integrated EMG (muscular effort); LD = M. latissimus dorsi; p = probability of committing a type 1 error; PM = M. pectoralis major, Pars sternalis; RA = M. rectus abdominis; RoA = range of activation; TB = M. triceps brachii, Caput laterale; TD = M. trapezius, Pars descendens.

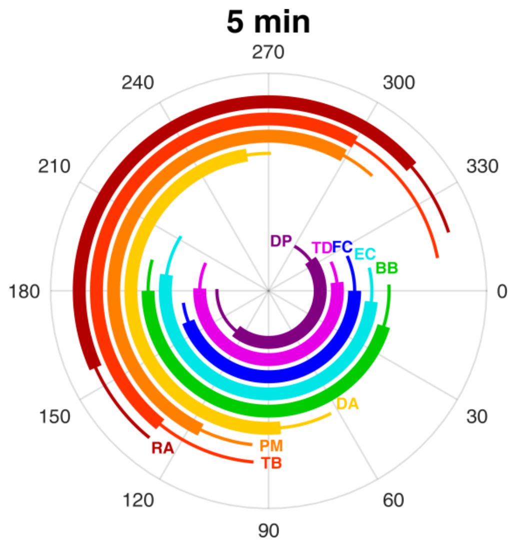

Fig. 23 Muscular activity above threshold with respect to crank angle at 5 min (left) and 30 min (right) of the continuous load trial

The thick lines represent muscular activity above 30%. The thin lines represent the standard deviation addition of the onsets and offsets. BB = M. biceps brachii, Caput breve; DA = M. deltoideus, Pars clavicularis; DP = M. deltoideus, Pars spinalis; EC = M. extensor carpi ulnaris (forearm extensors); FC = M. flexor carpi radialis (forearm flexors); PM = M. pectoralis major, Pars sternalis; RA = M. rectus abdominis; TB = M. triceps brachii, Caput laterale; TD = M. trapezius, Pars descendens.

4.4 Discussion

4.4.1 Fatigue-related alterations

To our knowledge, this study is the first to examine sport-specific fatigue and biomechanical alterations during the course of a CLT in handcycling. The participants performed the CLT at a P4 of 87 ± 12 W and had a heart rate and global RPE at the end of the test of 127 ± 20 min^{-1} and 13 ± 2, respectively (Quittmann et al. 2018a, Quittmann et al. 2018b). Compared to trained SCI handcyclists (149 ± 12 W, 166 ± 14 min^{-1}, 17 ± 2), the cardio-vascular and perceived response during the CLT was remarkably lower (Stangier et al. 2019). However, the metabolic response in terms of lactate concentration at 30 min was similar between able-bodied and SCI athletes (5.4 ± 1.9 and 5.1 ± 1.6 $mmol \cdot l^{-1}$, respectively). Three of twelve participants (25%) exceeded the steady-state criterion, which is consistent with findings in SCI athletes (33%) (Stangier et al. 2019). Combined with the higher locally perceived exertion, these findings indicate that the limiting factors of prolonged exercise differ between trained and untrained athletes (Abbiss and Laursen 2005). It is assumed that trained handcyclists improved their local mechanisms in a way that the gap between peripheral and central fatigue is reduced. Consequently, untrained individuals (like the participants of this study) suffer from locally-based fatigue before central (cardio-vascular) mechanisms are fully utilised. This is consistent with the peripheral failure theory stating that fatigue is related to the cellular mechanisms of excitation-contraction coupling (Allen et al. 2008). Based on these mechanisms, the physiological and biomechanical perspectives on (neuromuscular) fatigue merge. Hence, the assumption of locally-based fatigue can be substantiated by the biomechanical alterations during the course of the CLT.

Spontaneously chosen Cad was increased during the CLT which led to a concomitant reduction in crank torque. Since high muscle forces and an increased extent of vascular occlusion are assumed to be responsible for exhaustion in arm cranking exercises, this might be a strategy to reduce locally-based fatigue (Smith et al. 2001, Price et al. 2007, Quittmann et al. 2018b). Analogous to findings in conventional (leg) cycling, the wrist muscles (FC and EC) faced the highest fatigue in the CLT and seem to be responsible for the force transmission from the more proximal joints to the cranks (Elmer et al. 2012). The increase in iEMG and reduced RoM in RD is consistent with findings in incremental handcycling and indicates that the wrist increased in joint stiffness (Quittmann et al. 2018b, Quittmann et al. 2019). As a link between metabolic and biomechanical responses to prolonged exercise, the participants exceeding the lactate-steady state criterion demonstrated a higher increase in FC effort ($d = 1.74$) compared to those within steady-state ($d = 0.96$). In order to compensate for the higher wrist muscle forces required for an improved distal force transmission and avoiding peripheral fatigue, Cad was increased over time.

Due to the increase in Cad, joint angular velocities were predominantly increased in the sagittal plane (SF and EF). According to findings in incremental handcycling, W_{rot} contribution increased in favour of pulling and the highest increase in muscular effort was highest in DP (Quittmann et al. 2018b, Quittmann et al. 2019). This might be due to the fact that DP is considered as the initiator of the pull phase and thus sensitive to a reinforced pull phase propulsion. As a rather small muscle of the upper extremity, DP might be prone to fatigue in inexperienced participants. Another argument for a reinforced pull phase is the earlier onset of PM, BB, DA and FC indicating the need for supplementary muscular activation. Based on the findings of this study, the increase in muscular effort for TD, PM, DA, BB, TB, LD and RA mentioned elsewhere (Quittmann et al. 2019) and the increase in RoM for SA, SR and RA (Quittmann et al. 2018b) can be confirmed to result from an increase in exercise intensity. For FC, EC and DP, the findings of the preliminary study are – at least in parts – affected by exercise duration. LD demonstrates a rather low activation during continuous handcycling and contributes to propulsion exclusively at high workloads (Quittmann et al. 2019).

In contrast to conventional (leg) cycling, most of the rotational work was accomplished during the flexion movement; not the extension (Bini et al. 2010). Hence, corresponding muscles have to be assigned in accordance with this aspect. As one of the major force producers during the phase of lower W_{rot} contribution, the corresponding muscle for M. biceps femoris (cycling) is TB (handcycling). As demonstrated for M. biceps femoris in cycling, TB demonstrated a double burst pattern of activation in two participants (Suzuki et al. 1982). Suzuki et al. (1982) explained this behaviour by the nature of biarticular muscles in a multi-joint movement. Even though the lateral component of the M. triceps brachii inserts at the humerus and solely affects the elbow joint, another part (Caput longum) inserts at the scapula which might explain the activation behaviour of the co-activated part of the triceps.

4.4.2 Limitations

Based on the differences in power output and the cardio-vascular response between trained handcyclists and the participants of this study, these findings cannot be transferred to elite SCI athletes. However, since P4 was comparable to recreational handcyclists (91 ± 21 W) (Stone et al. 2019c), our findings can be generalised for moderately-trained individuals or newly injured spinal cord patients.

Cad was spontaneously chosen and not standardised during the CLT. This was due to the fact that the individually preferred coping strategy towards continuous load was considered. Previous research in arm-crank exercise found a significantly higher sum of iEMG when spontaneously chosen Cad was increased by 20 min^{-1} (Marais et al. 2004). On the other hand, a reduction in Cad by 20 min^{-1} did not affect iEMG measures. The spontaneously chosen cadences applied in this study corresponded to the literature (Smith et al. 2001). In conventional (leg) cycling, the relative moment contribution at the ankle, knee and hip joints was not affected by alterations in cadence (Mornieux et al. 2007).

Since participants were able to perform the 30-min continuous trial at a standardised intensity without failure, assessing neuromuscular fatigue is limited. Only three participants indicated metabolic fatigue in terms of a violation to the lactate steady-state criterion. Due to the fact that participants were rather inexperienced in handcycling, protocols that require a pacing strategy (e. g. in a time-trial protocol) should be performed with caution. Due to the risk of sweat contamination, longer CLT durations (e. g. in a time-to-exhaustion protocol) would have impeded proper sEMG measurements. However, the results of this study provide the initial insights into fatigue-related mechanisms in prolonged upper extremity cycling. To examine the mechanisms underlying sport-specific fatigue in handcycling, future studies should perform biomechanical analyses during time-trial exercises – even though these might be technically more challenging. Due to the necessity of an individualised pacing strategy in these exercise modes, it is recommended to measure trained and experienced handcyclists.

4.5 Conclusions

During a 30-min CLT at lactate threshold in handcycling, inexperienced individuals demonstrate an increased muscular effort of the forearm muscles (FC and EC) and the posterior part of the deltoideus (DP) at a rather high locally perceived exertion and low utilisation of the cardio-vascular system. This indicates that handcycling is predominantly limited by peripheral mechanisms if the individual is not used to prolonged upper extremity exercise. An increase in cadence might delay locally-based fatigue by a reduced muscle force and concomitant reduced vascular occlusion. It is assumed that the gap between peripheral and central fatigue is reduced due to sport-specific endurance training. Future studies should replicate this study by examining the biomechanics of time-trial handcycling in elite SCI handcyclists.

5 Normalising surface EMG in handcycling

Normalising surface EMG of ten upper-extremity muscles in handcycling: Muscle-specific vs. sport-specific MVICs

Oliver J. Quittmann[1], Joshua Meskemper[2], Kirsten Albracht[2,3], Thomas Abel[1,4], Tina Foitschik[1] & Heiko K. Strüder[1]

1 Institute of Movement and Neurosciences, German Sport University Cologne

2 Institute of Biomechanics and Orthopaedics, German Sport University Cologne

3 Faculty of Medical Engineering and Technomathematics, University of Applied Sciences Aachen

4 European Research Group in Disability Sport (ERGiDS)

Under Review in:

Journal of Electromyography and Kinesiology (Impact factor 2018: 1.753)

Submitted: 30 September, 2019

Abstract

Purpose: Muscular activity in terms of surface electromyography (sEMG) is usually normalised to maximal voluntary isometric contractions (MVICs). This study aims to compare muscle-specific and sport-specific MVIC-modes in handcycling and examine the effect of moving average window size.

Methods: Twelve able-bodied male competitive triathletes performed four sport-specific and ten muscle-specific MVIC trials; each at two distinct occasions. sEMG of ten muscles [M. trapezius (TD); M. pectoralis major (PM); M. deltoideus, Pars clavicularis (DA); M. deltoideus, Pars spinalis (DP); M. biceps brachii (BB); M. triceps brachii (TB); forearm flexors (FC); forearm extensors (EC); M. latissimus dorsi (LD) and M. rectus abdominis (RA)] was recorded and filtered using moving average window sizes of 150, 200, 250 and 300 ms.

Results: Sport-specific MVICs were higher compared to muscle-specific MVICs for TB, DA, DP and LD, whereas FC, TD, BB and RA demonstrated lower values. PM and EC demonstrated no significant difference between MVIC-modes. Moving average window size had no effect on MVIC outcomes.

Conclusions: MVIC-mode should be taken into account when normalised sEMG data are illustrated in handcycling. Sport-specific MVICs are advantageous in terms of time, fatigue and amplitude for some muscles (TB, DA, DP and LD), but should be augmented by muscle-specific MVICs for FC, TD, BB and RA.

5.1 Introduction

Surface Electromyography (sEMG) is a non-invasive method for examining muscular activity during movements in sports (de Luca 1997). Investigating the activation patterns of muscles helps to understand their interplay and the coordination underlying sport-specific movements. However, sEMG amplitude is influenced by many technical, anatomical and physiological factors that hinder their interpretation. For example, moving average window size affects sEMG amplitude up to factor 1.5 (Schwartz et al. 2017). In order to compare muscular activity between tasks, muscles and individuals, sEMG signals need to be normalised (Lehman and McGill 1999).

Normalisation of sEMG can be applied by using various methods that differ in terms of validity, reliability and specificity (Burden and Bartlett 1999). Maximal voluntary isometric contractions (MVICs) were found to be the most suitable method to set a reference value of 100% muscular activation since they demonstrate a high reliability and are not affected by contraction mode (Burden 2010). Nevertheless, MVICs need to be applied in an adequate position to attain the highest sEMG amplitude of a certain muscle. For complex joints with many degrees of freedom and biarticular muscles, finding an optimal MVIC position is challenging. When sEMG is measured for many muscles simultaneously, performing muscle-specific MVICs for every muscle is rather time-consuming and may induce fatigue. In order to reduce the amount of MVICs and thus the participants' effort for normalisation, performing sport-specific MVICs may be a suitable alternative (Rota et al. 2013).

In handcycling, the athletes propel their three-wheeled vehicle (called handcycle or handbike) with the power of their arms and trunk. Due to the synchronous crank mode, handcycling propulsion consists of a consecutive pull and push phase. As a Paralympic sport for people with spinal cord injury (SCI) or amputation of the lower extremity, handcycling can also be applied as a cross-training option in swimmers, rowers or biathletes. Investigating muscular activity in handcycling is relevant in terms of injury prevention (Arnet 2012), performance enhancement (Stone et al. 2019c), classification (Kouwijzer et al. 2018) and strength training needs (Nevin et al. 2018). In a recent study, the muscular activity of ten upper-extremity muscles during handcycling was normalised to sport-specific MVICs (Quittmann et al. 2019). However, it is not clear whether the percentage of MVICs illustrated in this study adequately represents activation effort in all muscles. Hence, the aim of this study is to compare the sEMG amplitude of ten upper extremity muscles between sport-specific and muscle-specific MVICs and moving average window sizes. Based on these findings, a suitable setup for MVIC normalisation methods in handcycling is derived. These findings are relevant for other studies examining activation of upper extremity muscles.

5.2 Methods

5.2.1 Participants

Twelve able-bodied male competitive triathletes (26.0 ± 4.4 yrs., 1.83 ± 0.06 m, 74.3 ± 3.6 kg) participated in the study. Participants gave their written informed consent before participating in the study. The study was approved by the German Sport University Cologne Ethics Committee (No. 52 / 2016) and complied with the ethical standards of the 1975 Helsinki Declaration modified in 1983.

5.2.2 Experimental protocol

Participants performed ten muscle-specific and four sport-specific MVIC trials; each on two distinct occasions that were separated by one week. MVIC trials consisted of three MVICs with a time under tension of two to three seconds and a duty-cycle of 1.0 (Doheny et al. 2008, Hansson et al. 2000). To ensure a standardised contraction pattern, the examiner provided verbal instructions for MVICs and recovery periods. Participants were instructed to increase tension and apply the highest force possible afterwards during MVICs. The muscular activity of ten muscles [M. trapezius, Pars descendens (TD); M. pectoralis major, Pars sternalis (PM); M. deltoideus, Pars clavicularis (DA); M. deltoideus, Pars spinalis (DP); M. biceps brachii, Caput breve (BB); M. triceps brachii, Caput laterale (TB); M. flexor carpi radialis (FC, forearm flexors); M. extensor carpi ulnaris (EC, forearm extensors); M. latissimus dorsi (LD) and M. rectus abdominis (RA)] was measured unilaterally on the dominant (right) side of the participants

Muscle-specific MVICs were applied against manual resistance applied by the examiner at positions based on the guidelines of SENIAM and the manufacturer (Hermens et al. 2000, Konrad 2006) (Fig. 24). In order to provide isometric conditions, the examiner adjusted the counterforce the best possible maner. For TD, the examiner applied a downward force in the participants' shoulders in a standing position (Al-Qaisi and Aghazadeh 2015). MVICs for PM were applied in a push-up position at a shoulder-abduction of 80° to 90°, an elbow angle of about 90° and the fingers pointing anteriorly. For DP and DA, the participants applied a posterior and anterior force with an extended arm near to neutral abduction (Hermens et al. 2000). MVICs for BB and TB were performed at an elbow-flexion angle of about 90° (Liu et al. 2015, Roman-Liu and Bartuzi 2018). The examiner stabilised the upper arm to improve and standardise activation conditions. For BB, the forearm was supinated, whereas a neutral forearm position was applied for TB. Elbow flexor (FC) and extensor (EC) MVICs were performed in a neutral wrist position (0° dorsal-flexion and 0° radial-duction) and extended fingers.

For FC, the forearm was supinated, whereas a pronated position was applied for EC. MVICs for LD were applied in a pull-up position (behind the neck) with the participants grasping a bar at a shoulder-abduction and elbow-flexion of approximately 90° (Park and Yoo 2013a). RA MVICs were performed as a trunk-flexion task in a crunch position with the examiner pushing against the shoulders (Lehman and McGill 1999).

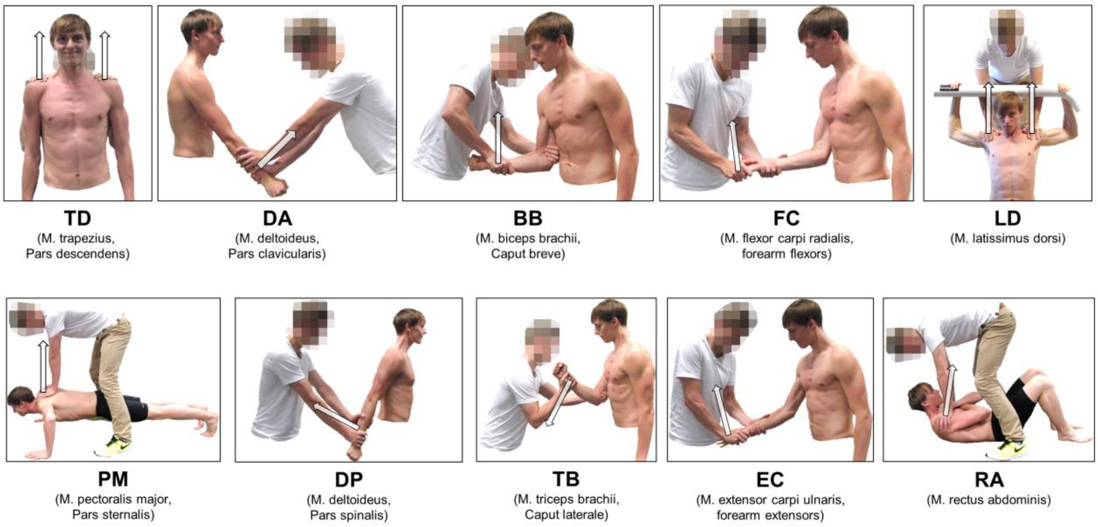

Fig. 24 Muscle-specific MVIC techniques

Muscle-specific MVIC techniques based on the guidelines of the Noraxon U.S.A. Inc. (Konrad 2006). The arrows indicate the force applied against manual resistance of the examiner. MVIC = maximal voluntary isometric contraction.

Sport-specific MVICs were performed in a recumbent racing handcycle (Shark S, Sopur, Sunrise Medical, Malsch, Germany) that was attached to a fully calibrated and validated ergometer (Cyclus 2, TE 2%, 8 Hz, RBM electronic-automation GmbH, Leipzig, Germany). During the sport-specific MVIC trials, the ergometer was mechanically blocked by a pin of steel that was plugged in the brake disk (Fig. 25). MVICs were applied against the blocked cranks at the foremost (0°), lowest (90°), nearest (180°) and highest (270°) crank position as described previously (Quittmann et al. 2019) (Fig. 26). On each occasion, the participants performed MVICs in the same order starting with sport-specific trials (0°, 90°, 180° and 270°) and muscle-specific trials (TD, DA, DP, PM, BB, TB, FC, EC, LD and RA) thereafter. Whereas the duration between each trial was about one minute, the duration between MVIC modes was three to ten minutes.

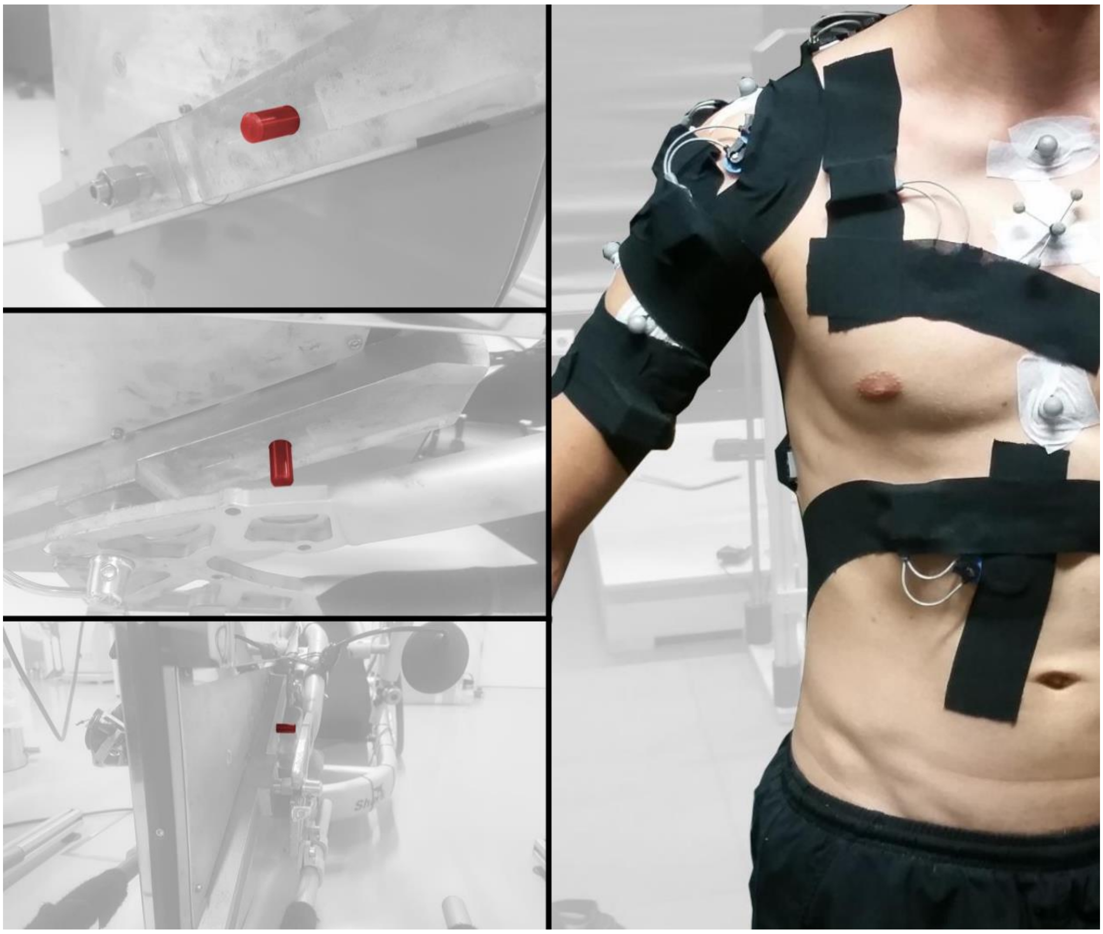

Fig. 25 Blocking of the ergometer using a pin of steel (left) and fixation of the electrodes and sensors (right)

The pin of steel (highlighted in red) was plugged in a hole of the ergometer's brake disk.

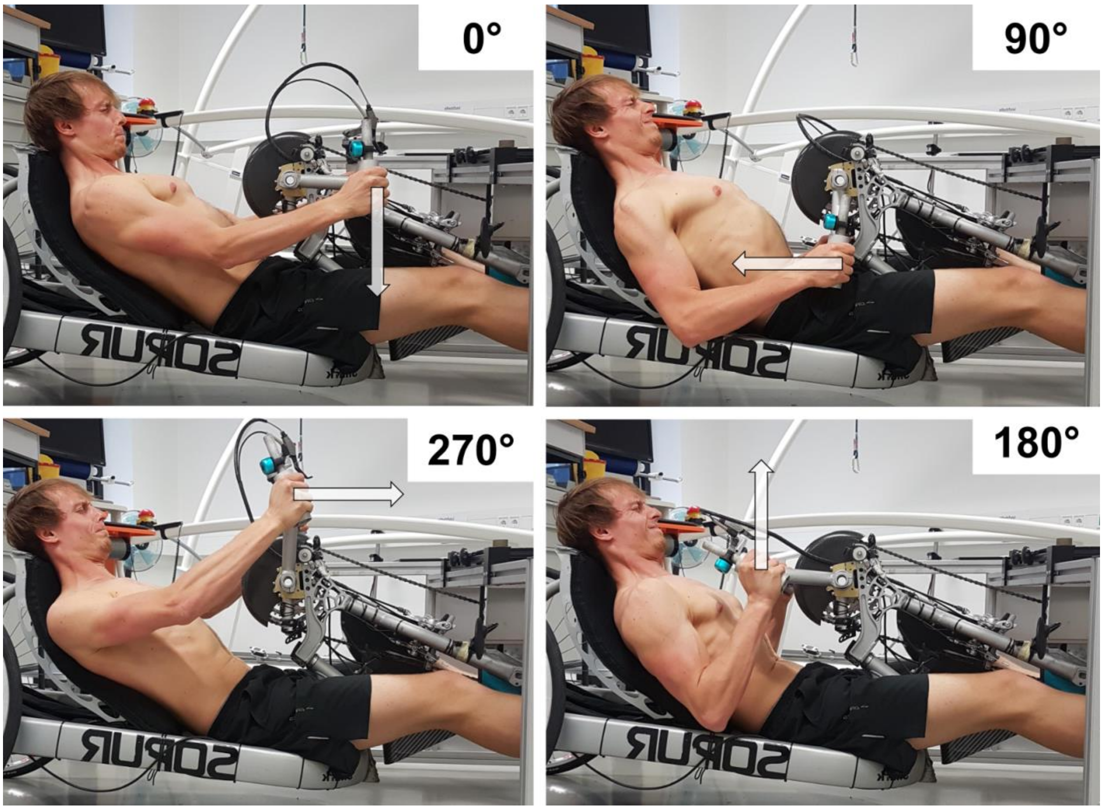

Fig. 26 Sport-specific MVIC positions

The arrows indicate the force applied against the cranks. MVIC = maximal voluntary isometric contraction.

5.2.3 Data recording

Muscular activity was measured using a wireless sEMG system (DTSEMG Sensor®, 1000 Hz, Noraxon Scottsdale, Arizona, USA) (Konrad 2006). The skin of the participants was prepared according to the standards for reporting EMG data of the International Society of Electromyography and Kinesiology (Hermens et al. 2000). Two single-use wet gel Ag/AgCl-electrodes (Ambu BlueSensor N, Ambu A/S, Ballerup, Denmark) were applied on each muscle according to the SENIAM guidelines (Hermens et al. 2000). Electrodes and senders were additionally fixed using kinesiology tape (Elyth®, WINpharma Herstellungs- und Vertriebs-GmbH, Wilhelmsburg, Germany) (Fig. 25).

5.2.4 Data processing

sEMG data were rectified and smoothed using a zero-lag moving average filter with a window size of 150, 200, 250 and 300 milliseconds using MATLAB (R2017b, MathWorks®, Natick, Massachusetts, USA). In order to compare MVIC modes, sport-specific MVICs were normalised to muscle-specific MVICs. Accordingly, for each muscle, the highest value of the muscle-specific MVIC trial was set to 100%. Sport-specific MVIC was set as the highest value attained in all (four) sport-specific MVIC trials. All trials were visually examined for signal quality and measurement errors (Fig. 27). In case a sport-specific trial attained inappropriate signals, the MVIC trial with the next highest sEMG amplitude was used for further analyses.

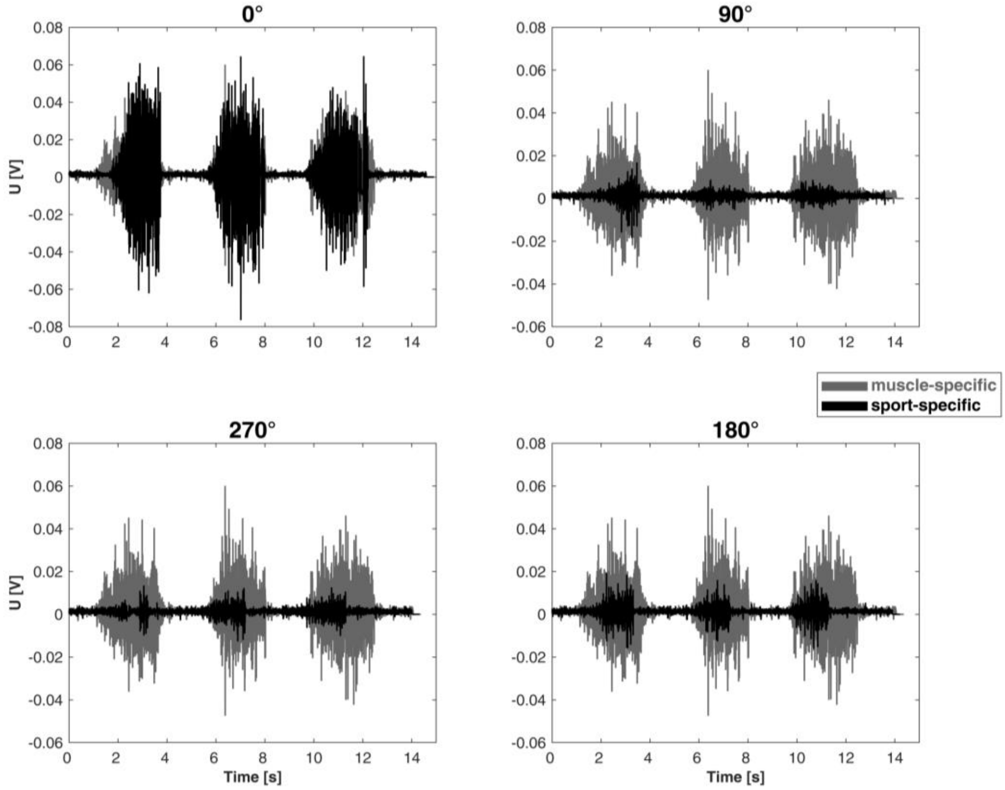

Fig. 27 Exemplary raw-data of sEMG signals during muscle- and sport-specific MVIC trials

The lines indicate the voltage measured of M. latissimus dorsi (LD, P04, T2) during the muscle-specific trial (grey) and the four sport-specific positions (black). At 90°, 180° and 270°, the sport-specific signal is remarkably lower when compared to the muscle-specific trial. At 0°, muscle- and sport-specific signals overlap and demonstrated a higher voltage during the sport-specific trials.

5.2.5 Statistics

Statistical analyses were performed using the Statistical Package for the Social Sciences software (25, SPSS Inc., Chicago, Illinois, USA). Since all (n = 12) participants performed the MVIC trials twice (T1 and T2), the analysis included a total sample size of N = 24. Differences between MVIC modes (muscle-specific and sport-specific) as well as between window sizes (150, 200, 250 and 300 ms) were analysed using a two-way (2 × 4) analysis of variance (ANOVA) with repeated measures. Mauchly's test was used to examine sphericity of window sizes. In case sphericity was violated, degrees of freedom were adjusted using the Greenhouse-Geisser method. Post-hoc comparisons between modes and windows were adjusted using Bonferroni's correction. To analyse the stability of the difference between muscle- and sport-specific trials between T1 and T2, student's t-test was applied. Normality was checked using Kolmogorov-Smirnov test with Lilliefors' correction. The calculated effect sizes for factors and mean differences were partial eta squared (η_P^2) and Cohen's d, respectively. The level of significance was set at $\alpha = 0.05$. To quantify the relevance of the sport-specific positions on sEMG amplitude for a certain muscle, the relative frequency a particular position attained the highest sEMG amplitude of all sport-specific MVIC trials was determined.

5.3 Results

Sport-specific MVICs were significantly higher compared to muscle-specific MVICs for TB ($\eta_P^2 = 0.402$, p = 0.001), DA ($\eta_P^2 = 0.385$, p = 0.001), DP ($\eta_P^2 = 0.213$, p = 0.020) and LD ($\eta_P^2 = 0.167$, p = 0.043) (Tab. 18). For DA and TB, more that 75% of all trials were above muscle–specific MVICs (Fig. 28). However, sport-specific MVICs were significantly lower compared to muscle-specific MVICs for FC ($\eta_P^2 = 0.405$, p = 0.001), TD ($\eta_P^2 = 0.283$, p =

0.006), BB (η_P^2 = 0.190, p = 0.029) and RA (η_P^2 = 0.158, p = 0.049). For FC and RA, more than 75% of all trials were lower compared to muscle–specific MVICs. PM (η_P^2 < 0.001, p = 0.997) and EC (η_P^2 = 0.010, p = 0.635) demonstrated no significant difference between sport- and muscle-specific MVICs. Window size between 150 and 300 ms had no effect on sEMG amplitude in all muscles.

Tab. 18 Sport-specific MVICs with respect to window size for all muscles

					mode		window	
	150 ms	200 ms	250 ms	300 ms	η_P^2	p	η_P^2	p
TD	78 ± 35	78 ± 35	78 ± 36	78 ± 36	**0.283****	0.006	0.005	0.785[g]
PM	101 ± 49	100 ± 46	99 ± 45	99 ± 45	< 0.001	0.977	0.057	0.253[g]
DA	149 ± 64	150 ± 65	150 ± 65	150 ± 65	**0.385*****	0.001	0.018	0.556[g]
DP	119 ± 37	119 ± 37	119 ± 62	118 ± 37	**0.213***	0.020	0.007	0.710[g]
BB	87 ± 30	86 ± 30	85 ± 31	85 ± 30	**0.190***	0.029	0.034	0.496[g]
TB	128 ± 35	127± 34	128 ± 35	128 ± 36	**0.402*****	0.001	0.013	0.647[g]
FC	69 ± 40	69 ± 40	68 ± 40	67 ± 39	**0.405*****	0.001	0.045	0.312[g]
EC	95 ± 42	96 ± 43	96 ± 43	96 ± 43	0.010	0.635	0.010	0.699[g]
LD	119 ± 42	119 ± 44	119 ± 44	119 ± 45	**0.167***	0.043	< 0.001	0.972[g]
RA	83 ± 43	82 ± 41	82 ± 41	82 ± 41	**0.158***	0.049	0.022	0.497[g]

Sport-specific MVICs are expressed in relation to muscle-specific trials [%] as mean ($\bar{x}$) and standard deviation (SD) Significant mode effects * p ≤ 0.05; ** p ≤ 0.01; *** p ≤ 0.001. BB = M. biceps brachii, Caput breve; DA = M. deltoideus, Pars clavicularis; DP = M. deltoideus, Pars spinalis; EC = M. extensor carpi ulnaris (forearm extensors); FC = M. flexor carpi radialis (forearm flexors); LD = M. latissimus dorsi; MVIC = maximal voluntary isometric contraction; p = probability of committing a type I error; PM = M. pectoralis major, Pars sternalis; RA = M. rectus abdominis; TB = M. triceps brachii, Caput laterale; TD = M. trapezius, Pars descendens; η_P^2 = partial eta squared.

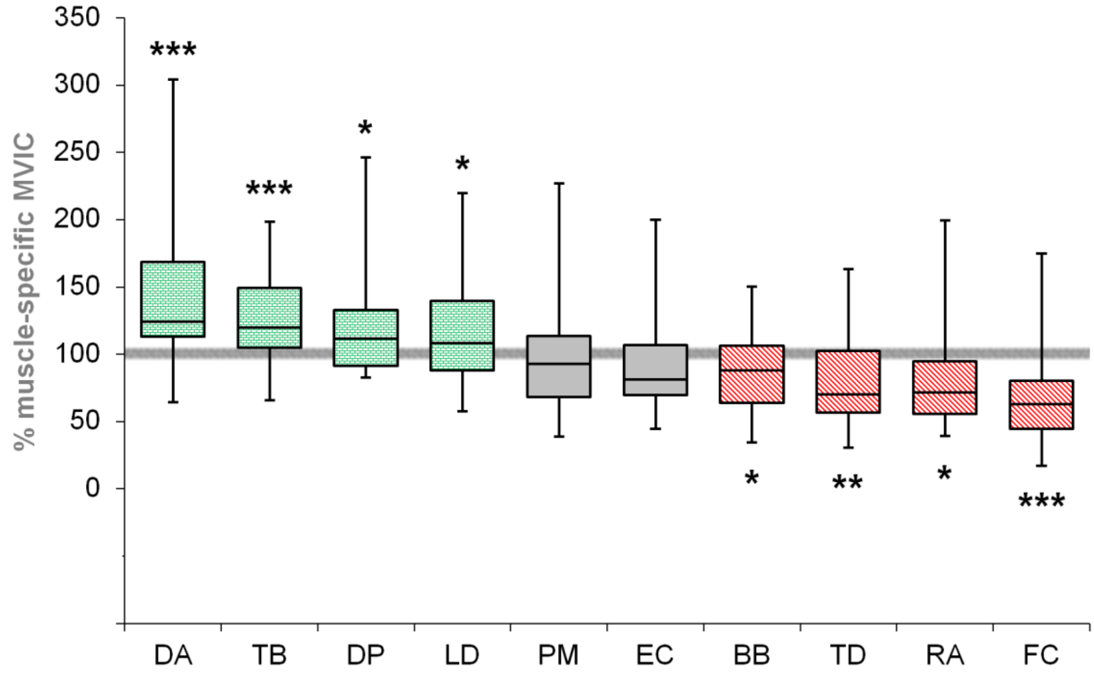

Fig. 28 Comparison of sport-specific and muscle-specific MVIC trials

Values are expressed as box-whisker plots including median, quartiles, minimum and maximum. Significant difference between sport-specific and muscle-specific MVICs (compared to 100%) * $p \leq 0.05$; ** $p \leq 0.01$; *** $p \leq 0.001$; MVIC = maximal voluntary isometric contraction.

Comparisons between occasions demonstrated a significant reduction of the ratio between sport-specific and muscle-specific MVICs (indicating a closer agreement between modes) for EC (d = 1.334, p = 0.003) and DA (d = 0.897, p = 0.010) (Tab. 19). For the other muscles, no significant difference between occasions was found.

Tab. 19 Differences in sport-specific MVICs between trials

	T1	T2	(T2-T1)	d	p
TD	84 ± 37	72 ± 34	-12 ± 49	0.236	0.429
PM	107 ± 57	92 ± 33	-15 ± 59	0.255	0.395
DA	178 ± 78	122 ± 31	-56± 63	**0.897****	0.010
DP	120 ± 45	117 ± 30	-3 ± 47	0.058	0.844
BB	81 ± 29	90 ± 32	+9 ± 37	0.255	0.395
TB	121 ± 35	134 ± 34	+13 ± 37	0.184	0.243
FC	74 ± 50	64 ± 28	-10 ± 54	0.356	0.538
EC	122 ± 47	70 ± 14	-58 ± 44	**1.334****	0.003
LD	126 ± 53	112 ± 33	-13 ± 53	0.251	0.402
RA	88 ± 54	76 ± 25	-12 ± 64	0.191	0.522

Sport-specific MVICs are expressed in relation to muscle-specific trials [%] as mean (x̄) and standard deviation (SD) for a window size of 200 ms. ** significant decrease from T1 to T2 ($p \leq 0.01$). BB = M. biceps brachii, Caput breve; d = Cohen’s d; DA = M. deltoideus, Pars clavicularis; DP = M. deltoideus, Pars spinalis; EC = M. extensor carpi ulnaris (forearm extensors); FC = M. flexor carpi radialis (forearm flexors); LD = M. latissimus dorsi; MVIC = maximal voluntary isometric contraction; p = probability of committing a type I error; PM = M. pectoralis major, Pars sternalis; RA = M. rectus abdominis; TB = M. triceps brachii, Caput laterale; TD = M. trapezius, Pars descendens.

For TD, the highest sport-specific MVICs were found at 90° (67%) and 180° (33%) (Fig. 29). For PM, the highest sport-specific MVICs were found at 270° (50%), 180° (46%) and 0° (4%). Whereas the highest sport-specific MVICs of DP were found at 90° (54%) and 0° (46%), the highest sport-specific MVICs of DA were found at 180° (75%) or 270° (25%). For BB, 90° (79%), 180° (13°) and 0° (8%) demonstrated the highest sport-specific MVICs. For TB, sport-specific MVICs were highest at 270° (71%), 180° (17%) and 0° (13%). For FC and EC, the highest sport-specific MVICs were found in almost all positions with the highest frequency found at 90° (58% and 62%, respectively). With only few exceptions, the highest sport-specific MVICs for LD and RA were found at 0° (96% and 92%, respectively).

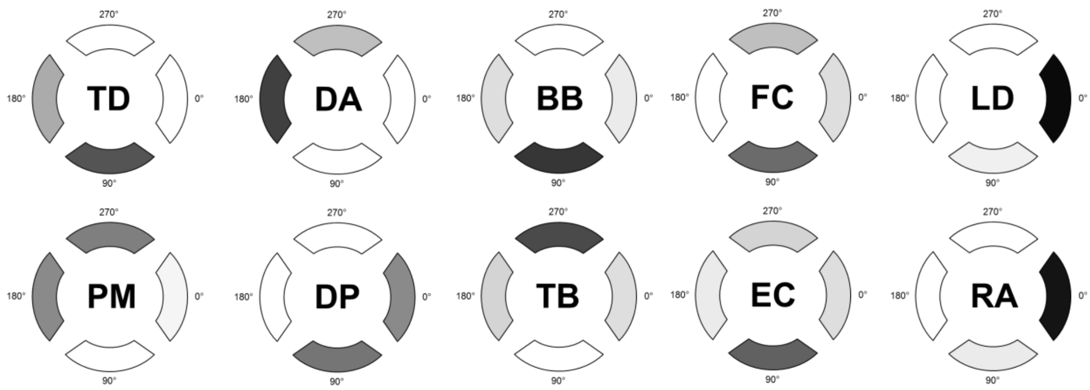

Fig. 29 Occurrence of the highest sport-specific MVIC for all muscles

Schematic illustration based on the percentage at which a certain position attained the highest voltage signal of all sport-specific MVIC trials. Black = 100%, white = 0%, grey = in between (the darker, the more frequent). BB = M. biceps brachii, Caput breve; DA = M. deltoideus, Pars clavicularis; DP = M. deltoideus, Pars spinalis; EC = M. extensor carpi ulnaris; FC = M. flexor carpi radialis; LD = M. latissimus dorsi; MVIC = maximal voluntary isometric contraction; PM = M. pectoralis major, Pars sternalis; RA = M. rectus abdominis; TB = M. triceps brachii, Caput laterale; TD = M. trapezius, Pars descendens.

5.4 Discussion

5.4.1 Normalisation of sEMG in handcycling

In order to derive a suitable setup for MVIC normalisation methods in handcycling, the aim of this study was to compare the sEMG amplitude of ten upper extremity muscles between sport-specific and muscle-specific MVICs and moving average window sizes between 150 and 300 ms.

TD activation was significantly lower in sport-specific MVICs when compared to muscle-specific MVICs indicating that sport-specific normalisation underestimates TD activation. This might be due to the fact that TD has a rather stabilising function during push and pull tasks and depends on how the participants realised sport-specific MVICs (Ho et al. 2019). Since participants were instructed to apply the highest force on the cranks, TD is maximally activated by chance. To improve TD activation during MVICs, movement instructions (e. g. "attempt to use only the shoulder muscles") might reduce amplitude variation (Al-Qaisi and Aghazadeh 2015). Furthermore, it was shown that TD activation is rather inhomogeneous during continuous trials (Holtermann and Roeleveld 2006) and reduced in patients who are suffering from sub-acromial pain syndrome (Hansson et al. 2000). TD activation should be normalised muscle-specifically by using the task described in this study or another task that is available in the literature. Further MVIC tasks for TD are shoulder-abduction task above 90° (Al-Qaisi and Aghazadeh 2015), shoulder-abduction with head rotation and lateral-flexion (Zanca et al. 2014) or the 'flexion 125' task (Boettcher et al. 2008).

Since PM activation did not significantly differ between muscle- and sport-specific MVICs, both modes can be used to adequately normalise MVICs in handcycling. In SCI athletes, performing a push-up might be challenging due to reduced hip and trunk stability. Hence, performing MVICs between 180° and 270° seems to be a suitable alternative.

For the deltoideus muscles, muscle-specific MVICs were found to be inadequate for referencing full activation. This might be due to the fact that deltoideus activation is higher for increasing shoulder-abduction (elevation in the frontal plane) which was rather low in this study (Park et al. 2008, Phillips and Karduna 2017). Hence, sport-specific MVICs between 0° and 90° for DP and between 180° and 270° for DA demonstrate higher amplitude and should be the preferred choice for sEMG in handcycling.

For the major elbow flexor (BB), sport-specific MVICs resulted in significantly lower sEMG amplitude compared to muscle-specific trials. This might be due to the fact that several muscles are activated during pulling which might reduce activation of a single muscle. Depending on the participants' pulling technique, the activation might shift between agonists (here, BB and DP) during a sport-specific task (Ho et al. 2019, Roman-Liu and Bartuzi 2018). Hence, muscle-specific MVICs around 90° should be performed for BB normalisation.

TB achieved higher sEMG amplitude during sport-specific MVICs compared to muscle-specific contractions. This might be due to the fact that elbow-flexion angle was lower and more extended (e. g. at 270° crank angle) compared to muscle-specific MVICs (at 90° elbow-flexion). In a previous study, TB activation tended to be higher for lower elbow-flexion angles (Doheny et al. 2008). Another argument for higher TB activation during sport-specific trials is that participants were able to push themselves against the backrest of the handcycle which facilitates maximal activation. Thus, TB should be normalised sport-specifically at a crank angle of approximately 270°.

The remarkably lower FC amplitudes during sport-specific MVICs highlight the necessity for muscle-specific normalisation. The large difference between modes might be due to the fact that the grip on the cranks was performed in a dorsal-flexed wrist (Quittmann et al. 2018b). An easy and reliable alternative for muscle-specific FC normalisation is a maximal grip task using a hydraulic hand grip dynamometer (Hashemi Oskouei et al. 2013).

EC amplitude did not differ between MVIC modes. Even though most of the highest sport-specific MVICs were found at 90°, EC demonstrated highest the activation in all positions. This might be influenced by the fact that forearm extensors demonstrate more variation in sEMG signals compared to the flexors (Salonikidis et al. 2011). To reduce variation during sport-specific MVICs, the participants might be instructed to perform a maximal grip task while pulling at the 90° position or using a hydraulic hand grip dynamometer.

LD activation during sport-specific MVICs at 0° was higher compared to muscle-specific trials. This corresponds to previous research demonstrating higher LD activation for lower shoulder elevation angles (Park and Yoo 2013b) and row style MVICs (Beaudette et al. 2014). Whereas LD MVICs are frequently applied in the frontal plane, the sport-specific MVICs of this study were applied in the sagittal plane. Since sEMG activity was not affected by movement planes (Park and Yoo 2013b), the findings of our study can be generalised. Hence, sport-specific MVIC normalisation of LD amplitude is a suitable approach in handcycling. However, it must be noted that LD activation using sEMG electrodes is overestimated when compared to intramuscular electrodes due to crosstalk contamination (Ginn and Halaki 2015).

For RA, lower amplitudes were found during sport-specific trials. This is not surprising since none of the positions performed seems to trigger full RA activation. Since trunk activation ability is a serious aspect in handcycling classification (Kouwijzer et al. 2018), a proper RA normalisation should be applied. Hence, a muscle-specific trunk-flexion movement against manual resistance seems to be more suitable for RA normalisation; especially if the upper and lower parts of RA are compared (Lehman and McGill 1999, Vera-Garcia et al. 2010).

Moving average window sizes (100 to 2000 ms) affected sEMG amplitude (Schwartz et al. 2017), whereas no effect was found in this study (150 to 300 ms). The windows of this study represent the most common range of window sizes (Phillips and Karduna 2017). However, previous research indicated that 500 ms improves intra-session repeatability (Schwartz et al. 2017).

5.4.2 Limitations

As a limitation of this study, MVIC trials were performed in a standardised (not randomised) order. This might lead to a carry-over effect from sport-specific to muscle-specific trials. The tendency for lower sport-specific MVICs (expressed as a percentage of muscle-specific MVICs) might be influenced by reduced fatigue due to familiarisation with MVIC procedures. However, it cannot be concluded which MVIC mode was (more) affected by familiarisation. For muscles demonstrating higher amplitude during sport-specific trials (DA, TB, DP and LD), these aspects should be taken into account. Furthermore, bilateral normalisation procedures (as applied during sport-specific trials) were found to attain an approximately 20% lower sEMG amplitude when compared to unilateral (muscle-specific) procedures (Bao et al., 1995). This aspect should be considered for muscles demonstrating lower amplitude during sport-specific trials (BB, TD, RA and FC).

To provide a practical normalisation procedure, muscle-specific MVICs were applied against manual and not mechanical resistance. Hence, the examiner's counterforce might affect the accuracy and reliability of sEMG amplitude during muscle-specific trials. Unfortunately, this study did not quantify the reliability of MVIC procedures. Removing and replacing electrodes on another occasion demonstrated a substantial reduction in reliability (Hashemi Oskouei et al. 2013), which is why reliability of sEMG amplitude was not assessed in this study. Future studies need to quantify intra-session reliability of muscle- and sport-specific MVICs in handcycling to assess their reproducibility and compare reliability between modes and window sizes.

5.4.2 Practical applications

Based on the findings of this study, the following eight trials (four sport-specific and four muscle-specific) should be performed for adequate sEMG normalisation in handcycling:

1. MVICs in foremost position (0°): Relevant for LD, DP, EC and PM.
2. MVICs in lowest position (90°): Relevant for DP and EC.
3. MVICs in nearest position (180°): Relevant for DA, PM and TB and EC.
4. MVICs in highest position (270°): Relevant for TB, PM, DA and EC.
5. MVICs on a hydraulic hand grip dynamometer: Relevant for FC and EC.
6. MVICs by using the shoulder elevation task: Relevant for TD.
7. MVICs by using elbow-flexion task (at 90° flexion): Relevant for BB.
8. MVICs by using the trunk-flexion task (lying position): Relevant for RA.

5.5 Conclusions

MVIC-mode should be taken into account when normalised sEMG data are illustrated in handcycling. Sport-specific MVICs are advantageous in terms of time, fatigue and amplitude for TB, DA, DP and LD, but should be augmented by muscle-specific MVICs for FC, TD, BB and RA. Moving average window sizes between 150 and 300 ms can be used interchangeably. These findings are relevant for sEMG normalisation of other upper extremity exercises (e. g. swimming, rowing and biathlon).

6 Maximal lactate accumulation rate in handcycling and cycling

Maximal lactate accumulation rate and post-exercise lactate kinetics in handcycling and cycling

Oliver J. Quittmann[1], Thomas Abel[1,2], Ramin Vafa[1], Jonas Mester[1], Yannick M. Schwarz[1] & Heiko K. Strüder[1]

[1] Institute of Movement and Neurosciences, German Sport University Cologne

[2] European Research Group in Disability Sport (ERGiDS)

Under Review in:

European Journal of Sport Science (Impact factor 2018: 2.376)

Submitted: 16 July, 2019

Abstract

Purpose: The aim of this study was to assess maximal lactate accumulation rate ($\dot{V}La_{max}$) and peak power output ($P_{max,AO15}$) in a 15-s all-out exercise in handcycling (HC) and cycling (C) in terms of (1) reliability, (2) correlations among and (3) differences between extremities.

Methods: Eighteen female and male competitive triathletes performed two trials (separated by one week) of a 15-s all-out sprint test in HC and C. Tests were performed in a recumbent racing handcycle and on the participants' own road bike which were both attached to an ergometer. Reliability was assessed using intraclass correlation coefficient (ICC).

Results: $P_{max,AO15}$ and $\dot{V}La_{max}$ demonstrated high reliability in HC (ICC = 0.972, ICC = 0.828) and C (ICC = 0.937, ICC = 0.872). $P_{max,AO15}$ (d = -2.54, p < 0.001) and $\dot{V}La_{max}$ (d = -1.62, p < 0.001) were lower in HC compared to C. $P_{max,AO15}$ and $\dot{V}La_{max}$ correlated in HC (r = 0.729, p = 0.001) and C (r = 0.710, p = 0.001). There was no significant correlation between extremities in $P_{max,AO15}$ (r = 0.442, p = 0.066) and $\dot{V}La_{max}$ (r = 0.455, p = 0.058).

Conclusions: $\dot{V}La_{max}$ attained in a 15-s all-out sprint test is highly reliable and related to anaerobic performance in both HC and C. The rather low correlation and individual differences in $\dot{V}La_{max}$ between HC and C indicate an extremity-specific adaptation of anaerobic metabolism. Future studies are encouraged to include $\dot{V}La_{max}$ as a parameter in exercise testing and assess the effects of extremity-specific training regimes on anaerobic metabolism and performance.

6.1 Introduction

Physiological differences between handcycling (HC) and (leg) cycling (C) arise from the relative muscle mass of the limbs, cross-sectional area (CSA) and fibre type of the recruited muscles. Whereas the relative segment mass of the limbs and CSA were shown to be higher for the lower extremities (Lovell et al. 2013, Zatsiorsky and Seluyanov 1985), differences in fibre type are not consistent in literature (Johnson et al. 1973, Polgar et al. 1973).

The physiology of HC and C is reflected in the utilisation of aerobic and anaerobic metabolism whose power can be quantified in exercise testing. Aerobic power is quantified as maximal oxygen uptake ($\dot{V}O_2max$) which was shown to be related to sport-specific performance in C (Craig et al. 1993, Jacobs et al. 2011) and HC (Janssen et al. 2001, de Groot et al. 2014, Fischer et al. 2015). In HC, $\dot{V}O_2max$ demonstrated high reliability in terms of intraclass correlation coefficient (ICC) in ramp-incremented (ICC = 0.85) and perceptually-regulated (ICC = 0.92) exercise (Hutchinson et al. 2017). $\dot{V}O_2peak$ was shown to be approximately 1.66 times higher in cyclists (62.5 ± 4.5 $ml \cdot min^{-1} \cdot kg^{-1}$) compared to handcyclists (37.5 ± 7.8 $ml \cdot min^{-1} \cdot kg^{-1}$) indicating that aerobic power is affected by the usage of muscle mass that is different between the limbs (Knechtle et al. 2004).

Besides aerobic power, measures of anaerobic or lactic power are also important for characterising the athlete's physiological profile, since anaerobic metabolism is utilised in short periods of high intensity exercise as applied in the start, passing manoeuvres or the final sprint of a race (Heck et al. 2003, Mader 2003). Lactic power is determined as maximal lactate accumulation rate ($\dot{V}La_{max}$) which has been applied in C (Hauser et al. 2014a, Adam et al. 2015, Manunzio et al. 2016) and HC (Quittmann et al. 2017, Quittmann et al. 2018a). In C, $\dot{V}La_{max}$ was shown to decrease during the preparation period of a long-distance race (Manunzio et al. 2016) and sprint interval training (Hommel et al. 2019). In HC, $\dot{V}La_{max}$ was shown to be positively correlated to anaerobic and negatively correlated to aerobic performance measures (Quittmann et al. 2018a).

Whereas $\dot{V}La_{max}$ was shown to be highly reliable in C (Adam et al. 2015), the reliability of $\dot{V}La_{max}$ as a measure of lactic power has not yet been assessed in HC. Furthermore, $\dot{V}La_{max}$ has not yet been investigated for differences and correlations between HC and C. In order to examine measures of anaerobic performance and power in HC and C, the aim of this study was to assess $\dot{V}La_{max}$ and peak power output in a 15-s all-out exercise ($P_{max,AO15}$) in terms of reliability, correlations among and differences between HC and C.

6.2 Methods

6.2.1 Design

The study contained two 15-s all-out sprint tests for the upper (HC) and lower (C) extremities that were performed within two consecutive weeks (T1 and T2). The order was standardized in the way that the sprint test in C preceded the sprint test in HC by approximately 48 hours (sprint tests on Mondays and Wednesdays). To avoid influences based on circadian rhythm, the participants performed the tests at the same time of the day. Participants had to be physically active with respect to the upper and lower extremities. Hence, competitive triathletes were recruited for this study. Based on an effect size of d = 0.80, a statistical power of 0.80 and a level of significance of 0.05, a required sample size of n = 15 was calculated.

6.2.2 Participants

Eighteen able-bodied female (n = 3) and male (n = 15) competitive triathletes (25.1 ± 2.8 yrs., 1.79 ± 0.08 m, 71.6 ± 6.3 kg) participated voluntarily in this study. Body fat was determined using ten-site skinfold thickness measures (Pařízková 1978). The mean body fat percentage of the participants was 14.4 ± 3.7%. The participants were used to a weekly training routine of 11.6 ± 4.3 h·wk^{-1} and had participated in triathlon competitions for 6.7 ± 4.7 yrs. (Tab. 20). The participants were given a medical check-up based on the guidelines of the European Society of Cardiology prior to any testing (Corrado et al. 2005). All procedures received institutional ethics approval (No. 124/2017) according to the Helsinki Declaration modified in 1983. There was no conflict of interest for the participants of this study.

Tab. 20 Descriptive statistics characterising participants

		Age [yrs.]	Height [m]	Mass [kg]	Body fat [%]	Training [h·wk^{-1}]	Experience [yrs.]
female	x̄ ± SD	23.7 ± 3.1	1.73 ± 0.01	65.7 ± 4.8	21.0 ± 2.3	9.7 ± 2.5	6.0 ± 7.8
(n = 3)	Min	21	1.72	61.1	18.4	7	2
	Max	27	1.73	70.7	22.3	12	15
male	x̄ ± SD	25.3 ± 2.8	1.80 ± 0.08	72.7 ± 6.0	13.1 ± 2.1	12.0 ± 4.6	6.8 ± 4.2
(n = 15)	Min	21	1.69	63.2	9.8	7	1
	Max	31	1.93	84.1	16.3	24	16
total	x̄ ± SD	25.1 ± 2.8	1.79 ± 0.08	71.6 ± 6.3	14.4 ± 3.7	11.6 ± 4.3	6.7 ± 4.7
(N = 18)	Min	21	1.69	61.1	9.8	7	1
	Max	31	1.93	84.1	22.3	24	16

Values are expressed as mean value (x̄) and standard deviation (SD). m = mass; Max = maximal value; Min = minimal value.

6.2.3 Experimental protocol

The sprint tests in C were performed on the participants' own road bikes that were attached to the same ergometer. Therefore, the teeth of the chain ring and the pinion as well as the length of the crank arm had to be known. The initial resistance of the sprint test in C was set to 2.0 N·kg^{-1} per kilogram body weight and cadence was limited to 130 min^{-1} (Adam et al. 2015). The sprint tests in HC were performed in a racing handcycle (Shark S, Sopur, Sunrise Medical, Malsch, Germany) in synchronous crank mode that was mounted on a fully calibrated and validated ergometer in isokinetic mode (TE 2%, Cyclus 2, 8 Hz, RBM electronic automation GmbH, Leipzig, Germany) (Reiser, Meyer, Kindermann, & Daugs, 2000). The handcycle was individually set according to previous research (Quittmann et al. 2018b). The initial resistance of the sprint test in HC was set to 0.5 $N \cdot kg^{-1}$ body weight and cadence was limited to 130 min^{-1} (Adam et al. 2015).

The participants performed a standardized low-intensity warm-up of ten minutes including three acceleration bursts (Ozkaya 2013). The basic load of the warm-up for HC and C was 30 W and 100 W, respectively (Coso and Mora-Rodríguez 2006, Weber et al. 2006). The acceleration bursts were applied for ten seconds each and power output was increased up to five times the basic load (150 W in HC and 500 W in C) (Fig. 30a). After the warm-up, the participants rested for five minutes in a sitting position. The beginning and end of the sprint tests were verbally announced by a count-down. Throughout the tests, the participants were verbally encouraged to maintain maximal effort by the examiners. After the warm-up, the participants rested for five minutes in a sitting position. The beginning and end of the sprint tests were verbally announced by a count-down. Throughout the tests, the participants were verbally encouraged by the examiners to maintain maximal effort. Since C and HC make use of a different amount of muscle mass, power output was normalised to lean segment mass (LSM). Therefore, the body segments primarily involved in C and HC were calculated based on previous research (Zatsiorsky and Seluyanov 1985, de Leva 1996). Fig. 30b illustrates the segment masses assumed for C and HC.

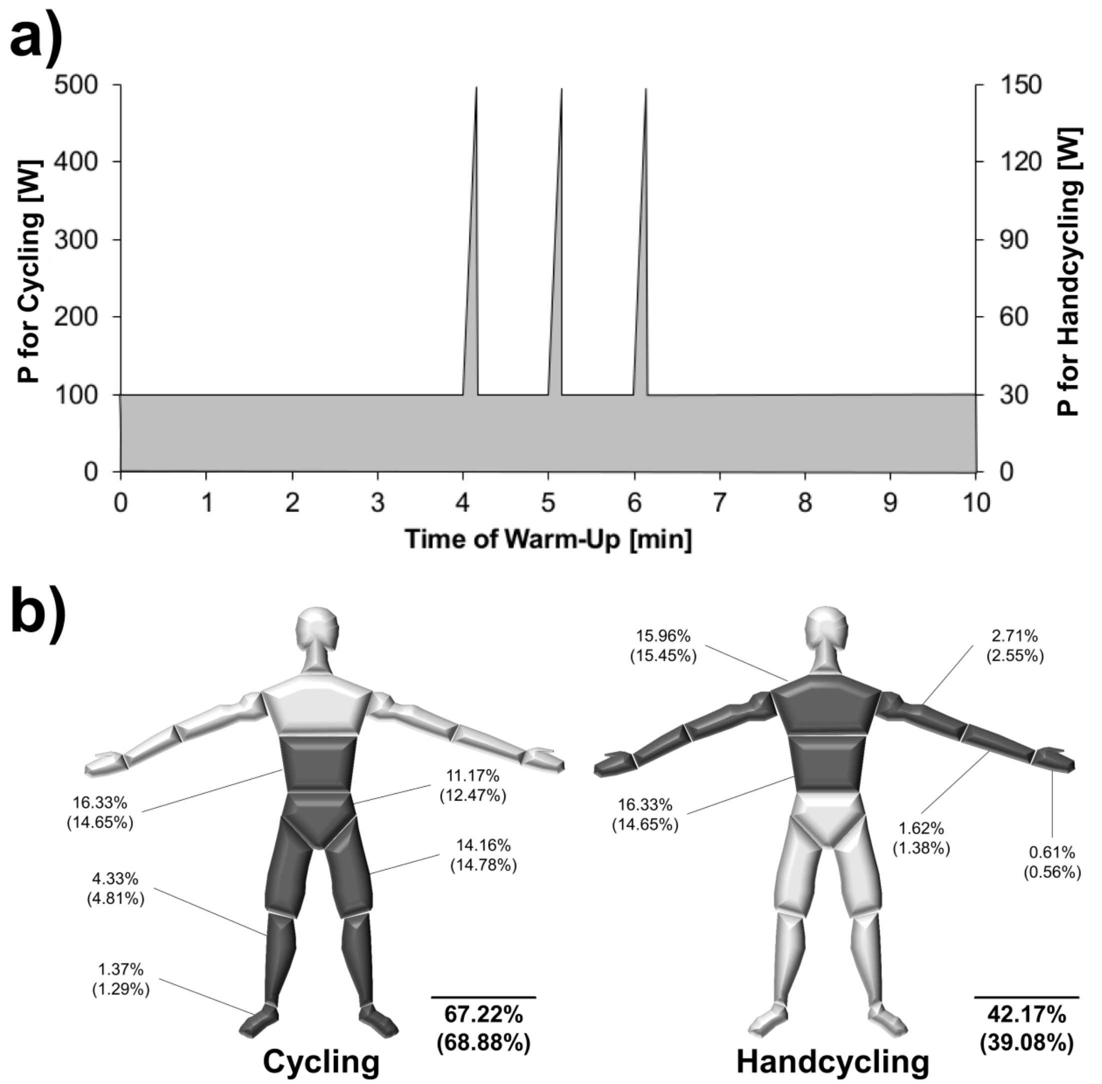

Fig. 30 Warm-up protocols and segmental masses for cycling and handcycling

a) Warm-up protocols (cycling on the primary y-axis, handcycling on the secondary y-axis) b) Segmental masses assumed for cycling (left) and handcycling (right). Relative factors based on the adjustments to Zatsiorsky et al. (de Leva 1996). Factors for females are expressed in parentheses. C = cycling; HC = handcycling; P = power output.

In order to consider the percentage of lean body mass, segmental masses were calculated according to Eq. (6):

$$\text{LSM} = \text{body mass} \cdot \text{segment mass factor} \cdot (100\% - \text{body fat percentage}) \qquad (6)$$

Where LSM = lean segment mass [kg]; segment mass factor in C = 0.6722 and 0.6888 in males and females, respectively; segment mass factor in HC = 0.4217 and 0.3908 in males and females, respectively; body fat percentage based on ten-site skinfold calliper (Pařízková 1978).

$P_{max,AO15}$ was identified as the peak value measured by the ergometer divided by the individual (and exercise modality-specific) LSM. Lactate concentration (La) of the arterialised ear lobe was determined using a stationary analyser (Biosen C-Line, EKF-diagnostics GmbH, Barleben, Germany). La was determined immediately before and immediately after the 15-s all-out sprint tests and every minute after exercise for ten minutes. Post-exercise lactate kinetics were interpolated using a modified biexponential time function based on Michaelis-Menten kinetics as described in previous research (Eq. 1) (Quittmann et al. 2018a).

$\dot{V}La_{max}$ was calculated as the difference between maximal interpolated post-exercise La and resting La that was divided by the difference between test time (15 s) and the period at the beginning of exercise for which no lactate formation is assumed (t_{alac}) (Eq. 2). The alactic time interval was individually set as the time until $P_{max,AO15}$ was reached (t_{pmax}) (Manunzio et al. 2016). Values at the beginning of exercise with a power output of zero were erased beforehand.

6.2.4 Statistics

Statistical analyses were done using Statistical Package for the Social Sciences software (25, SPSS Inc., Chicago, Ill., USA). Reliability of $P_{max,AO15}$, $\dot{V}La_{max}$, t_{pmax} and lactate interpolation parameters was assessed using intraclass correlation coefficient (ICC, Model: Two-way random, Type: Single measurements, Definition: Absolute agreement) (Koo and Li 2016). ICCs were classified as 'excellent' ($ICC \geq 0.90$), 'good' ($0.90 > ICC \geq 0.75$), 'moderate' ($0.75 > ICC \geq 0.50$) or 'poor' ($ICC < 0.5$) (Koo and Li 2016). Differences between extremities as well as between testing weeks were examined using a two-way (2 × 2) analysis of variance (ANOVA) with repeated measures. Post-hoc comparisons were adjusted using Bonferroni's correction. The calculated effect sizes for factors and mean differences were partial eta squared (η_p^2) and Cohen's d, respectively. In order to quantify differences in $P_{max,AO15}$ and $\dot{V}La_{max}$ between trials and extremities and to determine the limits of agreement (LoA), data were illustrated using Bland-Altman plots.

Parameters were initially checked for normal distribution using the Kolmogorov-Smirnov test with Lilliefors' correction. Correlations were calculated using Pearson's correlation coefficient. For parameters that violated the normal distribution assumption, the non-parametric correlation coefficient of Spearman was applied. To assess the relationship between anaerobic performance and metabolic response, correlations and linear regression analyses were performed between $P_{max,AO15}$ and $\dot{V}La_{max}$ in both C and HC at T2. To assess the concordance between extremities, correlations and regressions were calculated between C and HC in both $P_{max,AO15}$ and $\dot{V}La_{max}$ at T2. The level of significance for inferential analyses was set at α = 0.05.

6.3 Results

6.3.1 Reliability analyses

$P_{max,AO15}$ and $\dot{V}La_{max}$ demonstrated 'good' to 'excellent' reliability in HC and C (Tab. 21). However, the reliability of t_{pmax} and lactate interpolation parameters indicated partially 'poor' reliability. Only the amplitude parameter in C indicated 'good' reliability. In HC, k_2 demonstrated 'moderate' reliability. In C, the mean difference in $P_{max,AO15}$ between T1 and T2 was 0.22 $W \cdot kg_{LSM}^{-1}$ with LoA ranging from –2.18 to +2.62 $W \cdot kg_{LSM}^{-1}$ (Fig. 30a). In HC, the mean difference in $P_{max,AO15}$ was 0.26 $W \cdot kg_{LSM}^{-1}$ with LoA ranging from –0.90 to +1.43 $W \cdot kg_{LSM}^{-1}$ (Fig. 31b). Whereas the mean difference in $\dot{V}La_{max}$ was close to zero for upper and lower extremities, the LoA for C and HC ranged from -0.15 to +0.14 $mmol \cdot l^{-1} \cdot s^{-1}$ and -0.10 to +0.12 $mmol \cdot l^{-1} \cdot s^{-1}$, respectively (Fig. 31c-d). At T2, the mean difference in $P_{max,AO15}$ between C and HC was 7.74 W·kg_{LSM}^{-1} with LoA ranging from +1.35 to +14.12 W·kg_{LSM}^{-1} (Fig. 31e). For $\dot{V}La_{max}$, the mean difference between C and HC was 0.20 mmol·l^{-1}·s^{-1} with LoA ranging from –0.06 to +0.45 mmol·l^{-1}·s^{-1} (Fig. 31f).

Tab. 21 Reliability analyses of sprint-test parameters in handcycling and cycling

	C	HC
$P_{max,AO15}$	0.937 (0.843 - 0.976)	0.972 (0.921 - 0.990)
$\dot{V}La_{max}$	0.872 (0.691 - 0.950)	0.828 (0.603 - 0.932)
t_{pmax}	0.525 (0.038 - 0.801)	-0.115 (-0.586 - 0.378)
A	0.839 (0.622 - 0.937)	0.350 (-0.075 - 0.685)
k_1	0.55 (0.117 - 0.805)	0.314 (-0.114 - 0.661)
k_2	0.171 (-0.193 - 0.543)	0.736 (0.402 - 0.894)

Values are expressed as intraclass correlation coefficient (ICC, Model: Two-way random, Type: Single measurements, Definition: Absolute agreement) and 95% confidence intervals in parenthesis. A = Amplitude parameter describing post-exercise lactate kinetics of the 15-s all-out test; k_1 = Velocity constant describing the exchange of lactate from the previously active muscles; k_2 = Velocity constant describing the removal of lactate during passive recovery; $P_{max,AO15}$ = Maximal power output within the 15-s all-out sprint test; t_{pmax} = time until peak power output was reached; $\dot{V}La_{max}$ = Maximal lactate accumulation rate (glycolytic rate).

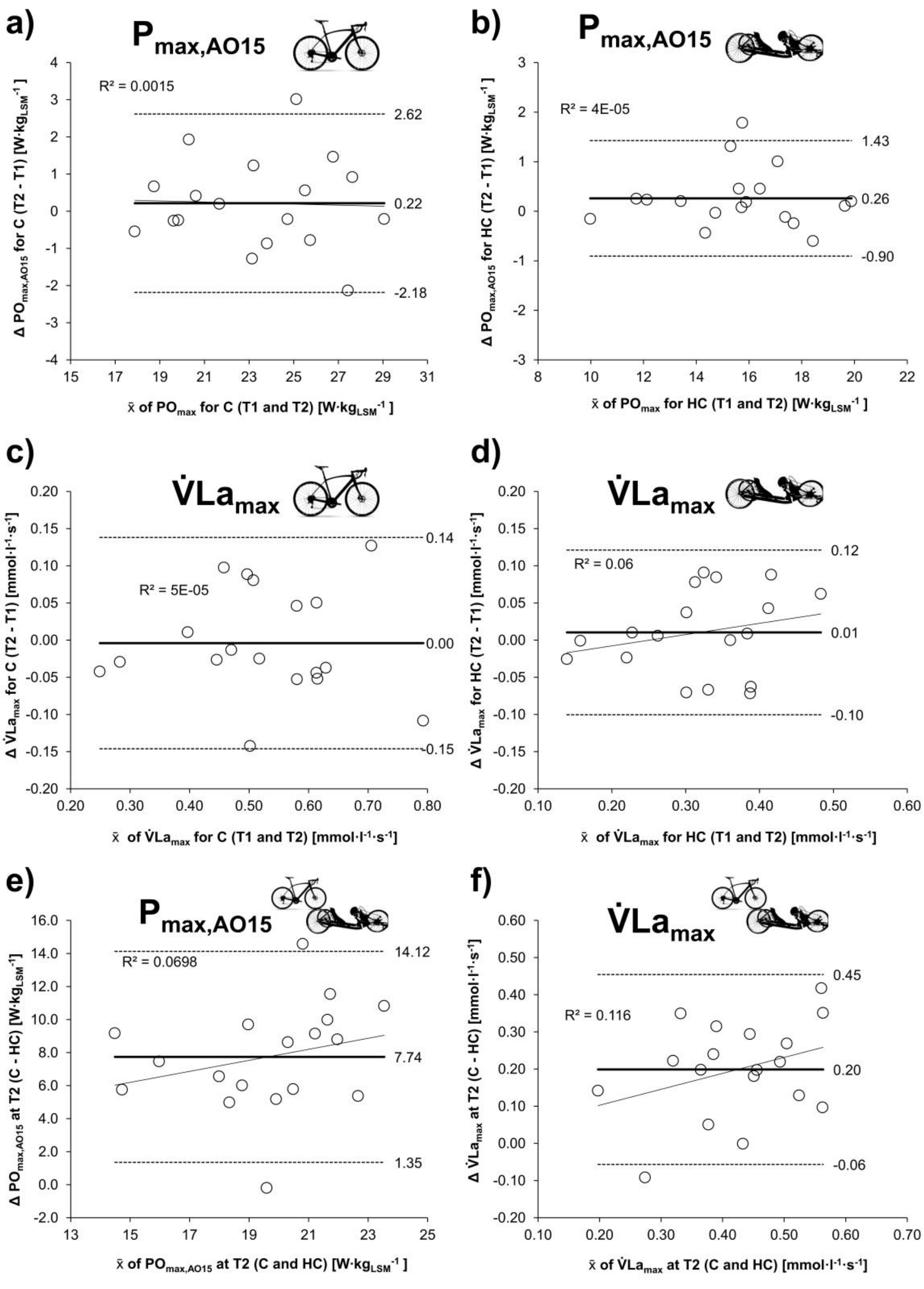

Fig. 31 Bland-Altman plots of $P_{max,AO15}$ and $\dot{V}La_{max}$ between trials and extremities

a) Difference of $P_{max,AO15}$ in C between T1 and T2; b) Difference of $P_{max,AO15}$ in HC between T1 and T2; c) Difference of $\dot{V}La_{max}$ in C between T1 and T2; d) Difference of $\dot{V}La_{max}$ in HC between T1 and T2; e) Difference in $P_{max,AO15}$ at T2 between C and HC; f) Difference in $\dot{V}La_{max}$ at T2 between C and HC. The solid lines illustrate the mean difference, whereas the dotted lines illustrate the limits of agreement (± 1.96 SD). $\bar{x}$ = mean value; C = cycling; HC = handcycling; $P_{max,AO15}$ = peak power output; $\dot{V}La_{max}$ = maximal lactate accumulation rate (glycolytic rate).

6.3.2 ANOVA and post-hoc test results

There was no significant time effect for all parameters (Tab. 22). Except for k_1 and t_{pmax}, all parameters demonstrated a significant effect of extremity. The highest extremity effects were observed for $P_{max,AO15}$ and $\dot{V}La_{max}$. The interaction of time and extremity was only significant for k_2 and A. From T1 to T2, a significant decrease of t_{pmax} was observed in C (Tab. 23). Whereas k_2 demonstrated a decrease from T1 to T2 in C, k_2 significantly increased in HC. All other parameters were not significantly different between trials.

Tab. 22 ANOVA results of physiological and performance parameters

	Time		Extremity		Time*Extremity	
	η_p^2	p	η_p^2	p	η_p^3	p
$P_{max,AO15}$	0.031	0.474	**0.953*** **	< 0.0001	< 0.0001	0.952
$\dot{V}La_{max}$	0.018	0.584	**0.742*** **	< 0.0001	0.005	0.766
t_{pmax}	0.157	0.093	**0.543*** **	< 0.0001	0.113	0.159
A	0.080	0.240	**0.577*** **	< 0.0001	**0.224***	0.041
k_1	0.152	0.099	0.099	0.189	0.115	0.155
k_2	0.002	0.863	**0.620*** **	< 0.0001	**0.455** **	0.002

A = Amplitude parameter describing post-exercise lactate kinetics of the 15-s all-out test; k_1 = Velocity constant describing the exchange of lactate from the previously active muscles; k_2 = Velocity constant describing the removal of lactate during passive recovery; p = Probability of committing a type I error; $P_{max,AO15}$ = Maximal power output within the 15-s all-out sprint test; t_{pmax} = time until peak power output was reached; $\dot{V}La_{max}$ = Maximal lactate accumulation rate (glycolytic rate); η_p^2 = partial eta squared. Significant factors * $p \leq 0.05$; ** $p \leq 0.01$; *** $p \leq 0.001$.

At T1, $P_{max,AO15}$, $\dot{V}La_{max}$ and A were significantly higher in C whereas k_1 and k_2 were significantly higher in HC (Tab. 23). The average C/HC ratio in $P_{max,AO15}$ was 1.50 indicating that $P_{max,AO15}$ was 50% higher in C. At T2, k_2 was significantly higher in HC whereas $P_{max,AO15}$, $\dot{V}La_{max}$ and A were significantly higher in C (Fig. 32). The average C/HC ratio in $\dot{V}La_{max}$ was 1.67 indicating that $\dot{V}La_{max}$ was 67% higher in C. There was no significant difference between extremities for t_{pmax} and k_1 at T2. As illustrated in Figure 32b, the absolute variation of post-exercise lactate concentration was higher in C compared to HC.

Tab. 23 Post-hoc comparisons between trials (lines) and extremities (columns)

		T1	T2	d	p
$P_{max,AO15}$ [W·kg_{LSM}^{-1}]	C	23.27 ± 3.44	23.49 ± 3.39	0.06	0.464
	HC	15.49 ± 2.66	15.75 ± 2.66	0.10	0.080
	d	**-2.53**$^{\#\#\#}$	**-2.54**$^{\#\#\#}$		
	p	< 0.001	< 0.001		
$\dot{V}La_{max}$ [mmol·l^{-1}·s^{-1}]	C	0.53 ± 0.14	0.52 ± 0.14	-0.03	0.820
	HC	0.31 ± 0.09	0.32 ± 0.10	0.11	0.445
	d	**-1.82**$^{\#\#\#}$	**-1.62**$^{\#\#\#}$		
	p	< 0.001	< 0.001		
t_{pmax} [s]	C	3.38 ± 0.85	2.87 ± 0.66	**-0.67****	0.004
	HC	3.09 ± 0.79	3.05 ± 0.69	-0.06	0.873
	d	-0.36	0.26		
	p	0.219	0.367		
A_{la} [mmol·l^{-1}]	C	7.58 ± 1.97	7.44 ± 1.89	-0.07	0.613
	HC	5.10 ± 1.24	6.02 ± 2.39	0.48	0.085
	d	**-1.50**$^{\#\#\#}$	**-0.66**$^{\#}$		
	p	< 0.001	0.017		
k_1 [min^{-1}]	C	0.77 ± 0.13	0.75 ± 0.14	-0.10	0.670
	HC	0.88 ± 0.22	0.76 ± 0.27	-0.48	0.094
	d	**0.64**$^{\#}$	0.05		
	p	0.025	0.875		
k_2 [min^{-1}]	C	0.042 ± 0.014	0.032 ± 0.012	**-0.75***	0.022
	HC	0.072 ± 0.031	0.084 ± 0.033	**0.34***	0.046
	d	**1.25**$^{\#\#\#}$	**2.03**$^{\#\#\#}$		
	p	< 0.001	< 0.001		

Values are expressed as mean value ($\bar{x}$) and standard deviation (SD). A = Amplitude parameter describing post-exercise lactate kinetics of the 15-s all-out test; C = cycling; d = Cohen's d; HC = handcycling; k_1 = Velocity constant describing the exchange of lactate from the previously active muscles; k_2 = Velocity constant describing the removal of lactate during passive recovery; p = Probability of committing a type I error; $P_{max,AO15}$ = Maximal power output within the 15-s all-out sprint test; T1 = familiarisation trial; T2 = testing trial; t_{pmax} = time until peak power output was reached; $\dot{V}La_{max}$ = Maximal lactate accumulation rate (glycolytic rate); Significant differences between trials * $p \leq 0.05$; ** $p \leq 0.01$; Significant differences between extremities $^{\#}$ $p \leq 0.05$; $^{\#\#\#}$ $p \leq 0.001$.

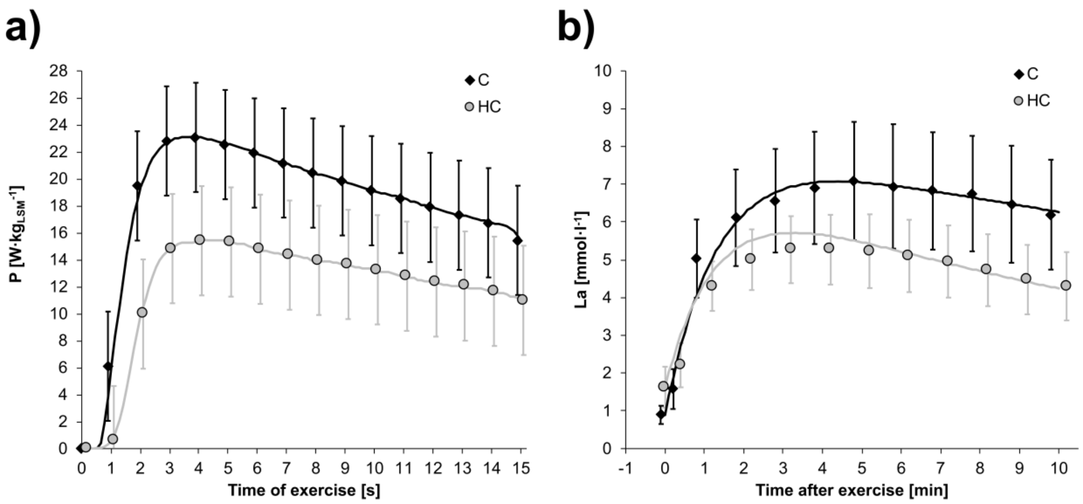

Fig. 32 Power output (left) and post-exercise lactate concentration (right) in handcycling and cycling

Values are expressed as mean value ($\bar{x}$) and standard deviation (SD). The solid lines illustrate mean interpolation parameters. C = cycling; HC = handcycling; La = lactate concentration; P = power output.

6.3.3 Correlation analyses

$P_{max,AO15}$ and $\dot{V}La_{max}$ demonstrated a significant correlation in C ($r = 0.710$, $p = 0.001$) and HC ($r = 0.729$, $p = 0.001$). In both extremities, $P_{max,AO15}$ and $\dot{V}La_{max}$ shared more than 50% of the variance (Fig. 33a-b). However, $P_{max,AO15}$ and $\dot{V}La_{max}$ were not significantly correlated between C ($r = 0.442$, $p = 0.066$) and HC ($r = 0.455$, $p = 0.058$). Between extremities, $P_{max,AO15}$ and $\dot{V}La_{max}$ shared around 20% of the variance (Fig. 33c-d).

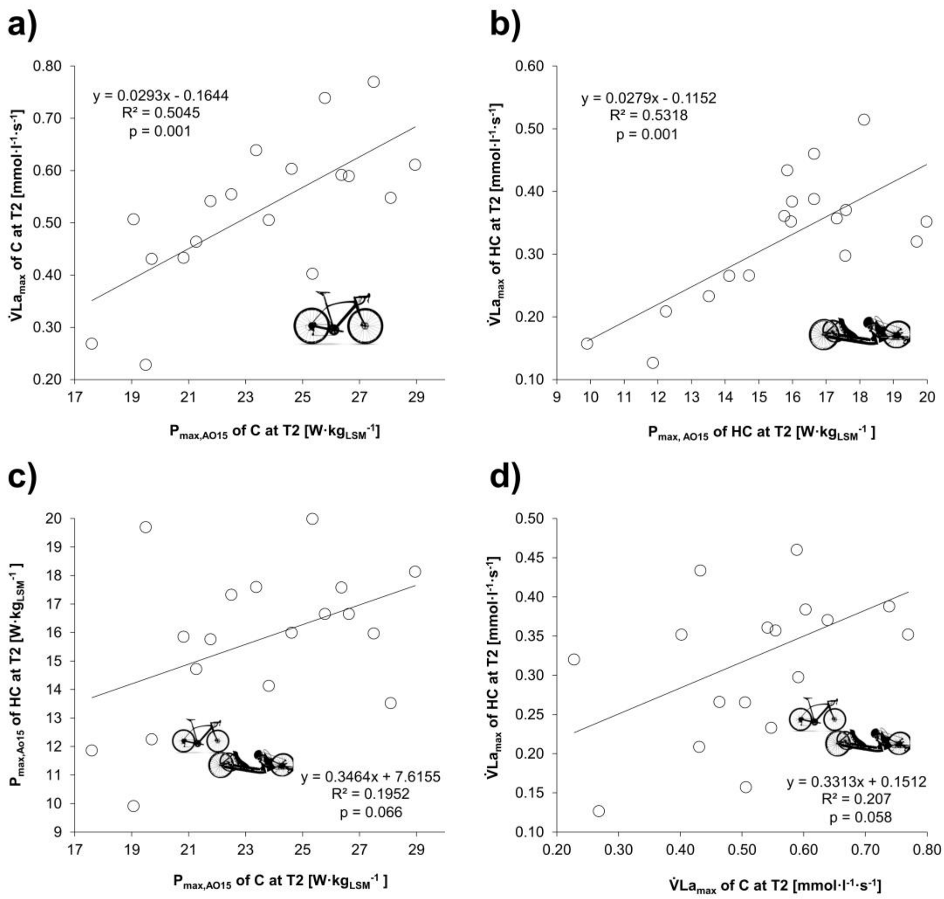

Fig. 33 Linear regression of $P_{max,AO15}$ and $\dot{V}La_{max}$ in handcycling and cycling

a) Regression between $P_{max,AO15}$ and $\dot{V}La_{max}$ in C at T2; b) Regression between $P_{max,AO15}$ and $\dot{V}La_{max}$ in HC at T2; c) Regression of $P_{max,AO15}$ between and C and HC at T2; d) Regression of $\dot{V}La_{max}$ between C and HC at T2; C = cycling; HC = handcycling; LSM = lean segment mass; $P_{max,AO15}$ = peak power output; $\dot{V}La_{max}$ = maximal lactate accumulation rate (glycolytic rate).

6.4 Discussion

6.4.1 Reliability

Even though participants were not experienced in HC, $\dot{V}La_{max}$ and $P_{max,AO15}$ demonstrated 'good' and 'excellent' reliability, respectively. This might be due to the fact that participants were performing swimming exercises on a regular basis and thus were used to upper extremity exercises. Based on previous findings in C, it is assumed that reliability does not increase after several familiarisation trials (Adam et al. 2015). In C, ICCs of $P_{max,AO15}$ and

$\dot{V}La_{max}$ agreed with previous research, although a different ergometer (Lode Excalibur Sport, Lode, Groningen, NL) and other period standardisation between trials (three to six days) were applied (Adam et al. 2015). The results of this study also concurred with previous literature demonstrating 'excellent' reliability of $P_{max,AO15}$ in C and arm-cranking exercise (Jaafar et al. 2015). As a part of $\dot{V}La_{max}$ calculation, t_{pmax} demonstrated 'poor' reliability in C. Since t_{pmax} values are rather small (around three seconds), small absolute differences result in high variability. The same applies to the velocity constants k_1 and k_2. The negative ICC for t_{pmax} in HC is due to a higher within-group than between-group variance. Since k_2 describes the removal of lactate during passive recovery, it is affected by the position and movements of the participants during recovery. Whereas the participants were leaning against the backrest of the handcycle after HC exercise, the participants remained seated on their road bike and kept their hands on the handlebars after the sprint test in C.

6.4.2 Differences between trials

According to reliability analysis, $\dot{V}La_{max}$ and $P_{max,AO15}$ demonstrated similar values at T1 and T2 in HC and C. However, LoA indicated that $\dot{V}La_{max}$ can vary between trials by up to 0.15 $mmol \cdot l^{-1} \cdot s^{-1}$ in C and 0.12 $mmol \cdot l^{-1} \cdot s^{-1}$ in HC. Compared to $\dot{V}La_{max}$ values ranging from around 0.15 to 0.70 $mmol \cdot l^{-1} \cdot s^{-1}$, this variation seems to be rather high. $P_{max,AO15}$ varied between T1 and T2 by around 2.5 $W \cdot kg_{LSM}^{-1}$ in C and around 1.5 $W \cdot kg_{LSM}^{-1}$ in HC which is equal to approximately 10% of $P_{max,AO15}$. These findings concurred with previous findings (Jaafar et al. 2015). Parameters of lactate kinetics demonstrated poor reliability and should be treated with caution on the first occasion.

6.4.3 Differences between extremities

$P_{max,AO15}$ of HC and C agreed with previous findings (Weber et al. 2006). The metabolic response to 15-s all-out exercise in terms of $\dot{V}La_{max}$ was significantly higher in C compared to HC. These findings concur with literature demonstrating significantly higher absolute $P_{max,AO15}$ and higher post-exercise La in lower extremity exercise (Lovell et al. 2013). However, previous findings indicated that $P_{max,AO15}$ in relation to the CSA is higher for upper- compared to lower extremity exercise (Lovell et al. 2013). The mean ratio of lactic power ($\dot{V}La_{max}$) attained during C to HC (1.67) was similar to the ratio of aerobic power ($\dot{V}O_2max$) attained by cyclists to handcyclists (1.66) (Knechtle et al. 2004). This indicates that aerobic and anaerobic power are affected by the type of extremity exercise to a similar extent.

Participants achieved $P_{max,AO15}$ after the same period of time in both C and HC. Since t_{pmax} was assumed to be alactic, energy supply in this period is formally provided by creatine phosphate metabolism. The time in which creatine phosphate is available is determined by the capacity (energy) of creatine phosphate stores and the turn-over rate (power) of its metabolism. Since t_{pmax} was not significantly different in C and HC, it is assumed that the turn-over rate of creatine phosphate metabolism in relation to its capacity is equal in lower- and upper extremity exercise. However, it cannot be stated to what extent the underlying parameters (energy and power) of creatine phosphate metabolism are different between extremities.

Post-exercise lactate interpolation parameters demonstrated significant differences between extremities. Since participants accomplished considerably more work during C and the increase in lactate concentration is proportional to the energy provided by lactic metabolism, it is not surprising that the amplitude parameter of whole body lactate concentration was higher in C compared to HC. However, previous findings indicate that the arms have a higher percentage of fast-twitch muscle fibres compared to the legs which might lead to higher intramuscular lactate concentrations in HC compared to C (Polgar et al. 1973, Johnson et al. 1973). Whereas $P_{max,AO15}$ was normalised to LSM, $\dot{V}La_{max}$ was compared in absolute values. The exchange of lactate from the previously active muscles (k_1) was similar between extremities after initial familiarisation. Post-exercise lactate concentration demonstrated less variation and a higher removal constant (k_2) in HC compared to C. This might be due to the fact that the amount of passive musculature and thus lactate distribution volume is higher in HC (Medbø and Toska 2001). Additionally, participants leaned against the backrest of the handcycle during recovery and thus had a more relaxed position which might have increased k_2.

6.4.4 Correlations within and between extremities

$\dot{V}La_{max}$ and $P_{max,AO15}$ shared around 50% of variance in both HC and C. This is consistent with previous findings in HC (Quittmann et al. 2018a). Hence, anaerobic performance and metabolic response are closely related indicating that $\dot{V}La_{max}$ is a valid parameter of anaerobic metabolism (lactic power) which has been hypothesized in simulation approaches (Mader 2003). However, the anaerobic performance and/or metabolic response attained in C explain only 20% of the variance attained in HC. This indicates that anaerobic performance and metabolic response in terms of lactic power are extremity-specific. Participants with a relatively high $P_{max,AO15}$ and $\dot{V}La_{max}$ attained in C only tend to demonstrate a relatively high $P_{max,AO15}$ and $\dot{V}La_{max}$ in HC even though the exact value is not precisely predictable. Hence, it seems reasonable that local adaptations (e.g. muscle fibre type) occur due to certain training emphases that result in extremity-specific alterations of lactic power (Esbjörnsson et al. 1993). This is highly important for sports that make use of both extremities (e. g. triathlon, rowing, etc.) and want to improve endurance performance in both limbs.

6.4.5 Limitations

Since the participants were not experienced in HC, it is likely that familiarisation effects affected our findings. However, the major parameters $P_{max,AO15}$ and $\dot{V}La_{max}$ demonstrated a high initial reliability. Furthermore, participants performed only two trials that were separated by one week. It is not known if and to what extent the reliability of the observed parameters would further increase by performing more than one familiarisation trial. The initial resistance of the sprint test was determined based on previous testing trials. Hence, the choice of initial resistance might additionally have influenced the differences observed between HC and C. Future studies are encouraged to assess the effect of initial resistance on both $P_{max,AO15}$ and $\dot{V}La_{max}$. Although the relation between $\dot{V}La_{max}$ and $P_{max,AO15}$ concurred with previous findings in able-bodied participants (Quittmann et al. 2018a), a validation of this finding in elite handcyclists has yet to be conducted. The fact that this sample consisted of both male and female participants limits the ability to extrapolate the results. However, for the reliability analyses there seems to be no reason why a mixed sample hinders the analyses.

6.5 Conclusions

This study adds new findings for HC and C exercise testing:

1. $\dot{V}La_{max}$ attained in a 15-s all-out sprint test is highly reliable and related to $P_{max,AO15}$ in both HC and C.
2. Since $\dot{V}La_{max}$ and $P_{max,AO15}$ are different and poorly correlated between extremities, anaerobic performance and power are assumed to be extremity-specific.
3. In exercise testing of HC and C, $\dot{V}La_{max}$ and $P_{max,AO15}$ can be determined to the nearest of approximately 0.12 mmol·l^{-1}·s^{-1} and 10% of $P_{max,AO15}$, respectively.
4. Leaning against a backrest during passive recovery might improve the reliability and amount of lactate removal following exercise.
5. With reference to previous findings, aerobic ($\dot{V}O_2max$) and anaerobic power ($\dot{V}La_{max}$) are affected by the type of extremity exercise to a similar extent.

Main findings and applications

The findings described in the previous chapters of this thesis pursue the physiological and biomechanical aspects of handcycling propulsion under various exercise modalities. The primary focus of these aspects lie in the physiology of anaerobic metabolism and the investigation of muscular activity patterns (MAPs), respectively. These results allow for new insights into the mechanics and energetics of handcycling and can be applied in future exercise testing and biomechanical measurements. Even though there are some indications for sport-specific strength and endurance training, the studies of this thesis need to be replicated in several elite handcyclists.

Physiological aspects of handcycling demonstrated that maximal lactate accumulation rate ($\dot{V}La_{max}$) is a promising parameter in exercise testing. This was due to the fact that $\dot{V}La_{max}$ attained high reliability (ICC = 0.828) and was correlated with both aerobic (r = -0.646, p = 0.023) and anaerobic performance (r = 0.604, p = 0.037). Other parameters of lactate kinetics are correlated with $\dot{V}La_{max}$ and can be used to accurately interpolate lactate concentration within and following handcycling exercise. But since these parameters (e. g. exchange and removal constants) are frequently lacking in reproducibility, they should be interpreted with caution. Based on Bland-Altman's limits of agreement (LoA), $\dot{V}La_{max}$ can be determined to the nearest of around ±0.12 $mmol \cdot l^{-1} \cdot s^{-1}$. Future studies should examine the effect of test conditions (in terms of initial load, cadence limitation and crank position at the start) to improve anaerobic exercise testing in handcycling.

Since $\dot{V}La_{max}$ demonstrated a similar specificity of extremity as aerobic power ($\dot{V}O_2max$), endurance sports with an emphasis on the upper extremity (e. g. rowing, kayaking, biathlon and triathlon) might need to determine their anaerobic power in terms of $\dot{V}La_{max}$ in both extremities. To improve the reproducibility of the lactate removal constant (k_2) and minimise active movements, the participants should lean against a backrest or the back of a chair during passive recovery. Future intervention studies should implement $\dot{V}La_{max}$ as a parameter in exercise testing to examine the effects of deliberate training on anaerobic metabolism. Since the suitability and accuracy of lactate threshold (P_4) seems to be influenced by individual lactate kinetics, simulation approaches of skeletal muscle phosphorylation (Mader et al. 1983, Hauser et al. 2014b) should be modified to provide a holistic illustration of the metabolic profile in terms of maximal lactate steady-state (MLSS) and fat oxidation of handcyclists. Therefore, complex procedures of aerobic and anaerobic metabolism have to be applied in handcycling exercise testing.

Biomechanical aspects of handcycling propulsion in terms of crank kinetics, joint kinematics and muscular activity demonstrated alterations in various exercise modalities. During the course of a 15-s all-out sprint test, the highest torque was measured at the initial pull of the very first revolution (R1). This indicates that a good starting manoeuvre requires a high maximal strength capacity. Since Paralympic athletes are prone to overuse injuries, the usage of maximal sprints in the training of elite handcyclists should be applied with caution (Athanasopoulos et al. 2009, Willick et al. 2013). To minimize the load on tendons and ligaments surrounding the joint and avoid a high maximum as observed at R1, sprint intervals should (most of the time) be performed in a flying start procedure. It is likely that crank position at the start determines which of the muscles involved is primarily demanded. Due to the athletes' strength abilities, an individual start position might be evaluated to attain a faster and higher peak power output that needs to be examined in future research. From the third revolution on, pull and push phase tended to be equal in the size of their maximal torque which indicates that both phases are equally relevant for later stages of all-out handcycling.

According to a preliminary study, crank torque demonstrated local maxima at around 90 and 270° and local minima at around 0 and 180° (Quittmann et al. 2018b). In the course of a continuous load trial (CLT), the pull phase increased in terms of relative work distribution which corresponded to previous findings in incremental handcycling (Quittmann et al. 2018b). There are two possibilities to interpret this finding. On the one hand, this might indicate that the increase in favour of pulling is not exclusively affected by intensity, but also by time in terms of fatigue. On the other hand, this might also be affected by a concomitant increase in spontaneously chosen cadence which was observed during the course of both exercise modalities. To exclude this factor, future studies may replicate both procedures at a fixed cadence to provide clearance. However, the participants chose to reinforce the pull phase to cope with either higher workloads or maintain power output over time. Hence, the stamina of the pulling motion might be emphasised in the strength training of elite handcyclists.

Joint kinematics demonstrated an increase in joint angular velocity during a 15-s all-out sprint and CLT which concurred with findings in incremental handcycling (Quittmann et al. 2018b). The angles of shoulder-abduction and internal-rotation attained during sprinting were higher when compared to high intensity handcycling (Quittmann et al. 2018b). Moreover, shoulder-abduction and internal-rotation increased during the course of the 15-s sprint test. This indicates that shoulder load is rather high in all-out handcycling and increases during the latter phase of a sprint exercise. However, this hypothesis has to be validated by inverse dynamic musculoskeletal modelling approaches. Since dorsal-flexion and radial-duction angles were considerably higher when compared to ergonomic recommendations, frequently performed sprint exercises seem to increase the risk of carpal tunnel syndrome in handcycling. During the course of a CLT, joint angles were hardly altered except for a reduced range of motion (RoM) for elbow-flexion and radial-duction. However, there are some alterations in handcycling propulsion that can only be observed on the level of muscular activation.

Muscular activity patterns (MAPs) in terms of muscular effort and coordination characteristics demonstrated a high reliability in handcycling. The studies of this thesis measured muscular activity for a total of ten muscles some of which (e. g. M. latissimus dorsi) have not yet been examined in the context of handcycling exercise. To achieve a ‘good’ to ‘excellent’ reliability in all parameters, six to ten consecutive cycles should be averaged, respectively. As indicated by the significantly higher ratings of perceived exertion (RPE) on a local level, handcycling exercise seems to be peripherally limited in inexperienced handcycling beginners. Based on the findings, the muscles of the upper extremity and trunk can be assigned to a certain function in the propulsion cycle at various exercise modalities. Furthermore, adequate normalisation techniques can be designated to each of the ten examined muscles.

M. deltoideus, Pars spinalis (DP) was found to be the initiator of the pull phase and highly affected by exercise intensity and duration. At low intensity, DP is activated at a crank angle of around 320 to 110° and increases the range of activation (RoA) at increasing workloads. In both exercise modalities, the incremental step test and the CLT, DP demonstrated the highest increase in muscular effort. This might be due to the fact that DP is poorly supported by other muscles (at the beginning of activation) and thus, the initiation of a reinforced pull phase, as observed in crank kinetics, relies solely on DP. Hence, this muscle seems to be highly important in handcycle athletes and might need additional strength training to improve stamina at high workloads and later stages of a race. Suitable strength training exercises should include rowing-like motions at a rather high number of repetitions with slight shoulder-abduction. Surface electromyography (sEMG) in DP should be normalised to sport-specific maximal voluntary isometric contractions (MVICs) performed at a crank position between 0 and 90°.

The upper part of M. trapezius (Pars descendens, TD) is the second muscle that is activated during the pull phase from around 350 to 190° at low intensity. Since TD demonstrated an increase in muscular effort due to increasing workloads, but remained constant over time in a CLT, TD does not seem to be prone to neuromuscular fatigue. It can be concluded that TD has a rather stabilising function for the shoulder blade in the crank cycle and is increasingly activated at high workloads. Especially at high fluctuations in shoulder-flexion and internal-rotation (as during the 15-s all-out sprint), the demands on TD seem to increase. Hence, additional exercises that improve the stability of the shoulder by means of the rotator cuff muscles might reduce the demands on TD. However, future studies need to validate this in elite handcyclists. The high values of muscular effort for TD (especially during sprinting) might be affected by the sport-specific normalisation procedure, which underestimates maximal TD activation. As highlighted in chapter 5, TD should be normalised muscle-specifically e. g. by performing the shoulder elevation task.

The forearm flexors (FC) and extensors (EC) provide the distal force transmission from the proximal limbs to the cranks and are primarily activated during the pull phase from around 0 to 180° at low intensity handcycling. Since their on- and offsets are almost equal, radial-duction RoM decreases during incremental and continuous exercise and muscular effort did not change during the course of a 15-s all-out sprint, it can be concluded that a stiff wrist improves distal force transmission. However, FC tends to demonstrate an earlier on- and offset when compared to the coordination characteristics of EC. Since FC and EC demonstrated the highest increase in muscular effort during the course of a CLT, these muscles seem to be prone to neuromuscular fatigue. This might be affected by the recruitment of able-bodied participants who are not used to applying high repetitive forces with their upper limbs. However, these findings are highly relevant in newly injured SCI patients who want to improve their endurance by handcycling exercise. It is assumed that the limiting effect of the forearm muscles is reduced with increasing experience and thus not as relevant in elite handcyclists. However, various elite handcyclists stated that the handgrip position is varied during the course of a race. This might be a strategy to shift the load on the forearm between different regions and thereby reduce overuse injuries and delay peripheral fatigue. Another strategy to improve forearm stamina is the involvement of additional strength exercises at a rather high number of repetitions. Whereas EC can be normalised using sport-specific MVICs, FC should be normalised by using muscle-specific MVICs by using a hydraulic handgrip dynamometer. It is assumed that this procedure might also be adventurous for EC normalisation.

As the major flexor muscle, M. biceps brachii (BB) is activated during the pull phase from around 10 to 170° at low intensity. BB demonstrated the lowest increase in muscular effort during incremental handcycling and was not affected by exercise duration in a CLT. This indicates that BB is not prone to neuromuscular fatigue in handcycling exercise. At higher intensities (especially during sprinting), BB demonstrates an earlier onset of activation which supports the initiation of the (reinforced) pull phase. Since high BB activation was found at low elbow-flexion and high shoulder internal-rotation angle, the tendons of BB might be prone to overuse injuries. Sport-specific MVICs demonstrated significant lower values when compared to muscle-specific techniques, which is why the elbow-flexion task should be applied to normalise BB activation.

The anterior part of M. deltoideus (Pars clavicularis, DA) initiates shoulder-flexion and acts as a mediator from pull to push phase. DA is activated from around 80 to 270°. Since DA demonstrated the highest increase in muscular effort during the course of a 15-s all-out sprint, it can be concluded that very high workloads and cadences increase the demands on DA. This might be due to the fact that shoulder-retroversion (performed by DP) was reduced and shoulder-flexion (performed by DA) was increased during most exercise tests. Accordingly, DA demonstrated an earlier onset in activation and thus higher period of co-contraction during incremental, continuous and all-out sprinting. Due to the function in crank cycle, DA should be exercised to increase in strength and shortening velocity. To improve DA's contribution in handcycling exercise, additional strength training at maximal activation (either maximal strength or maximal velocity) might be applied. Similar to DP, DA activation should be normalised to sport-specific MVICs at a crank angle between 180 and 270°.

As the initiator of the push phase, M. pectoralis major (PM) is activated from around 120 to 300° at low intensity handcycling. Since the lift-up sector (150 to 210°) was found to be a limiting factor in high intensity handcycling, PM has a high impact on the lift-up due to the coordination characteristics. As a rather large muscle, PM demonstrated a high increase in muscular effort during incremental and all-out handcycling, whereas no alteration was found in a CLT. It can be concluded that PM activation is important for performing higher workloads but does not seem to be prone to neuromuscular fatigue. However, during the course of a CLT, PM shifts the coordination characteristics by an earlier on- and offset and thereby supports DA activation in terms of co-contraction. In the strength training of handcyclists, PM should improve in maximal strength by performing exercises (e. g. bench press) at a medium number of repetitions. Due to the different parts of the M. pectoralis, various conditions (e. g. incline and decline) and grip positions (e. g. narrow and wide) should be performed at a high RoM. Since PM demonstrated similar amplitudes during sport-specific and muscle-specific MVICs, both techniques can be used for normalisation purposes. However, in SCI handcyclists sport-specific normalisation seems to be more applicable.

M. triceps brachii (TB) is responsible for elbow-extension during the push phase and activated from around 160 to 300° at low intensity handcycling. Similar to BB, TB significantly increased muscular effort during incremental cycling but was not affected during the course of a 15-s all-out sprint test and a CLT. As in the agonist of the push phase (PM), the RoA of TB increased due to an earlier onset at higher intensities to reduce the loss in cadence during the lift-up. This indicates that TB is not prone to neuromuscular fatigue but highly relevant for handcycling at higher intensities. A higher maximal strength of TB might minimise the limiting factor observed during the lift-up. Additional strength training exercises for TB (e. g. performing an isolated elbow-extension on a cable tower) might be helpful to improve force transmission during the push phase. In sEMG studies, TB should be normalised in sport-specific MVICs at crank angles between 180 and 270°.

The trunk muscle M. rectus abdominis (RA) was found to be predominantly activated at high to very high intensities. Findings indicate that RA is only marginally activated at low workloads and demonstrates a high activation during sprinting. It seems that RA supports the lift-up sector and push phase from around 170 to 320°. However, coordination characteristics in terms of on- and offset demonstrate a large variation between participants. Since muscular effort was not altered during a CLT, RA does not seem to be prone to fatigue. Depending on the lesion level, additional strength training of the trunk might assist the push phase at the start, passing manoeuvres or the final sprint of a race. Hence, trunk-flexion exercises should be applied where possible. Since RA demonstrated a significantly lower activation during sport-specific MVICs, RA should be normalised in a muscle-specific crunch position.

Similar to RA, M. latissimus dorsi (LD) was found to be exclusively activated at very high workloads. During the early steps of incremental handcycling and in the CLT, LD activation was marginal. Hence, the coordination characteristics of LD in terms of on- and offset is hindered by large inter-individual variation. Findings in all-out handcycling indicated that LD is activated from around 240 to 90° and thereby assists the transition from push to pull phase. LD seems to have a stabilising function at rather high intensities and cadences. Additional strength training of LD in terms of pull up exercises can be applied in handcyclists, even though there seems to be no necessity based on the sEMG results. Due to the contact to the backrest and risk of sweat contamination, investigating LD activation during continuous handcycling is challenging. However, sport-specific MVICs at a crank angle close to 0° should be performed instead of muscle-specific lateral pull exercises for normalisation purposes.

In conclusion, this thesis highlights the importance of anaerobic measures of handcycling exercise in terms of lactate kinetics and $\dot{V}La_{max}$. Augmenting exercise testing by means of $\dot{V}La_{max}$ helps to illustrate the metabolic profile in terms of aerobic and anaerobic metabolism. Biomechanical aspects of handcycling propulsion highlight the complex interplay of crank kinetics joint kinematics and muscular activity. Depending on the exercise modality, the muscles of the upper extremity seem to vary in effort and their sensitivity to muscular fatigue. However, adequate normalisation procedures have to be applied. Since DP demonstrated the highest demands during handcycling exercise, particular attention should be provided in the conditioning of this muscle.

Future studies should validate these findings in elite SCI handcyclists. Therefore, complex biomechanical measurements combining crank kinetics, joint kinematics and muscular activity have to be applied. To ensure sport-specific measurement in the individualised handcycle, suitable methods to estimate crank kinetics have to be developed. In a subsequent project, handgrips equipped with a measuring device are developed to provide 2D crank kinetics in the sagittal plane. Since these handgrips can be attached to the individual cranks, this could be a suitable method to improve exercise testing and applied biomechanical measurements in handcycling. Additionally, these measures could be used in inverse-dynamic musculoskeletal modelling approaches to estimate joint and muscle forces during various exercise modalities. Since interdisciplinary approaches require diverse expertise and the recruitment of several handcyclist appears to be rather challenging, there is a need for inter-lab collaboration of the European Research Group in Disability Sport (ERGiDS).

References

1. Abbiss CR, Laursen PB (2005) Models to explain fatigue during prolonged endurance cycling. Sports Medicine 35(10):865–898. doi: 10.2165/00007256-200535100-00004

2. Abel T, Burkett B, Schneider S, Lindschulten R, Strüder HK (2010) The exercise profile of an ultra-long handcycling race. The Styrkeprøven experience. Spinal cord 48(12):894–898. doi: 10.1038/sc.2010.40

3. Abel T, Burkett B, Thees B, Schneider S, Askew CD, Strüder HK (2015) Effect of Three Different Grip Angles on Physiological Parameters During Laboratory Handcycling Test in Able-Bodied Participants. Frontiers in physiology 6:331. doi: 10.3389/fphys.2015.00331

4. Abel T, Kroner M, Rojas Vega S, Peters C, Klose C, Platen P (2003) Energy expenditure in wheelchair racing and handbiking - a basis for prevention of cardiovascular diseases in those with disabilities. European journal of cardiovascular prevention and rehabilitation 10(5):371–376. doi: 10.1097/01.hjr.0000096542.30533.59

5. Abel T, Schneider S, Platen P, Strüder HK (2006) Performance diagnostics in handbiking during competition. Spinal cord 44(4):211–216. doi: 10.1038/sj.sc.3101845

6. Adam J, Öhmichen M, Öhmichen E, Rother J, Müller UM, Hauser T, Schulz H (2015) Reliability of the calculated maximal lactate steady state in amateur cyclists. Biology of sport 32(2):97–102. doi: 10.5604/20831862.1134311

7. Allen DG, Lamb GD, Westerblad H (2008) Skeletal muscle fatigue. Cellular mechanisms. Physiological reviews 88(1):287–332. doi: 10.1152/physrev.00015.2007

8. Al-Qaisi S, Aghazadeh F (2015) Electromyography Analysis. Comparison of Maximum Voluntary Contraction Methods for Anterior Deltoid and Trapezius Muscles. Procedia Manufacturing 3:4578–4583. doi: 10.1016/j.promfg.2015.07.475

9. Amann M (2011) Central and peripheral fatigue. Interaction during cycling exercise in humans. Medicine & Science in Sports & Exercise 43(11):2039–2045. doi: 10.1249/MSS.0b013e31821f59ab

10. Arnet U (2012) Handcycling. A biophysical analysis. Dissertation, Vrije Universiteit Amsterdam

11. Arnet U, Hinrichs T, Lay V, Bertschy S, Frei H, Brinkhof MWG (2016) Determinants of handbike use in persons with spinal cord injury. Results of a community survey in Switzerland. Disability and rehabilitation 38(1):81–86. doi: 10.3109/09638288.2015.1024339

12. Arnet U, van Drongelen S, Scheel-Sailer A, van der Woude LHV, Veeger DHEJ (2012a) Shoulder load during synchronous handcycling and handrim wheelchair propulsion in persons with paraplegia. Journal of rehabilitation medicine 44(3):222–228. doi: 10.2340/16501977-0929

13. Arnet U, van Drongelen S, Schlussel M, Lay V, van der Woude LHV, Veeger DHEJ (2014) The effect of crank position and backrest inclination on shoulder load and mechanical efficiency during handcycling. Scandinavian journal of medicine & science in sports 24(2):386–394. doi: 10.1111/j.1600-0838.2012.01524.x

14. Arnet U, van Drongelen S, van der Woude LHV, Veeger DHEJ (2012b) Shoulder load during handcycling at different incline and speed conditions. Clinical biomechanics 27(1):1–6. doi: 10.1016/j.clinbiomech.2011.07.002

15. Arnet U, van Drongelen S, Veeger DHEJ, van der Woude LHV (2012c) Are the force characteristics of synchronous handcycling affected by speed and the method to impose power? Medical engineering & physics 34(1):78–84. doi: 10.1016/j.medengphy.2011.07.001

16. Arnet U, van Drongelen S, Veeger DHEJ, van der Woude LHV (2013) Force Application during Handcycling and Handrim Wheelchair Propulsion. An Initial Comparison. Journal of Applied Biomechanics 29(6):687–695. doi: 10.1123/jab.29.6.687

17. Athanasopoulos S, Mandalidis D, Tsakoniti A, Athanasopoulos I, Strimpakos N, Papadopoulos E, Pyrros DG, Parisis C, Kapreli E (2009) The 2004 Paralympic Games. Physiotherapy Services in the Paralympic Village Polyclinic. The Open Sports Medicine Journal 3(1):1–8. doi: 10.2174/1874387000903010001

18. Azizpour G, Lancini M, Incerti G, Gaffurini P, Legnani G (2017a) An Experimental Method to Estimate Upper Limbs Inertia Parameters During Handcycling. Journal of Applied Biomechanics:1–27. doi: 10.1123/jab.2017-0136

19. Azizpour G, Ousdad A, Legnani G, Incerti G, Lancini M, Gaffurini P (2017b) Dynamic Analysis of Handcycling. Mathematical Modelling and Experimental Tests. In: Boschetti G, Gasparetto A (eds) Advances in Italian Mechanism Science. Springer International Publishing, Cham, pp 33–40

20. Bafghi HA, Haan A de, Horstman A, van der Woude LHV (2008) Biophysical aspects of submaximal hand cycling. International journal of sports medicine 29(8):630–638. doi: 10.1055/s-2007-989416

21. Bartlett R, Wheat J, Robins M (2007) Is movement variability important for sports biomechanists? Sports biomechanics 6(2):224–243. doi: 10.1080/14763140701322994

22. Basset DR, Howley ET (2000) Limiting factors for maximum oxygen uptake and determinants of endurance performance. Medicine & Science in Sports & Exercise:70. doi: 10.1097/00005768-200001000-00012

23. Batalha N, Raimundo A, Tomas-Carus P, Paulo J, Simão R, Silva AJ (2015) Does a land-based compensatory strength-training programme influences the rotator cuff balance of young competitive swimmers? European Journal of Sport Science 15(8):764–772. doi: 10.1080/17461391.2015.1051132

24. Beaudette SM, Unni R, Brown SHM (2014) Electromyographic assessment of isometric and dynamic activation characteristics of the latissimus dorsi muscle. Journal of Electromyography and Kinesiology 24(3):430–436. doi: 10.1016/j.jelekin.2014.03.006

25. Beneke R (2003a) Maximal lactate steady state concentration (MLSS). Experimental and modelling approaches. European journal of applied physiology 88(4-5):361–369. doi: 10.1007/s00421-002-0713-2

26. Beneke R (2003b) Methodological aspects of maximal lactate steady state-implications for performance testing. European journal of applied physiology 89(1):95–99. doi: 10.1007/s00421-002-0783-1

27. Beneke R, Hutler M, Jung M, Leithauser RM (2005) Modeling the blood lactate kinetics at maximal short-term exercise conditions in children, adolescents, and adults. Journal of applied physiology 99(2):499–504. doi: 10.1152/japplphysiol.00062.2005

28. Billat VL, Sirvent P, Py G, Koralsztein J-P, Mercier J (2003) The concept of maximal lactate steady state. A bridge between biochemistry, physiology and sport science. Sports Medicine 33(6):407–426. doi: 10.2165/00007256-200333060-00003

29. Bini RR, Carpes FP, Diefenthaeler F, Mota CB, Guimarães ACS (2008) Physiological and electromyographic responses during 40-km cycling time trial. Relationship to muscle coordination and performance. Journal of science and medicine in sport 11(4):363–370. doi: 10.1016/j.jsams.2007.03.006

30. Bini RR, Diefenthaeler F, Mota CB (2010) Fatigue effects on the coordinative pattern during cycling. Kinetics and kinematics evaluation. Journal of Electromyography and Kinesiology 20(1):102–107. doi: 10.1016/j.jelekin.2008.10.003

31. Blake OM, Wakeling JM (2012) Muscle coordination during an outdoor cycling time trial. Medicine & Science in Sports & Exercise 44(5):939–948. doi: 10.1249/MSS.0b013e3182404eb4

32. Boettcher CE, Ginn KA, Cathers I (2008) Standard maximum isometric voluntary contraction tests for normalizing shoulder muscle EMG. Journal of orthopaedic research 26(12):1591–1597. doi: 10.1002/jor.20675

33. Borg GA (1982) Psychophysical bases of perceived exertion. Medicine & Science in Sports & Exercise 14(5):377–381

34. Bressel E, Bressel M, Marquez M, Heise GD (2001) The effect of handgrip position on upper extremity neuromuscular responses to arm cranking exercise. Journal of Electromyography and Kinesiology 11(4):291–298. doi: 10.1016/S1050-6411(01)00002-5

35. Burden A (2010) How should we normalize electromyograms obtained from healthy participants? What we have learned from over 25 years of research. Journal of Electromyography and Kinesiology 20(6):1023–1035. doi: 10.1016/j.jelekin.2010.07.004

36. Burden A, Bartlett R (1999) Normalisation of EMG amplitude. An evaluation and comparison of old and new methods. Medical engineering & physics 21(4):247–257

37. Cohen J (1988) Statistical Power Analysis for the Behavioral Sciences, 2nd ed. Taylor and Francis, Hoboken

38. Corrado D, Pelliccia A, Bjornstad HH, Vanhees L, Biffi A, Borjesson M, Panhuyzen-Goedkoop N, Deligiannis A, Solberg E, Dugmore D, Mellwig KP, Assanelli D, Delise P, van-Buuren F, Anastasakis A, Heidbuchel H, Hoffmann E, Fagard R, Priori SG, Basso C, Arbustini E, Blomstrom-Lundqvist C, McKenna WJ, Thiene G (2005) Cardiovascular pre-participation screening of young competitive athletes for prevention of sudden death: Proposal for a common European protocol. Consensus Statement of the Study Group of Sport Cardiology of the Working Group of Cardiac Rehabilitation and Exercise Physiology and the Working Group of Myocardial and Pericardial Diseases of the European Society of Cardiology. European heart journal 26(5):516–524. doi: 10.1093/eurheartj/ehi108

39. Coso JD, Mora-Rodríguez R (2006) Validity of cycling peak power as measured by a short-sprint test versus the Wingate anaerobic test. Applied physiology, nutrition, and metabolism 31(3):186–189. doi: 10.1139/h05-026

40. Craig NP, Norton KI, Bourdon PC, Woolford SM, Stanef T, Squires B, Olds TS, Conyers RA, Walsh CB (1993) Aerobic and anaerobic indices contributing to track endurance cycling performance. European journal of applied physiology 67(2):150–158

41. Dallmeijer AJ, Ottjes L, Waardt E de, van der Woude LHV (2004a) A physiological comparison of synchronous and asynchronous hand cycling. International journal of sports medicine 25(8):622–626. doi: 10.1055/s-2004-817879

42. Dallmeijer AJ, Zentgraaff IDB, Zijp NI, van der Woude LHV (2004b) Submaximal physical strain and peak performance in handcycling versus handrim wheelchair propulsion. Spinal cord 42(2):91–98. doi: 10.1038/sj.sc.3101566

43. Damsgaard M, Rasmussen J, Christensen ST, Surma E, Zee M de (2006) Analysis of musculoskeletal systems in the AnyBody Modeling System. Simulation Modelling Practice and Theory 14(8):1100–1111. doi: 10.1016/j.simpat.2006.09.001

44. de Groot S, Hoekstra SP, Grandjean Perrenod Comtesse P, Kouwijzer I, Valent LJ (2018) Relationships between internal and external handcycle training load in people with spinal cord injury training for the handbikebattle. Journal of rehabilitation medicine 50(3):261–268. doi: 10.2340/16501977-2316

45. de Groot S, Postma K, van Vliet L, Timmermans R, Valent LJM (2014) Mountain time trial in handcycling. Exercise intensity and predictors of race time in people with spinal cord injury. Spinal cord 52(6):455–461. doi: 10.1038/sc.2014.58

46. de Leva P (1996) Adjustments to Zatsiorsky-Seluyanov's segment inertia parameters. Journal of biomechanics 29(9):1223–1230. doi: 10.1016/0021-9290(95)00178-6

47. de Luca CJ (1997) The Use of Surface Electromyography in Biomechanics. Journal of Applied Biomechanics 13(2):135–163. doi: 10.1123/jab.13.2.135

48. de Morree HM, Marcora SM (2012) Frowning muscle activity and perception of effort during constant-workload cycling. European journal of applied physiology 112(5):1967–1972. doi: 10.1007/s00421-011-2138-2

49. Decorte N, Lafaix PA, Millet GY, Wuyam B, Verges S (2012) Central and peripheral fatigue kinetics during exhaustive constant-load cycling. Scandinavian journal of medicine & science in sports 22(3):381–391. doi: 10.1111/j.1600-0838.2010.01167.x

50. Doheny EP, Lowery MM, Fitzpatrick DP, O'Malley MJ (2008) Effect of elbow joint angle on force-EMG relationships in human elbow flexor and extensor muscles. Journal of Electromyography and Kinesiology 18(5):760–770. doi: 10.1016/j.jelekin.2007.03.006

51. Elmer SJ, Marshall CS, Wehmanen K, Amann M, McDaniel J, Martin DT, Martin JC (2012) Effects of locomotor muscle fatigue on joint-specific power production during cycling. Medicine & Science in Sports & Exercise 44(8):1504–1511. doi: 10.1249/MSS.0b013e31824fb8bd

52. Esbjörnsson M, Hellsten-Westing Y, Balsom PD, Sjödin B, Jansson E (1993) Muscle fibre type changes with sprint training. Effect of training pattern. Acta physiologica Scandinavica 149(2):245–246. doi: 10.1111/j.1748-1716.1993.tb09618.x

53. Ettema G, Lorås HW (2009) Efficiency in cycling. A review. European journal of applied physiology 106(1):1–14. doi: 10.1007/s00421-009-1008-7

54. Fagher K, Lexell J (2014) Sports-related injuries in athletes with disabilities. Scandinavian journal of medicine & science in sports 24(5):e320-31. doi: 10.1111/sms.12175

55. Faupin A, Gorce P (2008) The effects of crank adjustments on handbike propulsion. A kinematic model approach. International Journal of Industrial Ergonomics 38(7-8):577–583. doi: 10.1016/j.ergon.2008.01.019

56. Faupin A, Gorce P, Campillo P, Thevenon A, Remy-Neris O (2006) Kinematic analysis of handbike propulsion in various gear ratios. Implications for joint

pain. Clinical biomechanics 21(6):560–566. doi: 10.1016/j.clinbiomech.2006.01.001

57. Faupin A, Gorce P, Meyer C (2011) Effects of type and mode of propulsion on hand-cycling biomechanics in nondisabled subjects. Journal of rehabilitation research and development 48(9):1049. doi: 10.1682/JRRD.2010.19.0199

58. Faupin A, Gorce P, Meyer C, Thevenon A (2008) Effects of backrest positioning and gear ratio on nondisabled subjects' handcycling sprinting performance and kinematics. Journal of rehabilitation research and development 45(1):109–116. doi: 10.1682/JRRD.2006.10.0139

59. Faupin A, Gorce P, Watelain E, Meyer C, Thevenon A (2010) A biomechanical analysis of handcycling. A case study. Journal of Applied Biomechanics 26(2):240–245

60. Felsner E-M, Litzenberger S, Mally F, Sabo A (2016) Musculoskeletal Modelling of Elite Handcycling Motion. Evaluation of Muscular On- and Offset. Procedia Engineering 147:168–174. doi: 10.1016/j.proeng.2016.06.208

61. Fischer G, Figueiredo P, Ardigo LP (2015) Physiological Performance Determinants of a 22-km Handbiking Time Trial. International journal of sports physiology and performance 10(8):965–971. doi: 10.1123/ijspp.2014-0429

62. Fischer G, Tarperi C, George K, Ardigò LP (2014) An exploratory study of respiratory muscle endurance training in high lesion level paraplegic handbike athletes. International journal of sports physiology and performance(24):69–75. doi: 10.1097/JSM.0000000000000003

63. Fletcher JR, Esau SP, MacIntosh BR (2010) Changes in tendon stiffness and running economy in highly trained distance runners. European journal of applied physiology 110(5):1037–1046. doi: 10.1007/s00421-010-1582-8

64. Flueck JL, Gallo A, Moelijker N, Bogdanov N, Bogdanova A, Perret C (2019) Influence of Equimolar Doses of Beetroot Juice and Sodium Nitrate on Time Trial Performance in Handcycling. Nutrients 11(7). doi: 10.3390/nu11071642

65. Freund H, Gendry P (1978) Lactate kinetics after short strenuous exercise in man. European journal of applied physiology 39(2):123–135. doi: 10.1007/BF00421717

66. Ginn KA, Halaki M (2015) Do surface electrode recordings validly represent latissimus dorsi activation patterns during shoulder tasks? Journal of Electromyography and Kinesiology 25(1):8–13. doi: 10.1016/j.jelekin.2014.10.008

67. Gonzalez RV, Buchanan TS, Delp SL (1997) How muscle architecture and moment arms affect wrist flexion-extension moments. Journal of biomechanics 30(7):705–712. doi: 10.1016/s0021-9290(97)00015-8

68. Goosey-Tolfrey VL, Alfano H, Fowler N (2008) The influence of crank length and cadence on mechanical efficiency in hand cycling. European journal of applied physiology 102(2):189–194. doi: 10.1007/s00421-007-0576-7

69. Goosey-Tolfrey VL, Lenton J, Goddard J, Oldfield V, Tolfrey K, Eston R (2010) Regulating intensity using perceived exertion in spinal cord-injured participants. Medicine & Science in Sports & Exercise 42(3):608–613. doi: 10.1249/MSS.0b013e3181b72cbc

70. Graham-Paulson T, Perret C, Goosey-Tolfrey VL (2018) Case Study. Dose Response of Caffeine on 20-km Handcycling Time Trial Performance in a Paratriathlete. International Journal of Sport Nutrition and Exercise Metabolism 28(3):274–278. doi: 10.1123/ijsnem.2017-0089

71. Green HJ (1997) Mechanisms of muscle fatigue in intense exercise. Journal of sports sciences 15(3):247–256. doi: 10.1080/026404197367254

72. Groen WG, van der Woude LHV, Koning JJ de (2010) A power balance model for handcycling. Disability and rehabilitation 32(26):2165–2171. doi: 10.3109/09638288.2010.505677

73. Groot S, van de Westelaken LHJ, Noordhof DA, Levels K, Koning JJ de (2018) Recovery of Cycling Gross Efficiency After Time-Trial Exercise. International

journal of sports physiology and performance 13(8):1028–1033. doi: 10.1123/ijspp.2017-0429

74. Hansson GA, Nordander C, Asterland P, Ohlsson K, Strömberg U, Skerfving S, Rempel D (2000) Sensitivity of trapezius electromyography to differences between work tasks - influence of gap definition and normalisation methods. Journal of Electromyography and Kinesiology 10(2):103–115

75. Hashemi Oskouei A, Paulin MG, Carman AB (2013) Intra-session and inter-day reliability of forearm surface EMG during varying hand grip forces. Journal of Electromyography and Kinesiology 23(1):216–222. doi: 10.1016/j.jelekin.2012.08.011

76. Hauser T (2012) Untersuchungen zur Validität und Praktikabilität des mathematisch bestimmten maximalen Laktat-steady-states bei radergometrischen Belastungen. Dissertation, Chemnitz University of Technology

77. Hauser T, Adam J, Schulz H (2014a) Comparison of calculated and experimental power in maximal lactate-steady state during cycling. Theoretical biology & medical modelling 11:25. doi: 10.1186/1742-4682-11-25

78. Hauser T, Adam J, Schulz H (2014b) Comparison of selected lactate threshold parameters with maximal lactate steady state in cycling. International journal of sports medicine 35(6):517–521. doi: 10.1055/s-0033-1353176

79. Heck H, Mader A, Hess G, Mucke S, Muller R, Hollmann W (1985) Justification of the 4-mmol/l lactate threshold. International journal of sports medicine 6(3):117–130. doi: 10.1055/s-2008-1025824

80. Heck H, Schulz H, Bartmus U (2003) Diagnostics of anaerobic power and capacity. European Journal of Sport Science 3(3):1–23. doi: 10.1080/17461390300073302

81. Hermens HJ, Freriks B, Disselhorst-Klug C, Rau G (2000) Development of recommendations for SEMG sensors and sensor placement procedures.

Journal of Electromyography and Kinesiology 10(5):361–374. doi: 10.1016/S1050-6411(00)00027-4

82. Hettinga FJ, Koning JJ de, Broersen FT, van Geffen P, Foster C (2006) Pacing strategy and the occurrence of fatigue in 4000-m cycling time trials. Medicine & Science in Sports & Exercise 38(8):1484–1491. doi: 10.1249/01.mss.0000228956.75344.91

83. Hintzy F, Tordi N, Perrey S (2002) Muscular efficiency during arm cranking and wheelchair exercise. A comparison. International journal of sports medicine 23(6):408–414. doi: 10.1055/s-2002-33734

84. Ho AJ, Cudlip AC, Ribeiro DC, Dickerson CR (2019) Examining upper extremity muscle demand during selected push-up variants. Journal of Electromyography and Kinesiology 44:165–172. doi: 10.1016/j.jelekin.2018.12.008

85. Holtermann A, Roeleveld K (2006) EMG amplitude distribution changes over the upper trapezius muscle are similar in sustained and ramp contractions. Acta physiologica 186(2):159–168. doi: 10.1111/j.1748-1716.2005.01520.x

86. Hommel J, Öhmichen S, Rudolph UM, Hauser T, Schulz H (2019) Effects of six-week sprint interval or endurance training on calculated power in maximal lactate steady state. Biology of sport 36(1):47–54. doi: 10.5114/biolsport.2018.78906

87. Hopker J, Coleman D, Passfield L (2009) Changes in cycling efficiency during a competitive season. Medicine & Science in Sports & Exercise 41(4):912–919. doi: 10.1249/MSS.0b013e31818f2ab2

88. Hopman MT, van Teeffelen WM, Brouwer J, Houtman S, Binkhorst RA (1995) Physiological responses to asynchronous and synchronous arm-cranking exercise. European journal of applied physiology 72(1-2):111–114. doi: 10.1007/bf00964124

89. Hug F, Dorel S (2009) Electromyographic analysis of pedaling: a review. Journal of Electromyography and Kinesiology 19(2):182–198. doi: 10.1016/j.jelekin.2007.10.010

90. Hultman E, Greenhaff PL, Ren JM, Söderlund K (1991) Energy metabolism and fatigue during intense muscle contraction. Biochemical Society transactions 19(2):347–353. doi: 10.1042/bst0190347

91. Hutchinson MJ, Paulson TAW, Eston R, Goosey-Tolfrey VL (2017) Assessment of peak oxygen uptake during handcycling. Test-retest reliability and comparison of a ramp-incremented and perceptually-regulated exercise test. PloS one 12(7):e0181008. doi: 10.1371/journal.pone.0181008

92. Internaional Paralympic Commitee (2015) IPC Athlete Classification Code. Rules, Policies and Procedures for Athlete Classification. https://www.paralympic.org/sites/default/files/document/150813212311788_Classification+Code_1.pdf

93. Jaafar H, Attiogbé E, Rouis M, Vandewalle H, Driss T (2015) Reliability of Force-Velocity Tests in Cycling and Cranking Exercises in Men and Women. BioMed research international 2015:954780. doi: 10.1155/2015/954780

94. Jacobs RA, Rasmussen P, Siebenmann C, Diaz V, Gassmann M, Pesta D, Gnaiger E, Nordsborg NB, Robach P, Lundby C (2011) Determinants of time trial performance and maximal incremental exercise in highly trained endurance athletes. Journal of applied physiology 111(5):1422–1430. doi: 10.1152/japplphysiol.00625.2011

95. Jacquier-Bret J, Faupin A, Rezzoug N, Gorce P (2013) A new postural force production index to assess propulsion effectiveness during handcycling. Journal of Applied Biomechanics 29(6):798–803. doi: 10.1123/jab.29.6.798

96. Jakobsen L, Ahlers FH (2016) Biomechanical analysis of hand cycling propulsion movement: A musculoskeletal modelling approach. Development of a wireless crank moment measurement-system for a handbike: Initial results of propulsion kinetics. Master theses (Sports technology), Aalborg University Denmark

97. Janssen TWJ, Dallmeijer AJ, van der Woude LHV (2001) Physical capacity and race performance of handcycle users. Journal of rehabilitation research and development 38(1):33–40

98. Jeacocke NA, Burke LM (2010) Methods to Standardize Dietary Intake before Performance Testing. International Journal of Sport Nutrition and Exercise Metabolism 20(2):87–103. doi: 10.1123/ijsnem.20.2.87

99. Johnson MA, Polgar J, Weightman D, Appleton D (1973) Data on the distribution of fibre types in thirty-six human muscles. An autopsy study. Journal of the neurological sciences 18(1):111–129. doi: 10.1016/0022-510x(73)90023-3

100. Jones AM, Burnley M, Black MI, Poole DC, Vanhatalo A (2019) The maximal metabolic steady state. Redefining the 'gold standard'. Physiological reports 7(10):e14098. doi: 10.14814/phy2.14098

101. Joyner MJ (1991) Modeling. Optimal marathon performance on the basis of physiological factors. Journal of applied physiology 70(2):683–687. doi: 10.1152/jappl.1991.70.2.683

102. Joyner MJ, Coyle EF (2008) Endurance exercise performance. The physiology of champions. The Journal of physiology 586(1):35–44. doi: 10.1113/jphysiol.2007.143834

103. Juel C, Halestrap AP (1999) Lactate transport in skeletal muscle - role and regulation of the monocarboxylate transporter. The Journal of physiology 517(3):633–642. doi: 10.1111/j.1469-7793.1999.0633s.x

104. Juhl JØ (2013) Non-circular Chainring Optimization for Handcycling. Journal of Lorempisum(1):1–8

105. Kayser B (2003) Exercise starts and ends in the brain. European journal of applied physiology 90(3-4):411–419. doi: 10.1007/s00421-003-0902-7

106. Kent-Braun JA, Fitts RH, Christie A (2012) Skeletal muscle fatigue. Comprehensive Physiology 2(2):997–1044. doi: 10.1002/cphy.c110029

107. Knechtle B, Müller G, Knecht H (2004) Optimal exercise intensities for fat metabolism in handbike cycling and cycling. Spinal cord 42(10):564–572. doi: 10.1038/sj.sc.3101612

108. Konrad P (2006) The ABC of EMG. A practical Introduction to Kinesiological Electromyography. Version of 1.4 March 2006. Noraxon U.S.A. Inc.:1–61

109. Koo TK, Li MY (2016) A guideline of selecting and reporting intraclass correlation coefficients for reliability research. Journal of chiropractic medicine 15(2):155–163. doi: 10.1016/j.jcm.2016.02.012

110. Kouwijzer I, Cowan RE, Maher JL, Groot FP, Riedstra F, Valent LJM, van der Woude, Groot S de (2019) Interrater and intrarater reliability of ventilatory thresholds determined in individuals with spinal cord injury. Spinal cord 57(8):669–678. doi: 10.1038/s41393-019-0262-8

111. Kouwijzer I, Nooijen CFJ, van Breukelen K, Janssen TWJ, Groot S de (2018) Effects of push-off ability and handcycle type on handcycling performance in able-bodied participants. Journal of rehabilitation medicine. doi: 10.2340/16501977-2343

112. Kraaijenbrink C, Vegter RJK, Hensen AHR, Wagner H, van der Woude LHV (2017) Different cadences and resistances in sub-maximal synchronous handcycling in able-bodied men. Effects on efficiency and force application. PloS one 12(8):e0183502. doi: 10.1371/journal.pone.0183502

113. Krämer C, Hilker L, Bohm H (2009a) Influence of crank length and crank width on maximal hand cycling power and cadence. European journal of applied physiology 106(5):749–757. doi: 10.1007/s00421-009-1062-1

114. Krämer C, Schneider G, Bohm H, Klopfer-Kramer I, Senner V (2009b) Effect of different handgrip angles on work distribution during hand cycling at submaximal power levels. Ergonomics 52(10):1276–1286. doi: 10.1080/00140130902971916

115. Leedham JS, Dowling JJ (1995) Force-length, torque-angle and EMG-joint angle relationships of the human in vivo biceps brachii. European journal of applied physiology 70(5):421–426. doi: 10.1007/bf00618493

116. Lehman GJ, McGill SM (1999) The importance of normalization in the interpretation of surface electromyography. A proof of principle. Journal of manipulative and physiological therapeutics 22(7):444–446

117. Leicht C, Perret C (2008) Comparison of blood lactate elimination in individuals with paraplegia and able-bodied individuals during active recovery from exhaustive exercise. The journal of spinal cord medicine 31(1):60–64. doi: 10.1080/10790268.2008.11753982

118. Lepers R, Hausswirth C, Maffiuletti N, Brisswalter J, van Hoecke J (2000) Evidence of neuromuscular fatigue after prolonged cycling exercise. Medicine & Science in Sports & Exercise 32(11):1880–1886. doi: 10.1097/00005768-200011000-00010

119. Lepers R, Maffiuletti NA, Rochette L, Brugniaux J, Millet GY (2002) Neuromuscular fatigue during a long-duration cycling exercise. Journal of applied physiology 92(4):1487–1493. doi: 10.1152/japplphysiol.00880.2001

120. Lepers R, Millet GY, Maffiuletti NA (2001) Effect of cycling cadence on contractile and neural properties of knee extensors. Medicine & Science in Sports & Exercise 33(11):1882–1888. doi: 10.1097/00005768-200111000-00013

121. Li J-D, Huang H-P, Lu T-W (2015) Effects of seat position on joint loads of the uper extremeties during handcyling in wheelcair-dependent individuals. International Conference on Biomechanics in Sports 33:406–409

122. Lindschulten R (2008) Leistungsphysiologische, hämatologische und elektromyographische Untersuchungen im Handbikesport bei Menschen mit einer Verletzung oder Erkrankung des Rückenmarks. Dissertation, German Sport University Cologne

123. Litzenberger S, Mally F, Sabo A (2015) Influence of different seating and crank positions on muscular activity in elite handcycling - a case study. Procedia Engineering 112:355–360. doi: 10.1016/j.proeng.2015.07.262

124. Litzenberger S, Mally F, Sabo A (2016) Biomechanics of elite recumbent handcycling. A case study. Sports Engineering 19(3):201–211. doi: 10.1007/s12283-016-0206-x

125. Liu P, Liu L, Clancy EA (2015) Influence of Joint Angle on EMG-Torque Model During Constant-Posture, Torque-Varying Contractions. IEEE transactions on neural systems and rehabilitation engineering 23(6):1039–1046. doi: 10.1109/TNSRE.2015.2405765

126. Lovell D, Shields D, Beck B, Cuneo R, McLellan C (2012) The aerobic performance of trained and untrained handcyclists with spinal cord injury. European journal of applied physiology 112(9):3431–3437. doi: 10.1007/s00421-012-2324-x

127. Lovell DI, Mason D, Delphinus E, McLellan C (2013) Upper and lower body anaerobic performance of semi-elite Rugby League players. The Journal of sports medicine and physical fitness 53(5):477–482

128. Lundby C, Montero D, Gehrig S, Andersson Hall U, Kaiser P, Boushel R, Meinild Lundby A-K, Kirk N, Valdivieso P, Flück M, Secher NH, Edin F, Hein T, Madsen K (2017) Physiological, biochemical, anthropometric, and biomechanical influences on exercise economy in humans. Scandinavian journal of medicine & science in sports 27(12):1627–1637. doi: 10.1111/sms.12849

129. Mader A (2003) Glycolysis and oxidative phosphorylation as a function of cytosolic phosphorylation state and power output of the muscle cell. European journal of applied physiology 88(4-5):317–338. doi: 10.1007/s00421-002-0676-3

130. Mader A, Heck H, Hollmann W (1983) A Computer Simulation Model of Energy Output in Relation to Metabolic Rate and Internal Enviroment. Modelling Approach, German Sport University Cologne

131. Mannion P, Toparlar Y, Clifford E, Hajdukiewicz M, Andrianne T, Blocken B (2019) The impact of arm-crank position on the drag of a paralympic hand-cyclist. Computer Methods in Biomechanics and Biomedical Engineering 22(4):386–395. doi: 10.1080/10255842.2018.1558217

132. Manunzio C, Mester J, Kaiser W, Wahl P (2016) Training Intensity Distribution and Changes in Performance and Physiology of a 2nd Place Finisher Team of the Race across America Over a 6 Month Preparation Period. Frontiers in physiology 7:642. doi: 10.3389/fphys.2016.00642

133. Marais G, Dupont L, Vanvelcenaher J, Clarys JP, Pelayo P (2004) Effects of spontaneously chosen crank rate variations on electromyographic responses in sub-maximal arm exercise in inexperienced subjects. European journal of applied physiology 92(4-5):598–601. doi: 10.1007/s00421-004-1187-1

134. Martinez-Valdes E, Guzman-Venegas RA, Silvestre RA, Macdonald JH, Falla D, Araneda OF, Haichelis D (2016) Electromyographic adjustments during continuous and intermittent incremental fatiguing cycling. Scandinavian journal of medicine & science in sports 26(11):1273–1282. doi: 10.1111/sms.12578

135. Medbø JI, Toska K (2001) Lactate Release, Concentration in Blood, and Apparent Distribution Volume after Intense Bicycling. Japanese Journal of Physiology 51(3):303–312. doi: 10.2170/jjphysiol.51.303

136. Merletti R, Knaflitz M, Luca CJ de (1990) Myoelectric manifestations of fatigue in voluntary and electrically elicited contractions. Journal of applied physiology 69(5):1810–1820. doi: 10.1152/jappl.1990.69.5.1810

137. Messias LHD, Gobatto CA, Beck WR, Manchado-Gobatto FB (2017) The Lactate Minimum Test. Concept, Methodological Aspects and Insights for Future Investigations in Human and Animal Models. Frontiers in physiology 8:389. doi: 10.3389/fphys.2017.00389

138. Messonnier L, Freund H, Denis C, Feasson L, Lacour J-R (2006) Effects of training on lactate kinetics parameters and their influence on short high-

intensity exercise performance. International journal of sports medicine 27(1):60–66. doi: 10.1055/s-2005-837507

139. Millet GY, Lepers R (2004) Alterations of neuromuscular function after prolonged running, cycling and skiing exercises. Sports Medicine 34(2):105–116. doi: 10.2165/00007256-200434020-00004

140. Momeni K, Faghri PD, Evans M (2014) Lower-extremity joint kinematics and muscle activations during semi-reclined cycling at different workloads in healthy individuals. Journal of neuroengineering and rehabilitation 11:146. doi: 10.1186/1743-0003-11-146

141. Mornieux G, Guenette JA, Sheel AW, Sanderson DJ (2007) Influence of cadence, power output and hypoxia on the joint moment distribution during cycling. European journal of applied physiology 102(1):11–18. doi: 10.1007/s00421-007-0555-z

142. Mossberg K, Willman C, Topor MA, Crook H, Patak S (1999) Comparison of asynchronous versus synchronous arm crank ergometry. Spinal cord 37(8):569–574. doi: 10.1038/sj.sc.3100875

143. Moxnes JF, Sandbakk O (2012) The kinetics of lactate production and removal during whole-body exercise. Theoretical biology & medical modelling 9:7. doi: 10.1186/1742-4682-9-7

144. Murray IR, Goudie EB, Petrigliano FA, Robinson CM (2013) Functional anatomy and biomechanics of shoulder stability in the athlete. Clinics in sports medicine 32(4):607–624. doi: 10.1016/j.csm.2013.07.001

145. Nevin J, Smith P, Waldron M, Patterson S, Price M, Hunt A, Blagrove R (2018) Efficacy of an 8-Week Concurrent Strength and Endurance Training program on Hand Cycling Performance. Journal of Strength and Conditioning Research 32(7):1861–1868. doi: 10.1519/JSC.0000000000002569

146. Nikooyan AA, Veeger DHEJ, Chadwick EKJ, Praagman M, van der Helm FCT (2011) Development of a comprehensive musculoskeletal model of the

shoulder and elbow. Medical & biological engineering & computing 49(12):1425–1435. doi: 10.1007/s11517-011-0839-7

147. Nikooyan AA, Veeger DHEJ, Westerhoff P, Bolsterlee B, Graichen F, Bergmann G, van der Helm FCT (2012) An EMG-driven musculoskeletal model of the shoulder. Human Movement Science 31(2):429–447. doi: 10.1016/j.humov.2011.08.006

148. Nikooyan AA, Veeger DHEJ, Westerhoff P, Graichen F, Bergmann G, van der Helm FCT (2010) Validation of the Delft Shoulder and Elbow Model using in-vivo glenohumeral joint contact forces. Journal of biomechanics 43(15):3007–3014. doi: 10.1016/j.jbiomech.2010.06.015

149. O'Bryan SJ, Brown NAT, Billaut F, Rouffet DM (2014) Changes in muscle coordination and power output during sprint cycling. Neuroscience letters 576:11–16. doi: 10.1016/j.neulet.2014.05.023

150. Olds TS, Norton KI, Lowe EL, Olive S, Reay F, Ly S (1995) Modeling road-cycling performance. Journal of applied physiology 78(4):1596–1611. doi: 10.1152/jappl.1995.78.4.1596

151. Ozkaya O (2013) Familiarization Effects of an Elliptical All-out Test and the Wingate Test Based on Mechanical Power Indices. Journal of sports science & medicine 12(3):521–525

152. Pařízková J (ed) (1978) Nutrition, physical fitness, and health. International series on sport sciences, vol 7. Univ. Park Press, Baltimore, Md.

153. Park S, Miyakawa S, Shiraki H (2008) EMG Analysis of upper extremity musces during isokinetic testing of the shoulder joint. Japanese Journal of Physical Fitness and Sports Medicine 57(1):101–110. doi: 10.7600/jspfsm.57.101

154. Park S-y, Yoo W-g (2013a) Comparison of exercises inducing maximum voluntary isometric contraction for the latissimus dorsi using surface electromyography. Journal of Electromyography and Kinesiology 23(5):1106–1110. doi: 10.1016/j.jelekin.2013.05.003

155. Park S-y, Yoo W-g (2013b) Selective activation of the latissimus dorsi and the inferior fibers of trapezius at various shoulder angles during isometric pull-down exertion. Journal of Electromyography and Kinesiology 23(6):1350–1355. doi: 10.1016/j.jelekin.2013.08.006

156. Phillips D, Karduna A (2017) Deltoid electromyography is reliable during submaximal isometric ramp contractions. Journal of Applied Biomechanics 33(3):237–240. doi: 10.1123/jab.2016-0224

157. Pigeon P, Yahia L, Feldman AG (1996) Moment arms and lengths of human upper limb muscles as functions of joint angles. Journal of biomechanics 29(10):1365–1370. doi: 10.1016/0021-9290(96)00031-0

158. Polgar J, Johnson MA, Weightman D, Appleton D (1973) Data on fibre size in thirty-six human muscles. An autopsy study. Journal of the neurological sciences 19(3):307–318. doi: 10.1016/0022-510x(73)90094-4

159. Powers SK, Beadle RE, Mangum M (1984) Exercise efficiency during arm ergometry. Effects of speed and work rate. Journal of applied physiology 56(2):495–499. doi: 10.1152/jappl.1984.56.2.495

160. Price MJ, Collins L, Smith PM, Goss-Sampson M (2007) The effects of cadence and power output upon physiological and biomechanical responses to incremental arm-crank ergometry. Applied physiology, nutrition, and metabolism 32(4):686–692. doi: 10.1139/H07-052

161. Quittmann OJ, Abel T, Albracht K, Strüder HK (2019) Reliability of muscular activation patterns and their alterations during incremental handcycling in able-bodied participants. Sports biomechanics. doi: 10.1080/14763141.2019.1593496

162. Quittmann OJ, Abel T, Strüder HK (2017) Relationship between physiology and performance of handcycling in able-bodied subjetcs. In: Ferrauti A, Platen P, Grimminger-Seidensticker E, Jaitner T, Bartmus U, Becher L, Marées M de, Mühlbauer T, Schauerte A, Wiewelhove T, Tsolakidis E (eds) 22nd Annual Congress of the European College of Sport Science. 5th - 8th July 2017,

MetropolisRuhr - Germany : book of abstracts, vol 22. Bochumer Universitätsverlag Westdeutscher Universitätsverlag, Bochum, pp 30–31

163. Quittmann OJ, Abel T, Zeller S, Foitschik T, Strüder HK (2018a) Lactate kinetics in handcycling under various exercise modalities and their relationship to performance measures in able-bodied participants. European journal of applied physiology 118(7):1493–1505. doi: 10.1007/s00421-018-3879-y

164. Quittmann OJ, Meskemper J, Abel T, Albracht K, Foitschik T, Rojas-Vega S, Strüder HK (2018b) Kinematics and kinetics of handcycling propulsion at increasing workloads in able-bodied subjects. Sports Engineering 21(4):283–294. doi: 10.1007/s12283-018-0269-y

165. Reiser M, Meyer T, Kindermann W, Daugs R (2000) Transferability of workload measurements between three different types of ergometer. European journal of applied physiology 82(3):245–249. doi: 10.1007/s004210050678

166. Robergs RA, Ghiasvand F, Parker D (2004) Biochemistry of exercise-induced metabolic acidosis. American journal of physiology 287(3):502-16. doi: 10.1152/ajpregu.00114.2004

167. Roman-Liu D, Bartuzi P (2018) Influence of type of MVC test on electromyography measures of biceps brachii and triceps brachii. International journal of occupational safety and ergonomics 24(2):200–206. doi: 10.1080/10803548.2017.1353321

168. Rota S, Rogowski I, Champely S, Hautier C (2013) Reliability of EMG normalisation methods for upper-limb muscles. Journal of sports sciences 31(15):1696–1704. doi: 10.1080/02640414.2013.796063

169. Ryan MM, Gregor RJ (1992) EMG profiles of lower extremity muscles during cycling at constant workload and cadence. Journal of Electromyography and Kinesiology 2(2):69–80. doi: 10.1016/1050-6411(92)90018-E

170. Salonikidis K, Amiridis IG, Oxyzoglou N, Giagazoglou P, Akrivopoulou G (2011) Wrist flexors are steadier than extensors. International journal of sports medicine 32(10):754–760. doi: 10.1055/s-0031-1280777

171. Sawka MN, Glaser RM, Wilde SW, Luhrte TC von (1980) Metabolic and circulatory responses to wheelchair and arm crank exercise. Journal of applied physiology 49(5):784–788

172. Sayers MGL, Tweddle AL, Every J, Wiegand A (2012) Changes in drive phase lower limb kinematics during a 60 min cycling time trial. Journal of science and medicine in sport 15(2):169–174. doi: 10.1016/j.jsams.2011.09.002

173. Schantz P, Randall-Fox E, Hutchison W, Tydén A, Astrand PO (1983) Muscle fibre type distribution, muscle cross-sectional area and maximal voluntary strength in humans. Acta physiologica Scandinavica 117(2):219–226. doi: 10.1111/j.1748-1716.1983.tb07200.x

174. Schoenmakers P, Reed K, van der Woude LHV, Hettinga FJ (2016) High Intensity Interval Training in Handcycling. The Effects of a 7 Week Training Intervention in Able-bodied Men. Frontiers in physiology 7:638. doi: 10.3389/fphys.2016.00638

175. Schwartz C, Tubez F, Wang F-C, Croisier J-L, Brüls O, Denoël V, Forthomme B (2017) Normalizing shoulder EMG. An optimal set of maximum isometric voluntary contraction tests considering reproducibility. Journal of Electromyography and Kinesiology 37:1–8. doi: 10.1016/j.jelekin.2017.08.005

176. Seiler S (2010) What is best practice for training intensity and duration distribution in endurance athletes? International journal of sports physiology and performance 5(3):276–291. doi: 10.1152/jappl.1984.56.2.495

177. Smekal G, Duvillard SP von, Pokan R, Hofmann P, Braun WA, Arciero PJ, Tschan H, Wonisch M, Baron R, Bachl N (2012) Blood lactate concentration at the maximal lactate steady state is not dependent on endurance capacity in healthy recreationally trained individuals. European journal of applied physiology 112(8):3079–3086. doi: 10.1007/s00421-011-2283-7

178. Smith PM, Chapman ML, Hazlehurst KE, Goss-Sampson MA (2008) The influence of crank configuration on muscle activity and torque production during arm crank ergometry. Journal of Electromyography and Kinesiology 18(4):598–605. doi: 10.1016/j.jelekin.2006.12.006

179. Smith PM, Doherty M, Price MJ (2006a) The effect of crank rate on physiological responses and exercise efficiency using a range of submaximal workloads during arm crank ergometry. International journal of sports medicine 27(3):199–204. doi: 10.1055/s-2005-837620

180. Smith PM, Doherty M, Price MJ (2007) The effect of crank rate strategy on peak aerobic power and peak physiological responses during arm crank ergometry. Journal of sports sciences 25(6):711–718. doi: 10.1080/02640410600831955

181. Smith PM, McCrindle E, Doherty M, Price MJ, Jones AM (2006b) Influence of crank rate on the slow component of pulmonary O(2) uptake during heavy arm-crank exercise. Applied physiology, nutrition, and metabolism 31(3):292–301. doi: 10.1139/h05-039

182. Smith PM, Price MJ, Doherty M (2001) The influence of crank rate on peak oxygen consumption during arm crank ergometry. Journal of sports sciences 19(12):955–960. doi: 10.1080/026404101317108453

183. Sperlich B, Zinner C, Heilemann I, Kjendlie P-L, Holmberg H-C, Mester J (2010) High-intensity interval training improves VO(2peak), maximal lactate accumulation, time trial and competition performance in 9-11-year-old swimmers. European journal of applied physiology 110(5):1029–1036. doi: 10.1007/s00421-010-1586-4

184. Stangier C, Abel T, Zeller S, Quittmann OJ, Perret C, Strüder HK (2019) Comparison of Different Blood Lactate Threshold Concepts for Constant Load Performance Prediction in Spinal Cord Injured Handcyclists. Frontiers in physiology 10:894. doi: 10.3389/fphys.2019.01054

185. Stone B, Mason BS, Bundon A, Goosey-Tolfrey VL (2019a) Elite handcycling. A qualitative analysis of recumbent handbike configuration for optimal sports performance. Ergonomics 62(3):449–458. doi: 10.1080/00140139.2018.1531149

186. Stone B, Mason BS, Warner MB, Goosey-Tolfrey VL (2019b) Horizontal Crank Position Affects Economy and Upper Limb Kinematics of Recumbent Handcyclists. Medicine & Science in Sports & Exercise. doi: 10.1249/MSS.0000000000002062

187. Stone B, Mason BS, Warner MB, Goosey-Tolfrey VL (2019c) Shoulder and thorax kinematics contribute to increased power output of competitive handcyclists. Scandinavian journal of medicine & science in sports 29(6):843–853. doi: 10.1111/sms.13402

188. Suzuki S, Watanabe S, Homma S (1982) EMG activity and kinematics of human cycling movements at different constant velocities. Brain Research 240(2):245–258. doi: 10.1016/0006-8993(82)90220-7

189. Taoutaou Z, Granier P, Mercier B, Mercier J, Ahmaidi S, Prefaut C (1996) Lactate kinetics during passive and partially active recovery in endurance and sprint athletes. European journal of applied physiology 73(5):465–470. doi: 10.1007/BF00334425

190. Union Cycliste Internationale (UCI) (2019) UCI Cycling Regulations. Part 16 Paracycling. https://www.uci.org/docs/default-source/rules-and-regulations/part-xvi--para-cycling.pdf?sfvrsn=47af1c56_34. Accessed 20 Oct 2019

191. Valent LJ, Dallmeijer AJ, Houdijk H, Slootman HJ, Post MW, van der Woude LHV (2008) Influence of hand cycling on physical capacity in the rehabilitation of persons with a spinal cord injury. A longitudinal cohort study. Archives of physical medicine and rehabilitation 89(6):1016–1022. doi: 10.1016/j.apmr.2007.10.034

192. Valent LJM (2009) The effects of handcycling on physical capacity in persons with spinal cord injury. Dissertation, Vrije Universiteit Amsterdam

193. van der Helm FCT (1994) A finite element musculoskeletal model of the shoulder mechanism. Journal of biomechanics 27(5):551–569. doi: 10.1016/0021-9290(94)90065-5

194. van der Woude LHV, Bosmans I, Bervoets B, Veeger DHEJ (2000) Handcycling. Different modes and gear ratios. Journal of Medical Engineering & Technology 24(6):242–249. doi: 10.1152/jappl.1984.56.2.495

195. van Drongelen S, Maas JC, Scheel-Sailer A, van der Woude LHV (2009) Submaximal arm crank ergometry. Effects of crank axis positioning on mechanical efficiency, physiological strain and perceived discomfort. Journal of Medical Engineering & Technology 33(2):151–157. doi: 10.1080/13561820802565676

196. van Drongelen S, van den Berg J, Arnet U, Veeger DHEJ, van der Woude LHV (2011) Development and validity of an instrumented handbike. Initial results of propulsion kinetics. Medical engineering & physics 33(9):1167–1173. doi: 10.1016/j.medengphy.2011.04.018

197. van Hall G (2010) Lactate kinetics in human tissues at rest and during exercise. Acta physiologica 199(4):499–508. doi: 10.1111/j.1748-1716.2010.02122.x

198. van Ingen Schenau GJ (1989) From rotation to translation. Constraints on multi-joint movements and the unique action of bi-articular muscles. Human Movement Science 8(4):301–337. doi: 10.1016/0167-9457(89)90037-7

199. Veeger DHEJ, Meershoek LS, van der Woude LHV, Langenhoff JM (1998) Wrist motion in handrim wheelchair propulsion. Journal of rehabilitation research and development 35(3):305–313

200. Veeger DHEJ, van der Helm FC, van der Woude LHV, Pronk GM, Rozendal RH (1991) Inertia and muscle contraction parameters for musculoskeletal modelling of the shoulder mechanism. Journal of biomechanics 24(7):615–629. doi: 10.1016/0021-9290(91)90294-w

201. Veeger DHEJ, Yu B, An KN, Rozendal RH (1997) Parameters for modeling the upper extremity. Journal of biomechanics 30(6):647–652. doi: 10.1016/s0021-9290(97)00011-0

202. Vegter RJK, Mason BS, Sporrel B, Stone B, van der Woude LHV, Goosey-Tolfrey VL (2019) Crank fore-aft position alters the distribution of work over the push and pull phase during synchronous recumbent handcycling of able-bodied participants. PloS one 14(8):e0220943. doi: 10.1371/journal.pone.0220943

203. Vera-Garcia FJ, Moreside JM, McGill SM (2010) MVC techniques to normalize trunk muscle EMG in healthy women. Journal of Electromyography and Kinesiology 20(1):10–16. doi: 10.1016/j.jelekin.2009.03.010

204. Verellen J, Janssens L, Meyer C, Vanlandewijck Y (2012) Development and application of a handbike ergometer to measure the 3D force generation pattern during arm crank propulsion in realistic handcycling conditions. Sports Technology 5(1-2):65–73. doi: 10.1080/19346182.2012.754894

205. Verellen J, Meyer C, Reynders S, van Biesen D, Vanlandewijck Y (2008) Consistency of within-cycle torque distribution pattern in hand cycling. Journal of rehabilitation research and development 45(9):1295. doi: 10.1682/JRRD.2007.12.0205

206. Verellen J, Theisen D, Vanlandewijck Y (2004) Influence of Crank Rate in Hand Cycling. Medicine & Science in Sports & Exercise 36(10):1826–1831. doi: 10.1249/01.MSS.0000142367.04918.5A

207. Vicon Motion Systems (2007) Upper Limb Model Guide. https://www.vicon.com/downloads/documentation/vicon-documentation/upper-limb-model-guide. Accessed 26 Aug 2016

208. Wahl P, Yue Z, Zinner C, Bloch W, Mester J (2011) A mathematical model for lactate transport to red blood cells. The journal of physiological sciences 61(2):93–102. doi: 10.1007/s12576-010-0125-8

209. Weber CL, Chia M, Inbar O (2006) Gender differences in anaerobic power of the arms and legs. A scaling issue. Medicine & Science in Sports & Exercise 38(1):129–137. doi: 10.1249/01.mss.0000179902.31527.2c

210. Willick SE, Webborn N, Emery C, Blauwet CA, Pit-Grosheide P, Stomphorst J, van de Vliet P, Patino Marques NA, Martinez-Ferrer JO, Jordaan E, Derman W, Schwellnus M (2013) The epidemiology of injuries at the London 2012 Paralympic Games. British journal of sports medicine 47(7):426–432. doi: 10.1136/bjsports-2013-092374

211. Wu G, van der Helm FCT, Veeger DHEJ, Makhsous M, van Roy P, Anglin C, Nagels J, Karduna AR, McQuade K, Wang X, Werner FW, Buchholz B (2005) ISB recommendation on definitions of joint coordinate systems of various joints for the reporting of human joint motion. Part II: Shoulder, elbow, wrist and hand. Journal of biomechanics 38(5):981–992. doi: 10.1016/j.jbiomech.2004.05.042

212. Wu W, Lee PVS, Bryant AL, Galea M, Ackland DC (2016) Subject-specific musculoskeletal modeling in the evaluation of shoulder muscle and joint function. Journal of biomechanics 49(15):3626–3634. doi: 10.1016/j.jbiomech.2016.09.025

213. Zajac FE (2002) Understanding muscle coordination of the human leg with dynamical simulations. Journal of biomechanics 35(8):1011–1018. doi: 10.1016/S0021-9290(02)00046-5

214. Zanca GG, Oliveira AB, Ansanello W, Barros FC, Mattiello SM (2014) EMG of upper trapezius--electrode sites and association with clavicular kinematics. Journal of Electromyography and Kinesiology 24(6):868–874. doi: 10.1016/j.jelekin.2014.06.012

215. Zatsiorsky VM, Seluyanov VN (1985) Estimation of the mass and inertia characteristics of the main segments of the human body. In: Winter DA, Norman RW, Wells RP, Hayes, K. C. Patla, A. E. (eds) Biomechanics IX-B. [proceedings of the Ninth International Congress of Biomechanics held in 1983

at Waterloo, Ontario, Canada]. Human Kinetics Publishers, Champaign, IL., pp 233–239

216. Zeller S, Abel T, Smith PM, Strüder HK (2015) Influence of noncircular chainring on male physiological parameters in hand cycling. Journal of rehabilitation research and development 52(2):211–220. doi: 10.1682/JRRD.2014.03.0070

217. Zeller S, Abel T, Strüder HK (2017) Monitoring Training Load in Handcycling. A Case Study. Journal of Strength and Conditioning Research 31(11):3094–3100. doi: 10.1519/JSC.0000000000001786

Summary

Handcycling is an efficient and aerobically demanding exercise for improving endurance in individuals with an spinal cord injury (SCI) or amputation of the lower limb/s. Even though handcycling was found to be mechanically less straining when compared to manual wheelchair propulsion, Paralympic athletes are prone to overuse injuries of the upper extremity. Physiological aspects of handcycling exercise during cross-sectional and longitudinal studies have primarily investigated aerobic metabolism in terms of maximal oxygen consumption ($\dot{V}O_2max$) and efficiency. Biomechanical aspects of handcycling propulsion demonstrated alterations due to the handbike setup and different intensities. However, studies combining crank kinetics, joint kinematics and muscular activity are primarily based on single-case studies. Hence, this thesis aimed to assess anaerobic metabolism in terms of lactate kinetics and maximal lactate accumulation rate ($\dot{V}La_{max}$) and examine the complex biomechanics underlying handcycling propulsion in several participants.

Two studies were performed in n = 12 and n = 18 able-bodied triathletes, respectively. In the first study, lactate kinetics, crank kinetics, joint kinematics and muscular activity were measured during three exercise modalities: an incremental step test until volitional exhaustion, a 15-s all-out sprint test and a 30-min continuous load trial at the individual lactate threshold (P_4). The tests were performed in a recumbent racing handcycle (Shark S, Sopur, Sunrise Medical, Malsch, Germany) that was mounted on an ergometer (8 Hz, Cyclus 2, RBM electronic automation GmbH, Leipzig, Germany). Lactate kinetics were determined by using an enzymatic-amperometric sensor chip system (Biosen C-Line, EKF-diagnostics GmbH, Barleben, Germany) and adequate interpolation approaches. Tangential crank torque was measured using a power meter (1000 Hz, Schoberer Rad

Messtechnik GmbH, Jülich, Germany) installed in the crank. Joint kinematics of the shoulder, elbow, wrist and trunk were calculated according to the Upper Limb Model of Vicon Nexus and ISB recommendation by using a 3D motion capturing system (100 Hz, Vicon Nexus 2.3, Vicon Motion Systems Ltd., Oxford, UK). Surface electromyography (sEMG) was performed for ten muscles of the upper extremity and trunk using a wireless sEMG system (1000 Hz, DTSEMG Sensor®, Noraxon Scottsdale, Arizona, USA). Additionally, different sEMG normalisation procedures were compared to determine adequate maximal voluntary isometric contraction (MVIC) positions. In the second study, peak power output and $\dot{V}La_{max}$ were compared between handcycling and conventional (leg) cycling in terms of reliability, differences between and correlations among extremities.

$\dot{V}La_{max}$ was identified as a promising parameter in handcycling exercise testing, since $\dot{V}La_{max}$ attained high reliability and correlated with both aerobic and anaerobic performance. Moreover, $\dot{V}La_{max}$ was found to be extremity-specific which might be relevant for exercise testing in endurance sports with an emphasis on both extremities (e. g. rowing and cross-country skiing). Based on the biomechanical measurements, the pull phase was found to increase in work distribution with exercise intensity and duration. The muscular activation patterns (MAPs) of the examined muscles were used to identify their function in propulsion cycle and assess their sensitivity to fatigue. As the initiator of the pull phase, the posterior part of M. deltoideus (DP) was found to be most affected by exercise intensity and duration which highlights the necessity for additional conditioning. Whereas some muscles can be normalised by sport-specific MVICs, some muscles should be normalised muscle-specifically. Future studies should replicate these studies, examine the effect of deliberate training on $\dot{V}La_{max}$ and investigate handcycling biomechanics in several elite SCI handcyclists/paratriathletes.

Summary (in German)

Handcycling stellt eine effiziente Fortbewegungsart für Menschen mit Querschnittslähmung oder Amputation der unteren Extremität dar, die zur Entwicklung und Aufrechterhaltung der Ausdauerleistungsfähigkeit beiträgt. Obwohl Handcycling im Vergleich zum Rollstuhlfahren mit einer geringeren Gelenkbelastung einhergeht, weisen Paralympische Athleten eine hohe Verletzungsanfälligkeit im Bereich der oberen Extremität auf. Studien, die sich mit den physiologischen Aspekten des Handcycling und dessen Training beschäftigt haben, befassten sich bisher vornehmlich mit dem aeroben Stoffwechsel im Sinne der maximalen Sauerstoffaufnahme ($\dot{V}O_2max$) und Bewegungsökonomie. In biomechanischen Untersuchungen wurde zwar der Einfluss verschiedener Handbikeeinstellungen und Intensitäten ausführlich untersucht; jedoch basieren die Erkenntnisse komplexer Studien, die gleichzeitig Kurbelkinetik, Gelenkkinematik und Muskelaktivität bestimmt haben, zumeist auf Einzelfällen. Daher widmet sich diese Arbeit der Untersuchung des anaeroben Stoffwechsels im Sinne der Laktatkinetik und maximalen Laktatbildungsrate ($\dot{V}La_{max}$) sowie einer komplexen, biomechanischen Betrachtung der Antriebsbewegung im Handcycling bei mehreren Probanden.

In zwei Studien wurden ambitionierte Triathleten (n = 12 und n = 18) untersucht. Die erste Studie widmete sich der Laktatkinetik, Kurbelkinetik, Gelenkkinematik und Muskelaktivität während drei verschiedener Belastungsmodalitäten: ein Stufentest bis zur subjektiven Ausbelastung, ein maximaler Sprinttest über 15 Sekunden sowie ein 30 minütiger Dauertest bei einer Intensität analog zu einer Laktatkonzentration von der 4 $mmol \cdot l^{-1}$ (P_4). Die Belastungstests wurden in einem wettkampforientierten Handbike (Shark S, Sopur, Sunrise Medical, Malsch, Germany) durchgeführt, welches in einem entsprechenden Ergometer (8 Hz, Cyclus 2, RBM electronic

automation GmbH, Leipzig, Germany) montiert wurde. Die Laktatkinetik wurde über ein stationäres Analysegerät (Biosen C-Line, EKF-diagnostics GmbH, Barleben, Germany) und geeignete Interpolationsgleichungen bestimmt. Ein in der Kurbel montierter Leistungsmesser (1000 Hz, Schoberer Rad Messtechnik GmbH, Jülich, Germany) ermöglichte die Bestimmung des tangentialen Drehmomentes. Die Kinematik des Schulter-, Ellenbogen- und Handgelenkes sowie des Rumpfes wurde, im Einklang mit dem Upper Limb Modell von Vicon Nexus und Empfehlungen der ISB, über ein 3D Bewegungsanalysesystem (100 Hz, Vicon Nexus 2.3, Vicon Motion Systems Ltd., Oxford, UK) bestimmt. Die Aktivität von zehn Muskeln der oberen Extremität und des Rumpfes wurde über eine kabellose Oberflächenelektromyographie (sEMG) ermittelt (1000 Hz, DTSEMG Sensor®, Noraxon Scottsdale, Arizona, USA). Des Weiteren wurde ein Vergleich zwischen sport- und muskelspezifischen maximalen willkürlichen isometrischen Kontraktionen (MVICs) durchgeführt, um geeignete Normalisierungspositionen der jeweiligen sEMG-Signale zu bestimmen. Im Rahmen der zweiten Studie wurde die maximale Leistung und $\dot{V}La_{max}$ im Handcycling und Radfahren hinsichtlich der Reliabilität sowie Differenzen und Korrelationen zwischen den Extremitäten untersucht.

Die $\dot{V}La_{max}$ stellte sich als vielversprechender Parameter heraus, da sie eine hohe Reliabilität aufwies und sowohl mit der aeroben als auch anaeroben Leistungsfähigkeit signifikant korrelierte. Außerdem erwies sich die $\dot{V}La_{max}$ als extremitätsspezifisch, was eine Relevanz für die Leistungsdiagnostik von Ausdauersportarten haben könnte, die obere und untere Extremitäten in vergleichbarer Weise einsetzen (wie z. B. Rudern und Skilanglauf). Die biomechanischen Messungen zeigten, dass die Zugphase bei zunehmender Belastungsintensität und -dauer an relativer Bedeutsamkeit gewinnt. Aus den sEMG Messungen konnten die Aktivierungsmuster der beteiligten

Muskeln (MAPs) erstellt werden, die eine Bestimmung der jeweiligen Funktion im Kurbelzyklus zulassen. Als Initiator der Zugphase zeigte der posteriore Anteil des M. deltoideus (DP) die stärksten Veränderungen bei zunehmender Belastungsintensität und -dauer auf, was auf die Notwendigkeit zusätzlichen Krafttrainings hinweist. Während die sEMG-Signale mancher Muskeln durchaus sportart-spezifisch normalisiert werden können, sollte man bei anderen wiederum MVICs in muskel-spezifischen Positionen durchführen.

Zukünftige Studien sollten die vorgestellten Verfahren bei trainierten (querschnittsgelähmten) Handbikern und/oder Paratriathleten replizieren und den Effekt verschiedener Trainingsbelastungen auf die $\dot{V}La_{max}$ untersuchen. Gleiches gilt für die Analyse komplexer, biomechanischer Aspekte im Handcycling unter besonderer Berücksichtigung der MAPs.

Acknowledgements

During the past three years, I had the opportunity to measure, discuss and talk with a lot of colleagues, scientists and friends, respectively. Even though I am grateful for everyone who accompanied my journey, I cannot mention every single one of them. Representatively, I want to express my gratitude to some of the most influential people during the course of my doctorate program and the ones who supported me in preparing this thesis.

My first thanks go to my doctoral supervisors Univ.-Prof. Dr. **Thomas Abel** and Jun.-Prof. Dr. **Kirsten Albracht**. **Thomas**, it is hard to describe how much you inspired and influenced my work as a scientist, lecturer and coach. You introduced me to the sport of people with disabilities and handcycling in particular, which spurred my interest in this unique field. Your personality and character sets you apart as a Professor, leader and supervisor, which I admire very much. The field of Paralympic Sports deserves to have more courageous people like you. **Kirsten**, I would like to thank you for enabling all biomechanical measurements. Without your initiative, support and trust, most of the procedures described would not have been performed. You helped me in developing my biomechanical skills, even though I'm more an exercise physiologist. Thank you so much.

Many thanks go to **Joshua Meskemper** for helping me conduct the biomechanical setup and measurements. Since I was in the wrong master program for performing such a study, sharing your experience saved me a lifetime. Also, I would like to thank **Alessandro Fasse** for introducing me to the world of Matlab.

I would like to deeply thank Dr. **Thomas Bscher** for supporting me in all the years. Based on your sponsorship, I could focus on my research and career as an exercise scientist. I appreciate your support very much.

I would like to express my gratitude to my esteemed colleague Dr. **Tina Foitschik** for providing medical background during experiments, assisting me in all medical issues and being one of the most reliable persons I know.

I want to thank Dr. **Gerard King** for his support and advice during my time at the GSUC. Chatting, working and exercising with you has always been a pleasure. The GSUC is lucky to have you at the International Office.

Univ.-Prof. mult. Dr. Dr. h.c. mult. **Wildor Hollman**, I always admired you for your holistic and profound knowledge in sport, medicine, physics and other disciplines and your incredible eloquence during lectures.

Sharing knowledge, experience and ideas with my colleagues and co-authors Dr. **Sebastian Zeller**, Dr. **Ramin Vafa**, **Daniel Appelhans**, **Yannick M. Schwarz** and others helped me a lot to gain knowledge in exercise testing and training. Thank you very much for your time over the years.

I would like to thank MD **Ingrid Kouwijzer**, Dr. **Marika T. Leving**, **Benjamin Stone**, **Rafael Muchaxo**, Dr. **Sonja de Groot**, Dr. **Ursina Arnet**, PD Dr. **Claudio Perret**, Prof. Dr. **Victoria L. Goosey-Tolfrey**, Prof. Dr. **Lucas H. V. van der Woude**, Prof. Dr. **Thomas W. J. Janssen**, Dr. **Riemer J. K. Vegter**, Dr. **Carla F. J. Nooijen**, **Cassandra Kraaijenbrink** and all the others for welcoming me into the field of Paralympic sport and inspiring my research. I would be glad to collaborate with you in future projects of the European Research Group in Disability Sport (ERGiDS).

A huge 'thank you' goes to my athlete and (more importantly) close friend **Benjamin Lenatz**. I am so grateful for the trust you have placed in my paratriathlon coaching skills. It has been such an interesting journey with so many diagnostics, training camps and events in terms of practical application from you. You've inspired my work as a scientist and coach and I've learned so much from you. I really hope that at least some of the findings help you to improve your handcycling performance. Based on the work, effort and time you put into this project over the years, you deserve to qualify for the Paralympics in Tokyo next year and visit this lovely island once more.

I want to thank **all participants** who took part in the studies of this thesis for their patience and commitment during the various exercise tests in the lab.

I want to thank **Oradjeha Tanshi** for proof-reading my thesis for typos and wording.

Last but not least, I would like to express my heartfelt appreciation to my mother **Britta**, my father **Rolf**, my 'little' sister **Emily**, my stepmom **Jutta**, my best friend (for more than 20 years) **Till** and my beloved girlfriend **Katrin**. Words cannot express how grateful I am for having you. Without your love, I wouldn't be the person I am today.

Appendices

Scientific output

Published articles

Quittmann OJ, Appelhans D, Abel T & Strüder HK. Evaluation of a sport-specific field test to determine maximal lactate accumulation rate and sprint performance parameters in running . *Journal of Science and Medicine in Sport,* 2020, 23(1), 27-34. (Impact factor 2018: 3.623)

Quittmann OJ, Abel T, Albracht K & Strüder HK. Reliability of muscular activation patterns and their alterations during incremental handcycling in able-bodied participants. *Sports Biomechanics,* 2019, epub ahead of print. (Impact factor 2018: 1.714)

Quittmann OJ, Abel T, Zeller S, Foitschik T & Strüder HK. Lactate kinetics in handcycling under various exercise modalities and their relationship to performance measures in able-bodied participants. *European Journal of Applied Physiology,* 2018, 118(7):1493–1505. (Impact factor 2018: 3.055)

Quittmann OJ, Meskemper J, Abel T, Albracht K, Foitschik T, Rojas-Vega S & Strüder HK. Kinematics and kinetics of handcycling propulsion at increasing workloads in able-bodied subjects. *Sports Engineering,* 2018, 21(4): 283–294.

Stangier C, Abel T, Zeller S, **Quittmann OJ**, Perret C & & Strüder HK. Comparison of Different Blood Lactate Threshold Concepts for Constant Load Performance Prediction in Spinal Cord Injured Handcyclists. *Frontiers in Physiology*, 2019, epub ahead of print. (Impact factor 2018: 3.201)

Gavanda S, Geisler S, **Quittmann OJ** & Schiffer T. The Effect of Block Versus Daily Undulating Periodization on Strength and Performance in Adolescent Football Players, *International journal of sports physiology and performance*, 2019, 14(6): 814–821. (Impact factor 2018: 3.979)

Manuscripts under review

Quittmann OJ, Abel T, Albracht K, Meskemper J, Foitschik T & Strüder HK. Biomechanics of handcycling propulsion in a 30-min continuous load test at lactate threshold: Kinetics, kinematics and muscular activity in able-bodied participants. *European Journal of Applied Physiology*. (Impact factor 2018: 3.055)

Quittmann OJ, Meskemper J, Albracht K, Abel T, Foitschik T & Strüder HK. Normalising surface EMG of ten upper-extremity muscles in handcycling: Muscle-specific vs. sport-specific MVICs. *Journal of Electromyography and Kinesiology*. (Impact factor 2018: 1.753)

Quittmann OJ, Schwarz YM, Mester J, Foitschik T, Abel T & Strüder HK. Maximal lactate accumulation rate in all-out exercise differs between cycling and running. *International Journal of Sports Medicine*. (Impact factor 2018: 2.132)

Quittmann OJ, Abel T, Vafa R, Mester J, Schwarz YM & Strüder HK. Maximal lactate accumulation rate and post-exercise lactate kinetics in handcycling and cycling. *European Journal of Sport Science*. (Impact factor 2018: 2.376)

Quittmann OJ, Abel T, Albracht K & Strüder HK. Biomechanics of all-out handcycling exercise: Kinetics, kinematics and muscular activity of a

15-s sprint test in able-bodied participants. *Sports Biomechanics*. (Impact factor 2018: 1.714)

Gavanda S, Geisler S, **Quittmann OJ**, Bauhaus H & Schiffer T. Three weeks of detraining does not decrease muscle thickness, strength or sport performance in adolescent athletes. *International Journal of Exercise Science*.

Manuscripts in preparation

Quittmann OJ, Bartsch P, Foitschik T, Abel T & Strüder HK. Road to Tokyo 2020: The 4-year journey of a spinal cord injured paratriathlete preparing for the Paralympics.

Quittmann OJ, Foitschik T, Vafa R, Freitag FJ, Sparmann N, Abel T & Strüder HK. Augmenting the metabolic profile of endurance runners: Applications of maximal lactate accumulation rate ($\dot{V}La_{max}$)

Conference contributions

2018: 6th International RehabMove State-of-the-art congress, Groningen, The Netherlands. *Kinematics, kinetics and muscular activity of 15-s all-out handcycling exercise in able-bodied participants*, **Oral presentation**.

2018: Symposium 'sport.movement.health' (Science Slam World Cup), Cologne, Germany. *Biomechanics of all-out handcycling exercise*, **Poster presentation**.

2017: 22nd Annual Congress of the European College of Sport Science, Bochum/Duisburg/Essen, Germany. Relationship between physiology and performance of handcycling in able-bodied subjects, **Oral presentation**.

2017: 35th International Conference on Biomechanics in Sports, Cologne, Germany. *Changes in the kinematic and kinetic profile of handcycling propulsion due to increasing workloads,* **Oral presentation**.

2016: Kongress Nachwuchsförderung NRW, Cologne, Germany. *Evidence based Performance Diagnostics: Metabolic Parameters in Endurance Sports*, **Oral presentation**.

2016: Kongress Nachwuchsförderung NRW, Cologne, Germany. *Simulated Reduction of Flight Time during Hurdle Clearance by Manipulation of Ground Reaction Forces*, **Poster presentation**.

2015: 46th Deutscher Sportärztekongress, Frankfurt, Germany. *Stoßwellenbehandlung der Skelettmuskulatur: Wirkung auf Schädigungs- und Entzündungsmarker*, **Mini-Oral presentation**.

2015: Kongress Nachwuchsförderung NRW, Cologne, Germany. *Competition-based potentials in paratriathlon: an explorative approach*, **Oral presentation**.

Reviewer activities

Nov 2019: *International Journal of Sports Physiology and Performance* (topic: determinants of handcycling performance)

Sep 2019: *International Journal of Sports Medicine* (topic: performance testing in handcycling)

Nov 2018: *International Journal of Sports Physiology and Performance* (topic: intensified training in paratriathletes)

Curriculum vitae

Personal Details

Name	Oliver Jan Quittmann
Date of Birth	15/10/1991
Place of Birth	Dortmund, North Rhine-Westphalia, Germany
Nationality	German

Education

Since Sep 2016	PhD student at the Institute of Movement and Neurosciences, German Sport University Cologne (GSUC), Germany
Oct 2014 – Sep 2016	Master student at the GSUC, Germany
	Degree: M.Sc. Exercise Science and Coaching (1.0)
Oct 2011 – Jul 2014	Bachelor student at the GSUC, Germany
	Degree: B.Sc. Sport and Performance (1.2)
Aug 2002 – Jul 2011	Pheonix High School Dortmund, Germany
Aug 1998 – Jul 2002	Eintracht Elementary School Dortmund, Germany

Professional Career

Since Apr 2019	Lecturer at the Institute of Movement and Neurosciences, GSUC, Germany

Since Jan 2017	Research scientist at the Institute of Movement and Neurosciences, GSUC, Germany
Since Oct 2016	Lecturer for the following classes - Diagnostics and training: Physical performance (SUL 9.1) - Potential of adaptation processes and performance development (SUL 6) - Selected sport discipline I: Triathlon (SUL 1.12) - Clinical and technical fundamentals of elite, recreational and rehabilitative sport (PE 1.5)
Aug 2015 – Dec 2016	Research assistant at the Institute of Movement and Neurosciences, GSUC, Germany
Oct 2013 – Dec 2016	Research assistant at the Institute of Exercise Training and Sport Informatics, GSUC, Germany
Feb 2012 – Jul 2014	Tutor for 'Methods and Statistics', Institute of Physiology and Anatomy, GSUC, Germany

Awards and Scholarships

Nov 2018	2nd place at the Science Slam World Cup, GSUC, Germany
Apr 2018	1st place at the GSUC Science-Picture of the year competition, GSUC, Germany
Jul 2017	Best graduate student of the year in the M.Sc. Exercise Science and Coaching program, GSUC, Germany

Jun 2015	August-Bier award for the best graduate student of all bachelor's degree programs, GSUC, Germany
Jun 2014	Teaching award for the tutorial 'Methods and Statistics', GSUC, Germany
Oct 2013 – Sep 2016	German Scholarship of the GSUC in the category high performance students
Jun 2013	Teaching award for the tutorial 'Methods and Statistics', GSUC, Germany

About the author

I was born on 15 October, 1991 in Dortmund as the first child of Britta and Rolf Quittmann. Even though I participated in several sports, I was not that serious about training and exercise in my early childhood. Things changed at the age of 14, when I started playing Badminton at the local sports club. Driven by the goal to play in the same league as my father used to back in the day, I increased my efforts and used every possibility to improve. In 2008, I became an umpire in badminton and participated at the European Para-Badminton Championships which took place in my hometown. This was the first time I came into contact with athletes with disabilities and I was fascinated by their attitude and performance right from the start. In order to increase my endurance in competition, I started running in the beautiful landscape of Dortmund's south. At the advanced sport course of my high school, I initially learned about the theoretical background of training and adaptation (especially in the field of endurance exercise) which shaped my unbounded interest in exercise science. Little by little, my passion for endurance sports and exercise science overtook my enthusiasm for badminton. In 2009, I was on vacation with my father in Hamburg where the biggest age-group triathlon took place. Egged on by my father, I decided to participate at this event myself the following year. At the first swimming sessions, the life guard was worried about my technique because it looked like I was drowning. Through my first triathlon event, I became infected by the 'triathlon-virus'. After performing the physical aptitude test (three times), I moved to Cologne and started my bachelor program at the German Sport University Cologne. Finally, my scientific curiosity was unleashed, and I absorbed every lecture and class like a nerdy sponge. For a seminar project in public health, I assisted a wheelchair user to re-start swimming exercise, which was a precious and personal experience. Not entirely by chance, I wrote my bachelor thesis in the field of paratriathlon and analysed the competition results of the last years to determine performance potentials. In the fall of 2014, I started my master program, became a research assistant at the chair of 'Paralympic Sports' and had a fateful encounter. Benjamin (Benny) Lenatz, a young wheelchair basketball player, wanted to start a professional career in paratriathlon and asked for support. I started to schedule his training in swimming, handcycling and wheelchair racing, without personal experience in the latter two disciplines. Since handcycling was found to be Benny's 'greatest potential for improvement', I wanted to gain a more profound understanding of handcycling propulsion and its underlying biomechanical characteristics. Hence, I examined crank kinetics, joint kinematics, muscular activity and lactate kinetics of handcycling under various exercise modalities during the course of my doctorate program. Besides this project, I performed studies in my own (favourite) sport to improve anaerobic exercise testing in running. About that time, I started to make music by playing the blues harp and producing my first (Oldschool Hip Hop and House) beats. In the fall of 2018, I merged my interests for music, exercise and science and participated at the first Science Slam Word Cup. This experience kindled my passion for delivering scientific findings in an entertaining manner and led to various Slams following thereafter. I still support Benny in his preparation for the Paralympics in Tokyo 2020 for which he will hopefully (and realistically) qualify. Either way, I'm very grateful for the journey so far.

Numbers and facts

During the 3-year journey of preparing this thesis, a lot of measurements and analyses were performed. Considering the work steps required for finishing this program sounds worse than it actually was. This section is a tribute to all statisticians and number-enthusiasts (such as me):

360	C3D-files had to be analysed. With a duration of 20 s each,
2:00	hours of biomechanical measures were recorded. More than
200	hours were required for labelling all C3Ds. A total of
500	electrodes were placed on the participants who performed
500	maximal contractions for normalisation with a total of
20	minutes maximal isometric force duration during the tests.
1000	markers were placed and attached on anatomical landmarks.
100	15-s all-out tests were performed during studies, resulting in
25	minutes of sprint power by the participants who suffered from
1600	blood samples collected from their earlobes. However, only
32	millilitres of blood were analysed during the measurements.
30	participants demonstrated courageous commitment during the exhausting procedures of the studies. Without their unbounded motivation to perform to the best of their ability and
150	hours spent in the lab, this thesis would not have been possible.